

UNIVERSITAT POLITÈCNICA DE CATALUNYA

Doctorate programme in Environmental Engineering



Ph.D. Thesis

**Analysis of the aerosol-radiation-cloud
interactions through the use of regional
climate/chemistry coupled models**

Rocío Baró Esteban

Director:
Dr. Pedro Jiménez Guerrero

Tutor:
Dr. Santiago Gassó i Domingo

Barcelona, June 2017

*A mi familia
y a todos los que han creído en mí*

*“The most difficult thing is the decision to act. The rest is merely tenacity.
The fears are paper tigers. You can do anything you decide to do.
You can act to change and control your life; and the procedure,
the process is its own reward”.*
Amelia Earhart

Acknowledgements

Si me permitís el símil, durante la última fase, he pensado en la Tesis como pintar un cuadro. Al principio el lienzo está en blanco, no tienes ni idea de nada. Vas haciendo bocetos, pero aún no tienes claro qué estás pintando y dudas de si sirves para esto. En más de una ocasión, te enfrentas con cosas que no sabes pintar bien, y te lías pintando sombras, se te pone todo negro...Te ahogas hasta en el vaso donde limpias los pinceles. Pero tienes a gente que te ayuda y que de un modo u otro, aportan *luz* a tu *lienzo* (científica y personalmente). Poco a poco, sigues pintando y va cogiendo forma. Al final te das cuenta de que las *sombras* fueron necesarias para acabar tu *cuadro* y lo mejor es, que lo *acabas*.

Aquí van mis agradecimientos a aquellas personas que de una forma y otra, han aportado *luz* a mi *cuadro*. En primer lugar, a los que han hecho posible la realización de esta Tesis. Mi director, *Pedro Jiménez*, prácticamente te tengo que agradecer *TODO*. Esto es muy tópico, pero si no hubiera sido por tí, no estaría donde estoy ahora. Gracias por recibirme con los brazos abiertos, por creer en mí cuando yo no lo hacía y por ejercer de *socorrista* cuando me ahogaba en un vaso de agua. Por mejorar mi inglés, por dejar que te cuente mi vida, por la música, por todo lo que he aprendido contigo. Y sobre todo, gracias porque además de mi director de Tesis, eres un gran amigo. Mi tutor de la Tesis, *Santiago Gassó*, muchas gracias por toda tu ayuda, tu paciencia y por todo el tiempo que me has dedicado. Gracias a tí ha sido posible tener el doctorado en Barcelona y la afiliación en Murcia. Gracias por hacerlo sencillo y sobre todo, posible.

He tenido la inmensa suerte de hacer la Tesis en el *Grupo de Modelización Atmosférica Regional (GMAR)* de la Universidad de Murcia. Cuando he estado fuera, me he dado cuenta de que no debemos envidiar a otros grupos de nuestro campo, ya que con muchos menos recursos, somos un pequeño *GRAN* grupo. Dentro de él, tuve la suerte de compartir mis años de Tesis con: *Juanpe*, *el jefe*, que se desvive por ayudar a sus alumnos y a mí me ha tratado mejor, imposible. Gracias por los chistes, por el “*no te preocupes, yo me encargo*”, por enseñarme tanto de ciencia como de la vida. *Juanjo*, siempre recordaré lo que me dijiste, “*hacer otra carrera es crecer horizontalmente, hacer un doctorado implica crecer hacia arriba*”. Gracias por lo que me has enseñado y aún me sigues enseñando. *Raquel*, gracias por nuestras charlas, por los días felices en el CIOyN y las cenas y *cerves* para alegrarnos un lunes. *Juanan*, gracias por todo lo que he aprendido contigo en las prácticas, por tu apoyo y cariño. *Sonia*, gracias por traer a *Bolita* y hacer que los días fueran más bonicos. *Marco*, gracias por formar parte de nuestro grupo. *Nuno*, por enseñarme cosas de este mundillo, por la buena música y por seguir volviendo a Murcia. Y los pequeños de la casa, *Laura* y *Chema*. *Laura*, gracias por enseñarme cosas también a mí y ayudarme cuando me bloqueaba. Por los buenos ratos, las risas, los foodtopías, los viajes improvisados y por considerarme como un ejemplo...¡Gracias!. *Chema*, por enseñarme cosas que no sabía, por las conversaciones sobre libros y por tener siempre un vídeo de Homer para amenizar nuestras horas en el despacho. Por último, sin ser del GMAR, pero podrían serlo: *La Vane*, gracias por los buenos ratos en Viena y por tu apoyo. Y *Félix*, gracias por contribuir a esos días felices y por entender y valorar mi afición gastronómica.

Quiero agradecer a la gente del CIOyN, con la que compartí casi toda mi Tesis. *Jesús*: por los cafés en BBAA, por escucharme y apoyarme, por las cenas en Los Navarros y tu cariño. *Juan Fran*, no tengo palabras para agradecer tu inmensa ayuda y paciencia con mis dudas de L^AT_EX. Gracias a ti he podido ganar las batallas y tener *el documento*. Millones de gracias. *Elisa*, por tener siempre una palabra bonita hacia mí, por tu apoyo y confianza. *María* ¡porque sólo tú entiendes mis indecisiones! Gracias por mostrarme tanto cariño. *Lisa*, por ser un ejemplo de fuerza, un diamante, un gran apoyo y por creer en mí. *Abellán*, por tus charlas en la sala del café, tu experiencia y tu cariño. Gracias *Manu, Pablo, Andrés, Miguel, Jaime y Rafa*, por vuestro apoyo y cariño. De la Facultad de Química, a Néstor, gracias por tu apoyo.

A mi familia, mis padres Carmen y Mariano, mis hermanos y cuñadas; Pablo y Rebeca, David y Susi. Por vuestro apoyo incondicional durante estos años. Por creer en que un día, esta Tesis llegaría a su fin y sobre todo por vuestros cuidados y cariño en la última fase de la Tesis. Mi pequeña *Pau*, por sacarme una sonrisa cuando más lo necesitaba. A todos mis tíos y primos que me han apoyado y se han preocupado tanto por mí.

A mis amigos:

Cris, gracias por creer tanto en mí, por los días felices, los sonoramas, los SOS, por ser mi *gemela*. *Susana y Ari*, gracias por las noches de godhas, por las excursiones, los Musiks, los antibandos, por apoyarme tanto y creer en mí. Por estar en las buenas y en las malas, por seguir ahí después de todo. ¡Gracias! Mis *pardis*, por preocuparos y apoyarme tanto durante esta época, por seguir juntas después de tantos años. *Diana*, por tu apoyo desde el principio, por los viajes hechos y los que nos quedan. Mis chicos, *Fer, Alex, Juan y Luis*, las noches en Musik, los conciertos, las cenas en verano y haberme apoyado durante esta etapa. A mis *ambientólogo@s, mi Soni, Abri, Laksh, Athe, Resu, Virginia* gracias por creer en mí y mandarme fuerza!

A mis chicos de la *impro*, gracias por esos días maravillosos en los que todo lo malo se olvidaba porque dos horas con vosotros eran *medicina*. Descubrir la *impro* ha sido una de las mejores cosas que me ha pasado en este último año y me ha ayudado mucho personalmente. Gracias a mis profes *Javi y Santi* por todo lo que me habéis enseñado y a mis compañeros: *Susana, Jon, Alberto, Laja, Elena, Diego, Risi, Josema, Antonio y Carmen*, por haber tenido la suerte de compartirlo con vosotros.

Mis supernenas, Sara y Anna, gracias por el apoyo, los ratos felices en San Francisco y por aprender de vosotras, y en especial, gracias Sara por tu ayuda en el depósito de la Tesis. Mis chicos del ZAMG: *María y Aitor*, gracias por vuestro apoyo y ayuda desde el minuto cero.

Agradezco al Ministerio de Educación, Cultura y Deporte la beca FPU (Ref. FPU12/05642) que ha financiado la realización de esta Tesis.

Last, this investigation was also possible thanks to the collaboration of many scientists. I would like to acknowledge all the co-authors of the publications done in the context of this Thesis. I also acknowledge the AQMEII Phase 2 activity (specially the WRF-Chem community), and the EuMetChem COST Action ES1004. And thanks to all my international friends who have encouraged and supported me over the last years.

Hay mucha gente que me dejo sin nombrar, pero que también han contribuido a que esta etapa haya sido una de las mejores de mi vida hasta el momento. A todos ellos, ¡muchas gracias!

¡Gracias! Thank you! Grazie! Merci! Danke!

Resumen

Los procesos climáticos que representan una mayor incertidumbre respecto a la modificación del balance radiativo terrestre son los relacionados con los aerosoles atmosféricos. Por tanto, este campo de investigación representa uno de los temas clave a la hora de establecer políticas de mitigación del cambio climático. Los estudios de las interacciones calidad del aire / clima (siglas en inglés, AQCI) son por tanto de especial relevancia, contribuyendo a su vez a la comprensión de las incertidumbres asociadas a los forzamientos antropogénicos. Con el fin de crear confianza en los estudios de AQCI, un campo científico de especial interés, el uso de modelos meteorológicos y químicos de escala regional acoplados está en alza. En este contexto, el principal objetivo de esta Tesis es la caracterización de las incertidumbres del sistema clima-química-aerosol-nubes-radiación, asociadas a los efectos radiativos directo e indirecto causados por los aerosoles sobre Europa.

El primer aspecto tratado en esta Tesis es la configuración del modelo acoplado, relacionado con la parametrización de la microfísica. Se han estudiado y analizado las diferencias al usar dos esquemas de microfísica diferentes con el modelo meteorológico acoplado con la química (siglas en inglés, WRF-Chem). Las simulaciones estudiadas han sido realizadas bajo la segunda fase de la iniciativa internacional sobre evaluación de la modelización de la calidad del aire (siglas en inglés, AQMEII). Se ha estimado el impacto de varias variables bajo los siguientes esquemas de microfísica: Morrison versus Lin, sobre periodos de tres meses durante el 2010 en Europa. Los resultados obtenidos muestran que la parametrización Morrison simula gotas de nube más pequeñas y más numerosas, siendo por tanto más efectivo a la hora de dispersar la radiación de onda corta.

Así mismo, se han estudiado los efectos de los aerosoles procedentes de la quema de biomasa (siglas en inglés, BB) sobre los vientos en superficie durante la ola de calor y fuegos de Rusia. La metodología consiste en tres simulaciones con el modelo WRF-Chem sobre Europa, realizadas bajo la iniciativa EuMetChem COST Action ES1004. Éstas difieren en la inclusión (o no) de las interacciones aerosol-radiación y aerosol-nubes (en inglés ARI y ACI, respectivamente). Los resultados muestran que estos aerosoles pueden afectar los vientos en superficie no solo sobre la fuente de emisión sino también alejados de ella. Los vientos locales disminuyen debido a que la radiación de onda corta que llega a la superficie se reduce, lo que supone un descenso en la temperatura a dos metros. Además, la estabilidad atmosférica aumenta cuando se tienen en cuenta las realimentaciones producidas por los aerosoles sobre la meteorología, provocando una menor altura de la capa límite planetaria.

Finalmente, esta Tesis evalúa la representación de las interacciones ACI en modelos de escala regional acoplados complementando el análisis colectivo de temperatura. Las simulaciones analizadas se llevaron a cabo bajo la segunda fase de AQMEII (sobre Europa en 2010) e incluyen las interacciones ARI+ACI. Las simulaciones son evaluadas frente datos de la Agencia Espacial Europea (siglas en inglés, ESA) del proyecto Cloud de la iniciativa sobre cambio climático (siglas en inglés, CCI). La variable fracción de nubes (CFR) se subestima (sobrestima) sobre tierra (océano), lo que puede ser debido a que los satélite infraestiman las nubes finas sobre el océano. El bias y el error absoluto medio (siglas en inglés, MAE) son menores al considerar el promedio del conjunto de simulaciones. En general, la profundidad óptica de la nube (siglas en inglés, COD), así como el camino de hielo líquido en la nube (siglas en inglés, CIP) son subestimadas

sobre todo el dominio. Las diferencias encontradas entre los modelos se deben a los diferentes esquemas de microfísica empleados.

El desarrollo de esta Tesis ha contribuido al estado del arte de los estudios sobre AQCI. A pesar de que incluir las realimentaciones de los aerosoles no contribuye a la mejora del sesgo de los modelos, hay una mejora en la variabilidad espacio-temporal así como los coeficientes de correlación. Son necesarios más estudios en el futuro con el fin de mejorar la representación de estas interacciones.

Abstract

The response of the climate systems to aerosols and their effect on the radiative budget of the Earth is the most uncertain climate feedback, and therefore represents one of the key topics of research in climate change mitigation. Air quality-climate studies (AQCI) are a key, but uncertain contributor to the anthropogenic forcing that remains poorly understood. To build confidence in the AQCI studies, regional-scale integrated meteorology-atmospheric chemistry models are in demand. In this context, the main objective of the present Thesis is the characterization of the uncertainties in the climate-chemistry-aerosol-cloud-radiation system associated to the aerosol direct and indirect radiative effects caused by aerosols over Europe, employing an ensemble of fully-coupled climate and chemistry model simulations.

The first topic covered here deals with the configuration related to the microphysics parameterization of an online-coupled model. The differences when using two microphysics schemes within the Weather Research and Forecasting coupled with Chemistry (WRF-Chem) model, are analyzed. The evaluated simulations are run under the umbrella of the Air Quality Model Evaluation International Initiative (AQMEII) Phase 2, during the year 2010, in Europe. The impact on several variables is estimated when selecting Morrison vs. Lin microphysics parameterizations. The results showed smaller and more numerous cloud droplets simulated with the Morrison parameterization, and therefore this scheme is more effective in scattering shortwave radiation.

Also, the impact of biomass burning (BB) aerosols on surface winds during the Russian heat wave and wildfires episode is studied. The methodology consists of three WRF-Chem simulations over Europe, run under the context of EuMetChem COST Action ES1004, differing in the inclusion (or not) of aerosol-radiation (ARI) and aerosol-cloud interactions (ACI). Results show that these aerosols can affect surface winds not only where emission sources are located, but also further from the release areas. Local winds decrease due to a reduction of shortwave radiation reaching the ground, which leads to decreases in 2-m temperature. Atmospheric stability increases when considering aerosol feedbacks, inducing a lower planetary boundary layer height.

This Dissertation also investigates the ability of an ensemble of simulations to elucidate the aerosol-radiation-cloud interactions. An assessment of whether the inclusion of atmospheric aerosol radiative feedbacks during two aerosol case studies (wildfires and dust) of an ensemble of on-line coupled models improves the simulation results for maximum, mean and minimum 2-m temperature is done. The simulations (EuMetChem COST Action ES1004) are evaluated against observational data from E-OBS gridded database. In both episodes, a general underestimation of the studied variables is found, being most noticeable in maximum temperature. The biases are improved when including ARI or ARI+ACI in the dust case, but no evident improvements are found for the heatwave/wildfires episode. Although the ensemble does not outperform the individual models (in general), the improvements found when including ARI+ARI are more remarkable for the ensemble than for the individual models. Last, an improvement of the spatio-temporal variability and correlation coefficients when atmospheric aerosol radiative effects are included is found.

Finally, this Thesis explores the representation of the ACI in regional-scale integrated models when simulating the climate-chemistry-cloud-radiation system. It complements the temperature

collective analyses. The evaluated simulations are run in the context of AQMEII Phase 2 (over 2010 and Europe) and include the ARI+ACI interactions. The model simulations are evaluated against the (ESA) Cloud_cci data. Results show an underestimation(overestimation) of cloud fraction (CFR) over land(ocean) areas, which could be related to satellite retrieval missing thin clouds. Lower bias and mean absolute error (MAE) are found in the ensemble mean. Cloud optical depth (COD) and cloud liquid ice path (CIP) are generally underestimated over the whole domain. The differences found can be attributed to differences in the microphysics schemes.

The development of this Thesis has contributed to the state of the art in AQCI studies. Despite the inclusion of the aerosol feedbacks does not modify the bias, the spatio-temporal variability and correlation coefficients are improved when atmospheric aerosol radiative effects are included. Further studies are needed in order to improve the representation of these interactions.

Publications

Included in this Thesis

1. **Baró, R.**, Stengel, M., Brunner, D., Curci, G., Hollmann, R., Forkel, R., Palacios-Peña, L., Savage, N., Schaap, M., Van der Gon, H., Hogrefe, C., Galmarini, S and Jiménez-Guerrero, P.: How good are aerosol-cloud interactions represented in online coupled regional models? Submitted to :*Atmospheric Chemistry and Physics*.
2. **Baró, R.**, Palacios-Peña, L., Baklanov, A., Balzarini, A., Brunner, D., Forkel, R., Hirtl, M., Honzak, L., Pérez, J. L., Pirovano, G., San José, R., Schröder, W., Werhahn, J., Wolke, R., Zabkar, R., and Jiménez-Guerrero, P. (2017): Regional effects of atmospheric aerosols on temperature: an evaluation of an ensemble of on-line coupled models, *Atmospheric Chemistry and Physics Discussions*, pp. 1–35, doi:10.5194/acp-2016-1157, <http://www.atmos-chem-phys-discuss.net/acp-2016-1157/>, 2017.
3. **Baró, R.**, Lorente-Plazas, R., Montávez, J.P., Jimenez-Guerrero, P (2017). Biomass burning aerosol impact on surface winds during 2010 Russian forest fires. *Geophysical Research Letters* 44, 1088–1094.
4. **Baró, R.**, Jiménez-Guerrero, P., Balzarini, A., Curci, G., Forkel, R., Grell, G., Hirtl, M., Honzak, L., Im, I., Lorenz, C., Perez, J.L., Pirovano, G., San Jose, R., Tuccella, P., Werhahn, J., Zabkar, R. (2015). Sensitivity analysis of the microphysics scheme in WRF-Chem contributions to AQMEII phase 2. *Atmospheric Environment*, 115, 620-629.

Derived from this Thesis

1. Palacios-Peña, L., **Baró, R.**, Baklanov, A., Balzarini, A., Brunner, D., Forkel, R., Hirtl, M., Honzak, L., López-Romero, J.M., Pérez, J. L., San José, R., Schröder, W., Werhahn, J., Wolke, R., Zabkar, R., and Jiménez-Guerrero, P. An assessment of aerosol optical properties from remote sensing observations and an ensemble of regional chemistry-climate coupled models over Europe. *To be submitted to Atmospheric Chemistry and Physics*.
2. Solazzo, E., Bianconi, R., Hogrefe, C., Curci, G., Alyuz, U., Balzarini, A., **Baró, R.**, Bellasio, R., Bieser, J., Brandt, J., Christensen, J.H., Colette, A., Francis, X., Fraser, A., Garcia Vivanco, M., Jimenez-Guerrero, P., Im, U., Manders, A., Nopmongkol, U., Kitwiroon, N., Pirovano, G., Pozzoli, L., Prank, M., Sokhi, R.S., Tuccella, P., Unal, A., Yarwood, G., Galmarini, S (2016). Evaluation Error Apportionment of an Ensemble of Atmospheric Chemistry Transport Modelling Systems: Multi-variable Temporal and Spatial Breakdown. *Atmospheric Chemistry and Physics*, 17, 3001–3054.
3. Palacios-Peña, L., **Baró, R.**, Guerrero-Rascado, J.L., Alados-Arboledas, L., Brunner, D., Jimenez-Guerrero, P (2016). Assessment of the radiative effects of aerosols in an on-line coupled model over the Iberian Peninsula. *Atmospheric Chemistry and Physics*, 17, 277–296.

4. Kioutsioukis, I., Im, U., Solazzo, E., Bianconi, R., Badia, A., Balzarini, A., **Baró, R.**, Bellasio, R., Brunner, D., Chemel, C., Curci, G., Denier van der Gon, H., Flemming, J., Forkel, R., Giordano, L., Jimenez-Guerrero, P., Hirtl, M., Jorba, O., Manders-Groot, A., Neal, L., Perez, J.L., Pirovano, G., San Jose, R., Savage, N., Schroder, W., Sokhi, R.S., Syrakov, D., Tuccella, P., Werhahn, J., Wolke, R., Hogrefe, C., Galmarini, S (2016). Improving the deterministic skill of air quality ensembles. *Atmospheric Chemistry and Physics*, 16, 15629–15652.
5. Palacios-Peña, L., **Baró, R.**, Jimenez-Guerrero, P (2015). An on-line modelling study of the direct effect of atmospheric aerosols over Europe. *Física de la Tierra*, 27,155–170.
6. Giordano, L., Brunner, D., Flemming, J., Im, U., Hogrefe, C., Bianconi, R., Badia, A., Balzarini, A., **Baró, R.**, Chemel, C., Curci, G., Forkel, R., Jimenez-Guerrero, P., Hirtl, M., Hodzic, A., Honzak, L., Jorba, O., Knote, C., Kuenen, J.J.P., Makar, P.A., Manders-Groot, A., Neal, L., Perez, J.L., Pirovano, G., Pouliot, G., San Jose, R., Savage, N., Schroder, W., Sokhi, R.S., Syrakov, D., Torian, A., Tuccella, P., Werhahn, J., Wolke, R., Yahya, K., Zabkar, R., Zhang, Y., Galmarini, S (2015). Assessment of the MACC/IFS-MOZART model and its influence as chemical boundary conditions in AQMEII phase 2. *Atmospheric Environment*, 115, 371–388.
7. San José, R., Pérez, J. L., Balzarini, A., **Baró, R.**, Curci, G., Forkel, R., Galmarini, S., Grell, G., Hirtl, M., Honzak, L., Im, U., Jimenez-Guerrero, P., Langer, M., Pirovano, G., Tuccella, P., Werhahn, J., Zabkar, R (2015). Evaluation of feedback effects in CBMZ/MOSAIC chemical mechanism. *Atmospheric Environment*, 115, 646–656.
8. Curci, G., Hogrefe, C., Bianconi, R., Im, U., Balzarini, A., **Baró, R.**, Honzak, L, Brunner, D., Forkel, R., Giordano, L., Hirtl, M., Honzak, L., Jimenez-Guerrero, P., Knote, K., Langer, M., Makar, P., Pirovano, G., Perez, J.L., San Jose, R., Syrakov, D., Tuccella, P., Werhahn, J., Wolke, R., Zabkar, R., Zhang, J. (2014) . Uncertainties of simulated aerosol optical properties induced by assumptions on aerosol physical and chemical properties: an AQMEII-2 perspective. *Atmospheric Environment*, 115, 541–552.
9. Forkel, R., Balzarini, A., **Baró, R.**, Bianconi, R., Curci, G., Jimenez-Guerrero, P., Hirtl, M., Honzak, L., Lorenz, C, Im, U., Perez, J.L., Pirovano, G., San Jose, R., Tuccella, P., Werhahn, J., Zabkar, R (2014). Analysis of the WRF-Chem contributions to AQMEII phase 2 with respect to aerosol radiative feedbacks on meteorology and pollutant distributions. *Atmospheric Environment*, 115, 630–645.
10. Im, U., Bianconi, R., Solazzo, E., Kioutsioukis, I., Badia, A., Balzarini, A., **Baró, R.**, Bellasio, R., Brunner, D., Chemel, C., Curci, G., Flemmig, J., Forkel, R., Giordano, L., Jimenez-Guerrero, P., Hirtl, M., Hodzic, A., Honzak, L., Jorba Casellas, O., Knote, C., Kuenen, J. J., Makar, P. A., Manders-Groot, A., Neal, L., Perez, J. L., Pirovano, G., Pouliot, G., San Jose, R., Savage, N., Schroder, W., Sokhi, R., Syrakov, D., Torian, A., Tuccella, P., Werhahn, J., Wolke, R., Yahya, K., Zabkar, R., Zhang, Y., Zhang, J., Hogrefe, C., Galmarini, S (2014). Evaluation of operational on-line-coupled regional air quality models over Europe and north America in the context of AQMEII Phase 2. Part I: Ozone. *Atmospheric Environment*, 115, 404–420.
11. Im, U., Bianconi, R., Solazzo, E., Kioutsioukis, I., Badia, A., Balzarini, A., **Baró, R.**, Bellasio, R., Brunner, D., Chemel, C., Curci, G., Denier van der Gon, H.A.C., Flemming, J., Forkel, R., Giordano, L., Jimenez-Guerrero, P., Hirtl, M., Hodzic, A., Honzak, L., Jorba, O., Knote, C., Makar, P.A., Manders-Groot, A., Neal, L., Perez, J.L., Pirovano, G., Pouliot, G., San Jose, R., Savage, N., Schroder, W., Sokhi, R.S., Syrakov, D., Torian, A., Tuccella, P., Werhahn, K., Wolke, R., Yahya, K., Zabkar, R., Zhang, Y., Zhang, J.,

- Hogrefe, C., Galmarini, S (2014). Evaluation of operational online-coupled regional air quality models over Europe and North America in the context of AQMEII phase 2. Part II: Particulate Matter, *Atmospheric Environment*, 115, 421–441.
12. Knote, C., Tuccella, P., Curci, G., Emmons, L., Orlando, J. J., Madronich, S., **Baró, R.**, Jimenez-Guerrero, P., Luecken, D., Hogrefe, C., Forkel, R., Werhahn, J., Hirtl, M., Perez, J.L., San Jose, R., Giordano, L., Brunner, D., Yahya, K., Zhang, Y (2014). Influence of the choice of gas-phase mechanism on predictions of key gaseous pollutants during the AQMEII Phase-2 intercomparison. *Atmospheric Environment*, 115, 553–568.
 13. Kong, X., Forkel, R., Sokhi, R. S., Suppan, P., Baklanov, A., Gauss, M., Brunner, D., **Baró, R.**, Balzarini, A., Chemel, C., Curci, G., Guerrero, P., Hirtl, M., Honzak, L., Im, U., Perez, J.L., Pirovano, G., San Jose, R., Schlünzen, H., Tsegas, G., Tuccella, P., Werhahn, J., Zabkar, R., Galmarini, S (2014). Analysis of Meteorology-Chemistry Interactions during Air Pollution Episodes using online coupled models within AQMEII Phase-2. *Atmospheric Environment*, 115, 527–540.
 14. Makar, P. A., Gong, W., Hogrefe, C., Zhang, Y., Curci, G., Zabkar, R., Milbrandt, J., Im, U., Galmarini, S., Balzarini, A., **Baró, R.**, Bianconi, R., Cheung, P., Forkel, R., Gravel, S., Hirtl, M., Honzak, L., Hou, A., Jimenez-Guerrero, P., Langer, M., Moran, M.D., Pabla, B., Perez, J.L., Pirovano, G., San Jose, R., Tuccella, P., Werhahn, J., Zhang, J (2014). Feedbacks between Air Pollution and Weather, Part 1: Effects on Chemistry. *Atmospheric Environment*, 115, 442–562.
 15. Makar, P. A., Gong, W., Hogrefe, C., Zhang, Y., Curci, G., Zabkar, R., Im, U., Balzarini, A., **Baró, R.**, Bianconi, R., Cheung, P., Forkel, R., Gravel, S., Hirtl, M., Honzak, L., Hou, A., Jimenez-Guerrero, P., Langer, M., Moran, M.D., Pabla, B., Perez, J.L., Pirovano, G., San Jose, R., Tuccella, P., Werhahn, J., Zhang, J., Galmarini, S (2014). Feedbacks between Air Pollution and Weather, Part 2: Effects on Weather. *Atmospheric Environment*, 115, 499–526.
 16. Campbell, P., Zhang, Y., Yahya, K., Wang, K., Hogrefe, C., Pouliot, G., Knote, C., San Jose, R., Perez, J.L., Jimenez-Guerrero, P., **Baró, R.**, Makar, P (2014). A Multi-Model Assessment for the 2006 and 2010 Simulations under the Air Quality Model Evaluation International Initiative (AQMEII) Phase 2 over North America: Part I. Indicators of the Sensitivity of O₃ and PM_{2.5} Formation Regimes. *Atmospheric Environment*, 115, 569–586.
 17. Wang, K., Yahya, K., Zhang, Y., Hogrefe, C., Pouliot, G., Knote, C., Hodzic, A., San Jose, R., Jimenez-Guerrero, P., **Baró, R.**, Makar, P., Bennartz, R (2014). A Multi-Model Assessment for the 2006 and 2010 Simulations under the Air Quality Model Evaluation International Initiative (AQMEII) Phase 2 over North America: Part II. Evaluation of Column Variable Predictions Using Satellite Data. *Atmospheric Environment*, 115, 587–603.
 18. Brunner, D., Savage, N., Jorba, O., Eder, B., Giordano, L., Makar, P., Badia, A., Balzarini, A., **Baró, R.**, Bianconi, R., Chemel, C., Curci, G., Forkel, R., Jimenez-Guerrero, P., Hirtl, M., Hodzic, A., Honzak, L., Im, U., Knote, C., Manders-Groot, A., Neal, L., Perez, J.L., Pirovano, G., San Jose, R., Schröder, W., Sokhi, R.S., Syrakov, D., Torian, A., Werhahn, J., Wolker, R., van Meijgaard, E., Yahya, K., Zabkar, R., Zhang, Y., Hogrefe, C., Galmarini, S (2014). Evaluation of the meteorological performance of coupled chemistry-meteorology models in the context of AQMEII phase 2. *Atmospheric Environment*, 115, 470–498.

Book chapters

1. Montávez, J.P., Gómez-Navarro, J.J., Jerez S., **Baró, R.**, Lorente-Plazas, R., García-Valero, J.A., Jiménez-Guerreo, P. Análisis del papel de la elección de la base de datos reticular observacional en la evaluación de modelos climáticos regionales. Cambio climático. Extremos e impactos. 15, 153-163. Asociación Española de Climatología, 2012. ISBN 978-84-695-4331-3.

International Conferences and Workshops

1. **Baró, R.**, Palacios-Peña, L., Baklanov, A., Balzarini, A., Brunner, D., Forkel, R., Hirtl, M., Honzak, L., Pérez, J.L., Pirovano, G., San José, R., Schröder, W., Werhahn, J., Wolke, R., Zabkar, R., and Jiménez-Guerrero, P. Regional effects of atmospheric aerosols on temperature: an evaluation of an ensemble of on-line coupled models. Viena, Austria. 04/2017.
2. Palacios-Peña, L., **Baró, R.**, Jiménez-Guerrero, P. An evaluation of uncertainty in the aerosol optical properties as represented by satellites and an ensemble of chemistry-climate coupled models over Europe. EGU General Assembly. Viena, Austria. 04/2016.
3. Palacios-Peña, L., **Baró, R.**, Alados-Arboledas, L., Jiménez-Guerrero, P. Evaluation of the aerosol-radiation and aerosol-cloud interactions in an online-coupled model over the Iberian Peninsula. AIR QUALITY - Science and application. Milano, Italy 03/2016.
4. **Baró, R.**, Palacios-Peña, L., Brunner, D., Bianconi, R., Curci, G., Honzak, L., Forkel, R., Manders, A., Neal, L., Shaap, M., Tuccella, P., Van der Gon, H., Werhahn, W., Zabkar, R., Jiménez-Guerrero, P. How good are aerosol-cloud interactions in online coupled models?. AIR QUALITY - Science and application. Milano, Italy 03/2016.
5. **Baró, R.**, Palacios-Peña, L., Jiménez-Guerrero, P. Study of the aerosol cloud interactions over the Iberian Peninsula. 3rd Iberian Meeting on Aerosol Science and Technology, RICTA 2015, Elche, Alicante, España. 06/2015.
6. Palacios-Peña, L., **Baró, R.**, Jiménez-Guerrero, P. How good are aerosol radiative feedbacks represented in on-line coupled models? An assessment over the Iberian Peninsula. 3rd Iberian Meeting on Aerosol Science and Technology, RICTA 2015, Elche, Alicante, España. 06/2015
7. **Baró, R.**, Lorente-Plazas, R., Jerez, S., Montávez, J.P., Jiménez-Guerrero, P. Are atmospheric aerosols able to modify the surface winds? A sensitivity study of the biomass burning aerosols impact on the spatially-distributed wind over Europe. EGU General Assembly. Viena, Austria. 04/2015.
8. Forkel, R., Brunner, D., Balzarini, A., **Baró, R.**, Hirtl, M., Jiménez-Guerrero, P., Jorba, O., Pérez, J.L., Pirovano, G., San José, R., Schröder, W., Werhahn, J., Wolke, R., Zabkar, R. Case studies on aerosol feedback effects in online coupled chemistry-meteorology models during the 2010 Russian fire event. European Geosciences Union. Viena, Austria. 04/2015
9. Palacios-Peña, L., **Baró, R.**, Jiménez-Guerrero, P. Direct radiative effect of atmospheric aerosols over Europe: An on-line modelling approach. Gloream 25th Workshop On Tropospheric Chemical Transport Modelling. Aveiro, Portugal. 11/2014.
10. Campbell, P., Zhang, Y., Yahya, K., Wang, K., Christoph, K., Hodzic, A., San José, R., Pérez, J.L., Jiménez-Guerrero, P., **Baró, R.**, Makar, P. A multi-model assessment for the 2006 and 2010 simulations under the air quality model evaluation international initiative (AQMEII) Phase 2 over north America: indicators of the sensitivity of O3 and

PM2.5 formation regimes. Community Modeling and Analysis System (CMAS). Chape Hill, Carolina del Norte, United States. 10/2014.

11. Knote, C., Emmons, L., Hodzic, A., Madronich, S., Orlando, J., **Baró, R.**, Jiménez-Guerrero, P., Brunner, D., Giordano, L., Curci, G., Tuccella, P., Forkel, R., Hirtl, M., Hogrefe, C., Luecken, D., San José, R., Pérez, J.L., Wolke, R., Zhang, Y. Evaluation of the performance of different WRF-chem configurations with a focus on the gas-phase mechanisms. 15th Annual WRF Users' Workshop. Boulder, Colorado, United States. 06/2014
12. Jiménez- Guerrero, P., Balzarini, A., **Baró, R.**, Curci, G., Forkel, R., Hirtl, M., Honzak, L., Langer, M., Pérez, J.L., Pirovano, G., San José, R., Tuccella, P., Werhahn, J., Zabkar, R. Describing the direct and indirect radiative effects of atmospheric aerosols over Europe by using coupled meteorology-chemistry simulations: a contribution from the AQMEII-Phase II exercise. European General Assembly. Viena, Austria. 04/2014
13. Werhahn, J., Forkel, R., Balzarini, A., **Baró, R.**, Curci, G., Hirtl, M., Honzak, L., Jiménez-Guerrero, P., Pérez, J.L., Pirovano, G., San José, R., Tuccella, P., Zabkar, R. Analysis of the WRF-Chem simulations for the AQMEII Phase II exercise with respect to aerosol impact on precipitation. European General Assembly. Viena, Austria. 04/2014.
14. Forkel, R., Balzarini, A., **Baró, R.**, Curci, G., Jiménez-Guerrero, P., Hirtl, M., Honzak, L., Pérez, J.L., Pirovano, G., San José, R., Tuccella, P., Werhahn, J., Zabkar, R. WRF-CHEM simulations on the effect of aerosol-meteorology feedback on regional pollutant distributions over Europe. Garmisch-Partenkirchen, Alemania. 03/2014.

Acronyms

ACCMIP Atmospheric Chemistry and Climate Model Intercomparison Project.

ACI Aerosol-Cloud Interactions.

ACT Atmospheric Chemical Transport.

ACTMs Atmospheric Chemistry Transport Models.

ACTRIS Aerosols, Clouds, and Trace gases Research InfraStructure Network.

AEROCOM Aerosol Comparisons between Observations and Models.

AERONET AErosol RObotic NETwork.

AOD Aerosol Optical Depth.

AQCI Air Quality-Climate Interactions.

AQMEII Air Quality Model Evaluation International Initiative.

AR4 Fourth Assessment Report.

AR5 Fifth Assessment Report.

ARI Aerosol-Radiation Interactions.

ASY Asymmetry parameter.

BB Biomass Burning.

BC Black Carbon.

CAM3 Community Atmosphere Model.

CB05 Carbon Bond mechanism version 05.

CBM-Z Carbon-Bond Mechanism version Z.

CCN Cloud Condensation Nuclei.

CCSM Community Climate System Model.

CFR Cloud Fraction.

CH₄ Methane.

CIP Cloud liquid Ice Path.

CLOUDNET Network of stations for the continuous evaluation of cloud and aerosol profiles.

- CMAQ** Community Multiple Air Quality.
- CMIP5** Coupled Model Intercomparison Project Phase 5.
- CO₂** Carbon dioxide.
- COD** Cloud Optical Depth.
- CTM** Chemistry Transport Model.
- CWP** Cloud liquid water Path.
- DMS** Dimethylsulfide.
- D_p** Diameter particle.
- DRF** Direct Radiative Forcing.
- DWD** German Weather Service.
- EARLINET** European Aerosol Research Lidar Network.
- EC** Elemental Carbon.
- ECMWF** European Centre for Medium-Range Weather Forecasts.
- EMEP** European Monitoring and Evaluation Programme.
- EPA** Environmental Protection Agency.
- ERF** Effective Radiative Forcing.
- ERFaci** Aerosol-Cloud Interactions Effective Radiative Forcing.
- ERFari** Aerosol-Radiation Interactions Effective Radiative Forcing.
- ESA** European Space Agency.
- EU** Europe.
- EuMetChem** European framework for online integrated air quality and meteorology modelling.
- GATOR-GCMOM** Gas Aerosol Transport Radiation, General Circulation Mesoscale, Ocean Model.
- GCMs** Global Climate Models.
- GHGs** Greenhouse gases.
- GOCART** Global Ozone Chemistry Aerosol Radiation and Transport model.
- HNO₃** Nitric acid.
- IN** Ice Nuclei.
- IPCC** Intergovernmental Panel on Climate Change.
- LM-MUSCAT** Local Model Multiscale Chemistry Aerosol Transport.

LW LongWave.

MADE Modal Aerosol Dynamics Model for Europe.

MADRID Model of Aerosol Dynamics, Reaction, Ionization, and Dissolution.

MAE Mean Absolute Error.

MFB Mean Fractional Bias.

MIRAGE Model for Integrated Research on Atmospheric Global Exchanges.

MODIS Moderate Resolution Imaging Spectroradiometer.

MOSAIC Model for Simulating Aerosol Interactions and Chemistry.

NA North America.

NB Normalized Bias.

NCAR National Center for Atmospheric Research.

NH₃ Ammonia.

NH₄⁺ Ammonium.

NMSE Normalized Mean Square Error.

NO₃⁻ Nitrate.

NO_x Nitrogen oxides.

NO_y Total reactive nitrogen.

O₃ Ozone.

OA Organic Aerosol.

OC Organic Carbon.

OM Organic Matter.

PBAP Primary Biological Aerosol Particles.

PBL Planetary Boundary Layer.

PBLH Planetary Boundary Layer Height.

PCC Pearson Correlation Coefficient.

PM Particulate Matter.

PM₁₀ Particulate Matter with an aerodynamic diameter less than or equal to 10 μm .

PM_{2.5} Particulate Matter with an aerodynamic diameter less than or equal to 2.5 μm .

POA Primary Organic Aerosol.

ppbv Parts per billion in volume.

ppm Parts per million.

QCLOUD Cloud Water Mixing Ratio.

QNDROP Droplet Number Mixing Ratio.

RACM Regional Atmospheric Chemistry Mechanism.

RADM2 Regional Acid Deposition Model version 2.

RAINC Accumulated Convective Precipitation.

RAINNC Accumulated Total Grid scale Precipitation.

RCP Representative Concentration Pathways.

RE Radiative Effect.

RF Radiative Forcing.

RH Relative Humidity.

RMSE Root Mean Square Error.

RRTMG Rapid Radiative Transfer Method for Global.

Sfc Surface.

SILAM System for Integrated modeLing of atmospheric coMposition.

SLP Sea Level Pressure.

SO₂ Sulphur dioxide.

SO₄⁻² Sulphate.

SO_x Sulphur oxides.

SOA Secondary Organic Aerosol.

SORGAM Secondary Organic Aerosol Model.

SSA Single Scattering Albedo.

SW ShortWave.

SWDNB ShortWave Downwelling flux at Bottom.

SWUPB Shortwave Upwelling flux at the Bottom.

T2 Temperature at 2 meters.

TNO Netherlands Organization for Applied Scientific Research.

TOA Top Of the Atmosphere.

US United States.

VOCs Volatile organic compounds.

WRF-Chem Weather Research and Forecasting Chemistry model.

WS10 Wind Speed at 10 meters.

Contents

Acknowledgements	vii
Resumen	xi
Abstract	xv
Publications	xix
Acronyms	xxv
1 Introduction	1
1.1 State of the art of atmospheric aerosol	1
1.1.1 Aerosol properties	3
1.1.1.1 Mass concentration and size distribution	4
1.1.1.2 Optical properties	6
1.1.2 Aerosol-radiation-cloud Interactions	9
1.1.2.1 Effective radiative forcing by the aerosol-radiation interactions	9
1.1.2.2 Effective radiative forcing by the aerosol-cloud interactions . .	12
1.1.2.3 Types of aerosols and their radiative effects	12
1.1.2.4 Aerosol and climate change	17
1.1.2.5 Forcing, Rapid Adjustments and Feedbacks	19
1.1.3 Aerosol processes	21
1.1.3.1 Radiation schemes	22
1.1.3.2 Nucleation, condensation and coagulation	22
1.1.3.3 Dry deposition	23
1.1.3.4 Wet deposition	24
1.1.4 Approaches to study atmospheric aerosols	24
1.1.4.1 Extractive techniques	25
1.1.4.2 In situ or ground-based measurements	25
1.1.4.3 Remote sensing techniques	25
1.1.4.4 Aerosol modeling	28
1.1.4.5 Online-coupled meteorology and chemistry models	32
1.1.4.6 Short description of WRF-Chem model	36
1.1.4.7 Aerosol feedbacks modeling studies	37
1.2 Objectives	44
1.3 Scope and structure	46
2 Sensitivity analysis of the microphysics scheme in WRF-Chem contributions to AQMEII Phase 2	49
2.1 Introduction	50
2.2 Methodology	51
2.2.1 Emissions	52

2.2.2	Model configuration	53
2.2.3	Microphysics schemes	53
2.3	Results and discussion	55
2.3.1	Sensitivity study	55
2.3.2	Numerical model comparison and evaluation	61
2.4	Summary and conclusions	63
3	Biomass burning aerosol impact on surface winds during the 2010 Russian heatwave	65
3.1	Introduction	65
3.2	Simulations and methods	67
3.2.1	Model configuration	67
3.2.2	Experimental design	68
3.3	Results	69
3.3.1	Base case meteorological situation	69
3.3.2	Effects on wind speed	72
3.3.3	Causes of wind variation	72
3.3.3.1	Wind correlation	74
3.4	Conclusions	75
4	Regional effects of atmospheric aerosols on temperature: an evaluation of an ensemble of on-line coupled models	77
4.1	Introduction	78
4.2	Methodology	79
4.2.1	Participating models	80
4.2.2	Emissions and boundary conditions	81
4.2.3	Observational database	82
4.2.4	Validation methodology	82
4.3	Results	84
4.3.1	Bias	84
4.3.2	Temporal correlation	89
4.3.3	Temporal variability	93
4.3.4	Spatial variability	98
4.4	Summary and conclusions	100
5	How good are aerosol-cloud interactions represented in online-coupled regional models?	103
5.1	Introduction	104
5.2	Methodology	107
5.2.1	Model simulations	107
5.2.2	Observational data	110
5.2.3	Evaluation methodology	110
5.3	Results	112
5.3.1	Cloud fraction, CFR	112
5.3.2	Cloud optical depth, COD	118
5.3.3	Cloud ice path, CIP	121
5.3.4	Cloud water path, CWP	124
5.3.5	Spatial correlation and variability	127
5.4	Summary and conclusions	129
6	Conclusions and future perspectives	133
6.1	General conclusions	133

6.1.1	Sensitivity analysis of the microphysics scheme	134
6.1.2	Biomass burning aerosol impact on surface winds	135
6.1.3	Atmospheric aerosol effects on temperature	136
6.1.4	Aerosol-cloud interactions representation in online-coupled models . . .	137
6.2	Future works and development	138
Bibliography		141

List of Figures

1.1	Comparison of an unpolluted and polluted area of Beijing (PM ₁₀)	2
1.2	Mass distribution of atmospheric aerosols	5
1.3	Simplified diagram of the scatter and absorbing light	6
1.4	CIMEL Sun Photometer	7
1.5	Average seasonal AOD by MODIS	8
1.6	Schematic of the new terminology used in the AR5	10
1.7	Schematic of aerosol-radiation interactions	11
1.8	Diagram of the semi-direct effect	11
1.9	Schematic that represents aerosol-cloud interactions	13
1.10	Image of sulfate aerosols (the spherical structures)	14
1.11	A mixed organic/sulfate below-cloud aerosol	15
1.12	Transmission electron microscope image of BC	16
1.13	Mineral dust particle	17
1.14	Sea salt particle that consists of a sodium chloride crystal, mixed-cation sulfate, and filamentous organic material	17
1.15	Principal component of the RF of climate change	19
1.16	Multi-model CMIP5 average changes in the annual mean radiation anomaly at the TOA over 2081-2100.	20
1.17	CMIP5 multi-model changes in annual mean total cloud fraction (in %) relative to 1986-2005 for 2081-2100.	20
1.18	Overview of the forcing and feedback pathways involving GHGs, aerosols and clouds	21
1.19	Aerosol particles interaction	21
1.20	Schematic representation of the nucleation process and subsequent growth process	23
1.21	Schemematic representation of the wet deposition processes	24
1.22	Schematic diagram of a High Volume Sample	25
1.23	Nephelometer schematic	26
1.24	AERONET stations	28
1.25	Particle size distribution approach	29
1.26	Interactions of the integrated system of meteorology and ACTMs.	34
1.27	Flowchart of the WRF-Chem system.	38
2.1	(Top panel): (First row) Winter 2010 (left) and summer 2010 (right) mean cloud water mixing ratio (Q_CLOUD) in MORRAT simulations (g kg ⁻¹). (Second row) Winter 2010 (left) and summer 2010 (right) mean differences between MOR- RAT and LINES (g kg ⁻¹). (Bottom panel) Id. for droplet number mixing ratio (Q_DROP) (kg ⁻¹).	56

2.2	(Top panel): (First row) Winter 2010 (left) and summer 2010 (right) mean downwelling shortwave flux at bottom (SWDNB) in MORRAT simulations (W m^{-2}). (Second row) Winter 2010 (left) and summer 2010 (right) mean differences between MORRAT and LINES (W m^{-2}). (Bottom panel) Id. for upwelling shortwave flux at the top of the atmosphere (SWTU) (W m^{-2}).	58
2.3	(First row) Winter 2010 (left) and summer 2010 (right) T2 in MORRAT simulations (K). (Second row) Winter 2010 (left) and summer 2010 (right) mean differences between MORRAT and LINES (K).	59
2.4	(Top panel): (First row) Winter 2010 (left) and summer 2010 (right) mean convective precipitation (RAIN _C) in MORRAT simulations (mm). (Second row) Winter 2010 (left) and summer 2010 (right) mean differences between MORRAT and LINES (mm). (Bottom panel) Id. for grid scale precipitation (RAIN _{NC}) (mm).	60
3.1	Total PM ₁₀ fire emissions during the fire episode (25 July-15 August 2010). The region affected by the wildfires is highlighted with a circle.	70
3.2	Mean values during Russian forest fires. First row represents the Base case; second row DRF-Base differences, third row RF-Base differences.	71
3.3	Aerosol effects on WS10. First row represents the Base case; second row DRF-Base differences and third row RF-Base differences.	73
3.4	Spatial correlation over Russian area of WS10 differences and differences in several meteorological variables: SWDNB, T2, PBLH, SLP, AOD and RH. Correlations are computed for the spatial differences between experiments RF (triangles) and DRF (circles) and Base case, i.e., Figure 3.3 versus Figure 3.2.	74
4.1	(Top row) Maximum temperature (TMAX) for the fires (left) and dust (right) episodes, as derived from E-OBS database (in K). The panel below represents the bias for the fires (left) and dust (right) episodes of each simulation with respect to the E-OBS database. NRF: no radiative feedbacks; ARI: aerosol-radiation interactions; ARI+ACI: as ARI including aerosol-cloud interactions.	85
4.2	(Top row) Mean temperature (TEMP) for the fires (left) and dust (right) episodes, as derived from E-OBS database (in K). The panel below represents the bias for the fires (left) and dust (right) episodes of each simulation with respect to the E-OBS database. NRF: no radiative feedbacks; ARI: aerosol-radiation interactions; ARI+ACI: as ARI including aerosol-cloud interactions.	87
4.3	(Top row) Minimum temperature (TMIN) for the fires (left) and dust (right) episodes, as derived from E-OBS database (in K). The panel below represents the bias for the fires (left) and dust (right) episodes of each simulation with respect to the E-OBS database. NRF: no radiative feedbacks; ARI: aerosol-radiation interactions; ARI+ACI: as ARI including aerosol-cloud interactions.	88
4.4	(Top row) Time determination coefficient (ρ^2) (model vs. E-OBS) of the maximum temperature (TMAX) for the fires (left panel) and dust (right panel) episodes. The first column in each panel below represents the value of ρ^2 of the no radiative feedback case with respect to the E-OBS database. The center and right columns indicate the increase (red values) or decrease (blue value) of each simulation with respect to the case not including feedbacks. NRF: no radiative feedbacks; ARI: aerosol-radiation interactions; ARI+ACI: as ARI including aerosol-cloud interactions.	90

4.5	(Top row) Time determination coefficient (ρ^2) (model vs. E-OBS) of the mean temperature (TEMP) for the fires (left panel) and dust (right panel) episodes. The first column in each panel below represents the value of ρ^2 of the no radiative feedback case with respect to the E-OBS database. The center and right columns indicate the increase (red values) or decrease (blue value) of each simulation with respect to the case not including feedbacks. NRF: no radiative feedbacks; ARI: aerosol-radiation interactions; ARI+ACI: as ARI including aerosol-cloud interactions.	91
4.6	(Top row) Time determination coefficient (ρ^2) (model vs. E-OBS) of the minimum temperature (TMIN) for the fires (left panel) and dust (right panel) episodes. The first column in each panel below represents the value of ρ^2 of the no radiative feedback case with respect to the E-OBS database. The center and right columns indicate the increase (red values) or decrease (blue value) of each simulation with respect to the case not including feedbacks. NRF: no radiative feedbacks; ARI: aerosol-radiation interactions; ARI+ACI: as ARI including aerosol-cloud interactions.	92
4.7	(Top row) Standard deviation (STD) of the maximum temperature (TMAX) for the fires (left) and dust (right) episodes, as derived from E-OBS database (in K). The panel below represents the bias for the standard deviation of the fires (left) and dust (right) episodes of each simulation with respect to the E-OBS database. NRF: no radiative feedbacks; ARI: aerosol-radiation interactions; ARI+ACI: as ARI including aerosol-cloud interactions.	94
4.8	(Top row) Standard deviation (STD) of the mean temperature (TEMP) for the fires (left) and dust (right) episodes, as derived from E-OBS database (in K). The panel below represents the bias for the standard deviation of the fires (left) and dust (right) episodes of each simulation with respect to the E-OBS database. NRF: no radiative feedbacks; ARI: aerosol-radiation interactions; ARI+ACI: as ARI including aerosol-cloud interactions.	96
4.9	(Top row) Standard deviation (STD) of the minimum temperature (TMIN) for the fires (left) and dust (right) episodes, as derived from E-OBS database (in K). The panel below represents the bias for the standard deviation of the fires (left) and dust (right) episodes of each simulation with respect to the E-OBS database. NRF: no radiative feedbacks; ARI: aerosol-radiation interactions; ARI+ACI: as ARI including aerosol-cloud interactions.	97
4.10	Taylor diagrams for (left) maximum temperature, (center) mean temperature, and (right) minimum temperature for the simulations included in the analysis. The top row represents the Taylor diagrams for the fires episode, while the bottom row stands for the dust episode. The cases included are: no radiative feedbacks (filled circle), ARI (asterisk) and ARI+ACI (empty squares). Each configuration is shown in a different color: CS1 (green), CS2 (dark blue), DE3 (red), ES1 (yellow), ES3 (pink) and ENS (black).	99
5.1	MEAN BIAS ERROR (bias) CFR. First row represents the mean satellite values of 2010, JFM, AMJ, JAS, OND. Following rows represent the bias of CFR for the same time periods.	114
5.2	MEAN ABSOLUTE ERROR (MAE) CFR. First row represents the mean satellite values of 2010, JFM, AMJ, JAS, OND. Following rows represent the MAE of CFR for the same time periods.	115
5.3	Temporal correlation (r) for the whole year 2010. First row represents the mean satellite values of 2010 where each column represents a cloud variable. Following rows show the r of each model and cloud variable.	116

5.4	MEAN BIAS ERROR (bias) COD. First row represents the mean satellite values of 2010, JFM, AMJ, JAS, OND. Following rows represent the bias of COD for the same time periods.	119
5.5	MEAN ABSOLUTE ERROR (MAE) COD. First row represents the mean satellite values of 2010, JFM, AMJ, JAS, OND. Following rows represent the MAE of COD for the same time periods.	120
5.6	MEAN BIAS ERROR (bias) CIP. First row represents the mean satellite values of 2010, JFM, AMJ, JAS, OND. Following rows represent the bias of CIP for the same time periods.	122
5.7	MEAN ABSOLUTE ERROR (MAE) CIP. First row represents the mean satellite values of 2010, JFM, AMJ, JAS, OND. Following rows represent the MAE of CIP for the same time periods.	123
5.8	MEAN BIAS ERROR (BIAS) CWP. First row represents the mean satellite values of 2010, JFM, AMJ, JAS, OND. Following rows represent the bias of CWP for the same time periods.	125
5.9	MEAN ABSOLUTE ERROR (MAE) CWP. First row represents the mean satellite values of 2010, JFM, AMJ, JAS, OND. Following rows represent the MAE of CWP for the same time periods.	126

List of Tables

1.1	Radiation schemes.	22
1.2	Passive remote sensing techniques and relevant satellite instruments and missions for observing atmospheric aerosols (Boucher, 2015).	27
1.3	Features of aerosol approaches	30
1.4	Main aerosol modules in CTMs.	31
1.5	Photolysis schemes.	32
1.6	Gas-phase schemes.	33
1.7	Online-coupled models.	35
1.8	WRF-Chem features	37
2.1	Model configuration options.	53
2.2	Statistical evaluation of MORRAT and LINES simulations against variables with available observations within the ENSEMBLES system	62
2.3	Comparison of the two simulations taking MORRAT as reference for those variables not available within ENSEMBLES	63
3.1	WRF-Chem parameterizations included in this study.	68
4.1	Modeling systems participating and their contributions to the case studies	81
5.1	Some of the AQMEII2 models features of the simulations studied.	109
5.2	Source of the data used in the simulations inputs for the initial conditions (IC), boundary (BC) and aerosols emissions	110
5.3	Mean Satellite, models and Ensemble values for CFR, COD, CIP and CWP.	117
5.4	Spatial correlation and standard deviation ratio values for CFR, COD, CIP and CWP over the periods: 2010, JFM, AMJ, JAS, OND. r : correlation coefficient; σ_P/σ_O : ratio between the standard deviation of the models (σ_P) and the observations (σ_O).	128

Chapter 1

Introduction

This chapter reviews the state of the art of atmospheric aerosols. It is focused on the study of the optical properties and their effect on climate. Hence, it will not be focused on the aerosol effects on air quality. This Thesis is structured in such a way that each chapter covers one work related to the aerosol-radiation-cloud interactions. In this sense, there is not a Chapter devoted to the methodology itself since it is structured as a compilation of different studies, in which a more specific review and the employed methodology are described.

1.1 State of the art of atmospheric aerosol

Human health and the environment are affected by poor air quality. Its impacts are clear: it damages health (Pope et al., 2009), adversely affects ecosystems (Lovett et al., 2009) and leads to the corrosion and soiling of materials (EEA, 2010). By way of example, Figure 1.1 shows a comparison of an unpolluted and polluted situation in the same area of Beijing related to particulate matter with an aerodynamic diameter less than or equal to $10\ \mu\text{m}$ (PM_{10}) particles. Besides health, air quality also affects people's well-being (Welsch, 2007; Akay et al., 2013). Within air pollution, aerosol particles also play a key role in meteorology and climate. Exposure to fine particulates has been associated with increased morbidity and mortality (Pope et al., 2009). Complex analyses of North American epidemiological data by the U.S. Environmental Protection Agency (EPA) indicate wide variability in morbidity and mortality rates that are associated with exposure to fine particles (Kennedy, 2007).

An aerosol is a suspension of finely divided (liquid or solid) matter dispersed in a gaseous medium such as air (Seinfeld and Pandis, 2006). They are often mixtures of different chemical components and their typical feature is that undergo constant physical and chemical transformation cycles during their lifetime, typically in the order of 1 week in the lower troposphere.



Figure 1.1: Comparison of an unpolluted and polluted area of Beijing (PM_{10}), from http://news.bbc.co.uk/2/hi/in_pictures/7506925.stm

Aerosol particles originate from both natural and anthropogenic sources. Natural aerosol sources include wind-blown soil from arid regions, natural weathering, volcanic emissions, sea spray, biomass burning from wildfires and biogenic aerosol formation. Anthropogenic aerosol sources are divided into four categories: fuel combustion, industrial processes, non industrial fugitive sources and transport.

Atmospheric aerosols can be formed either as a result of the wind's action on the Earth's surface (land or ocean) or in situ by nucleation from the gaseous phase (AIAA, 1999). They are subject to changes in size and composition by the processes of condensation, evaporation and coagulation. Water-soluble aerosols may also change size in response to changes in atmospheric humidity (Saarikoski, 2008). They are also subject to modification by cloud processes, where aerosols are integrated into cloud droplets and may later be regenerated as a result of evaporation. Cloud processes are also responsible for removing a considerable part of the aerosols from the atmosphere within rain or snow. Aerosol concentrations and compositions depend on locations in relation to source regions, production and removal rates, transport and altitude. The most significant sources of atmospheric aerosols lie within the planetary boundary layer (PBL). Sources may vary in time, e.g., seasonal variation (formation of desert dust plumes by spring-time surface wind erosion or in the annual cycle of biomass burning and smoke production in tropical countries). Examples of sporadic aerosol production are those formed as a result of volcanic activity or forest fires (AIAA, 1999).

The study of atmospheric aerosols is important for several reasons (Hsu et al., 2011):

1. Their direct and indirect effects on climate are complex and have not been well assessed.
2. Heavy aerosol loadings in urban areas lead to poor air quality, with adverse effects on

human health.

3. Transported aerosols provide nutrients such as iron, which come from mineral dust and volcanic ash, important for fertilization.
4. Knowledge of aerosol loading is important for studying potential yields from solar energy sources.

The importance of atmospheric aerosols to issues of social concern has motivated much research, which intends to describe their loading, distribution and properties and to develop understanding of controlling processes to address both issues that produce air pollution and the influence of aerosol on climate. Atmospheric aerosols exert a substantial influence on Earth's climate, and currently interest in studying atmospheric aerosols has increased given the need to quantify this influence. They are a complex disperse system of solid and liquid particles of different sizes, shapes, chemical compositions and reactivities (Hauck et al., 2004). Atmospheric aerosols affects the Earth's radiation budget, which is also known as the aerosol radiative effect (RE) or as radiative forcing (RF). The former refers to both natural and anthropogenic aerosols while the latter refers explicitly to anthropogenic aerosols. Both cases, imply a secular change in the flux of an atmospheric radiation component, which affects the Earth's energy balance, expressed in units of watts per square meter: W m^{-2} (Boucher, 2015). It is a useful metrics to investigate the potential impacts of aerosol emission reductions on climate (Forster et al., 2007). A warming influence is denoted by positive forcing, and a cooling influence, by negative forcing (Buseck and Schwartz, 2003). As a result of their short atmospheric residence times (according to Ramanathan et al. (2001a), 1 or 2 weeks), tropospheric aerosol particles are highly variable in space and time.

1.1.1 Aerosol properties

Aerosol properties encompass mass concentration, particle size and size-dependent composition, optical properties, solubility, and the ability to serve as nuclei of cloud particles (Ghan and Schwartz, 2007). Physical, chemical and optical properties vary considerably depending on the aerosol because of not only the great non homogeneity of aerosols in the atmosphere, but also atmospheric conditions. Size distribution together with their composition, sources and sinks, is a key element to understand and control aerosol effects on health, visibility and climate (Stanier et al., 2004).

The important radiative properties of atmospheric aerosols (both direct and indirect) are determined by aerosol composition and size distribution. Nevertheless, in relation to direct

radiative effect calculations, and also assessments of uncertainties, these properties can be subsumed into a small set of parameters. Knowledge of a set of four quantities of the wavelength function is necessary to translate aerosol burdens into first aerosol optical depths, and then radiative perturbation: mass light-scattering efficiency (sp), the functional dependence of light-scattering on relative humidity (RH), the single-scattering albedo (SSA) and the asymmetry parameter (ASY, g) (Charlson et al., 1992).

1.1.1.1 Mass concentration and size distribution

Mass concentration is the most commonly measured aerosol property, defined as the mass of particulate matter (PM) in a unit volume of gas (for atmospheric aerosol usually $\mu\text{g m}^{-3}$). Aerosol concentration can also be expressed as a number concentration, which is the number of particles per unit volume of aerosol (usually number/cm³). In contrast to gaseous contaminants, volume ratio or mass ratio in parts per million (ppm) is not used for aerosols because two phases are involved and aerosol concentrations are numerically very low when expressed in this way. Mass concentration is the equivalent to the density of the ensemble of aerosol particles in air (Hinds, 1999).

Particles in an aerosol are characterized by size distribution, which is one of their core physical parameters. It determines various properties, like mass and number concentration or optical properties.

The size of a particle is the main quantity for characterizing the behaviour of particles as most properties of aerosols depend on particle size. The diameter of atmospheric aerosol particles ranges from a few nanometers to several hundreds of micrometers. As the smallest aerosol particles approach the size of gas molecules, they have many similar properties to them. Large aerosol particles are visible grains whose properties can be depicted by Newtonian Physics. Particle aerodynamic diameter is defined as the diameter of the spherical particle with a unit density (1 g cm^{-3}), which has the same settling velocity as the actual particle does.

Figure 1.2 shows the mass distribution of atmospheric aerosols, which can be represented in four different modes: nucleation, Aitken, accumulation and coarse particle mode:

- Ultrafine particles, which include the nucleation mode (Diameter particle $[D_p] < 20\text{-}25$ nm) and Aitken mode ($20 \text{ nm} < D_p < 0.1 \mu\text{m}$) particles, have the majority of particles by number (usually $> 90\%$), but account for a few percent of the total mass of atmospheric particles because of small size. Ultrafine particles consist of combustion particles formed by the condensation of the hot vapors or fresh particles formed in the atmosphere by nucleation. They are usually found near combustion sources, close to highways or places

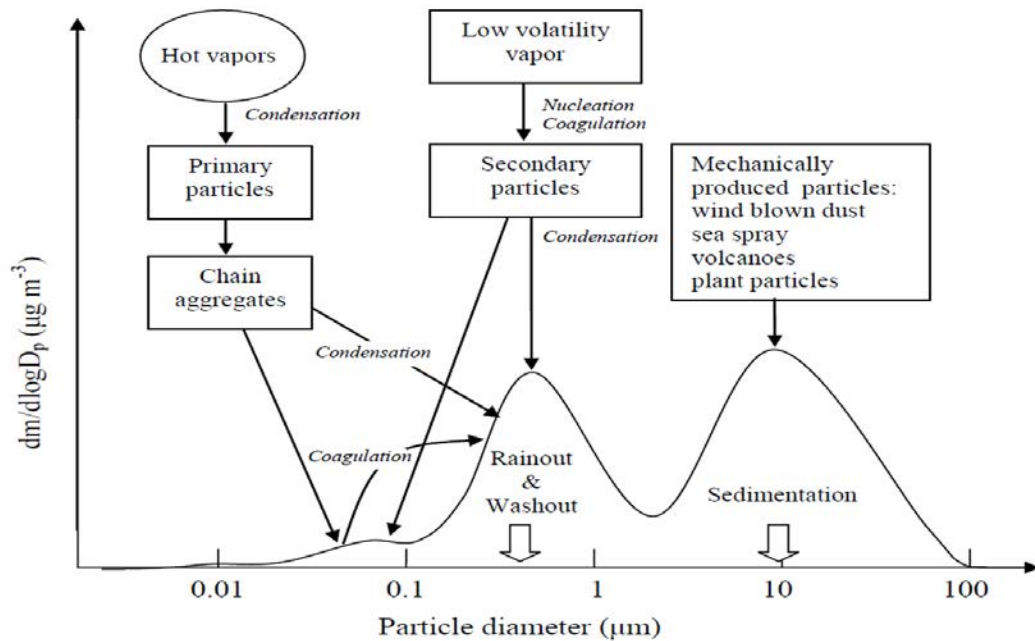


Figure 1.2: Mass distribution of atmospheric aerosols (Seinfeld and Pandis, 2006).

where the nucleation of biogenic volatile organic compounds (VOCs) arise (Kulmala et al., 2001). Owing to the large number of particles in the ultrafine mode, they can coagulate rapidly with each other, as well as with particles, in the accumulation mode. Nucleation mode particles have short lifetimes (usually a few hours), while Aitken mode particles can be found far away from their sources.

- Accumulation mode (size range from 0.1 to 1 μm) usually has a substantial fraction of the total particulate mass. The source of these particles is the coagulation of ultrafine particles as well as particles that have grown to accumulation size through condensation of vapors toward existing particles and by cloud processing. Accumulation mode particles can be removed from the atmosphere by rainout or washout, but are less efficient because they remain for many days and consequently travel long distances in the atmosphere. Accumulation mode particles cause most of the visibility effects of atmospheric particles since the accumulation size range includes the wavelength range of visible light (Hinds, 1999).
- Coarse mode particles ($> 1 \mu\text{m}$) are formed by mechanical processes. Within this size range man-made and natural dust particles are usually included. Coarse mode particles are made of large sea salt particles and particles from volcanic eruptions. These particles are removed from the lower atmosphere by sedimentation or inertial impaction over a reasonably short time scale (typically from hours to 1 day) due to their large size. Although coarse particles have a limited lifetime in the atmosphere, they can cause exposure to

people close to the particle source.

The accumulation and coarse mode are the aerosol sizes that primarily impact the radiative energy budgets of the atmosphere. On a global scale, the accumulation size mode is dominated by sulfate and carbonaceous aerosol, while coarse size is characterized by sea salt and dust (Kinne et al., 2006).

Size distribution measurements are needed to evaluate of regional and global chemical transport and climate models, which attempt to include size distributed aerosols as active constituents (WMO, 2003). Other number size distribution applications include:

- Adjustment of observed cloud condensation nuclei (CCN) through modeling.
- Explaining observed particle mass within a given size range or observed light-scattering coefficients.

1.1.1.2 Optical properties

Aerosol optical properties cause many atmospheric effects (coloured sunsets, halos around the sun or moon, and rainbows) as well as visibility degradation due to atmospheric pollution, and are required to evaluate their radiative impact. They depend on particle size distribution, mixing state, composition and refractive index, among others (Yu et al., 2012). If electromagnetic radiation goes through a medium made of molecules and particles, its intensity will always diminish. This is due to either scattering or absorption (Figure 1.3). During the scattering process, some incident radiation is re-radiated in all directions at different rates, its polarization state alters, but its wavelength (λ) remains constant. The sum of lost contributions due to *scattering* and *absorption* is called *extinction*, which is a process in which the aerosol particles illuminated by a beam of light scatter and absorb some light so that the intensity of the beam reduces. Usually aerosol particles scatter light and the absorbing aerosols absorb light (Hinds, 1999).

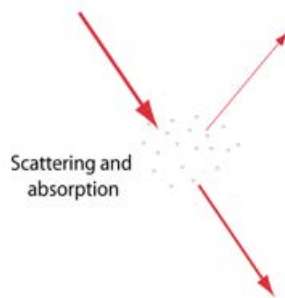


Figure 1.3: Simplified diagram of the scatter and absorbing light (Goosse et al., 2009).

The coefficient of light extinction (Equation 1.1) by PM σ_{ep} , is the sum of the scattering and absorption coefficients (σ_{sp} and σ_{ab} , respectively):

$$\sigma_{ep} = \sigma_{sp} + \sigma_{ab} \quad (1.1)$$

Radiative important properties of atmospheric aerosols are determined mainly by the aerosol composition and size distribution. Nevertheless for direct radiative forcing (DRF) calculation purposes, some quantities as a function of wavelength should be known, such as aerosol optical depth (AOD), SSA, ω_0 and the ASY, g (Charlson et al., 1992).

Aerosol optical depth

AOD is a quantitative measure of solar radiation extinction by aerosol scattering and absorption between the point of observation and the top of the atmosphere (TOA) and is the main variable for aerosol-climate interaction (Chung, 2012). It is a measure of the integrated columnar aerosol load and the single most important parameter for evaluating DRF. AOD can be determined by satellite, aircraft, and can be ground-based such as sunphotometers (Figure 1.4) or filter radiometers (WMO, 2003). Figure 1.5 shows the average seasonal AOD by Moderate Resolution Imaging Spectroradiometer (MODIS).

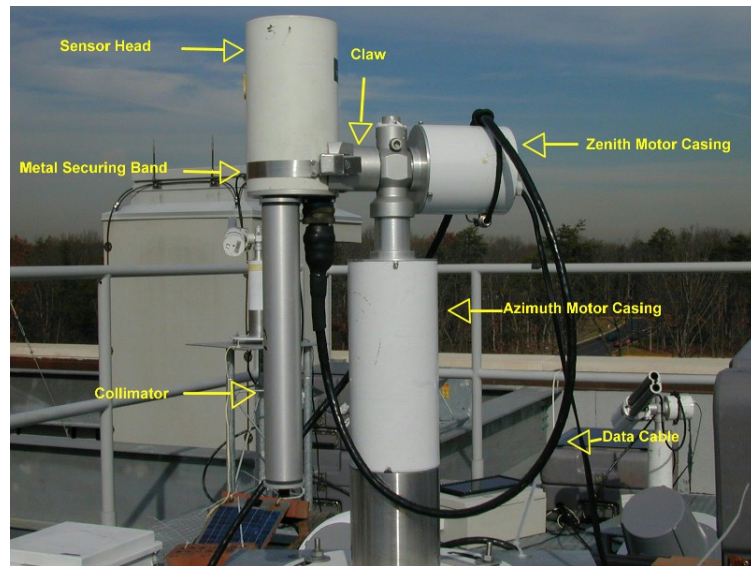


Figure 1.4: CIMEL Sun Photometer. From the Aerosol Robotic Network (AERONET).

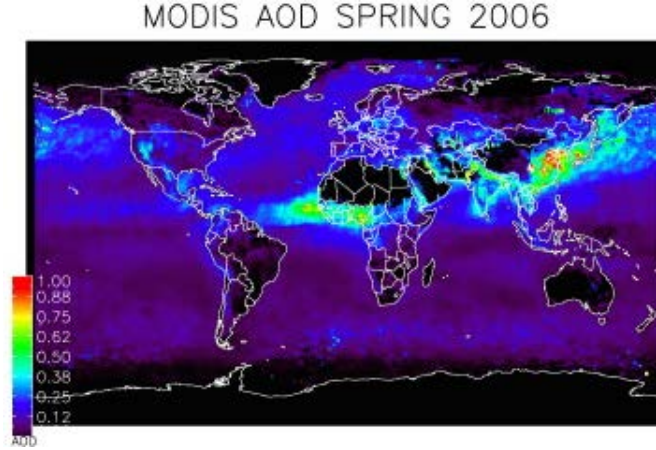


Figure 1.5: Average seasonal AOD by MODIS (De Meij et al., 2012).

As Equation 1.2 shows, AOD (τ) is a vertical integral of the aerosol extinction coefficient from the Earth surface (Sfc) to TOA.

$$\tau_{\lambda} = \int_{Sfc}^{TOA} k_{\lambda} \rho dz \quad (1.2)$$

Where k_{λ} is the mass extinction cross-section (in units of area per mass). So AOD is a function of wavelength and the standard value of AOD is usually 550 nm (Chung, 2012). There are many networks that measure this optical property such as AERONET (Holben et al., 2001) which is a major global network with central calibration facilities in the USA and France.

By increasing AOD, anthropogenic emissions of aerosols and their precursors contribute to solar radiation reduction on the surface. Therefore, worsening air quality leads to regional aerosol effects on radiation (Forster et al., 2007).

Single scattering albedo

SSA, ω , is defined as the ratio of scattering to extinction, Equation 1.3 (where extinction was the sum of scattering and absorption). It is the particulate extinction fraction resulting from scattering (Buseck and Schwartz, 2003). When photons are scattered, the wavelength remains unchanged and SSA is a wavelength function (Chung, 2012).

$$\omega = \sigma_{sp} / (\sigma_{sp} + \sigma_{ab}) \quad (1.3)$$

SSA is also a key variable in assessing the climatic effect of aerosols. Values range from about 0.7 for very absorbing particles to 1 for aerosols that only scatter light. According to Hansen et al. (1981), aerosols with a SSA lower than 0.85 generally warm the planet whereas those with more than 0.85 cool the planet.

Asymmetry parameter

ASY, g is the cosine-weighted average of the phase function (Equation 1.4), which is the probability of radiation being scattered in a given direction (Ogren et al., 2006). When it approaches +1 for scattering, it strongly peaks in the forward direction. When it comes close to -1 for scattering strongly, it peaks in the backward direction. Generally, $g=0$ indicates the scattering directions distributed uniformly between the forward and backward directions.

The ASY is defined as:

$$g = \frac{1}{2} \int_{-1}^1 P(\cos \Theta) \cos \Theta d \cos \Theta \quad (1.4)$$

where P is the phase function and Θ is the angle between the direction of incoming light and that of scattered light.

1.1.2 Aerosol-radiation-cloud Interactions

The Fifth Report of the Intergovernmental Panel on Climate Change (IPCC AR5)(Boucher et al., 2013; Myhre et al., 2013b) distinguishes between aerosol-radiation interactions (ARI), which encompass the traditional direct and semi-direct effect and also the aerosol-cloud interactions (ACI) that account for the indirect effects. A new term, effective RF (ERF), is defined in the AR5, which adds the RE from rapid adjustments, caused mainly by cloud changes (Figure 1.6). This new concept avoids confusion with the traditional RF definition and is generally a better predictor of the eventual surface temperature change induced by a forcing mechanism (Hansen et al., 2005). The traditional semi-direct effect is better seen as a rapid adjustment associated with ARI. The effective RF due to ARI (ERFari) is therefore the sum of direct and semi-direct effects. The ACI forcing component, the so called indirect aerosol effects, can be more easily compiled into an effective RF due to ACI (ERFaci). These indirect effects can be interpreted as rapid adjustments associated with the initial modification of the concentrations of CCN and ice nuclei (IN).

1.1.2.1 Effective radiative forcing by the aerosol-radiation interactions

Radiative effect due to aerosol-radiation interactions or direct effect (REari)

The RE due to ARI is defined by the IPCC AR5 (Boucher et al., 2013; Myhre et al., 2013b) as the change in the radiative flux caused by the combined scattering and absorption of radiation by anthropogenic and natural aerosols (Figure 1.7). ARI occur essentially under cloud

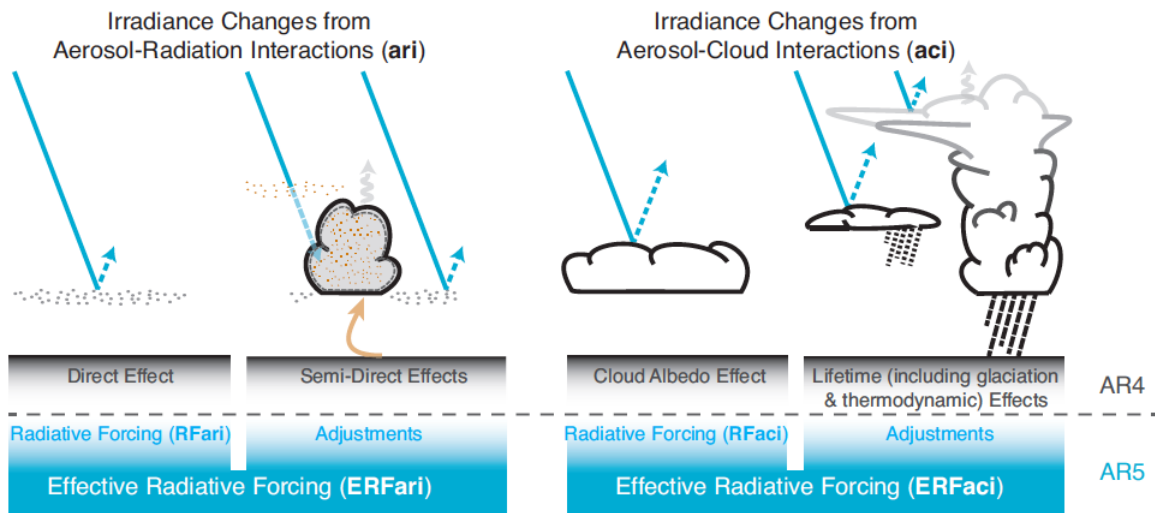


Figure 1.6: Schematic of the new terminology used in the AR5 ARI and ACI and its relations with the Fourth Assessment Report (AR4) terminology. Blue arrows depict solar radiation, grey arrows terrestrial radiation and the brown arrow symbolizes the importance of couplings between the surface and the cloud layer for rapid adjustments (Boucher et al., 2013).

free conditions since clouds themselves are good scatterers, so the modification of the TOA flux solar radiation by the atmospheric aerosols is more effective in clear sky conditions (Boucher, 2015). ARI does not only depend on the properties of aerosols, but also on the properties of the solar radiation that interacts with them (Boucher, 2015).

To estimate REari, aerosol and environmental properties, and the fraction of the aerosol of anthropogenic origin, needs to be known. Characterizing the natural aerosol only by observation methods is difficult since aerosols are present everywhere. For this reason, most of the aerosol RE requires using modeling approaches.

REari is influenced by: radiative properties of the surface, atmospheric trace gases and clouds. Under cloud-free conditions it is typically negative at the TOA, but can be weakened and become positive due to increasing aerosol absorption, a decreasing upscatter fraction or increasing albedo. Under cloudy conditions, REari is weaker except when the cloud layer is thin or when absorbing aerosols are located above or between clouds (Chand et al., 2009). The REari on the surface is negative and can be much stronger than the REari at the TOA over regions where aerosols are absorbing (Li et al., 2010).

Zanis (2009) studied the total DRF of aerosol as derived from models and observations, which was estimated to be $-0.5 \pm 0.4 \text{ W m}^{-2}$ in global scale. The Aerosol Comparisons between Observations and Models (AEROCOM) Phase 1 (Schulz et al., 2006) showed a global DRF that resulted from 16 models of -0.22 W m^{-2} and in its Phase 2 (Myhre et al., 2013a) of -0.35 W m^{-2} . This could be due to the addition of new species such as nitrate and secondary

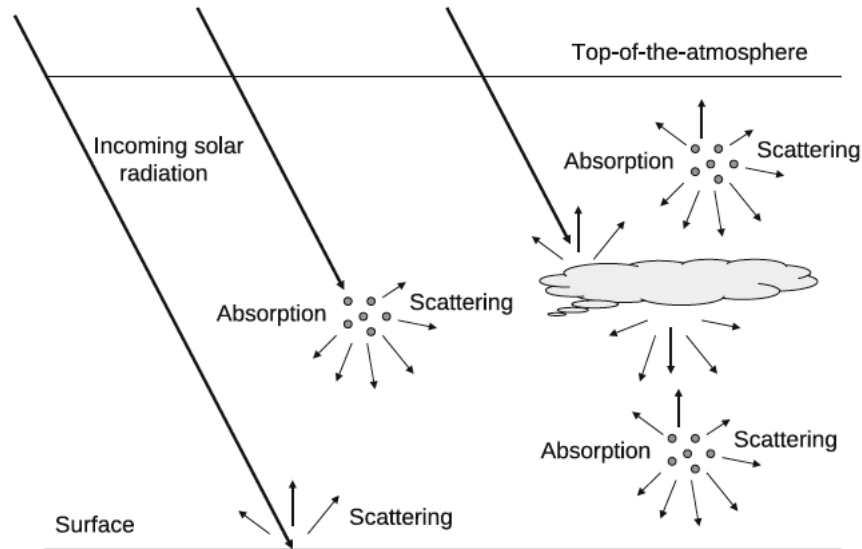


Figure 1.7: Schematic of the aerosol-radiation interactions (Boucher, 2015).

organic aerosol (SOA).

Rapid adjustments to aerosol-radiation interactions or semi-direct effect

Incoming solar radiation can also be absorbed by aerosols consisting of black carbon (BC) and mineral dust, heating the local atmosphere and possibly reducing the incidence of cloud formation (Figure 1.8) (Hansen et al., 1997). Solar radiation absorption can cool the surface below thus increasing the stability of lower atmosphere leading to inhibition of convection (Sanap et al., 2014). Ramanathan and Carmichael (2008) estimated that the light absorbed by BC particles may have a global warming effect comparable to that of carbon dioxide (CO_2). This phenomenon gives rise to rapid adjustments and contributes to ERF (Boucher et al., 2013)

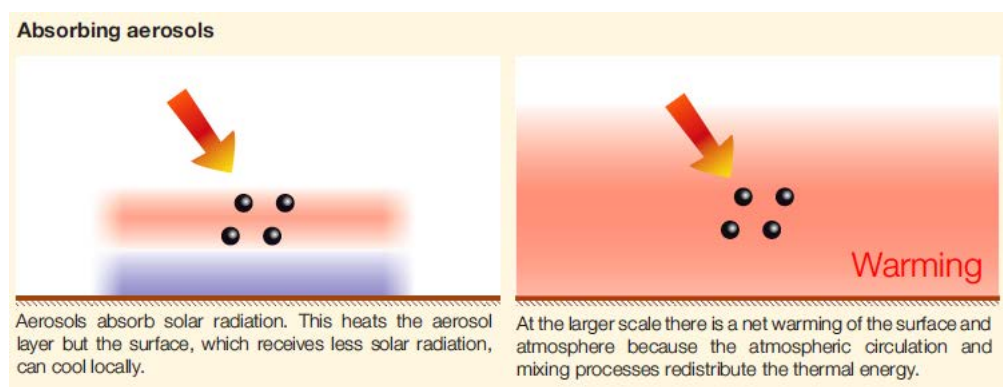


Figure 1.8: The left panels show the instantaneous radiative effects of aerosols, while the right panels show their overall impact after the climate system has responded to their radiative effects. (Stocker et al., 2013).

1.1.2.2 Effective radiative forcing by the aerosol-cloud interactions

Atmospheric aerosols influence cloud microphysical properties in a number of ways (Figure 1.9). Previously, these influences were largely known as aerosol indirect effects. As aerosols act as CCN and/or IN, they may affect cloud microphysics and, thus, influence overall cloud radiative properties through interactions referred to as the “first indirect effect” or “Twomey effect” (Twomey, 1974, 1977, 1991; Chapman et al., 2009; Yu and Zhang, 2011). This effect can be associated with radiative forcing (RF_{aci}) calculations, at least in principle if the preindustrial aerosol concentration is known. For a fixed cloud cover and liquid water content, an increase in cloud droplet concentration results in smaller cloud droplets but an increase in the total scattering cross section, and thus the cloud reflectivity increases (Boucher, 2015). Aerosols can act as IN by three ways: contacting with supercooled cloud droplets (contact freezing), by initiating freezing from within a cloud droplet by immersion or condensation freezing, or by acting as deposition nuclei. This is also named the “cloud albedo effect”. Clouds that form with many CCN have more numerous small droplets, and will thus be whiter and optically “thicker”, leading to a cooling effect on the planet (as less solar radiation is absorbed by the Earth’s surface).

Additionally, the aerosols that act as CCN may affect precipitation efficiency, cloud life-time, and cloud thickness, and may thus further influence weather and climate through the “second indirect effect” (Albrecht, 1989), also named the “cloud lifetime effect”. Since the droplets in clouds that form with many available CCN have smaller droplets, the number of droplets in the cloud that can fall out of the cloud as rain or drizzle is lower.

The RF due to the first indirect effect is estimated to be -0.7 W m^{-2} (ranging from -1.8 to 0.3 W m^{-2}) with a poor level of scientific understanding (Forster et al., 2007). The second indirect effect is estimated as being practically as large as the Twomey effect (Lohmann and Feichter, 2005; Zanis, 2009).

1.1.2.3 Types of aerosols and their radiative effects

Both natural and anthropogenic atmospheric aerosols originate in two ways: emissions of primary particulate matter and the formation of secondary particulate matter from gaseous precursors. The main constituents of atmospheric aerosols are inorganic species (sulfate [SO_4^{-2}], nitrate [NO_3^-], ammonium [NH_4^+], sea salt and dust), organic species (organic aerosol, OA), BC (formed from the incomplete combustion of fossil and biomass based fuels under certain conditions), mineral species (mostly desert dust) and primary biological aerosol particles (PBAP). Mineral dust, sea salt, BC and PBAP enter the atmosphere as primary particles, whereas non-

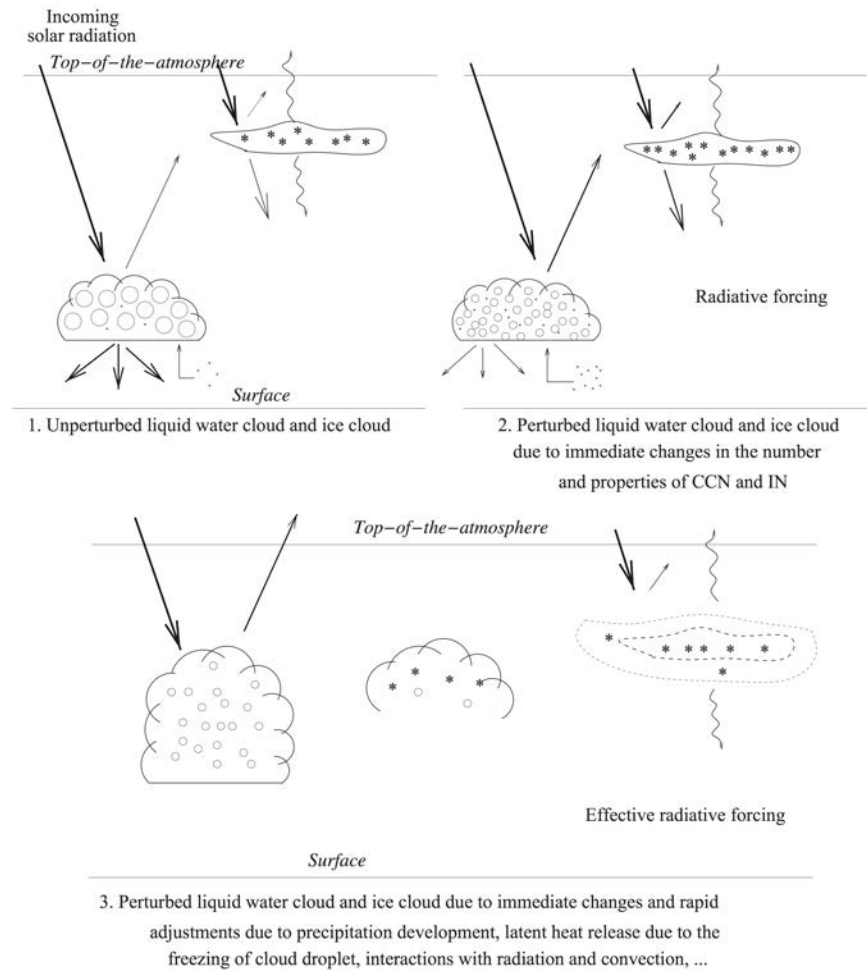


Figure 1.9: Schematic representing aerosol-cloud interactions by Boucher (2015).

sea salt SO_4^{-2} , NO_3^- and NH_4^+ predominantly derive from secondary aerosol formation processes. OA has both significant primary and secondary sources. In the present-day atmosphere, the majority of BC, SO_4^{-2} , NO_3^- and NH_4^+ come from anthropogenic sources, whereas sea salt, most mineral dust and PBAP are predominantly of natural origin. Primary organic aerosols (POA) and SOA are influenced by both natural and anthropogenic sources. The paragraphs that follow describe the different types of aerosols and their relation to the RF.

Secondary inorganic aerosols (sulfates, nitrates and ammonium)

Atmospheric SO_4^{-2} aerosol compositions range from sulphuric acid to ammonium sulfate and are present as liquid droplets or partly crystallized (Figure 1.10). They constitute a major aerosol type in the troposphere, and are probably the best known because of this. They either nucleate homogeneously or form on existing particles from gaseous precursors of both natural and anthropogenic origins, and the anthropogenic fraction dominates (Pósfai and Buseck, 2010). Dimethylsulfide (DMS) is a significant natural source of SO_4^{-2} ; this is an organic compound

whose production by phytoplankton and its release to the atmosphere depends on climatic factors. SO_4^{-2} aerosol tends to cool the Earth surface by scattering part of the incoming solar radiation (Denman et al., 2007). On a global scale, the main source of SO_4^{-2} aerosol is via sulfur dioxide (SO_2) emissions from fossil fuel burning (about 72%), with a minor contribution made by biomass burning (about 2%), while natural sources come from DMS emissions by marine phytoplankton (about 19%) and by SO_2 emissions from volcanoes (about 7%). According to the IPCC AR5 (Myhre et al., 2013b), the global mean RF due to SO_4^{-2} aerosol is -0.40 W m^{-2} .

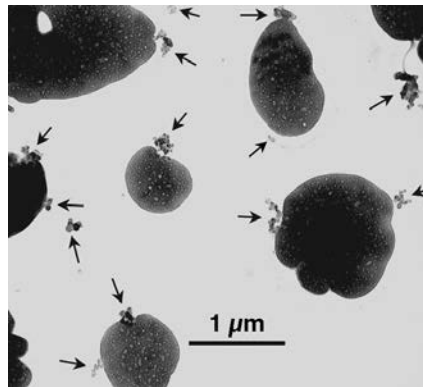


Figure 1.10: Image of sulfate aerosols (spherical structures) (Pósfai et al., 1999).

NO_3^- aerosol is formed chemically in the atmosphere from precursor species ammonia (NH_3) and nitric acid (HNO_3). NH_3 sources include agricultural sources, oceans, biomass burning, crops and soil. Typical sources of nitrogen oxides (NO_x), which are the main precursor of HNO_3 , include fossil fuel combustion, soils, biomass burning and lightning. The most important impact of NO_x emissions on the climate is through the formation of tropospheric ozone (O_3), which is the third largest single contributor to positive RF. NO_x emissions generate indirect negative RF by shortening the atmospheric lifetime of methane (CH_4) (Prather, 2002; Forster et al., 2007). NH_3 contributes to the formation of SO_4^{-2} and NO_3^- aerosols, which thereby contribute to aerosol cooling and the aerosol indirect effect. According to the AR5 (Myhre et al., 2013b) the global mean RF for NO_3^- is estimated to be -0.11 W m^{-2} .

Organic carbon

Organic carbon (OC) is a complex mixture of chemical compounds that contain the carbon-carbon bonds produced from fossil fuel and biofuel burning as well as natural biogenic emissions (Figure 1.11). They can be emitted as primary aerosol particles or formed as secondary aerosol particles from the condensation of organic gases, which are considered to be semi-volatile or have low volatility. As there are lots of different atmospheric organic compounds, modeling the

direct and indirect effects is a huge challenge. According to AR4 (Forster et al., 2007), for OC, different modeling studies have shown mean RF of $+0.24 \text{ W m}^{-2}$ from biomass burning and fossil fuel emissions.

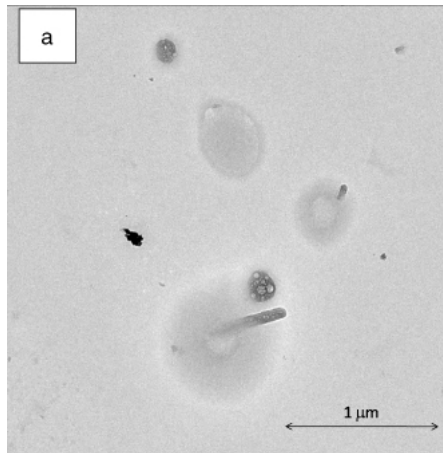


Figure 1.11: A mixed organic/sulfate below-cloud aerosol. From the DYCOMS-II project (Stevens et al., 2003).

Black carbon

The atmospheric science community commonly uses the terms BC for the strongly absorbing component of aerosols, and elemental carbon (EC) for the most refractory part of carbonaceous aerosol that oxidizes above a certain threshold in combustion experiments (Pósfai and Buseck, 2010; Petzold et al., 2013). It is a primary aerosol (Figure 1.12), that strongly absorbs solar radiation, emitted directly at the source produced by the combustion of fossil fuels, residential biofuel, and biomass, so therefore much atmospheric BC is of anthropogenic origin. Ramanathan et al. (2001b) studied the importance of absorption by aerosol in the atmospheric column. The observations showed a local surface forcing of -23 W m^{-2} , which was significantly stronger than the local RF at the TOA, -7 W m^{-2} . According to the AR5 (Myhre et al., 2013b) the mean RF was estimated as $+0.40 \text{ W m}^{-2}$.

Biomass burning aerosols

Biomass burning aerosols consist of two major chemical components: BC, which mainly absorbs solar radiation; OC, which mainly scatters solar radiation. Sources of biomass burning aerosols include burning forests and agriculture, burning agricultural waste and substances burned for fuel (wood, dung and peat). Not all biomass aerosol comes from anthropogenic activities, as naturally vegetation fires regularly occur. The anthropogenic biomass aerosol fraction is difficult to deduce. According to the AR4 (Forster et al., 2007), a contribution to RF of roughly -0.40 W m^{-2} from scattering components (mainly OC and inorganic compounds) and of $+0.20 \text{ W m}^{-2}$ from absorbing components (BC) has been reported, which led to an estimate

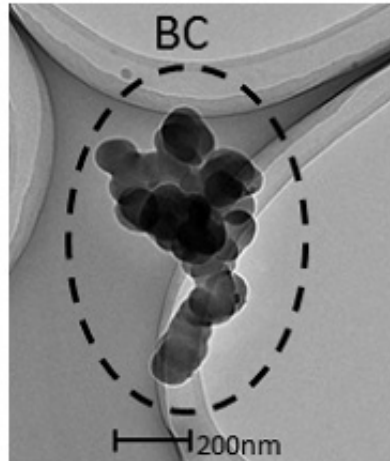


Figure 1.12: Transmission electron microscope image of BC collected at a stationary point over the Arctic Ocean (Taketani et al., 2016).

of the RF of -0.20 W m^{-2} with a factor of uncertainty of 3. The RF is grouped into a single estimation because biomass burning emissions are essentially uncontrolled.

Mineral dust

Mineral dust aerosols (Figure 1.13) are soil particles that the wind blows into the atmosphere. Most mineral dust in the troposphere originates from the dust belt, a chain of arid regions that includes the Sahara and Middle East and China deserts. They are the single largest component of the Earth's atmospheric aerosol arsenal, and include half the total aerosol mass. Dust impacts radiation to varying degrees, depending on the composition of the minerals that dust grains comprise. Prospero et al. (2002) have reported that mineral dust from anthropogenic sources originates mainly from agricultural practices such as harvesting, ploughing, overgrazing, changes in surface water (Caspian and Aral Sea, Owens Lake) and industrial practices (cement production, transport). According to the AR4 (Forster et al., 2007), RF due to anthropogenic mineral dust falls with a range of $+0.40$ to -0.60 W m^{-2} , the related mineral aerosols fall within the range of -0.56 to $+0.1 \text{ W m}^{-2}$ and with global mean RF of -0.10 W m^{-2} (AR5) (Myhre et al., 2013b).

Sea Salt

Sea salt aerosols (Figure 1.14) are generated by different physical processes, especially by bursting air bubbles that rise to the sea surface (Monahan and Mac Niocaill, 1986), which results in a strong dependence on wind speed. In mass terms, an abundance of sea salt particles is second only to mineral dust in the troposphere (Tomasi et al., 2016). This aerosol may be the dominant contributor to the light scattering and cloud nuclei in those regions of the marine

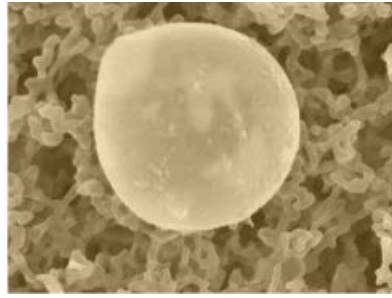


Figure 1.13: Mineral dust particle (Baltensperger, 2010).

atmosphere where wind speeds are high and/or no other aerosol sources exist (Forster et al., 2007). Sea salt particles are very efficient CCN and, therefore, characterisation of their surface production is of major importance for aerosol indirect effects.

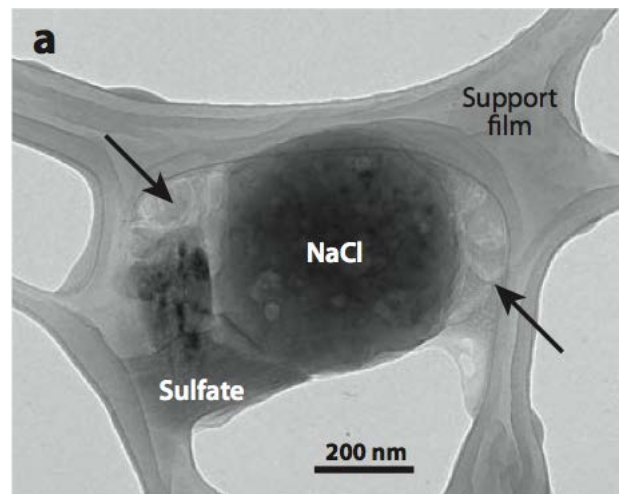


Figure 1.14: Sea salt particle that consists of a sodium chloride crystal, mixed-cation sulfate, and filamentous organic material (Pósfai and Buseck, 2010).

1.1.2.4 Aerosol and climate change

As discussed above, aerosols play an important role in the global climate balance, and could, therefore, be important in climate change. Natural sources like volcano eruptions, are recognized as significant climate forcing (by altering the Earth's radiation balance) as they cause global temperature change. Human activities alter atmospheric aerosols near the ground, by industrial emissions and also at the lower stratosphere (aircraft emissions) and thus possibly affect climate. The particles in the troposphere influence global climate. Since the response of climate systems to aerosols and their effect on the Earth's radiative budget is the most uncertain climate feedback (Randall et al., 2007), our current understanding of how aerosols affect weather and climate incurs considerable uncertainties that must be reduced in order to better estimate the impact of anthropogenic emissions on the atmosphere. Aerosol negative RF causes

changes in atmospheric thermal structure, and also in synoptic and regional circulation systems, rainfall removal and leads to a loss of efficient atmospheric pollutants removal (Ramanathan and Feng, 2009). Positive RF could lead to significant regional climate effects as BC can absorb radiation and can heat air, which partly offset aerosol scattering effects (Jacobson, 2001c).

The uncertainty in the RF of the Earth's radiation budget by anthropogenic aerosols, which occurs mainly in the lower troposphere, greatly exceeds that of all the other forcing mechanisms combined, as stated in IPCC AR5 (Stocker et al., 2013). Consequently, studying aerosol components is crucial to assess the impact of human activities on climate and air quality (Zanis, 2009). Aerosols of anthropogenic origin are composed mainly of SO_4^{-2} , carbonaceous particles (BC and EC), NO_3^- , NH_4^+ and mineral dust of industrial origin (Stanhill and Cohen, 2001). BC, SO_4^{-2} and organics play a major role in solar dimming at the Earth's surface (Stocker et al., 2013).

Aerosol as well as changes to cloud and radiation fields from aerosols, affect O_3 as it depends on the photo-oxidation of precursors emissions. Therefore, these short-lived species are significant for their climate and air quality impacts, being important in near-term mitigation efforts. The O_3 RF is about 0.4 W m^{-2} and for aerosols, forcing range from 0.3 (for BC) to -2.2 W m^{-2} (for reflecting aerosols; sulfates, organic matter [OM], nitrates and aerosol-cloud changes) based on emission changes from 1750 to the present day (Forster et al., 2007). Absorbing aerosols are thought to inhibit surface O_3 formation by reducing the photolysis rates in polluted areas; whereas reflecting aerosols are thought to increase O_3 formation (He and Carmichael, 1999). Thus, future forcing depend on emission scenarios and relative changes in the distribution of precursors and reflecting versus absorbing aerosols (BC)(Menon et al., 2008).

In accordance with other greenhouse gases, Ramanathan and Carmichael (2008) estimated that the light absorbed by BC particles may have a global warming effect that is comparable to that of CO_2 . Figure 1.15 shows the principal components of the RF of climate change. They are associated with human activities or natural processes. The thin black line attached to each coloured bar represents the range of uncertainty for the respective value. Contrary to CO_2 and greenhouse gases, tropospheric aerosols and O_3 may last in the atmosphere from days to weeks. Thus, these pollutants are usually most potent near their source of emission, where they can force local or regional perturbations to the climate (Myhre et al., 2013b).

Understanding and quantifying the influence of anthropogenic sources on atmospheric aerosol loading is of growing interest since public debate about climate change has begun to focus on potential mitigation measures and regulatory actions. In this sense, the AR5 includes a chapter about climate projections for the near term (the next few decades). As an example, Figures

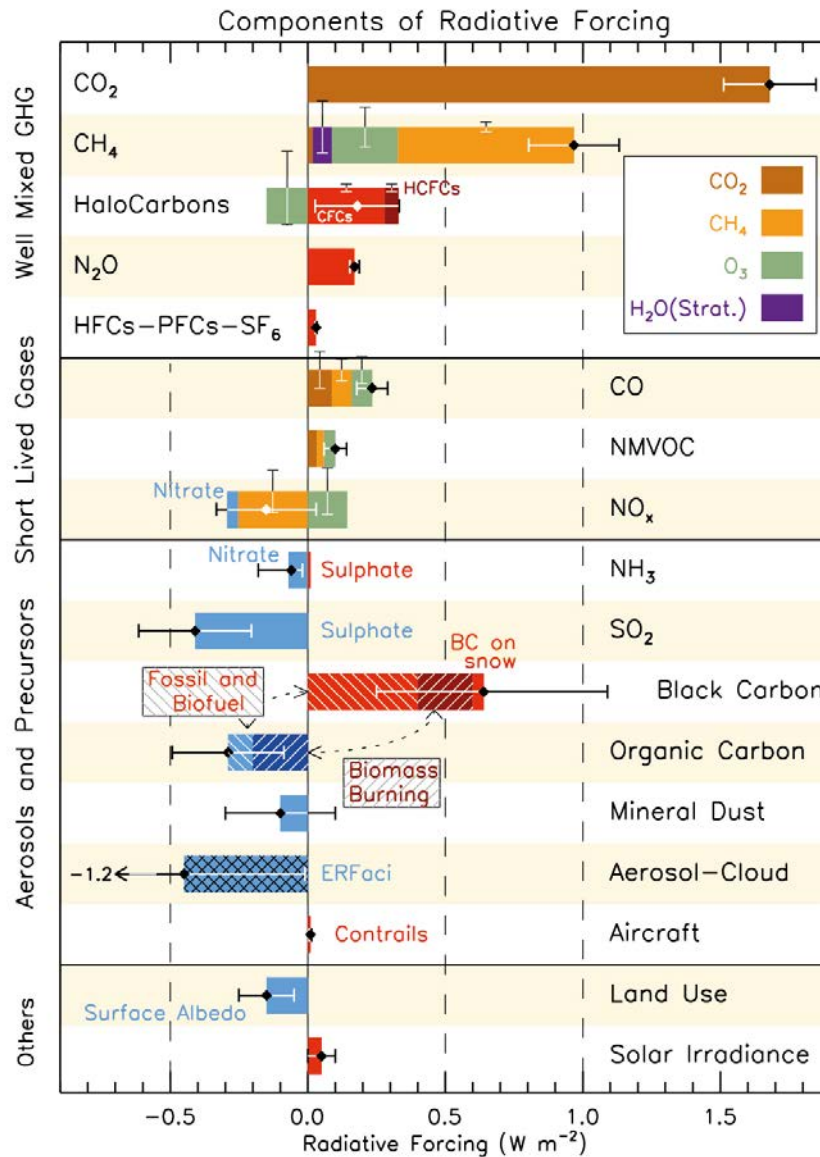


Figure 1.15: Principal component of the RF of climate change (Myhre et al., 2013b).

1.16 and 1.17 show the changes in the mean radiation and cloud fraction respectively for future climate change scenarios by means of the Coupled Model Intercomparison Project Phase 5 (CMIP5). This newness shows the growing importance of adaptation alongside mitigation in the portfolio of policy responses to climate change (Chalmers et al., 2012).

1.1.2.5 Forcing, Rapid Adjustments and Feedbacks

It is important to distinguish between RF, rapid adjustments and climate feedback (Figure 1.18). As previously explained, the term *forcing* is associated with radiative imbalance due to climate perturbation. Forcing agents, such as greenhouse gases (GHGs) and aerosols, act on the global mean surface temperature by changing the global radiative (energy) budget (Boucher

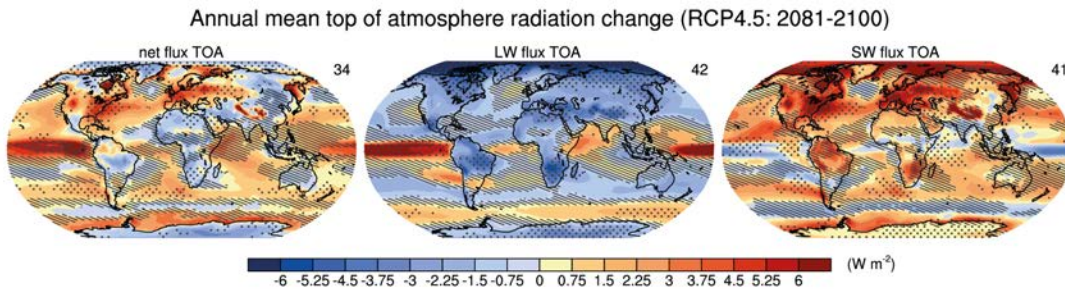


Figure 1.16: Multi-model CMIP5 average changes in the annual mean (left) net total radiation anomaly at the TOA, (middle) net longwave radiation anomaly at the TOA and the (right) net shortwave radiation anomaly at the TOA for the Representative Concentration Pathways (RCP) 4.5 scenario averaged over the periods 2081-2100 (Collins et al., 2013).

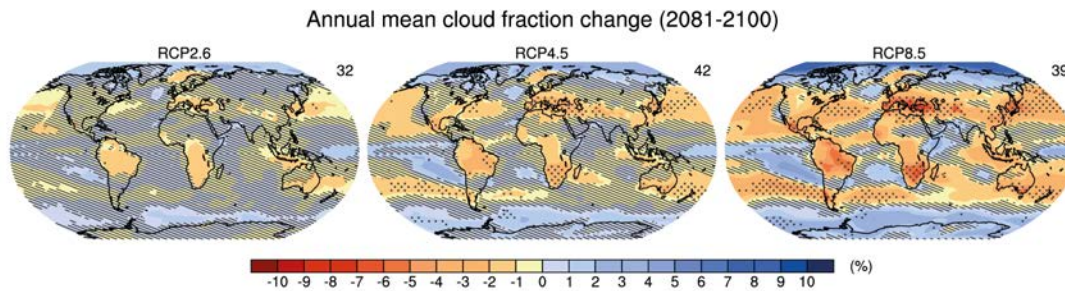


Figure 1.17: Principal component of the RF of the climate CMIP5 multi-model changes in the annual mean total cloud fraction (in %) in relation to 1986-2005 for 2081-2100 under the RCP2.6 (left), RCP4.5 (centre) and RCP8.5 (right) forcing scenarios (Collins et al., 2013).

et al., 2013).

Rapid Adjustments appear when forcing agents affect the cloud cover or other components of the climate system in a short loop, and consequently modify the global radiative budget, without operating through changes in the global mean surface temperature (indirect alteration). Therefore, rapid adjustments are related to the re-equilibration of fast climate system components, such as the atmospheric water cycle and the energetics of the atmosphere (Boucher, 2015). Adding the rapid adjustment concept helps to redefine the RF concept as the change in TOA irradiance after rapid adjustments have taken place but before the average surface temperature has changed.

Lastly, *feedbacks* are associated with changes in climate variables mediated by a change in the global mean surface temperature. They contribute to amplify or damp global temperature changes via their impact on the radiative budget (Boucher et al., 2013). According to Boucher (2015), many climate feedbacks exist: water vapor feedback, the cloud feedback, surface albedo feedbacks, etc.

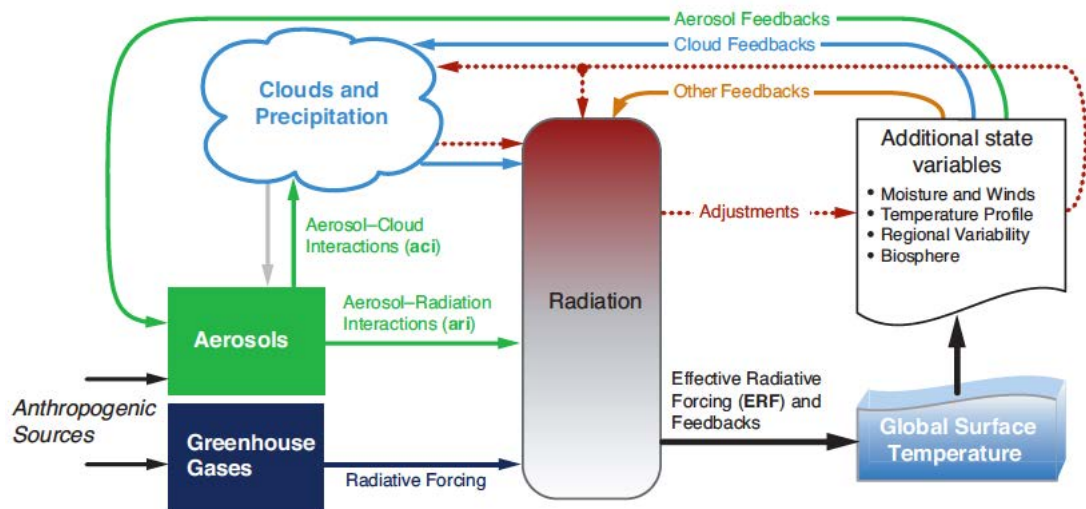


Figure 1.18: Overview of the forcing and feedback pathways involving GHGs, aerosols and clouds from Boucher et al. (2013).

1.1.3 Aerosol processes

As the origin of atmospheric aerosol particles can be either as primary particles or secondary particles, the main aerosol process is the emission of aerosol particles and precursor gases, gas-to-particle conversion and other atmospheric chemical reactions, transport, and the processes by which particles are removed from the atmosphere. The following subsections describe the main processes by which particles are removed and transformed. Figure 1.19 represents the aerosol particle interaction due to some of the processes described below.

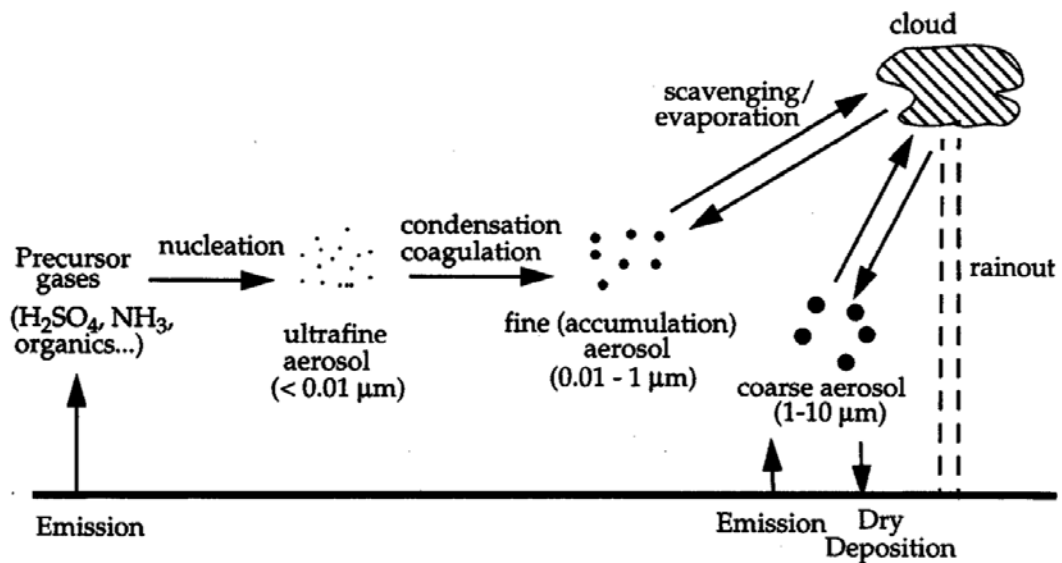


Figure 1.19: Aerosol particles interaction (Jacob, 1999).

1.1.3.1 Radiation schemes

Radiation is the main force that controls the surface energy budget. There are some variables, such as surface temperature (T) and PBL height (PBLH) that depend on accurate calculation of both shortwave (SW) and longwave radiations (LW). All these variables are important as meteorological inputs to air quality models. Radiative heating (Equation 1.5) is computed as net radiation fluxes:

$$\left(\frac{\delta T}{\delta t}\right)_{rad} = -\frac{g}{c_p} \frac{\delta F}{\delta p} \quad (1.5)$$

where F is a net flux (sum of the upward and downward fluxes) (Planton and Maynard, 2004). Table 1.1 shows the main radiation schemes available.

Table 1.1: Radiation schemes.

Name	LW/SW	Reference
GFDL	LW/SW	Fels and Schwarzkopf (1975); Schwarzkopf and Fels (1991)/ Lacis and Hansen (1974)
CAM	LW/SW	Ramanathan and Downey (1986)
Goddard	SW	Chou and Suarez (1994)
Goddard	LW/SW	Chou and Suarez (1999)
Goddard	LW	Chou et al. (2001)
RRTM	LW/SW	Mlawer et al. (1997)/ Mlawer and Clough (1998)
RRTMG	LW/SW	Morcrette et al. (2007)/ Morcrette et al. (2008)

1.1.3.2 Nucleation, condensation and coagulation

Nucleation is the gas-to-particle conversion, in which low volatile gas-phase species are converted into aerosol particles and is, hence, a source of new particles in the Earth's atmosphere (Figure 1.20). These new particles start to form when they are less than 2 nm in diameter. If conditions are suitable, these can then grow to larger sizes (50-100 nm). These particles are interesting from a climate point of view as they can serve as seeds for clouds. Nucleation contributes to the number of CCN (Haywood and Boucher, 2000; Kazil et al., 2010; Mashayekhi and Sloan, 2013), which form cloud droplets. Therefore it acts upon cloud radiative properties, cloud lifetimes, and precipitation rates via the first and second indirect aerosol effect.

The nucleation process takes place through the condensation of molecules and coagulation. *Condensation* occurs when a vapor condenses on a particle population or when material evaporates from the aerosol to the gas-phase, hence changes the particle diameters and size distribution of the population $n(v, t)$ shape (Seinfeld and Pandis, 2006). *Coagulation* occurs when the aerosol particles suspended in a fluid come into contact given their Brownian motion or as a result of their motion produced by hydrodynamic, electrical, gravitational forces, among others. This process modifies aerosol size distribution and reduces the particles number and is

more efficient for the smallest particles in the nucleation and Aitken modes.

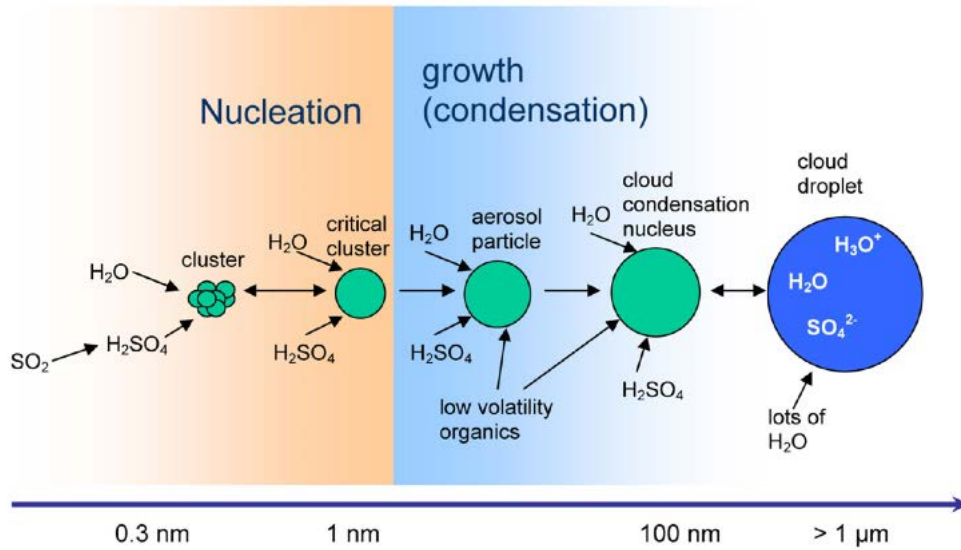


Figure 1.20: Schematic representation of the nucleation process and subsequent growth process for atmospheric binary homogeneous nucleation (Curtius, 2006).

1.1.3.3 Dry deposition

This process can be defined as the transport of gaseous and particulate species from the atmosphere onto surfaces when precipitation is absent. The factors that influence dry deposition are (Seinfeld and Pandis, 2006):

- Atmospheric turbulence.
- The chemical properties of depositing species (solubility of species in water).
- The nature of the surface itself (terrain and type of surface cover).
- Whether the substance is present in the gaseous or particulate form.
- The amount of precipitation in the region.

Solubility and chemical reactivity can affect uptakes on the surface of gaseous species, while size, density and shape can determine the capture of particle species. In relation to the surface, natural surfaces (such as vegetation) generally promote dry deposition. Therefore dry deposition (of gases and particles) is a basic process which removes atmospheric aerosols from the atmosphere. Generally, the parameter used to model the deposition rate is deposition velocity v_d , defined as (Equation 1.6):

$$v_d = -\frac{F_c}{C_z} \quad (1.6)$$

where F_c is the vertical dry deposition flux and C_z is the concentration at height z .

1.1.3.4 Wet deposition

It refers to the natural processes by which a material is scavenged by atmospheric hydrometeors (cloud and fog drops, rain, snow) and is deposited on the Earth's surface. Wet deposition is also known as precipitation scavenging, wet removal, washout, and rainout. Rainout usually refers to in-cloud scavenging, while washout refers to below-cloud scavenging by falling rain, snow, etc. Figure 1.21 shows necessary steps for wet removal: first gas or particle species must be placed in the presence of condensed water. Then species must be scavenged by hydrometeors, and finally need to be deposited on the Earth's surface (Seinfeld and Pandis, 2006).

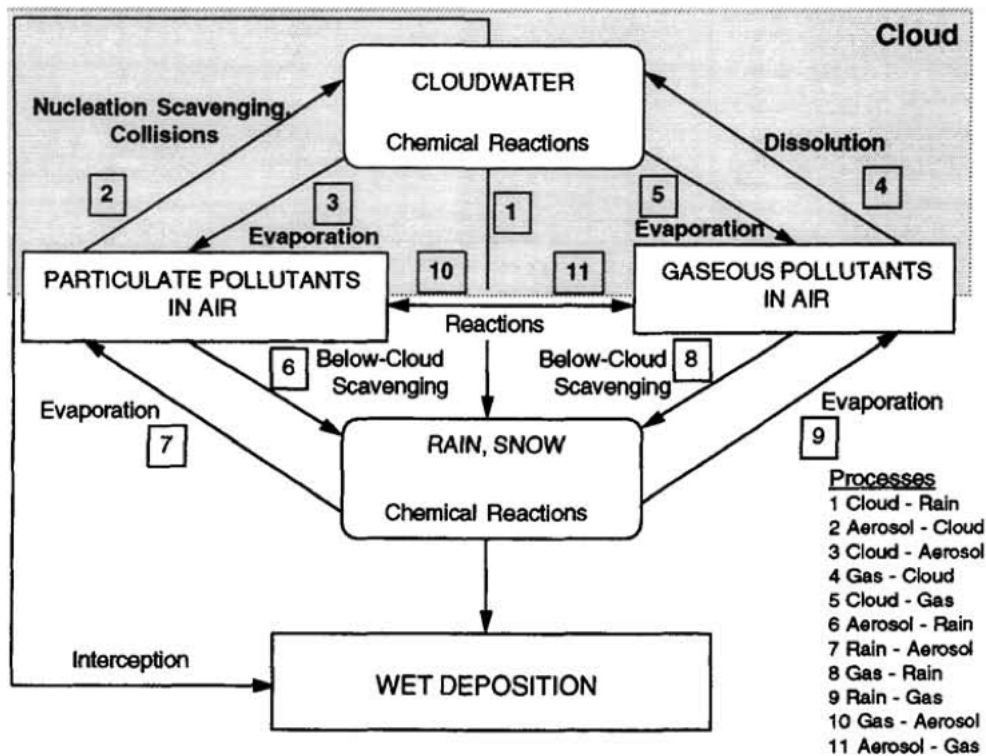


Figure 1.21: Schematic representation of the wet deposition processes (Seinfeld and Pandis, 2006).

1.1.4 Approaches to study atmospheric aerosols

Several approaches are available to study and measure aerosol properties such as extractive, in situ and remote sensing techniques. This section presents some of the techniques used for characterize the properties of aerosols. Observation systems have increasingly been used in the last years, but improvement are required (Seinfeld et al., 2016) because of the large range of scales and the fact that various measuring systems tend to address different scales. Seinfeld

et al. (2016) compiled some large-scale field experiments, which are planned to address aerosol-cloud-climate interactions.

1.1.4.1 Extractive techniques

They consist of collecting samples for further laboratory analysis. These methods are highly sensitive and selected, but offer poor real-time monitoring. The principal instrument used to collect samples is the High Volume collector (Figure 1.22). This instrument uses a continuous duty blower to suck in an air stream by collecting aerosol particles and depositing them on a filter for later chemical and mineralogical analyses. Different size ranges can be selected (PM_{10} , particulate matter with an aerodynamic diameter less than or equal to $2.5 \mu\text{m}$ [$PM_{2.5}$]... etc).

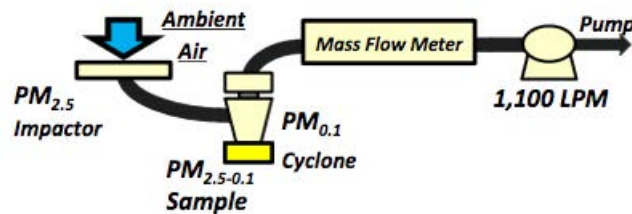


Figure 1.22: Schematic diagram of a High Volume Sample from Okuda et al. (2015).

1.1.4.2 In situ or ground-based measurements

Ground-based measurement networks are a very useful and accurate way to assess aerosol optical properties (Holben et al., 2001). In situ measurements provide accurate local information on aerosol concentrations and properties but cannot properly sample the atmosphere to characterize the spatial and temporal variability of the global aerosol.

Examples of in situ instruments to monitor aerosol optical properties are: Nephelometer (Figure 1.23)(it measures the radiation that is scattered or backscattered by aerosols which are directed into a tube); Aethalometer or Particle Soot Absorption Photometer and Photo-Acoustic Absorption Measurement which measures aerosol absorption (Boucher, 2015).

1.1.4.3 Remote sensing techniques

Remote sensing techniques include all the measurements taken remotely; i.e., not-coming into physical contact with it (Boucher, 2015). Hence, one advantage is that the studied sample is not perturbed. Besides, the electromagnetic waves used are sensitive to different aerosol properties and can provide point, column or profile data.

There are two main platforms that measure aerosol properties by remote sensing: the Earth's

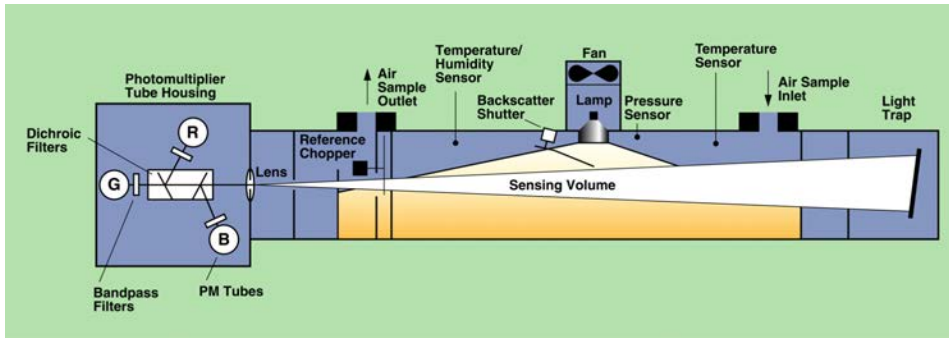


Figure 1.23: Nephelometer schematic from https://www.esrl.noaa.gov/gmd/aero/gallery/aerosol_instrumentation/nephelometer/.

surface (ground-based measurement) and from the space (by means of satellites). Ground-based measurement provides reliable information about aerosol optical properties but its drawback is limited spatial data coverage. Although satellite data are not as reliable as ground-based observations, they provide valuable information with a higher spatial coverage. Furthermore, remote sensing techniques can also be classified by the radiation source as: passive techniques (using natural radiation, e.g., sun photometers and spectroradiometers) and active techniques (using artificial sources that emit radiation, such as lidar or radar). Remote sensing of aerosols from the ground and from space is thus essential for monitoring and understanding atmospheric aerosols and their role in the climate system (Boucher, 2015). Some of the passive remote sensing techniques and relevant satellite instruments and missions for observing atmospheric aerosols can be found in Table 1.2.

Table 1.2: Passive remote sensing techniques and relevant satellite instruments and missions for observing atmospheric aerosols (Boucher, 2015).

Instruments	Measure	Reference
AERONET PHOTONS	Extinction and scattering of solar radiation from the ground and from space, respectively	Shaw (1983) Holben et al. (2001) Twitty (1975) Nakajima et al. (1983) Dubovik and King (2000)
SAGE, OSIRIS GOMOS, MAESTRO	Extinction of solar radiation from space	Kent et al. (1991)
AVHRR, MERIS, MODIS, MISR, SCIAMACHY, POLDER, ATSR, AATSR, SEVIRI, PARASOL, VIIRS, 3MI	Scattering of solar radiation from space	Nagaraja Rao et al. (1989) Herman et al. (1997) Remer et al. (2005) Tanré et al. (2011)
METEOSAT, SEVIRI, AIRS, IASI, IASI-NG	Infrared radiation at nadir	Ackerman (1997) Legrand et al. (1989) Pierangelo et al. (2004)

It is worth point out two European ground-based remote sensing networks; the Aerosols, Clouds, and Trace gases Research InfraStructure Network (ACTRIS) and AERONET. The aim of ACTRIS is to integrate European ground-based stations equipped with advanced atmospheric probing instrumentation for aerosols, clouds, and short-lived gas-phase species (<http://www.actris.net/language/en-GB/Project.aspx>). ACTRIS integrates three typical data repositories: EBAS (near-surface aerosol and trace gas data), European Aerosol Research Lidar Network (EARLINET) for the remote sensing of vertical aerosol distribution, and Network of stations for the continuous evaluation of cloud and aerosol profiles (CLOUDNET). The AERONET program is a federation of ground-based remote sensing aerosol networks established by NASA and PHOTONS (University of Lille 1, CNES, and CNRS-INSU) which provides globally distributed observations of spectral AOD, inversion products, and precipitable water in diverse aerosol regimes. Two data versions (Versions 1 and 2) and three quality levels (Levels 1.0, 1.5, 2.0) exist for each product. While Levels 1.0 and 1.5 are provided in near real-time, a 12-month or longer delay (due to a final calibration and manual inspection) ensures that the highest quality data can be found in Version 2, Level 2.0 data products. Version 2 AOD processing now includes fine and coarse mode AOD as well as fine mode fraction. AOD at different wavelengths (AOD470, AOD555 and AOD675) are compared to available AERONET data, with information from 85 stations for Europe. We will have also one station to validate

O₃ sounding (<http://aeronet.gsfc.nasa.gov/>). Figure 1.24 shows the AERONET stations worldwide.



Figure 1.24: AERONET stations. From http://aeronet.gsfc.nasa.gov/new_web/aerosols.html.

Satellite-based remote sensing continues to be the primary source of global data for ACI, but concerns persist regarding how measurement artefacts affect retrievals of both aerosol (Li et al., 2010) and cloud properties. Observations can not measure RFari directly, only useful constraints to aspects of the global RFari. Given their high cost, in situ observations cannot provide sufficient coverage of these spatial and temporal scales to calculate the climate forcing by aerosol particles. Consequently, the utility of in-situ observations cannot be fully realized until closely coupled with numerical models and satellite observations. Models require the numerical values of the parameters used in the calculation of spatial distribution and optical properties for each chemical or aerosols type predicted (Ogren, 1995).

1.1.4.4 Aerosol modeling

Ground measurements provide data with high temporal resolution and in real time but, they sometimes have only a sparse spatial resolution. Satellite data covers regions where no ground-based stations are available but are representative of larger regions and only serve data at specific times of the day. Air Quality models fill in the sparse temporal and spatial sampling of the measurements and connect them in a physically consistent manner.

The aim of aerosol modeling is to provide a detailed description of aerosol particle concentrations, composition and size distribution, and to collect expressions for relevant physical processes (chemical reactions, nucleation, condensation, coagulation, ... etc) (Whitby and Mc-

Murry, 1997), since these processes cannot be obtained by measurements alone. This requires advanced modeling techniques and innovation, plus reliable validation data of particle characteristics. Therefore modeling plays a key role to quantitatively integrate knowledge and to evaluate our understanding of physical and chemical processes in the atmosphere.

To mathematically describe the distribution for a given aerosol mode, functions that can cover a large range of sizes are useful. The most popular function is lognormal distribution (Equation 1.7), which describes well the typical distributions observed in the atmosphere (Seinfeld and Pandis, 2006):

$$\frac{dN}{d \ln r} = N_0 \frac{1}{\sqrt{2\pi}\sigma_0} \exp\left(-\frac{1}{2} \left(\frac{\ln(r/r_0)}{\sigma_0}\right)^2\right) \quad (1.7)$$

There are three approaches to represent aerosol total volume: bulk, sectional and modal, although commonly-used approaches are sectional and modal. In the sectional approach (Figure 1.25), size distribution is discretized into sections (or bins) and particle properties are assumed constant over particle size sections (Spracklen et al., 2005). The particle number concentration and mass concentrations are tracked separately for each section (Bergman et al., 2011). In the modal approach (Zhang et al., 2010), size distribution is considered by several modes and particle properties are assumed uniform in each mode (Zhang et al., 1999). Bulk representations are considered as sectional approaches involving one single bin.

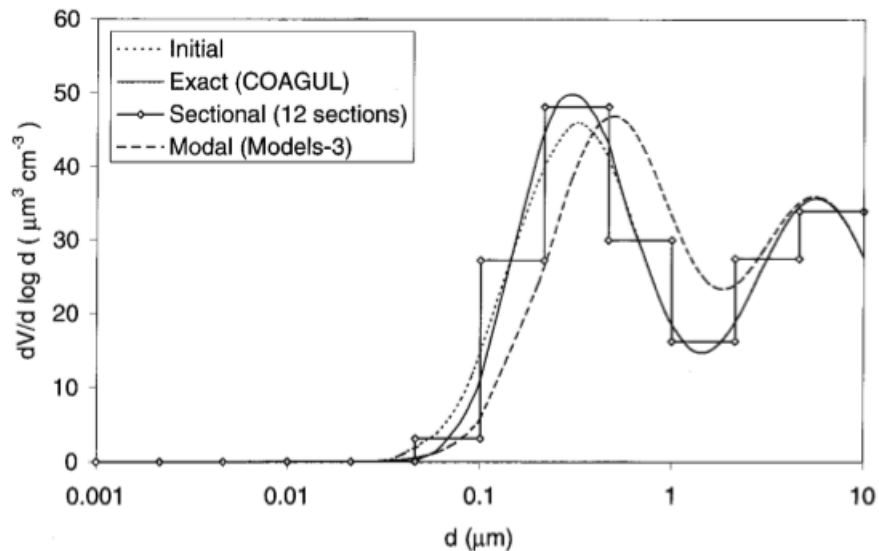
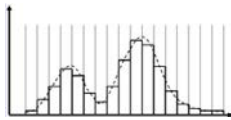


Figure 1.25: Particle size distribution approach (Zhang et al., 1999).

The sectional approach is accurate for coagulation and can reproduce the major characteristics of particle size distribution evolution for condensational growth with the moving-center and hybrid algorithms. It is the most accurate and flexible approach in terms of size distribu-

tion shape, despite being computationally most demanding (Bergman et al., 2011). The modal approach provides more accurate results according to coagulation and condensation growth and is used in Models-3, which follows a modal approach with 3 log-normal distributions and constant standard deviations to represent Aitken nuclei, accumulation, and coarse modes. In global models, modal approaches are still preferred to sectional approaches because of lower computational costs (Mann et al., 2012) although this could change as technology is improving. Table 1.3 summarizes the features of the three aerosol approaches.

Table 1.3: Features of aerosol approaches (Bellouin, 2013).

Bulk	Sectional	Modal
Simulate modal mass for an external mixture of species		Simulate modal mass and number for an internal mixture of selected species
Size distribution is prescribed globally	Decompose the size distribution in bins	The mean radius of the size distribution depends on mass and number
Mass and number are co-varying	Does not usually represent the mixing state	Width of the size distribution is generally fixed

Aerosol modules

Several models have been developed as an extension of the global/regional chemistry transport model (CTM) to better process aerosol effects in these models. A reliable aerosol model must be able to resolve the wide particle size range and the chemical complexity that arises from many different primary and secondary aerosol species, and must also include reliable treatments for simulating the various chemical and microphysical processes. Aerosols of different types and origins can be composed of various chemical species. Including each species in an aerosol model is not feasible due to computational cost. Therefore, different aerosol models are designed according to the accuracy desired for a given application (Zaveri et al., 2008). Table 1.4 compiles the main aerosol modules used in state of the art CTMs.

MADE is based on the regional particulate model (Binkowski and Shankar, 1995). The size distribution of the submicrometer aerosol is represented by two modes, and lognormal distribution is assumed. Chemical composition is computed in the sulfate nitrate ammonium and water system. Emission and nucleation are used for modeling aerosol sources. Coagulation,

condensation, transport and deposition are considered as processes modifying the aerosol load in the atmosphere. Aerosol dynamics calculations are made on-line in the chemistry-transport model Ackermann et al. (1998). SOA have been incorporated into MADE by Schell et al. (2001), through the Secondary Organic Aerosol Model (SORGAM).

Table 1.4: Main aerosol modules in CTMs.

Name	Representation	Organic/Inorganic	Reference
MADE	Modal	Inorganic	Ackermann et al. (1998)
GOCART	Bulk	Inorganic	Chin et al. (2000)
SORGAM	Modal	Organic	Schell et al. (2001)
AERO3	Modal	Organic and inorganic	Binkowski (1999)
AERO4	Modal	Organic and inorganic	Binkowski and Roselle (2003)
MADRID	Modal and sectional	Organic and inorganic	Zhang et al. (2004)
MOSAIC	Sectional	Organic and inorganic	Zaveri et al. (2008)

The GOCART (Goddard Chemistry Aerosol Radiation and Transport model) module (Chin et al., 2000) simulates the distribution of sulfur species in the atmosphere and solves the continuity equation, including the emissions, chemistry, convection, advection, diffusion, dry and wet deposition. It has a bulk aerosol scheme. MADRID treats all major aerosol chemical and microphysical processes including inorganic aerosol thermodynamic equilibrium, SOA formation, nucleation, condensation, gas/particle mass transfer, and coagulation Zhang et al. (2004). AERO3 Binkowski (1999) simulates the transformations of gas-phase chemical species, which are either directly emitted or produced from gas-phase reactions, to aerosol and calculates aerosol mass, number and surface concentrations. The difference between AERO3 and AERO4 (Binkowski and Roselle, 2003) is that AERO4 includes the sea salt aerosol. MOSAIC (Model for Simulating Aerosol Interactions and Chemistry) (Zaveri et al., 2008) handles all the major aerosol species at urban, regional, and global scales. These include sulfate, methanesulfonate, NO_3 , chloride, carbonate, NH_4^+ , sodium, calcium, BC, OC, and liquid water. In order to represent aerosol size distribution, they can be implemented by either the modal or sectional approach.

Apart from the aerosol module, there are two components that are fundamental for the chemistry modeling: photolysis and gas-phase mechanism.

Photolysis

Photolysis reactions play a key role in atmospheric chemistry, as the Sun is the source of energy that drives the entire system of atmospheric reactions (Seinfeld and Pandis, 2006). Photolysis rate coefficient J_i (Equation 1.8) for a gaseous species i depend on the wavelength

λ and is defined as:

$$J_i = \int_{\lambda} \sigma_i(\lambda, P, T) \phi_i(\lambda, P, T) F(\lambda) d\lambda \quad (1.8)$$

where σ_i is the absorption cross section, ϕ_i is the quantum yield of species i and F is the representative actinic flux of irradiance that reaches the level where J is calculated. The variables σ_i and ϕ_i are specific to photolysed species i , whereas F depends on the position of the sun but also on the presence of clouds and aerosols. Photolysis rates can be modified by the aerosols and clouds inside the layer but also below and above it (Real and Sartelet, 2011). Some studies have shown the effects of aerosols on photolysis rates in the presence of clouds (Liao et al., 1999; Yang and Levy II, 2004; Liu et al., 2009). Table 1.5 summarizes the different photolysis schemes included in several state of the art CTMs.

Table 1.5: Photolysis schemes.

Name	Model	Reference
2-stream	GISS CTM	Isaksen et al. (1977)
δ -Eddington	WRF-Chem; CMAQ	Joseph et al. (1976)
Madronich	WRF-Chem; CMAQ	Madronich (1987)
Fast-J	WRF-Chem; UCI CTM; NMMB/BSC-CHEM	Wild and Prather (2000)
Fast-J2	UCI CTM	Bian and Prather (2002)
Fast-TUV/FTUV	MOZART-4; CMAQ	Tie et al. (2003)
Fast-JX	p-TOMACT	Neu et al. (2007)

Gas-phase

The gas-phase mechanism is a critical module of CTMs that comprise inorganic species, such as NO_x , HO_x and sulphur oxides (SO_x) and organic species, mainly VOCs. The chemical reaction mechanism describes how VOCs and NO_x interact to produce O_3 and other oxidants (Dodge, 2000). It is essential to understand the photochemistry of the troposphere in order to comprehend the changes in RF and to predict the future atmospheric composition (Emmerson and Evans, 2009). Table 1.6 summarizes the different gas-phase schemes included in several CTMs.

1.1.4.5 Online-coupled meteorology and chemistry models

Historically, given the complexity and lack of appropriate computer power, meteorology/climate and chemistry feedbacks have been separately studied. Air chemistry and weather forecasts have developed as separate disciplines, which has led to the development of separate modeling systems that are only loosely coupled (offline) (Grell and Baklanov, 2011). Simulating climate and aerosols offline leads to inconsistencies in transport and no climate-chemistry-aerosol-

Table 1.6: Gas-phase schemes.

Name	Model	Reference
LCC	CIT	Lurmann et al. (1987)
CBM-IV	Models-3; CMAQ; NMMB/BSC-CHEM	Gery et al. (1989)
RADM2	Models-3; CMAQ; WRF-Chem	Stockwell et al. (1990)
EMEP	EMEP MSC-W	Simpson et al. (1993)
RACM	EURAD; WRF-Chem	Stockwell et al. (1997)
MELCHIOR1	CHIMERE	Lattuati (1997)
MELCHIOR2	MACC CHIMERE	Lattuati (1997)
CBM-Z	WRF-Chem	Zaveri and Peters (1999)
SAPRC	CMAQ	Carter (2000)
CBM-05	CMAQ; NMMB/BSC-CHEM	Yarwood et al. (2005)
CACM	CIT	Griffin et al. (2002)
CB05-TU	Polair-3D	Whitten et al. (2010)
CB06	CAMx	Yarwood et al. (2010)

cloud-radiation feedbacks (Sanderson et al., 2006). As aerosol is one of the key properties in simulations of the Earth's climate (Kinne et al., 2006), fully-coupled meteorology-climate, and chemistry models provide the possibility to account for these feedback mechanisms between simulated aerosol concentrations and meteorological variables. Figure 1.26 shows the interaction between meteorology and the Atmospheric Chemistry Transport Model (ACTMs). It is also a promising way toward for future atmospheric simulation systems that lead to a new generation of models for improved meteorological, environmental and chemical weather forecasting (Baklanov et al., 2008b, 2014). Nevertheless, this fact presents significant challenges in both scientific understanding and computational demand terms. Forkel et al. (2012) highlights that further studies with higher cloud resolving resolution are therefore necessary to investigate the aerosol indirect effect and also the development of the semi-direct effect in more detail. Moreover, as Grell and Baklanov (2011) showed, considering the many uncertainties in air quality forecasting (such as emission inventories), more research and studies are needed to show that models with online chemistry are able to perform well enough to meet these standards.

Online modeling systems have been developed and used by the research community since the 1990s. The earliest online approach may have been the Gas Aerosol Transport Radiation, General Circulation Mesoscale, Ocean Model (GATOR-GCMOM) a model developed by Jacobson (Jacobson, 1994, 2001a,b). Both offline and online models are actively used in current regional and global models and are useful for different applications:

- Offline models: in ensembles and operational forecasting, inverse/adjoint modeling, and sensitivity simulations.
- Online models: where feedbacks are important (locations with high frequencies of clouds

and large aerosol loadings, among others), where the local scale wind and circulation system change quickly, and also when coupled meteorology-air quality modeling is essential for accurate model simulations (real-time operational forecasting or simulating the impact of future climate change on air quality).

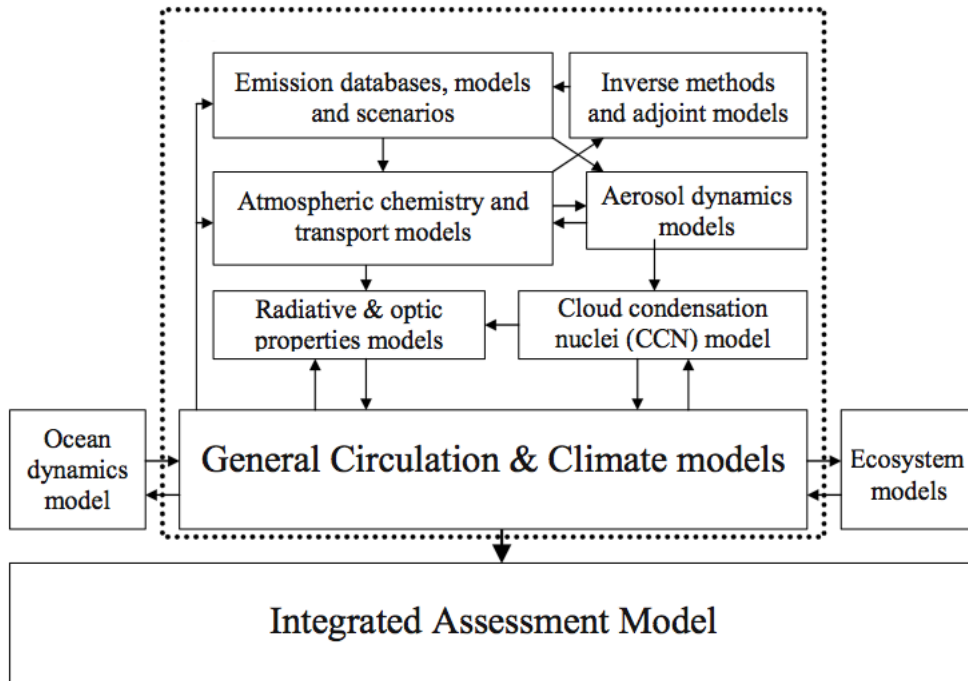


Figure 1.26: Interactions of the integrated system of meteorology and ACTMs (Baklanov et al., 2008b).

Many online-coupled global climate models (GCMs) were developed for simulating global climate change and air quality studies more than three decades ago, whereas fewer coupled climate/meteorology chemistry models at urban and regional scales (Zhang, 2008). Table 1.7 shows some online models from Europe (EU) and the United States (US).

According to European online models, COSMO-ART (Steppeler et al., 2003) processes reactive gases and aerosols including secondary aerosols, soot, mineral dust, sea salt and biological matter. It compiles modules for emissions of mineral dust, sea salt and pollen grains. Processes such as the emissions, coagulation, condensation, dry deposition, wet removal, and sedimentation of aerosols are taken into account. Online coupling enables the calculation of interactions of gases and aerosols with the state of the atmosphere. It ranges from the continental to the regional scale, and is the operational weather forecast model of the German Weather Service (DWD). LM-MUSCAT (Wolke et al., 2004) is based on the “Lokal-Modell” (LM), which is the operational weather prediction model of the DWD, the online-coupled Multiscale Chemistry Aerosol Transport model (MUSCAT). The Enviro-HIRLAM (Environment-High Resolution Limited Area Model) is a fully online-coupled ACT-NWP which can be applied

to regional-, meso- and urban-scale applications. The NWP part has been developed by the HIRLAM consortium, and has been used for operational weather forecasting (Baklanov et al., 2008a). NMMB/BSC-Chem, which is under development at the Earth Sciences Department of BSC-CNS <http://www.bsc.es/earth-sciences/nmmbbsc-project>, is a fully online integrated system used for meso to global scale applications. The meteorological driver is the NCEP/NMMB numerical weather prediction and the CBM-05 chemical mechanism. The BOLCHEM model Maurizi et al. (2011) online couples the mesoscale meteorological model BOLAM (BOlogna Limited Area Model) and modules for transport and transformation of chemical species.

Table 1.7: Online-coupled models.

Model	EU/US	Reference
COSMO-ART	EU	Steppeler et al. (2003)
LM-MUSCAT	EU	Wolke et al. (2004)
DMI-Enviro-HIRLAM	EU	Baklanov et al. (2008a)
NMMB/BSC-CHEM	EU	Jorba et al. (2010)
BOLCHEM	EU	Maurizi et al. (2011)
GATOR-GCMOM	US	Jacobson (2001a,b)
WRF-Chem	US	Grell et al. (2005)
CAM3	US	Collins et al. (2006)
MIRAGE2	US	Ghan and Easter (2006)
WRF-CMAQ(online)	US	Mathur et al. (2010)

Among the American online models, we find GATOR-GCMOM (Jacobson, 2001a,b), a one-way nested (from the global to the local scale) gas, aerosol, transport, radiation, general circulation, mesoscale, and ocean model. The Community Atmosphere Model version 3.0 (CAM3)(Collins et al., 2006) represents the sixth generation of the Atmospheric General Circulation Models developed by the climate community in collaboration with the National Center for Atmospheric Research (NCAR). It has been designed as a modular and versatile model suitable for climate studies by the general scientific community. When coupled to the Community Climate System Model (CCSM) it interacts with fully prognostic land, sea-ice, and ocean models. The name of the model series has been changed from the Community Climate Model to the Community Atmosphere Model to reflect the role of CAM3 in the fully coupled climate system. MIRAGE (Model for Integrated Research on Atmospheric Global Exchanges) is designed to study the impacts of anthropogenic aerosols on the global environment. It consists of a CTM coupled online with a GCM. The CTM simulates trace gases, aerosol number, and aerosol chemical component mass (sulfate, methane sulfonic acid, BC and OC, sea salt, and mineral dust) for four aerosol modes (Aitken, accumulation, coarse sea salt, and coarse mineral dust) by the modal aerosol dynamics approach. WRF-CMAQ (Weather Research Forecast Model)

coupled with the EPA's Community Multiple Air Quality (CMAQ) (Mathur et al., 2010), is an online meteorology-chemistry model that simulates the two-way feedback between meteorology and chemistry in a single simulation. It takes into account the interactions of estimated aerosol mass on incoming shortwave radiation through the Rapid Radiative Transfer Method for Global (RRTMG) radiation scheme for the shortwave aerosol direct effect. It does not simulate the effects of aerosols on long wave radiation and cannot be used with the CAM radiation scheme. This release also uses a core-shell model to perform the aerosol optics calculation rather than the volume mixing technique used in the previous WRF-CMAQ version.

For this Thesis the WRF model coupled with Chemistry (WRF-Chem) (Grell et al., 2005) has been used. A short description is done in the following Section. The online integrated design of WRF-Chem has served to comply with the objectives of this work, as explained in Section 1.2

1.1.4.6 Short description of WRF-Chem model

In this section we focus on describing the main features of this model. WRF-Chem simulates the emission, transport, mixing, and chemical transformation of trace gases and aerosols simultaneously with the meteorology. The model is used for investigating regional-scale air quality, field program analyses, and cloud-scale interactions between clouds and chemistry. It represents the first community open-code, supported, online-coupled model (publicly available) and also conditioned the election of this model for Thesis. Unlike the coarse spatial resolution of GCMs, feedback processes over a wide range of spatial scales can be investigated with WRF-Chem. Supermicrometer particles are included in WRF-Chem by adding an interactive coarse mode (Schell et al., 2001).

Model features

The WRF-Chem model consists of the following components, and some are compiled in Table 1.8:

- Gas-phase chemical mechanisms: the Regional Acid Deposition Model version 2 (RADM2) of Chang et al. (1990), the Regional Atmospheric Chemistry Mechanism (RACM) of (Stockwell et al., 1997). Carbon-Bond Mechanism version Z (CBM-Z) (Zaveri and Peters, 1999) and the 2005 version of Carbon Bond mechanism version 05 (CB05) of (Yarwood et al., 2005) and (Sarwar et al., 2008).
- Aerosol module: the Modal Aerosol Dynamics Model for Europe (MADE) (Ackermann et al., 1998) with the Secondary Organic Aerosol Model (SORGAM) of Schell et al.

(2001) (MADE/SORGAM). Model for Simulating Aerosol Interactions and Chemistry (MOSAIC) (Zaveri et al., 2008). Model of Aerosol Dynamics, Reaction, Ionization, and Dissolution (MADRID) (Zhang et al., 2004) and a total mass aerosol module from the Global Ozone Chemistry Aerosol Radiation and Transport model (GOCART) (Chin et al., 2000).

- Photolysis scheme: Fast-J scheme (Fast et al., 2006), Madronich scheme (Madronich, 1987) and F-TUV photolysis scheme (scheme faster than the previous Madronich scheme option).
- Aerosol direct effect through interactions with atmospheric radiation, photolysis, and micro physics routines. Available for GOCART, MOSAIC or MADE/SORGAM options.
- Aerosol indirect effect through interaction with atmospheric radiation, photolysis, and microphysics routines. Available for MOSAIC or MADE/SORGAM.

A more detailed description of the model can be found in Grell et al. (2005) and Fast et al. (2006). Figure below (1.27) shows the flowchart for the WRF-Chem modeling system.

Table 1.8: WRF-Chem features (Zhang, 2008).

Feature	Name	References
Gas-phase	RADM2, RACM, CBM-Z, CB05 (156-237 reactions, 52-77 species)	Chang et al. (1990); Stockwell et al. (1997); Zaveri and Peters (1999); Yarwood et al. (2005); Sarwar et al. (2008)
Aerosol module	MADE/SORGAM, MADRID, MOSAIC, GOCART	Ackermann et al. (1998); Schell et al. (2001); Zhang et al. (2004); Zaveri et al. (2008)
Photolysis	Madronich, F-TUV, Fast-J	Madronich (1987); Madronich and Weller (1990); Fast et al. (2006)
Direct effect	Available for GOCART, MOSAIC or MADE/SORGAM	Chin et al. (2000); Zaveri et al. (2008); Schell et al. (2001)
Indirect effect	Available for MOSAIC or MADE/SORGAM	Zaveri et al. (2008); Schell et al. (2001)
Emissions	Online: biogenic and sea salt emissions Offline: anthropogenic emissions and other natural emissions	
Applications	Forecast/hindcast, Met/chem feedbacks; O ₃ , PM _{2.5} ; Aerosol direct and indirect effects	

1.1.4.7 Aerosol feedbacks modeling studies

Including aerosol interactions implies a major advance in air quality modeling. It is also important for developing integrated emissions control strategies for both air quality management and climate change mitigation (Yu et al., 2013; Rosenfeld et al., 2014). The commonest method to address the study of the aerosol-radiation-cloud interactions is to use different modeling set-ups, for both the regional and global scale. Regarding ARI, available works focus on several

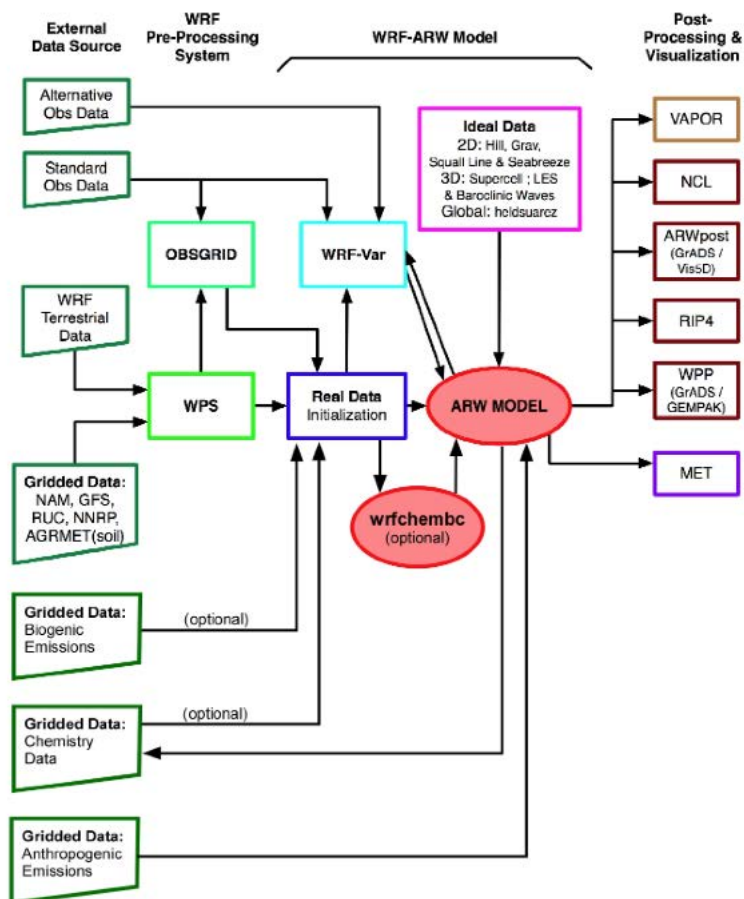


Figure 1.27: Flowchart of the WRF-Chem system (Peckham et al., 2012).

climatic and meteorological variables such as T, SW, AOD and PBLH. On the other hand, in ACI studies, CCN, cloud cover, precipitation efficiency are the most widely studied variables. The semi-direct effect is reflected in changes in T, PBL, cloud cover or in solar heating rates.

Chapman et al. (2009) coupled the aerosol-radiation-cloud system into WRF-Chem, and tested it with a simulation that contained all anthropogenic emission sources and another one with removed emissions. They focused on a north-eastern North America (NA) domain in summer of 2004. They found a reduction of 5 W m^{-2} due to the effect of aerosols. Moreover, fewer clouds were found when removing emissions. Other studies have computed different model setups, which include aerosol effects, or did not; i.e., a baseline case without any aerosol feedback on meteorology, a simulation with the direct effect included and a simulation including the direct as well as the indirect aerosol effect. The difference between these setups provides an idea of the influence of the aerosol effect on the studied variable. Forkel et al. (2012) studied a two-month episode (June to July 2006) to allow medium range effects of the direct and indirect aerosol effects on meteorological variables and air quality. These authors found a slightly lower T over western Europe when they included atmospheric aerosol feedbacks. This reduction

followed the same pattern as PBLH. The inclusion of the indirect aerosol effect led to reduced cloud water content by up to 70% and also to a significantly higher mean rain water content over the North Atlantic. The mean O₃ mixing ratios in July were modified by up to 4 ppb over continental Europe, which were related mainly to changes in cloud cover. In July 2006, Meier et al. (2012) found a general decrease in 0.14 K on T at 2 meters (T2) when simulating absorbing aerosol in upper layers compared to an aerosol-free troposphere over land surface. During the Russian forest fires episode in summer 2010, Péré et al. (2014) showed a SW reduction up to 80-150 W m⁻² and daily mean surface temperature reductions between 0.2 to 2.6 K, due to the presence of high aerosol loads. Kumar et al. (2013) performed a study during a pre-monsoon season (April-June) in India, and showed that the impact of dust aerosol effects was minor on a regional scale, but was significant locally. They also found a cooling effect on the surface (-8.0 ± 3.3 W m⁻²) and TOA (-2.9 ± 3.1 W m⁻²) and conversely a warming itself due to dust particles (5.1 ± 3.3 W m⁻²).

Some studies have shown the importance of including the ACI, which contributes to good performance when simulating aerosol properties; e.g., a work led by Yang et al. (2011a), used the WRF-Chem model in a study on the northern Chilean and southern Peruvian coasts from 15 October to 16 November 2008. They performed a simulation including ACI and compared it to another one with fixed CDNC and simplified cloud and aerosol treatments. When taking ACI into account, it strengthens the temperature and humidity gradients within the inversion layer and reduced the marine boundary layer depth. They also found that, the coupling simulation of ACI improved cloud optical and microphysical properties. Moreover, a better agreement of the mean TOA outgoing fluxes with observations is found in ACI simulation.

Among international initiatives, within GCMs, the AEROCOM initiative (Schulz et al., 2006), compiles a number of observations and results from more than 14 global models to document and compare state of the art modeling of global aerosols. Regarding the RF from the ARI, in the phase I (Schulz et al., 2006) estimated the direct radiative TOA forcing (without nitrate and dust) as 0.22 W m⁻². After phase I, more attention was paid to the direct aerosol effect due to anthropogenic nitrate and SOA. In AEROCOM Phase II, (Myhre et al., 2013a), 16 global aerosol models were used to assess the RF of the anthropogenic direct aerosol effects, with a mean of -0.27 W m⁻². In the same initiative, Quaas et al. (2009) evaluated 10 different GCMs against satellite data, by taking into account aerosol-radiation-cloud interactions. They computed the statistical relationships between AOD and various cloud and radiation quantities. Results found suggested that the second aerosol indirect effect had to be revised in the GCMs (mainly regarding an autoconversion parameterisation). The Atmospheric Chemistry

and Climate Model Intercomparison Project (ACCMIP) (Shindell et al., 2013) examined the short-lived drivers of climate change in current climate models. Ten ACCMIP models including aerosols, of which 8 also participated in CMIP5, were evaluated. They studied the ERF which includes the direct + indirect effects. They observed an aerosol ERF of -1.17 W m^{-2} ; (ranging from -0.71 to -1.44 W m^{-2}) for the period 1850–2000, being greater than forcing RF.

The AQMEII Phase 2 Initiative

The Air Quality Model Evaluation International Initiative (AQMEII) (Rao et al., 2011; Alapaty et al., 2012) (<http://aqmeii.jrc.ec.europa.eu>) was launched in May 2009. Its goal was to promote research on regional air quality model evaluation across European and North American atmospheric modeling communities. According to the importance of atmospheric aerosols, and in order to quantify these effects, the second phase of the AQMEII exercise (Alapaty et al., 2012) emerged in 2012 and focused on online-coupled meteorology-chemistry models. Its goal was to assess how well the current generation of coupled regional scale air quality models can simulate the spatio temporal variability in the optical and radiative characteristics of atmospheric aerosols and the associated feedbacks among aerosols, radiation, clouds, and precipitation. Therefore, it focuses on helping build credibility for coupled models and to provide a better representation of feedback processes, namely, aerosol, radiation, cloud interactions and changes in the air quality-climate interactions that result from emission changes (Alapaty et al., 2012; Galmarini et al., 2015). This will lead to a better understanding of the interactions of climate change and air quality, and to linkages between human health and ecosystems.

EuMetChem COST Action ES1004

On this basis, a coordinated exercise of working groups 2 and 4 of the COST Action ES1004 emerged to take into account the radiative feedbacks of atmospheric aerosol effects on meteorology. The COST Action - European framework for online integrated air quality and meteorology modeling (EuMetChem, <http://eumetchem.info>) - focused on a new generation of online integrated Atmospheric Chemical Transport (ACT) and Meteorology modeling with two-way interactions between different atmospheric processes including chemistry (both gases and aerosols), clouds, radiation, boundary layer, emissions, meteorology and climate. The establishment of such a European framework will enable the EU to develop world class capabilities in integrated ACT/NWP-Climate modeling systems, including research, education and forecasting. In this

initiative, two important episodes with high loads of atmospheric aerosols were analyzed which were identified in the previous AQMEII Phase 2 modeling intercomparison exercise. They were selected for their strong potential for aerosol-radiation and aerosol-cloud interactions (Makar et al., 2015b,a; Forkel et al., 2015).

As a result of the AQMEII Phase 2 initiative and EuMetChem COST Action, several studies into the analysis of the ARI+ACI feedbacks to meteorology in EU and NA have been done. The majority of the studies used an ensemble of simulations. Regarding model evaluation over EU, Brunner et al. (2015) carried out an operational analysis of model performance regarding the key meteorological variables. Among them, WS10 was significantly overpredicted by most models (mainly at night). According to T2, seasonal evolution was well captured with monthly mean biases below 2 K over all the domains. In contrast, solar incoming radiation, precipitation and PBLH, showed a notable spread between models and observations, which led the authors to conclude that important challenges still remain in the simulating relevant meteorological parameters for air quality and for chemistry climate interactions on the regional scale. Im et al. (2015a,b) performed an operational analysis of model performance as regards O₃ and PM₁₀, respectively, over EU and US during the whole 2010. In Im et al. (2015a), the results in both domains suggested that models tended to underestimate surface O₃ and that simulated levels depended on meteorological and chemical model configurations. Besides, they saw that boundary conditions strongly influenced O₃ predictions (which were more important in winter and autumn). According to PM₁₀ (Im et al., 2015b), in the EU domain, all the models underestimated it in almost all seasons and sub-regions (largest underestimations in the Mediterranean). The overestimations in the PM_{2.5} levels suggested that the large underestimations in the PM₁₀ levels mainly came from the natural dust emissions. Over North US, a general underestimation in PM₁₀ was also found, in all seasons and sub-regions, which was mainly due to underpredictions in soil dust. The differences found on AOD at 550 nm in both domains, were attributed to differences in the concentration of the main species and to the way of estimating AOD. Lastly, dust and sea salt emissions can extensively impact the simulated PM. For the NA domain, the study of Campbell et al. (2015) made a multi-model evaluation over NA of the O₃ and PM_{2.5} indicators. They saw over southeast US an overprediction in the extent of VOC-limited chemistry, and how the O₃ indicators, total reactive nitrogen (NO_y) and O₃/NO_y were the most robust (compared to H₂O₂/HNO₃, HCHO/NO_y and HCHO/NO₂), whereas PM_{2.5} was the least one. Moreover, the inter-model agreement for O₃ indicator sensitivities was good, which indicated a governing change to more NO_x-limited conditions in 2010 compared to 2006. As an extension of Campbell et al. (2015), Wang et al. (2015) performed a multi-model evaluation for column

variables against satellite data over NA in 2010. They found a good prediction of radiation budgets and major column gases. Variables AOD, cloud optical thickness, liquid water path, CCN and CDNC were largely underpredicted from most studied simulations. They stated that there were still many uncertainties related to the parameterizations of the aerosol indirect effects. Giordano et al. (2015) performed an operational evaluation of the MACC re-analysis data and to assess their influence as chemical boundary conditions. They found different degrees of agreement between the measurements and the MACC re-analysis (better performed over the US domain). According to the boundary condition effects, a strong influence is shown over O_3 . The CO background concentrations near the boundary domain were closer to observations compared to the interior of both domains. Results showed that inputs in future linked global/regional modeling studies needed to be harmonized of inputs in future linked global/regional modeling studies since emissions differences have an impact on model performance.

Focusing on the effects of including the aerosol feedbacks, Forkel et al. (2015) carried out a study using 8 WRF-Chem simulations over EU in 2010, differing in the models parameterizations. A notable feedback effects were found during the Russian forest fire episode (summer 2010), reducing the seasonal mean solar radiation by 20 W m^{-2} and mean T by 0.25° . As aerosol concentration was underestimated by up to 50%, this results should be considered as a lower limit. The areas where lower indirect aerosol effects were found coincided with those with low aerosol concentration (as the Atlantic and Northern EU). Finally, including the aerosol feedbacks reduces the bias and improves correlations (in some episodes and regions). The domain and time averaged performance statistics did not generally improve. Forkel et al. (2016) and Kong et al. (2015), focused on the COST Action episodes. Forkel et al. (2016) studied the 2010 Russian wildfire episode, where presence of atmospheric aerosols decreased the mean temperature during summer 2010 by 0.25 K over the target area. Kong et al. (2015) focused on both episodes (Russian forest fires and the Saharan dust event). They compared simulation without aerosol effects, direct effect only and direct+indirect effects. When comparing the different simulations with the observations made from a station in Moscow, these authors showed that the best skilled was the aerosol direct effect simulation. According to the model evaluation, a reduction of 10% to 20% of the bias in PM_{10} was found when including aerosol direct effects. The authors concluded that it is important to include the meteorology and chemistry interactions in online-coupled models and, as models performed better when including only direct effects, this indicates that aerosol indirect effect representation needs to be improved.

Makar et al. (2015a,b) also studied the role of feedback effects on model meteorological and chemical performance, respectively, for EU and NA in 2006 and 2010. According to the

aerosol effects on weather (Makar et al., 2015b), they compared two simulations, one without any feedback effects and a second simulation including the aerosol feedbacks. They saw that including both feedbacks types systematically changed to forecast predictions of meteorological variables in, both time and space terms, with the strongest impacts occurring in the summer and near large sources of pollution. After taking into account only direct effects, reductions in T, surface downward and upward shortwave radiation, precipitation and PBLH were found, while an increasing of upward shortwave radiation, in both domains was noted. In contrast, the aerosol feedbacks response of models taking into account both direct and indirect effects, varied across models, suggesting the details of implementation of the indirect effect have a large impact on model results, and hence should be a focus for future research. These authors also found that feedback implementation improved forecasts of meteorological parameters (as T2 and precipitation), which suggests that meteorological forecasts could be improved by using fully coupled feedback models, or by adding improved climatologies of aerosol properties. Regarding the aerosol feedbacks on chemistry (Makar et al., 2015a), they changed the ozone-forming chemical regime, within NO_x^- and VOC-limited environments. Moreover, feedbacks have an important influence on biogenic hydrocarbon emissions and concentrations, showing in NA an average decrease of isoprene concentration were found and on the contrary, in direct effect simulations during the Russian forest fire. Feedbacks were also important, as it affected atmospheric chemical transport (such as forest fires plumes). During summer, O_3 was improved whereas performance for PM was decreased. This suggests that current parameterizations for in- and below cloud processes, may over- or under-predict the strength of these processes. In that study, the authors recommended using online-coupled models when simulating large scale urban/industrial and forest fire plumes and process parameterization comparison for further future studies. For EU and NA domain, Knote et al. (2015) made a comparison of the tropospheric gas-phase mechanisms used in AQMEII Phase 2. They intercompared their performance under tight constraints for environmental parameters, photolysis rates, removal processes and emissions. Besides, they computed box model simulations representing mean boundary layer concentrations, and different sets of conditions. For the O_3 box model, differences between models of 4 ppbv (5%) were found for in both domains. Larger differences for predicted concentrations were found for NO_x (up to 25%), OH (40%) HO_2 (25%) and particularly NO_3 by more than 100%. The authors concluded that the gas-phase mechanism choice is significant in model simulations for regulatory purposes and emission scenarios since uncertainties still exist.

San José et al. (2015) studied the inclusion of the aerosol feedback within the WRF-Chem model and the gas-phase chemistry CBM-Z. They used two simulations, one without any feed-

back effects and a second simulation with both the direct and the indirect aerosol effects. Results shown that including the aerosol feedbacks increased solar radiation, mainly over cloudy areas (up to 70%, due to the indirect aerosol effects) and decreased over sunny areas (10% through scattering). Water vapor also increased (around 3%) and PBLH decreased (20%) over the entire domain (but for the Sahara, where the highest load are found).

Curci et al. (2015) focused on EU in July 2010 and calculated the optical properties from several AQMEII Phase 2 simulations by applying the same assumptions. The assumption of the mixing ratio was found to be the most important factor of uncertainty on simulated AOD and SSA (30 to 35%). For the ASY, the choice of the mixing state is the order of 10%. In contrast, the core composition in the core-shell representation resulted crucial for SSA but not important for AOD. These authors concluded that future modeling research should be focused on accurate representation of the aerosol mixing state to reduce the uncertainty of simulated aerosol properties. Last, a sensitivity study of the microphysic scheme is done in Baró et al. (2015) and will be described in Chapter 2.

Overall, the studies carried out under the umbrella of AQMEII Phase 2 and the EuMetChem COST Action initiatives have pointed out the improvements of using online-coupled models and also that uncertainties as to the aerosol-radiation-cloud interactions still remain. In Galmarini et al. (2015) an overview of these initiatives is compiled.

1.2 Objectives

As previously shown, the main hypothesis on which this Ph.D. Thesis stands on is that climate-chemistry-aerosol-radiation-cloud feedbacks are important processes occurring in the atmosphere, and that they should be accurately simulated in order to reduce the uncertainties related to climate change projections. The study of these feedbacks requires fully-coupled meteorology, climate and chemistry models. To further deepen the insights of this main hypothesis, the main objective is defined as the *characterization of the uncertainties in the climate-chemistry-aerosol-radiation-cloud system associated to the aerosol direct and indirect radiative effects caused by aerosols over Europe, employing an ensemble of fully-coupled climate and chemistry model simulations.*

The development of this Thesis has been done within the framework of AQMEII Phase 2 and the EuMetChem COST Action initiatives, contributing to study some of the top ranked interactions recommended by the expert survey, as aerosol direct effects on radiation and temperature.

The specific objectives can be summarized as:

- Investigate the impact of different cloud microphysics schemes within two one-year WRF-Chem simulations, over Europe.
- Estimate the influence of biomass burning (BB) aerosols on spatially-distributed winds over Europe and, specially over the Russian area.
- Assess whether the outputs of an ensemble of regional on-line coupled models simulations including aerosol radiative feedbacks, during two important atmospheric aerosol episodes of the year 2010, improves the prognostic for maximum, mean and minimum temperature at 2 meters over Europe.
- Assess the representation of the ARI+ACI interactions in regional-scale integrated models when simulating the climate-chemistry-cloud-radiation system.

As this Thesis has been undertaken under the umbrella of the AQMEII Phase 2, this had led to contribute to its general objectives:

1. Exchanging expert knowledge in regional air quality modeling.
2. Identifying knowledge gaps in air quality science.
3. Developing methodologies to evaluate uncertainty in air quality modeling building a common strategy on model development and future research priorities.
4. Establishing methodologies for model evaluation to increase knowledge on processes.
5. Support the use of models for policy development preparing coordinated research projects and inter-comparison exercises.

Having contributed to the mentioned initiatives have provided us the analytical tools to reach a better understanding of the air quality-climate interactions as well as to value the various physical and chemical processes incorporated in the coupled modeling systems. We have taken profit from the valuable database generated in this initiatives, which will serve to develop the main objective of this Thesis which goes beyond the initiative's objectives.

As derived objectives, thanks to the huge and valuable data base generated, it could be used to study other interest factors in order to establish an air quality climatology over the target areas. A data base has been created with the results from the different simulations done under this Thesis. This data base have had an appropriate organization and format according to the specific requirements in AQMEII and is available to the members of the project as well as the scientific community.

It is interesting to highlight that for the first time (to our knowledge), the direct and indirect effect of aerosols (natural and anthropogenic) have been studied over a whole year by an ensemble of regional climate-chemistry simulations, and thus not confined to a short period of time or starting from an episodic approach.

1.3 Scope and structure

The present document shows the discussion and main results of this Ph.D. Thesis entitled: *Analysis of the aerosol-radiation-cloud interactions through the use of regional climate/chemistry coupled models*. As stated above, the document does not include a Chapter devoted to the methodology itself since this Thesis is structured as a compilation of different studies. Each topic composes an organized view of the analysis of aerosol-radiation-cloud interactions. Therefore each Chapter/topic includes the description of the methodology, together with a more specialized review of the state-of-the art.

In order to accomplish with the defined objectives, the Thesis document is organized as follows. **Chapter 1** reviews the state of the art of the atmospheric aerosols. The importance of atmospheric aerosols to issues of social concern has motivated a number of research initiatives intended to describe their loading, distribution, and properties and to develop understanding of the controlling processes to address the aerosol influences on climate. Atmospheric aerosols exert a substantial influence on Earth's climate, and the current interest in studying atmospheric aerosol has grown given the need to quantify this influence. Hence, this section focuses on the aerosols role in modifying the Earth's radiative balance, and does not focus so much on the impacts of aerosols on health, which have been widely covered in the scientific literature. According all this information, the objectives of this Ph.D. Thesis have been stated.

The first topic covered in this Thesis has to do with the configuration of the on-line coupled model, especially in those aspects related to microphysics parameterization. **Chapter 2** shows a sensitivity analysis of the microphysics scheme used in the WRF-Chem model. Aerosol indirect effects are related to the microphysical processes, since they govern the formation, growth and dissipation of hydrometeors. Here, the differences when using two microphysics schemes which are able to take into account the aerosol-radiation-cloud interactions are analyzed and discussed.

Once the configuration of the model is set up (by confirming the selected microphysics scheme), the atmospheric aerosol effects on meteorological variables during a case study were estimated. This topic is covered in **Chapter 3**, which elucidates the impact of BB aerosols on surface winds for the Russian heat wave and wildfires episode between 25th July and 15th August 2010. An important component of atmospheric aerosols are those coming from BB,

which strongly absorbs solar radiation, having an impact on cloud processes and playing an important role in the Earth's climate system.

After studying this episode, this Thesis explores the ability of an ensemble of simulations to elucidate aerosol-radiation-cloud interactions. This is reflected in **Chapter 4**, which includes an assessment of whether the inclusion of atmospheric aerosol radiative feedbacks of an ensemble of on-line coupled models improves the simulation results for maximum, mean and minimum temperature at 2 meters over Europe or not.

Since a cloud free condition prevailed during the Russian forest fires (and therefore aerosol impacts are produced mainly in the ARI), in order to be able to study the ACI, in **Chapter 5**, an assessment of the representation of aerosol-cloud interactions interactions in regional-scale integrated models when simulating the climate-chemistry-cloud-radiation system is done. Up to now, all the collective studies performed used global models; regional climate analysis do not usually take into account ARI+ACI. Hence, It complements the temperature collective analyses shown in **Chapter 4**.

Last, **Chapter 6** provides not only the main conclusion drawn from this Thesis, but also suggestions for future works derived from continuing the research line done within the framework of this Ph.D. Thesis.

Chapter 2

Sensitivity analysis of the microphysics scheme in WRF-Chem contributions to AQMEII Phase 2

Published in Atmospheric Environment: Baró, R., Jiménez-Guerrero, P., Balzarini, A., Curci, G., Forkel, R., Grell, G., Hirtl, M., Honzak, L., Langer, M., Pérez, J.L., Pirovano, G., San José, R., Tuccella, P., Werhahn, J., and Zabkar, R (2015). Sensitivity analysis of the microphysics scheme in WRF-Chem contributions to AQMEII Phase 2. Atmospheric Environment, 115, 620-629.

The parameterization of cloud microphysics is a crucial part of fully-coupled meteorology-chemistry models, since microphysics governs the formation, growth and dissipation of hydrometeors and also aerosol cloud interactions. The main objective of this study, which is based on two simulations for Europe contributing to the Phase 2 of the Air Quality Model Evaluation International Initiative (AQMEII), is to assess the sensitivity of WRF-Chem to the selection of the microphysics scheme. Two one-year simulations including aerosol cloud interactions with identical physical-chemical parameterizations except for the microphysics scheme (Morrison -MORRAT vs Lin -LINES) are compared. The study covers the difference between the simulations for two three-month periods (cold and a warm) during the year 2010, allowing thus a seasonal analysis. Overall, when comparing to observational data, no significant benefits from the selection of the microphysical schemes can be derived from the results. However, these results highlight a marked north-south pattern of differences, as well as a decisive impact of the aerosol pollution on the results. The MORRAT simulation resulted in higher cloud water mixing ratios over remote areas with low cloud condensation nuclei (CCN) concentrations, whereas

the LINES simulation yields higher cloud water mixing ratios over the more polluted areas. Regarding the droplet number mixing ratio, the Morrison scheme was found to yield higher values both during winter and summer for nearly the entire model domain. As smaller and more numerous cloud droplets are more effective in scattering shortwave radiation, the downwelling shortwave radiation flux at surface was found to be up to 30 W m^{-2} lower for central Europe for the MORRAT simulation as compared to the simulation using the LINES simulation during wintertime. Finally, less convective precipitation is simulated over land with MORRAT during summertime, while no almost difference was found for the winter. On the other hand, non-convective precipitation was up to 4 mm lower during wintertime over Italy and the Balkans for the case of including Lin microphysics as compared to the MORRAT simulation.

2.1 Introduction

Anthropogenic aerosols exert a substantial influence on Earth's climate, and the current interest in studying the atmospheric aerosol has increased due to the need to quantify this influence. Aerosols influence climate by modifying both the global energy balance through absorption and scattering of radiation (direct effects), the reflectance and persistence of clouds and the development and occurrence of precipitation (indirect effects)(Ghan and Schwartz, 2007; Forkel et al., 2012). Aerosols act as CCN (first indirect effect), thus affecting cloud albedo and lifetime (Twomey, 1977; Lohmann and Feichter, 2005) and their impacts also include an increase in liquid water content, cloud cover and lifetime of low level clouds and suppression or enhancement of precipitation, which is the second indirect effect (Bangert et al., 2011).

Indirect effects are related to the microphysical processes, which play an important role in how convection develops. Cloud microphysical processes are also very important to predictions of the atmosphere at temporal scales ranging from minutes to centuries, owing to the effects of latent heat release due to the phase changes of water and the interactions between clouds and radiation (Stensrud, 2007).

Several studies have addressed the influence of the aerosols in microphysics. For example, Rosenfeld et al. (2008) studied how aerosol influences precipitation, showing that clouds with lower amounts of CCN rain out more quickly than polluted clouds, which evaporate water before precipitation can occur. Twohy et al. (2005) evaluated the aerosol indirect effect in marine stratocumulus clouds, showing that clouds formed in air with high particle concentrations had higher droplet concentrations, smaller droplet sizes, and lower drizzle rates.

As aerosol is one of the key properties in simulations of the Earth's climate (Kinne et al., 2006; Grell and Baklanov, 2011), fully-coupled meteorology-climate, and chemistry models are

required to provide the possibility to account for these feedback mechanisms between simulated aerosol concentrations and meteorological variables in numerical climate and weather prediction models. Within this context, the microphysics parametrization scheme accounts for the processes that govern the formation, growth and dissipation of cloud particles (freezing, sublimation, evaporation, melting and deposition) (Jérez et al., 2013). There are several schemes describing these interactions. Most of these schemes are “single-moment” schemes, meaning that only the total mixing ratio is predicted. “Double-moment” implies additional prediction of number concentrations. If the aerosol effect on microphysical processes and cloud/precipitation evolution is studied, the use of a double-moment scheme will be necessary. The prediction of the number concentration will affect simulated particle sizes and hence gravitational settling, collision/coalescence and cloud radiative properties, and precipitation efficiency (Ghan et al., 1997).

In order to investigate the impact of different cloud microphysics schemes on results of WRF-Chem, two one-year simulations for Europe from the AQMEII Phase 2 modeling exercise are analysed. Both simulations include aerosol cloud interactions for grid scale clouds and differ only by the choice of the cloud physics parameterization.

In this sense, the main objective of this paper focuses on the following question: Which is the sensitivity of WRF-Chem simulations to the selection of the cloud microphysics schemes? Hence, this work is not focused on characterizing the aerosol radiative effects and feedbacks, which are covered by the study of Forkel et al. (2015); Curci et al. (2015); San José et al. (2015) (in this issue).

2.2 Methodology

The WRF-Chem model (Grell et al., 2005) has been used for assessing two different simulations differing only in the microphysics scheme selected. WRF-Chem allows an interactive coupling and simulates the emission, transport, mixing, and chemical transformation of trace gases and aerosols simultaneously with the meteorology. The model is used for investigation of regional-scale air quality, field program analysis, and cloud-scale interactions between clouds and chemistry. In contrast with the coarse spatial resolution of GCMs, feedback processes over a wide range of spatial scales can be investigated with WRF-Chem. The simulations have been done within the framework of AQMEII Phase 2 (Alapaty et al., 2012) (<http://aqmeii.jrc.ec.europa.eu>) which emerged in 2012 and focuses on online-coupled meteorology-chemistry models. Its goal is to assess how well the current generation of coupled regional scale air quality models can simulate the spatio temporal variability in the optical

and radiative characteristics of atmospheric aerosols and associated feedbacks among aerosols, radiation, clouds, and precipitation.

The target domain covers Europe for the year 2010. The spatial configuration employed consists of one single domain centered on latitude 50°N, and longitude 12°E. The Lambert Conformal projection has been used according to the project specifications. The vertical model coordinate system consists of 33 vertical sigma levels, the lowest layer height at 24 m and the model top 50 hPa. The horizontal resolution is 23 km and the total number of grid points is 60.750.

The simulations were integrated by continuous runs with 2-days of time slices. The chemistry was restarted from the previous run whereas the meteorology is restarted each time slot. This keeps the simulations consistent with large-scale analysis fields while allowing for the feedback processes to work. The simulation was driven by ECMWF operational analyses (with data at 00 and 12 UTC) and with respective forecasts (at 3/6/9 etc. hours), so that the time interval of meteorological fields used for boundary conditions was 3 hours. The chemical initial conditions (IC) were provided by the European Centre for Medium-Range Weather Forecasts (ECMWF) IFS-MOZART model, which are available in 3-hour time intervals and provided in daily files with 8 times per file.

2.2.1 Emissions

The anthropogenic emissions used were provided by the Netherlands Organization for Applied Scientific Research (TNO). The dataset is a follow-on to the widely used TNO-MACC database (Pouliot et al., 2012). The provided species are CH₄, CO, NO_x, SO_x, non-methane VOC, NH₃, PM_{coarse}, PM_{2.5}. A separate PM bulk composition profile file is composed based on the information by source sector by country. The different chemical components represented are EC, OC, SO₂, sodium and other mineral components.

Biogenic emissions were estimated using MEGAN (Guenther et al., 2006) which are calculated online. MEGAN is a global model with a base resolution of around 1 km that serves for estimating the net emission of gases and aerosols from terrestrial ecosystems into the atmosphere. Driving variables include land cover, weather, and atmospheric chemical composition.

Fire emissions data were obtained from the IS4FIRE Project (<http://is4fires.fmi.fi>). The emission dataset is estimated by re-analysis of fire radiative power data obtained by MODIS instrument onboard of Aqua and Terra satellites. The fire assimilation system information is processed into the emission input for the System for Integrated modeling of Atmospheric composition (SILAM) for a subsequent evaluation of the impact of fires on atmospheric composition

and air quality. The emission data is available for Europe with 0.1×0.1 degree spatial resolution.

2.2.2 Model configuration

Within all WRF-Chem simulations included in AQMEII Phase 2 (see Forkel et al. (2015) for further details), the focus of this paper is on two equal simulations differing only in the microphysics scheme. The first simulation (MORRAT) uses the Morrison microphysics scheme (Morrison et al., 2009). The second simulation (LINES) relies on the Lin microphysics scheme (Lin et al., 1983). WRF-Chem configurations used include the following options (Table 2.1): RADM2 chemical mechanism (Stockwell et al., 1990); MADE/SORGAM aerosol module (Schell et al., 2001) including some aqueous reactions; Fast-J photolysis scheme (Fast et al., 2006); Goddard shortwave radiation parameterization (Chou and Suarez, 1994); Yonsei University scheme (YSU) (Hong and Pan, 1996) for the Planetary Boundary Layer (PBL); dry deposition follows the Wesely resistance approach (Wesely, 1989), while wet deposition is divided into convective wet deposition and grid-scale wet deposition (Easter et al., 2004).

Table 2.1: Model configuration options.

OPTION	NAME
Gas phase mechanism	RAMD2 (Stockwell et al., 1990)
Aerosol mechanism	MADE/SORGAM (Schell et al., 2001)
Organic module	SORGAM (Schell et al., 2001)
Aerosol size	3 modes (Aitken, accumulation and coarse)
Planetary Boundary Layer	YSU (Hong and Pan, 1996)
Dust model	MOSAIC MADE/SORGAM (Schell et al., 2001)
Photolysis option	Fast-J (Fast et al., 2006)
Microphysics option	Lin (Lin et al., 1983) modified by Chapman et al. (2009)
Shortwave radiation	Morrison (Morrison et al., 2009)
Longwave radiation	Goddard (Chou and Suarez, 1994)
Prognostic cloud condensation nuclei	RRTM (Iacono et al., 2008)
Direct feedback	Yes
Indirect feedback	Yes
Wet deposition	Yes
Wet deposition	Gris scale wet deposition (Easter et al., 2004)
Dry deposition	Wesely resistance approach (Wesely, 1989)

2.2.3 Microphysics schemes

The Morrison scheme (Morrison et al., 2009) is a double moment scheme including the following six species of water: vapour, cloud droplets, cloud ice, rain, snow and graupel/hail. While single-moment bulk microphysics schemes only predict the mixing ratios of hydrometeors, double-moment methods include an additional prognostic variable that is related to the size distribution, such as number concentration. Prognostic variables include number concentrations and mixing ratios of cloud ice, rain, snow and graupel/hail, cloud droplets and water vapour (total 10 variables). Moreover, several liquid, ice, and mixed-phase processes are included. Particle size distributions are treated using gamma functions, with the associated intercept and

slope parameters derived from the predicted mixing ratio and number concentration.

The Lin scheme, based on Lin et al. (1983) and Rutledge and Hobbs (1984), is a single moment scheme including some modifications, as saturation adjustment following Tao et al. (1989) and ice sedimentation, which is related to the sedimentation of small ice crystal (Mitchell et al., 2008). It includes six classes of hydrometeors: water vapor, cloud water, rain, cloud ice, snow, and graupel. This scheme was one of the first to parameterize snow, graupel, and mixed-phase processes (such as the Bergeron process and hail growth by riming) and it has been widely used in numerical weather studies.

According to Li et al. (2008), the one-moment microphysical scheme is unsuitable for assessing the aerosol-clouds interactions as it only predicts the mass of cloud droplets and does not represent the number concentration of cloud droplets. The prediction of two moments provides a more robust treatment of the particle size distributions, which is a key for computing the microphysical process rates and cloud/precipitation evolution. Therefore, prediction of additional moments allows greater flexibility in representing size distributions and hence microphysical process rates.

In this sense, although the Lin microphysics is presented as a single moment scheme, WRF-Chem model allows to transform the single into a double moment scheme. This implementation is described in Chapman et al. (2009). Following Ghan et al. (1997), a prognostic treatment of cloud droplet number was added, which treats water vapour and cloud water, rain, cloud ice, snow, and graupel. The autoconversion of cloud droplets to rain droplets depends on droplet number follows Liu et al. (2005). Droplet-number nucleation and (complete) evaporation rates correspond to the aerosol activation and resuspension rates. Ice nuclei based on predicted particulates are not treated. However, ice clouds are included via the prescribed ice nuclei distribution following the Lin scheme. Finally, the interactions of clouds and incoming solar radiation have been implemented by linking simulated cloud droplet number with the Goddard shortwave radiation scheme, representing the first indirect effect, and with Lin microphysics, which represents the second indirect effect (Skamarock et al., 2005). Therefore, droplet number will affect both the calculated droplet mean radius and cloud optical depth when using Goddard shortwave radiation scheme.

In order to summarize the main differences between the two schemes, cloud droplets spectrum is represented by gamma distribution for Morrison scheme (Morrison et al., 2009) whereas an exponential distribution is used for Lin. All the other hydrometer types are represented by the exponential function in the Morrison scheme.

2.3 Results and discussion

2.3.1 Sensitivity study

The difference between MORRAT and LINES for several WRF variables (such as cloud water mixing ratio, droplet number mixing ratio, 2-m temperature, accumulated cumulus and total grid precipitation and shortwave radiation) is estimated, giving an idea of the sensitivity of the results to the selected microphysics scheme. Mean values for a cold period (January-February-March, JFM) and a warm period (July-August-September, JAS) are considered.

The results of the differences between the two simulations are presented in this section (Figures 2.1 to 2.4), where MORRAT has been taken as reference. That is, positive (negative) values indicate that MORRAT simulates higher (lower) levels of the studied variable.

Figure 2.1 shows the mean values of cloud water mixing ratio (QCLOUD) and droplet number mixing ratio (QNDROP). MORRAT and LINES simulate similar cloud water mixing ratio for both seasons, with MORRAT providing higher QCLOUD in winter over the northeastern part of the domain, between 60°N to 70°N (+0.05 g kg⁻¹) and remote areas (Mediterranean Sea and Atlantic Ocean; western Scandinavian peninsula; here the differences are up to +0.10 g kg⁻¹) where the CCN concentration is lower. LINES gives higher values of this mixing ratio over central Europe (-0.06 g kg⁻¹) and the British Islands (-0.05 g kg⁻¹). Differences over land are negligible during summertime, but MORRAT simulates a notably higher QCLOUD (up to +0.08 g kg⁻¹) over the Atlantic Ocean during this part of the year.

Regarding the droplet number mixing ratio, MORRAT simulations indicate higher values of QNDROP both during winter and summer for nearly all the domain of simulation. Highest differences are found for JFM (+2.5·10⁻⁷ kg⁻¹). In summer, QNDROP is more similar between the two runs. As cloud water mixing ratio values are similar for MORRAT and LINES, higher droplet number mixing ratio in MORRAT indicates that cloud droplets have a lower diameter in MORRAT than in LINES, especially during winter. Therefore, smaller and more numerous cloud droplets as simulated in MORRAT should be more effective in scattering shortwave radiation. This is clearly observed in Figure 2.2, showing the differences of the mean shortwave downwelling flux at bottom (SWDNB) and shortwave upwelling flux at the top of the atmosphere (SWTU), for JFM and JAS over 2010. According to these variables, MORRAT has lower(higher) levels for SWDNB(SWTU) radiation up to 30 W m⁻² (20 W m⁻²) for central Europe during JFM especially during wintertime, reducing to a general MORRAT-LINES difference of -15 W m⁻² for SWDNB for JAS, with a maximum difference of -20 W m⁻² in downwelling shortwave radiation at bottom.

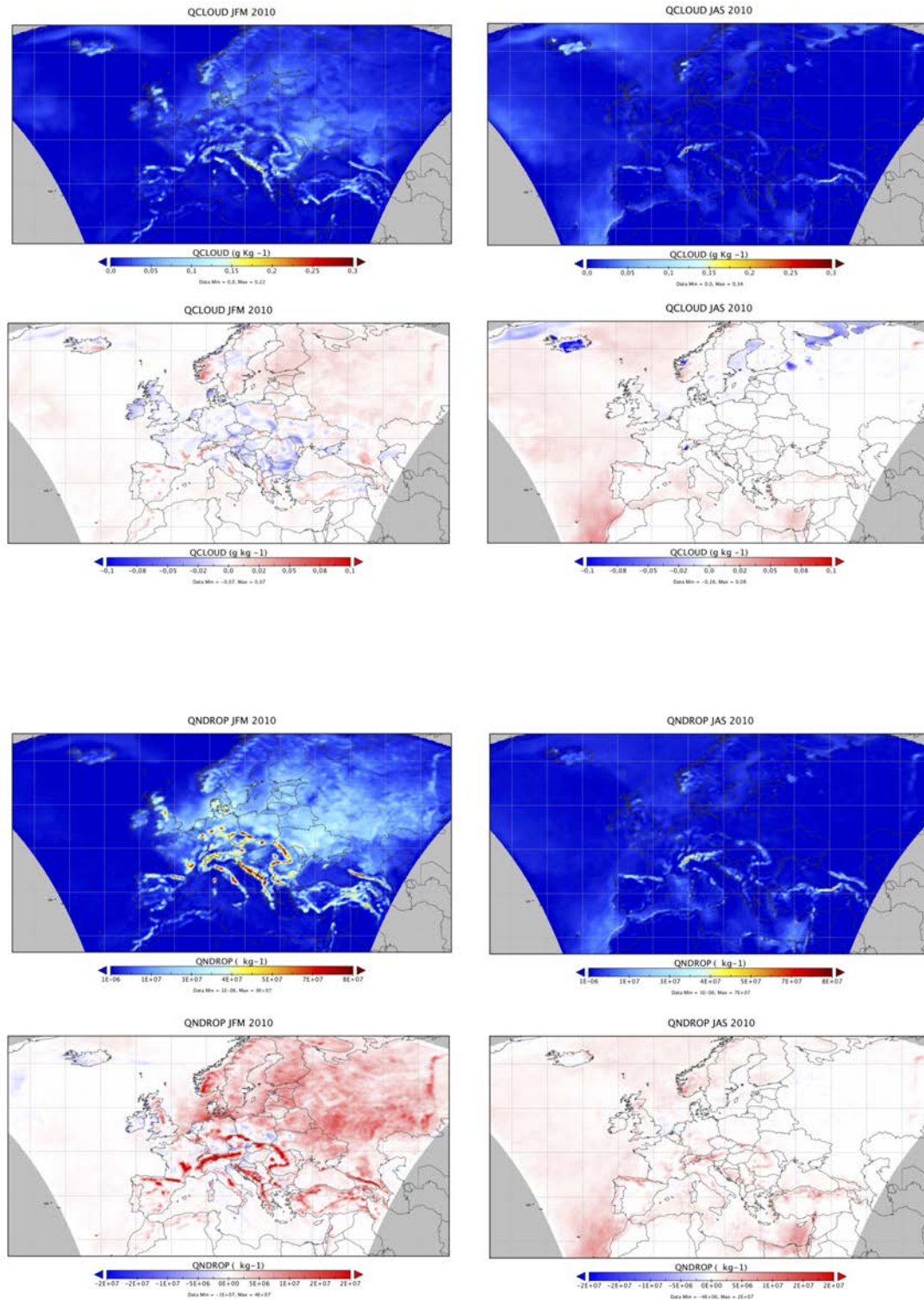


Figure 2.1: (Top panel): (First row) Winter 2010 (left) and summer 2010 (right) mean cloud water mixing ratio (QCLOUD) in MORRAT simulations (g kg^{-1}). (Second row) Winter 2010 (left) and summer 2010 (right) mean differences between MORRAT and LINES (g kg^{-1}). (Bottom panel) Id. for droplet number mixing ratio (QNDROP) (kg^{-1}).

This fact is conditioned by the higher levels of cloud droplets in MORRAT, leading to a more effective scattering. Conversely, MORRAT-LINES difference for SWTU is maximum (+25

W m^{-2}) over the Atlantic Ocean both for JFM and JAS; and minimum ($+1 \text{ W m}^{-2}$) in the cold period over north-eastern Europe (Russia, Baltic Countries and Scandinavia).

However, taking a look at 2-m temperature in Figure 2.3, higher winter average temperatures are simulated with MORRAT than with the case of including Lin microphysics in the northernmost part of the domain (Nordic countries and Russia, 50°N to 70°N , with differences of $+2.5 \text{ K}$). Only small differences are observed for the Mediterranean area and the Atlantic Ocean, where LINES simulates slightly higher temperatures (differences under -0.2 K). The spatial pattern of differences for QNDROP and T2 are highly correlated. MORRAT simulations having higher QNDROP (and therefore, higher levels of cloud droplets) cause lower temperature during the day (as less shortwave radiation reaches the ground), but higher temperature during night (because of more longwave radiation reflected towards the ground, not shown). Between the two effects, the latter prevails, and thus the daily average temperature increases (as observed during wintertime, when QNDROP differences are higher). Furthermore, in winter at these latitudes shortwave heating will be smaller so the longwave effect will be more important. This phenomenon is also described in Forkel et al. (2015).

Last, Figure 2.4 shows the differences of the accumulated convective precipitation (RAINNC) and accumulated total grid scale precipitation (RAINNC). As previously stated in Figure 2.1, MORRAT showed higher levels of QNDROP, involving a higher droplet number mixing ratio, but less liquid water droplet. This could be related to the lower convective precipitation simulated over land with MORRAT during summertime (difference up to -1.0 mm over land), while no important differences are found for winter. On the other hand, for non-convective precipitation, highest differences are found over Italy and the Balkans, with negative MORRAT-LINES values up to -4.0 mm (differences are negligible for summertime).

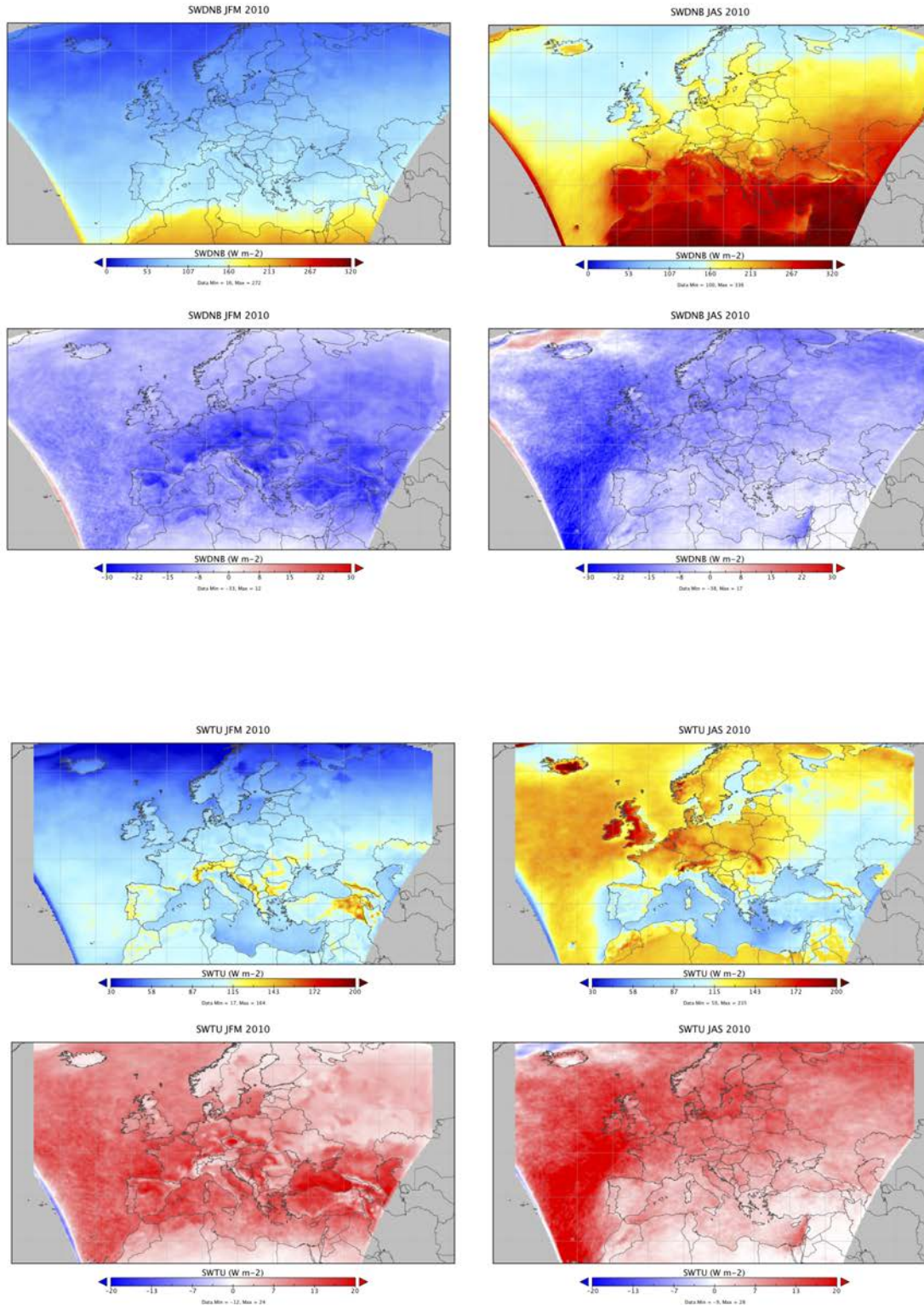


Figure 2.2: (Top panel): (First row) Winter 2010 (left) and summer 2010 (right) mean downwelling shortwave flux at bottom (SWDNB) in MORRAT simulations (W m^{-2}). (Second row) Winter 2010 (left) and summer 2010 (right) mean differences between MORRAT and LINES (W m^{-2}). (Bottom panel) Id. for upwelling shortwave flux at the top of the atmosphere (SWTU) (W m^{-2}).

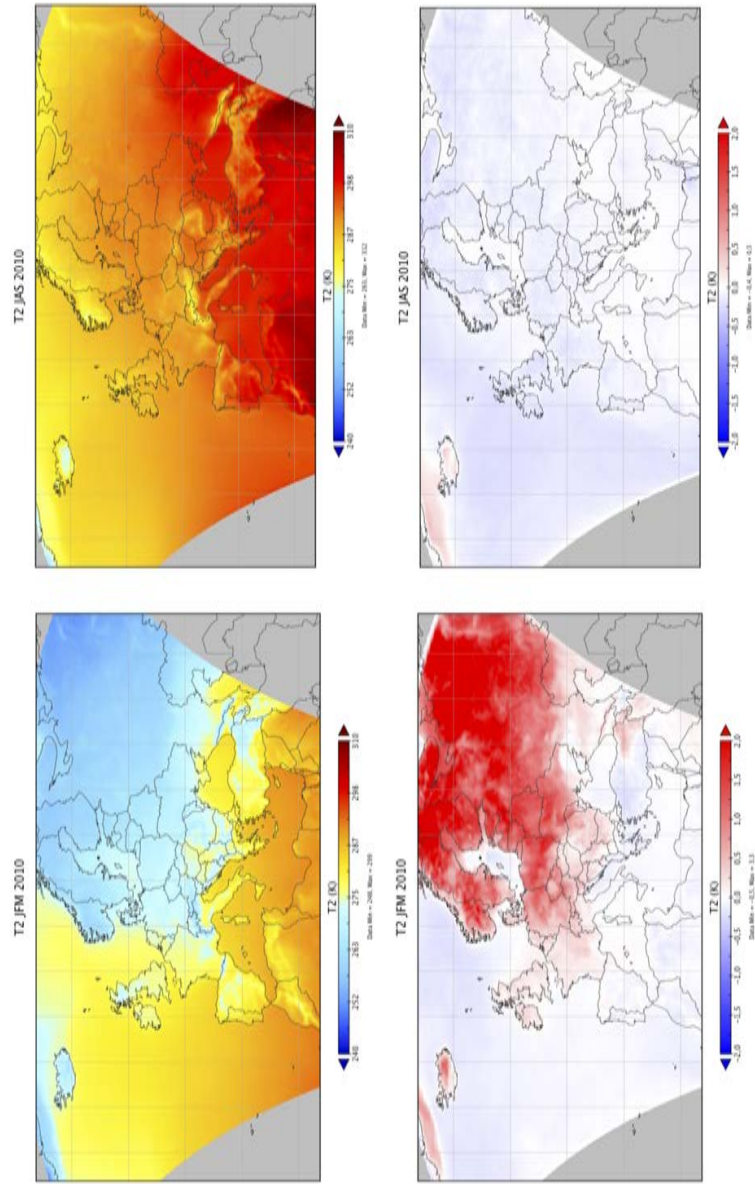


Figure 2.3: (First row) Winter 2010 (left) and summer 2010 (right) T2 in MORRAT simulations (K). (Second row) Winter 2010 (left) and summer 2010 (right) mean differences between MORRAT and LINES (K).

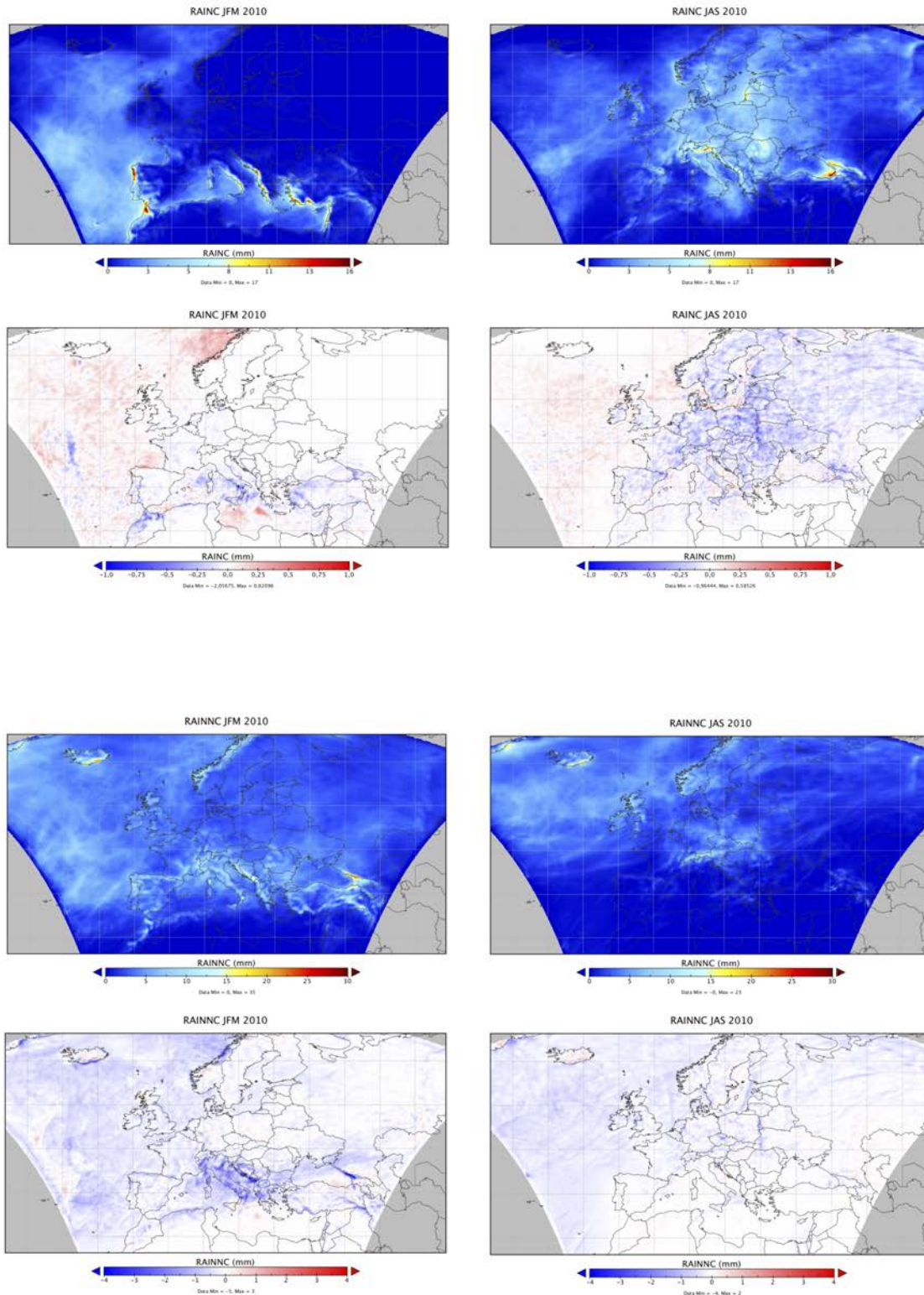


Figure 2.4: (Top panel): (First row) Winter 2010 (left) and summer 2010 (right) mean convective precipitation (RAIN) in MORRAT simulations (mm). (Second row) Winter 2010 (left) and summer 2010 (right) mean differences between MORRAT and LINEs (mm). (Bottom panel) Id. for grid scale precipitation (RAINNC) (mm).

2.3.2 Numerical model comparison and evaluation

This section is devoted to the evaluation of the two simulations against observations, when available. The reader should bear in mind that the aim of this paper is not to provide a comprehensive model evaluation, which has been already done within the study performed by Im et al. (2015a,b) for pollutants and Brunner et al. (2015) for meteorology; studies also developed under the umbrella of AQMEII Phase 2. However, in order to highlight the differences between the two simulations, several variables are evaluated using the web-based platform for model intercomparison and multi-model ensemble analysis ENSEMBLE (<http://ensemble2.jrc.ec.europa.eu/public/>) hosted at the Joint Research Centre (JRC) (Bianconi et al., 2004; Galmarini et al., 2012). Observations include hourly data collected by the AirBase, AERONET and the European Monitoring and Evaluation Programme (EMEP). Several classical statistics are used, such as bias, normalized bias (NB), mean fractional bias (MFB), normalized mean square error (NMSE), root mean square error (RMSE) and the Pearson correlation coefficient (PCC).

As the results presented in Section 2.3.1 indicate a marked north-south difference in the patterns (e.g., for T2 or QNDROP), results have been divided into two domains, northern (from 50°N to 70°N) and southern Europe (from 30°N to 50°N), to check whether the models present any spatial-related bias. Table 2.2 shows the performed statistics over both domains for those variables with observations available within the ENSEMBLE system. Broadly, the sensitivity of the results to the selection of the microphysics scheme is very limited, since the results of the model evaluation are quite similar for both simulations in northern and southern Europe. No significant benefits from the selection of the microphysics schemes can be derived from the results. For instance, both simulations underpredict air pollutants such as SO₂, PM₁₀ and PM_{2.5} in all domains. The most importance differences are found for tropospheric ozone (O₃) in the southern domain (30°N to 50°N), where the bias is 8.3 $\mu\text{g m}^{-3}$ for MORRAT and reduces to 2.8 $\mu\text{g m}^{-3}$ in LINES. However, the differences in the PCC are low for all these pollutants. In this sense, it should be highlighted that the selection of the different microphysics does not seem to improve the time reproducibility of the simulations in both domains.

Table 2.2: Statistical evaluation of MORRAT and LINES simulations against variables with available observations within the ENSEMBLES system

VARIABLE	SIMULATION	BIAS ¹	NB ²	MFB ²	NMSE ¹	RMSE ¹	PCC
NORTHERN EUROPE							
TEMP	MORRAT	-0.4557	-0.0016	0.0051	0.0001	2.8577	0.9582
	LINES	-0.5845	-0.0021	-0.0014	0.0001	3.0333	0.9553
PM_{2.5}	MORRAT	-5.9173	-0.4190	-0.3183	2.2049	15.9850	0.3044
	LINES	-6.7524	-0.4783	-0.3889	2.6480	16.5949	0.2406
O₃	MORRAT	-7.4301	-0.1235	-0.0641	0.1809	23.9560	0.6011
	LINES	-10.873	-0.1807	-0.1053	0.2158	25.2972	0.5975
SO₂	MORRAT	-2.7626	-0.5598	-0.6135	4.4752	6.9260	0.4979
	LINES	-2.8481	-0.5951	-0.6981	4.9115	6.9625	0.5078
PM₁₀	MORRAT	-7.7279	-0.3826	-0.2763	0.5053	22.9020	0.1940
	LINES	-8.9224	-0.4417	-0.3450	0.5511	23.5194	0.1518
SOUTHERN EUROPE							
TEMP	MORRAT	-0.8091	-0.0028	-0.0018	0.0001	3.1894	0.9374
	LINES	-0.7816	-0.0027	-0.0018	0.0001	3.1850	0.9379
PM_{2.5}	MORRAT	-3.5182	-0.3184	-0.3184	0.9605	8.9402	0.3782
	LINES	-4.0872	-0.3699	-0.3768	1.0789	9.1112	0.3733
O₃	MORRAT	8.2815	0.1332	0.1185	0.1632	26.7421	0.5432
	LINES	2.7612	0.0444	0.0709	0.2416	25.3991	0.5467
SO₂	MORRAT	-4.4496	-0.6080	-0.5337	25.9405	23.3353	0.2005
	LINES	-5.1143	-0.6984	-0.6916	34.1846	23.3353	0.2005
PM₁₀	MORRAT	-21.931	-0.5915	-0.5556	3.4689	44.1400	0.2807
	LINES	-22.883	-0.6172	-0.6061	3.7784	44.5957	0.2818

¹RMSE and BIAS are in units of K for T; $\mu\text{g m}^{-3}$ for PM₁₀ and O₃; ppbv for SO₂, mm for PREC and W m^{-2} for SWUPB and SWDNB.

²Parts per units.

Table 2.3 shows the comparison of the statistics for those variables whose observations are not included within ENSEMBLE (observations not available) at receptors taking MORRAT simulation as reference. This has allowed comparing the behaviour of LINES with respect to MORRAT. Hence, LINES minus MORRAT statistics are computed: as an example, a positive bias for a certain variable implies that LINES has a higher value of that variable. The differences for total precipitation are negligible both for northern Europe and southern Europe. The biases are below +0.01 mm, with LINES giving higher precipitation for both domains of study; normalized biases are under +5%, indicating LINES tendency for a higher precipitation. However, a low correlation is observed for both simulations with respect to precipitation (0.52 in northern Europe and 0.62 in southern Europe), indicating a different timing of precipitation in both simulations. Last, shortwave radiation differences are also low (under 15% for both shortwave upwelling flux at the bottom [SWUPB] and SWDNB), being these variables strongly correlated between the two simulations.

Table 2.3: Comparison of the two simulations taking MORRAT as reference for those variables not available within ENSEMBLES

VARIABLE	BIAS ¹	NB ²	MFB ²	NMSE ¹	RMSE ¹	PCC
NORTHERN EUROPE						
PREC	0.0054	0.0381	0.0075	0.6078	0.1119	0.5233
SWUPB	8.2893	0.1536	0.0986	0.1473	22.2506	0.9400
SWDNB	28.8298	0.1108	0.963	0.0779	76.5125	0.9566
SOUTHERN EUROPE						
PREC	0.0075	0.0457	0.0051	0.4748	0.1152	0.6246
SWUPB	4.9325	0.0636	0.0578	0.0449	16.944	0.9754
SWDNB	21.465	0.0544	0.0566	0.0296	67.852	0.9760

¹RMSE and BIAS are in units of mm for PREC and W m^{-2} for SWUPB and SWDNB.

²Parts per units.

2.4 Summary and conclusions

Although many aspects related to the microphysics processes are still not completely understood, it is well known that they play an important role in how moist convection develops and evolves, as well as in the radiative energy budget of the Earth-atmosphere system. Therefore, the sensitivity of the selection of the microphysics scheme within WRF-Chem model has been assessed in this contribution. The impact on several variables (such as cloud water mixing ratio, droplet number mixing ratio, shortwave radiation, 2-m temperature, of precipitation) is estimated when selecting two different microphysics parameterizations: Morrison (MORRAT) vs. Lin (LINES). Mean values for winter and summer are considered, allowing a seasonal interpretation of the analysis.

MORRAT provides higher cloud water mixing ratio in winter mainly over remote areas, where the CCN concentrations are lower; while LINES gives higher values over most polluted areas. Regarding the droplet number mixing ratio, MORRAT simulations indicate higher values of this variable both during winter and summer for nearly all the domain of simulation. This fact indicates that smaller and more numerous cloud droplets are simulated with the Morrison parameterization, and therefore this scheme is more effective in scattering shortwave radiation (as clearly observed when assessing both the differences in the mean upwelling shortwave flux and the downwelling shortwave flux at bottom).

It is worth nothing that the spatial pattern of differences for the droplet number mixing ratio T2 are highly correlated for wintertime. MORRAT simulations having higher levels of cloud droplets allow less shortwave radiation to reach the ground, but also higher longwave radiation to be reflected towards the ground. Between the two effects, the latter prevails, and

thus the daily average temperature increases in northern areas (50°N to 70°N) in MORRAT with respect to LINES.

Despite the differences found in the behaviour of both simulations, the sensitivity of the results to the selection of the microphysics scheme is very limited when comparing the results to observations. No significant benefits from the selection of the microphysics schemes can be derived from the results neither in northernmost areas nor in southern-Mediterranean Europe.

Because of the limitations in this sensitivity analysis (which is restricted to just two simulations implemented in just one model), future research on this topic should be devoted to further studies that examine the impact of aerosols on cloud properties using other microphysics and convective parameterizations, also in other target domains. In this sense, further analysis of the simulations included in Phase 2 of the AQMEII initiative could help deepen the study of these processes.

Chapter 3

Biomass burning aerosol impact on surface winds during the 2010 Russian heatwave

Published in Geophysical Research Letters: Baró, R., Lorente-Plazas, R., Montávez, J.P., and Jiménez-Guerrero, P (2016). Biomass burning aerosol impact on surface winds during the 2010 Russian heatwave. Geophysical Research Letters, 44, 1088–1094.

This work elucidates the impact of the biomass burning aerosols (BB) on surface winds for the Russian fires episode during 25 July to 15 August 2010. The methodology consists of three Weather Research and Forecasting model coupled with Chemistry (WRF-Chem) simulations over Europe differing in the inclusion (or not) of aerosol-radiation and aerosol-cloud interactions. The presence of BB reduces the 10-m wind speed over Russia during this fire event by 0.2 m s^{-1} (10%). Aerosol interactions imply a decrease of the shortwave downwelling radiation at the surface leading to a reduction of the 2-m temperature. This decrease reduces the turbulence flux, developing a more stable PBL. Moreover, cooling favours an increase of the surface pressure over Russian area and also it extends nearby northern Europe.

3.1 Introduction

Aerosols radiative effects, which depend mainly on the aerosol optical properties, affect radiation, temperature, stability, clouds and precipitation. But, to what extent do aerosol particles affect the wind? Jacobson and Kaufman (2006) tried to answer this question for a case study in California during February and August, 2002–2004. These authors found a reduction of the

near-surface wind speeds below them by up to 8% locally. They attributed this wind speed reduction due to the enhancement in stability caused by the aerosols directly and to aerosol-enhanced clouds. Aerosols and aerosol-enhanced clouds decreased near-surface air temperature, which increased stability and reduced turbulent kinetic energy as well as the vertical transport of horizontal properties. Moreover, wind speed reductions over China were found (average of 5.5% between February and August) where lots of biofuel burning occurred. Aside from this study, scientific literature about aerosol effects on wind is scarce. A reason of the lack of these studies could be the difficulty understanding of the physical causes of the feedbacks between aerosols and winds.

The Fifth Assessment Report of the Intergovernmental Panel on Climate Change (IPCC AR5 (Boucher et al., 2013; Myhre et al., 2013b) distinguishes between aerosol-radiation interactions (ARI) and aerosol-cloud interactions (ACI). ARI encompass the traditional aerosol direct and semi-direct effect, and ACI mainly account for the indirect effects. Direct effects influence climate by means of absorption and scattering of solar radiation, which modify the energy balance. On the other hand, indirect effects affect the reflectance and persistence of clouds and the growth and occurrence of precipitation (Ghan and Schwartz, 2007; Forkel et al., 2012). The consideration of different aerosols interactions (ARI and ACI) could play a key role to understand the interplay between aerosols and winds. For instance, atmospheric aerosol affects buoyancy processes and wind shear in the atmospheric boundary layer (Baidya and Sharp, 2013) by modifying meteorological variables such as temperature. Consequently, turbulence characteristics and atmospheric stability change, which directly affect wind fields. Several studies have demonstrated the implications of atmospheric stability on winds (Gualtieri and Secci, 2011; Sathe et al., 2011; Wharton and Lundquist, 2012; Lorente-Plazas et al., 2016). On the other hand, aerosol levels depend on winds by different processes, leading to wind-dependent emission of particles over land or ocean (for example, Boucher et al. (2013); Prijith et al. (2014); Li et al. (2015)).

An important component of aerosols are those coming from BB. They consist mainly in black carbon, which strongly absorbs solar radiation, having an impact on cloud processes and playing an important role in the Earth's climate system (Bond et al., 2013). The AR5 gives an estimate of +0.2 (+0.03 to +0.4) W m^{-2} as the black carbon contribution to the radiative forcing caused by ARI for the period 1750–2010, relying on Bond et al. (2013).

During the end of July and mid August extensive heatwave/fires occurred over Russia and specifically over the Moscow area. According to Konovalov et al. (2011), high levels of particles were caused by the mix of smoke particles plus accumulated urban and industrial

atmospheric pollution, with values of daily PM_{10} up to $700 \mu\text{g m}^{-3}$. Moreover, there was an important influence of the aerosol solar extinction on the photochemistry. Simulation results from Péré et al. (2015) showed reductions of the photolysis rate of NO_2 and O_3 (especially over the entire boundary layer). Several studies (e.g. Chubarova et al. (2012); Péré et al. (2014)) analysed the properties of particles from an optical and radiative point of view during this heatwave. These latter authors found a solar radiation reduction at the ground up to $80\text{-}150 \text{ W m}^{-2}$. However, these results were found by using off-line coupled models and only included direct effects (ARI). Despite Péré et al. (2014) find a wind reduction over the target domain, their methodology neglects the importance of on-line chemistry-climate coupling. Wind changes may be conditioned by AOD, who is strongly influence by the aerosol feedbacks affecting aerosol vertical distribution (Mishra et al., 2015) and vertical profiles of meteorological variables by absorbing and scattering solar radiation (Zhang et al., 2015). These feedbacks cannot be characterize by off-line coupling.

Therefore, the contribution presented here goes one step beyond previous studies by including on-line feedbacks between aerosols and meteorology in a regional climate-chemistry coupled model, and by solving online ARI in addition to ACI (and hence considering aerosol feedbacks with meteorology). Those effects are not considered in offline simulations. Moreover, the novelty of this work is related to the target area covered: our aim is to assess the influence of BB aerosols on spatially-distributed winds over Europe and, specially over the Russian area. This study also contributes to verify the results found with global-to-urban models in other areas as California or China (Jacobson and Kaufman, 2006).

3.2 Simulations and methods

3.2.1 Model configuration

The version 3.4.1 of the WRF-Chem online-coupled meteorology and chemistry model (Grell et al., 2005; Skamarock et al., 2008) was used in order to perform the simulations. The experiments are focused over Europe to study Russian wildfires during 25 of July to 15 of August 2010. The simulations presented here have been run in the context of the EuMetChem COST ES1004 Action (http://www.cost.eu/COST_Actions/essem/ES1004). For a detailed description of the simulations, the reader is referred to Forkel et al. (2015) and Baró et al. (2015). Nevertheless, Table 3.1 depicts a short description of the modeling parameterizations. Meteorological variables and particles have been extensively evaluated in Brunner et al. (2015) and Im et al. (2015b) and are therefore not included in this work for the sake of brevity.

Table 3.1: WRF-Chem parameterizations included in this study.

Parameterizations	Name	References
Microphysic option	Lin	Lin et al. (1983)
Photolysis option	Fast J	Fast et al. (2006)
Shortwave radiation	Goddard	Chou and Suarez (1994)
Longwave radiation	RRTMG	Morcrette et al. (2008)
Planetary Boundary Layer	YSU	Hsu et al. (2011)
Cummulus option	Grell 3D	Grell and Dévényi (2002)
Dust model	MOSAIC	Schell et al. (2001)
	MADE/SORGAM	Zaveri et al. (2008)
Gas phase mechanism	RADM2	Stockwell et al. (1990)
Aerosol mechanism	MADE/SORGAM	Schell et al. (2001)
Organic module	SORGAM	Schell et al. (2001)
Wet deposition	Grid scale	Easter et al. (2004)
Dry deposition	Wesley resistance	Wesely (1989)
Aerosol size	Aitken, accumulation and coarse	
Anthropogenic emissions	TNO-MACC	Pouliot et al. (2012)
Biogenic emissions	MEGAN	Guenther et al. (2006)
Fire emissions	IS4FIRE	http://is4fires.fmi.fi

The simulation domain uses a horizontal resolution of 0.22° (approximately 23 km) with a Lambert Conformal projection and complains with Euro-CORDEX requirements. 33 vertical sigma levels are used for vertical resolution (lowest layer at 24 m). The model top has been set at 50 hPa. Data provided by the European Centre for Medium-Range Weather Forecasts (ECMWF) operational analyses (with data at 00 and 12 UTC) and with respective forecasts have been used as initial (IC) and boundary conditions (BC) (time interval of 3 hours used as BC). Chemical IC were provided by ECMWF IFS-MOZART (Model for OZone and Related chemical Tracers) (Brasseur et al., 1998). Wildfires emission data come from the IS4FIRE Project (Sofiev et al., 2009), where emissions are estimated by re-analysis of fire radiative power data obtained by MODIS instrument (onboard Aqua and Terra satellites).

3.2.2 Experimental design

Three different simulations are constructed differing only in the inclusion (or not) of ARI and ACI: (1) No aerosol feedbacks (Base, NRF), (2) only ARI (simulation includes only the direct radiative forcing, DRF) and (3) ARI+ACI feedbacks (all radiative feedbacks, RF). It is important to clarify that although the Base case does not include any aerosol radiation interactions, there is a standard aerosol assumption for aerosol-radiation and aerosol-cloud interactions of some continental aerosol. No heat released is considered in the simulations of this study.

With the purpose of studying the effects of BB aerosols on surface winds, a sensitivity

analysis were conducted by taking the Base case as reference. Differences between DRF and RF with respect to the Base case have been assessed. Positive (negative) values means that DRF and RF have higher (lower) values than the Base case. These spatial differences are inspected for the 10-m wind speed (WS10), shortwave downwelling radiation at the surface (SWDNB), 2-m temperature (T2), planetary boundary layer height (PBLH), AOD at 550 nm, relative humidity (RH), and sea level pressure (SLP). The impact of the BB aerosols on WS10 is assessed by computing spatial correlation between the variation in WS10 and the rest of meteorological variables found for DRF-Base and RF-Base simulations. Correlations are 95% significant according to a correlation significance test (Wilks, 2011).

3.3 Results

3.3.1 Base case meteorological situation

As stated by several works (e.g. Im et al. (2015b) or Forkel et al. (2015)), the BB aerosols generated by the Russian wildfires had a very important impact on PM_{10} ground levels, with concentrations largely exceeding $700 \mu\text{g m}^{-3}$. This increase was evidenced by satellite observations like Terra-MODIS (not shown), results from WRF-Chem simulation are in agreement with these previous findings. Figure 3.1 shows the time aggregation of PM_{10} emissions averaged during the fires period, where largest values are gathered over the region where wildfires took place.

First row of Figure 3.2 shows the mean values of the Base case (no aerosol interactions) for SWDNB, T2, PBLH, AOD, and RH (vertically averaged). The SLP mean spatial pattern (first row in Figure 3.2(b)) shows a high pressure system over the northeast of the target area with a strong positive SLP anomaly for this period. This led to a strong positive surface temperature anomaly and weak winds from the southeast. Regarding the AOD, values between 1 to 1.8 are found over Russian area and RH values are around 50%.

The highest WS10 average (over 7 m s^{-1}) is found offshore, over the Baltic sea, Sweden and Finland coastline. Also large WS10 values are found in south Russia, south Ukraine and over Azov Sea (around $6\text{--}7 \text{ m s}^{-1}$) while in the center of the subdomain winds are around 3 m s^{-1} .

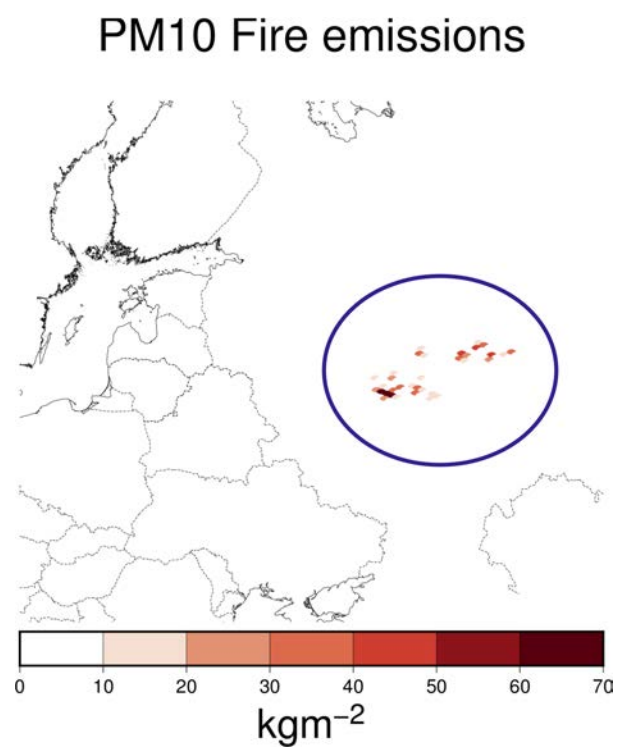


Figure 3.1: Total PM_{10} fire emissions during the fire episode (25 July-15 August 2010). The region affected by the wildfires is highlighted with a circle.

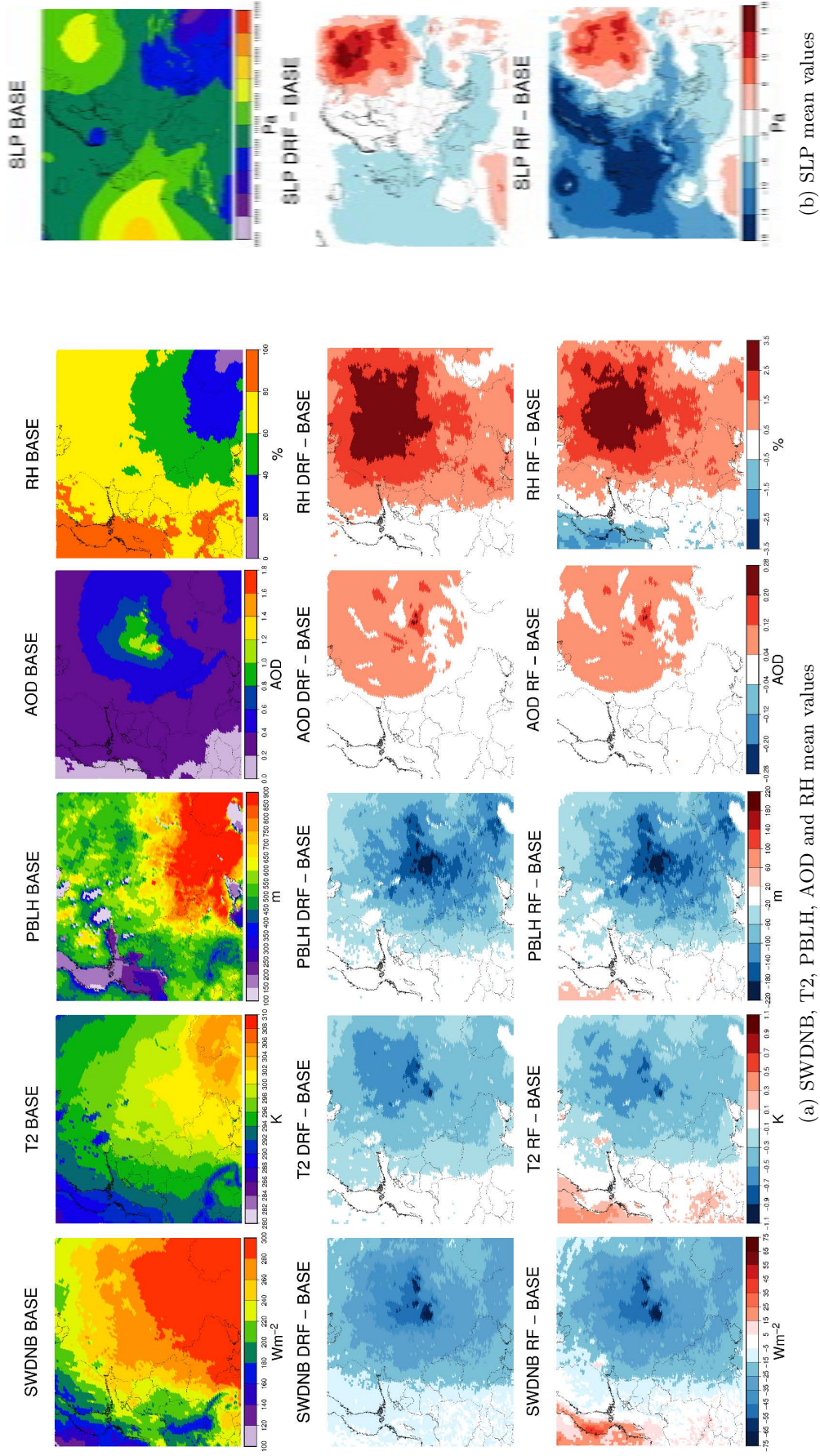


Figure 3.2: Mean values during Russian forest fires. First row represents the Base case; second row DRF-Base differences, third row RF-Base differences.

3.3.2 Effects on wind speed

The analysis of the BB aerosols impacts on WS10 with respect to the Base case (Figure 3.3 second and third row) shows a strong heterogeneity in the spatial patterns of differences for both DRF and RF simulations. However, there is a clear WS10 reduction up to 10% (mean reduction of 0.2 m s^{-1} with respect to average WS10 of 2 m s^{-1}) over the target area. Some areas present a WS10 reduction up to 0.35 m s^{-1} for both DRF and RF simulation. In Péré et al. (2014), horizontal wind speed over Moscow during 8 August was reduced between $0.05\text{--}0.86 \text{ m s}^{-1}$. Our mean values for the whole period are included in that range.

3.3.3 Causes of wind variation

In order to explore the physical causes of the WS10 changes, we have examined several meteorological variables (as SWDNB, T2, PBLH, AOD, RH and SLP), some of them also covered on previous studies (Jacobson and Kaufman, 2006). Second and third rows in Figure 3.2 represent the differences found for DRF and RF cases, respectively. Variables SWDNB, T2, PBLH, AOD and RH are represented over the Russian area whereas SLP is represented over the whole Europe for a better understanding of this variable and since its effects extend beyond the Russian area.

The impact of considering aerosols feedbacks in the on-line simulations is analyzed by comparing with the Base simulation. Differences between DRF and RF are similar over the Russian wildfires area because the processes are mainly related to the ARI, occurred during this event. In both cases (DRF and RF) the aerosol effects imply a decrease of SWDNB. The maximum differences are around 80 W m^{-2} over Russia as the period mean. This difference involves a T2 reduction up to 0.9 K over Russia (consistent with Péré et al. (2014), who found reductions of 0.2 to 2.5 K). The temperature decrease diminishes the convective processes and the turbulence, resulting in a lower PBLH with lower values up to 300 m with respect to Base case over the target area. Changes in AOD are found when considering aerosol feedbacks, resulting in an increase up to 0.25 over the Russian area. This could be related to the increase of the RH (with values around 3.5%) which is directly related to the hygroscopic growth, which in turn is related to the effective radius and hence to the particle extinction (Curci et al., 2015). This increased RH may explain the increase of AOD during the fires. Positive differences are also found for SLP, because the decrease of the temperature enhances the SLP not only over the Russian area but also extended over the North of Europe. Hence, the reduction is directly related to an increase of the atmospheric stability where lower PBLH is found and there was an increase of the SLP. Jacobson and Kaufman (2006) also explored the effects of clouds on winds;

however clear skies are found over the entire target period.

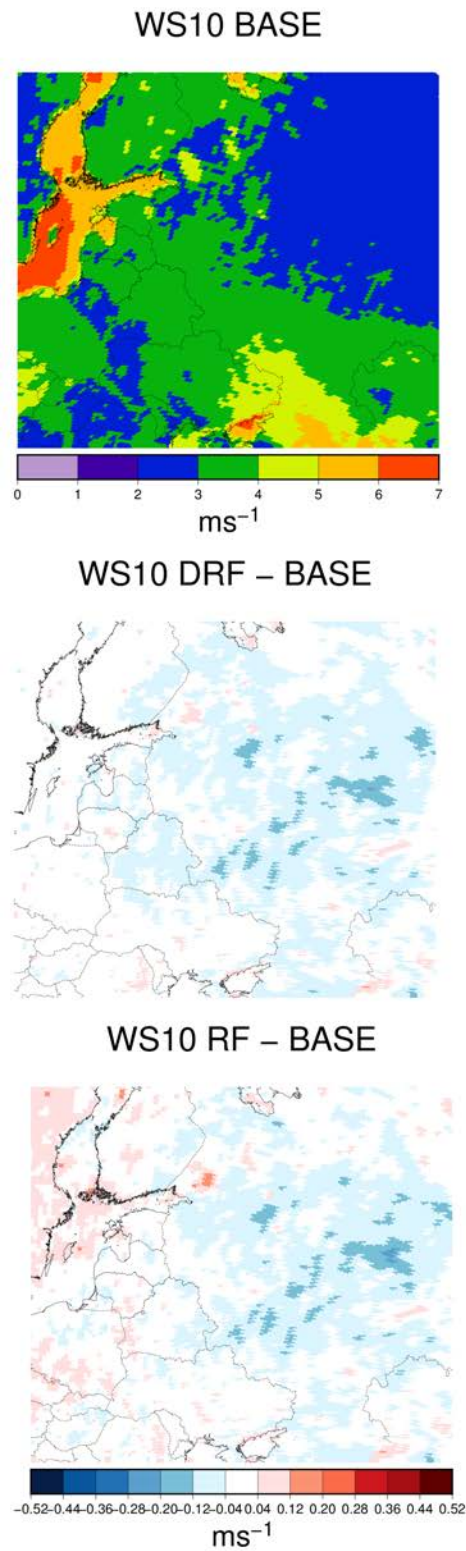


Figure 3.3: Aerosol effects on WS10. First row represents the Base case; second row DRF-Base differences and third row RF-Base differences.

3.3.3.1 Wind correlation

To assess whether changes in the WS10 may be attributed to changes in meteorological variables (SWDNB, T2, PBLH, AOD, RH and SLP) correlations are computed between the meteorological variables (Figure 3.2) and WS10 (Figure 3.3) for the spatial differences of Base case minus RF or DRF. Estimations cover the Russian area. In general, correlations are lower than $+0.6$ and higher than -0.6 . The correlations of Δ WS10 with Δ SWDNB, Δ T2 and Δ PBLH are in the order of $+0.45$ to $+0.55$. Δ WS10 is anticorrelated with Δ SLP, Δ AOD and Δ RH, and anticorrelation is higher for DRF than for RF (-0.4 versus -0.35). In general, slight differences are found between DRF and RF case since this fire episode is mainly explained by ARI. ARI only increase or decrease the radiation which is directly related with the meteorological variables assessed. Including ACI implies more complex physical hampering to attribute the causes of the changes.

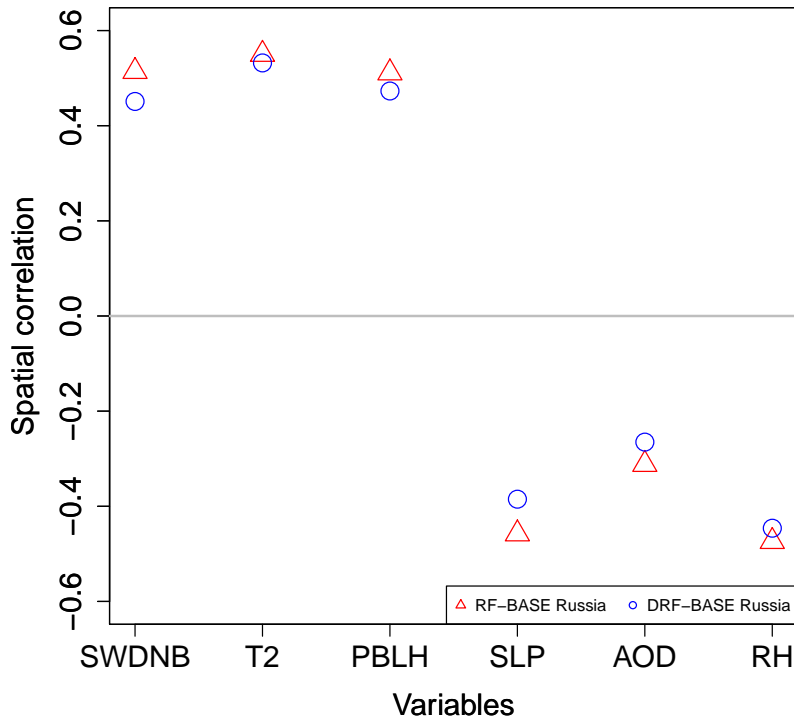


Figure 3.4: Spatial correlation over Russian area of WS10 differences and differences in several meteorological variables: SWDNB, T2, PBLH, SLP, AOD and RH. Correlations are computed for the spatial differences between experiments RF (triangles) and DRF (circles) and Base case, i.e., Figure 3.3 versus Figure 3.2.

3.4 Conclusions

Focusing on the heatwave/wildfires episode that took place during summer 2010 over Russia, this study demonstrates that considering BB aerosols feedbacks could play a key role when simulating surface winds. Results show that these aerosols can affect surface winds not only where emission sources are located, but also further from the release areas. Local winds decrease due to a reduction of SWDNB which leads to decreases in T2. In addition, atmospheric stability increases when considering aerosol feedbacks, inducing a lower PBLH. Meanwhile, the presence of BB aerosols in the atmosphere can change the SLP, producing changes in mesoscale circulations and an increase of surface winds over distant regions.

With the present analysis, we highlight the relevance of including aerosols feedbacks when simulating surface winds, which could contribute both to the skill of weather prediction and improve climatological studies. For instance, better understanding of feedbacks between aerosols and winds could help the decision making on fires management and could condition the planning on wind energy. Albeit this promising conclusion, this work only analyzes a particular episode and more case studies will be needed to support these conclusions.

Chapter 4

Regional effects of atmospheric aerosols on temperature: an evaluation of an ensemble of on-line coupled models

Published under discussion: Baró, R., Palacios-Peña, L., Baklanov, A., Balzarini, A., Brunner, D., Forkel, R., Hirtl, M., Honzak, L., Pérez, J.L., Pirovano, G., San José, R., Schröder, W., Werhahn, J., Wolke, R., Zabkar, R., and Jiménez-Guerrero, P (2017). Regional effects of atmospheric aerosols on temperature: an evaluation of an ensemble of on-line coupled models, Atmospheric Chemistry and Physics Discussions, pp. 1–35, doi:10.5194/acp-2016-1157, <http://www.atmos-chem-phys-discuss.net/acp-2016-1157/>, 2017.

The climate effect of atmospheric aerosols is associated to their influence on the radiative budget of the Earth due to the direct aerosol-radiation interactions (ARI) and indirect effects, resulting from aerosol-cloud interactions (ACI). On-line coupled meteorology-chemistry models permit the description of these effects on the basis of simulated atmospheric aerosol concentrations, although there is still some uncertainty associated to the use of these models. In this sense, the objective of this work is to assess whether the inclusion of atmospheric aerosol radiative feedbacks of an ensemble of on-line coupled models improves the simulation results for maximum, mean and minimum temperature at 2 meters over Europe. The evaluated models outputs originate from EuMetChem COST Action ES1004 simulations for Europe, differing in the inclusion (or omission) of ARI and ACI in the various models. The cases studies cover two important atmospheric aerosol episodes over Europe in the year 2010, a heat wave event and a forest fires episode (July-August 2010) and a more humid episode including a Saharan desert dust outbreak in October 2010. The simulation results are evaluated against observational

data from E-OBS gridded database. The results indicate that, although there is only a slight improvement in the bias of the simulation results when including the radiative feedbacks, the spatio-temporal variability and correlation coefficients are improved for the cases under study when atmospheric aerosol radiative effects are included.

4.1 Introduction

Atmospheric aerosol particles are known to have an impact on Earth's radiative Budget due to their interaction with radiation and clouds properties, which are dependent on their optical, microphysical and chemical properties, and are considered to be the most uncertain forcing agent. They influence climate by modifying the global energy balance through both absorption and scattering of radiation (direct effect) and by acting as cloud condensation nuclei, thus affecting clouds droplet size distribution, lifetime (Twomey, 1977; Lohmann and Feichter, 2005; Chung, 2012) and reflectance (indirect effects) (Ghan and Schwartz, 2007; Yang et al., 2011b). Depending on the atmospheric aerosol concentration, aerosol cloud interactions may result in an increase or decrease in liquid water content, cloud cover, and lifetime of low level clouds and a suppression or enhancement of precipitation (Bangert et al., 2011). Besides, aerosol absorption may decrease low-cloud cover by heating the air and reducing relative humidity. This leads to a positive radiative forcing, termed the semi-direct effect, which amplifies the warming influence of absorbing aerosols (Hansen et al., 1997). The Fifth Report of the Intergovernmental Panel on Climate Change (IPCC AR5) (Boucher et al., 2013; Myhre et al., 2013a) distinguishes between aerosol-radiation interactions (ARI), which encompass the aerosol direct and semidirect effect, and the aerosol-cloud interactions (ACI), which encompass the indirect effects.

In order to account for these atmospheric aerosol effects, the use of fully-coupled models is needed for meteorological, chemical and physical processes. On-line coupled models include the interaction of atmospheric pollutants (gaseous-phase compounds and aerosols) with meteorological variables (Baklanov et al., 2014). In this context, in its phase 2, the air quality model evaluation international initiative (AQMEII) (Alapaty et al., 2012; Galmarini et al., 2015), focused on the assessment of how well the current generation of coupled regional scale air quality models can simulate the spatio-temporal variability in the optical and radiative characteristics of atmospheric aerosols and associated feedbacks among aerosols, radiation, clouds and precipitation. On this basis, a coordinated exercise of working groups 2 and 4 of the COST Action ES1004 (EuMetChem, <http://eumetchem.info>) emerged in order to take into account the radiative feedbacks of atmospheric aerosol effects on meteorology. In this initiative, two important episodes with high loads of atmospheric aerosols were analyzed which were identified during the

previous AQMEII Phase 2 modeling intercomparison exercise (Galmarini et al., 2015). They were selected on behalf of their strong potential for aerosol-radiation and aerosol-radiation-cloud interactions (Makar et al., 2015b,a; Forkel et al., 2015).

As a result of the AQMEII Phase 2 initiative and EuMetChem COST Action, several studies covering the analysis of the ARI+ACI feedbacks to meteorology have been done (e.g. Baró et al. (2015); Forkel et al. (2015, 2016); Kong et al. (2015); San José et al. (2015)). Focusing on the effects of including ARI+ACI on temperature, Forkel et al. (2015) focused on the 2010 Russian wildfire episode, where the presence of the atmospheric aerosols decreased the mean temperature during summer 2010 by 0.25 K over the target area. For the same episode, Péré et al. (2014) showed daily mean surface temperature reductions between 0.2 to 2.6 K. In Forkel et al. (2012) they studied a two-month episode (June to July 2006) for allowing medium range effects of the direct and indirect aerosol effect on meteorological variables and air quality. They found a slightly lower temperature over western Europe when including atmospheric aerosol feedbacks. This reduction followed the same pattern as the planetary boundary layer height. Moreover, Meier et al. (2012) found during July 2006 a general decrease of 0.14 K on 2-m temperature when simulating absorbing aerosol in upper layers compared to an aerosol-free troposphere over land surface.

However, all these studies are based on individual model evaluations and do not take into account an ensemble of regional models, in order to build confidence on model simulations and to characterize the uncertainty associated to the use of different modeling systems. Therefore, the objective of this work is to assess whether the outputs of an ensemble of regional on-line coupled models simulations including aerosol radiative feedbacks, during two important atmospheric aerosol episodes of the year 2010, improves the prognostic for maximum, mean and minimum temperature at 2 meters over Europe.

4.2 Methodology

The analyzed model outputs are the results of a coordinated modeling exercise which was performed within the COST Action ES1004 (EuMetChem). In order to analyze the ARI or ARI+ACI effect on temperature, it was suggested to run three case studies for two episodes with different on-line coupled models with identical meteorological boundary conditions and anthropogenic emissions. The two considered episodes are: the Russian heatwave and wildfires episode in the summer of 2010 (25 July-15 August 2010) and an autumn Saharan dust episode, including the dust transport to Europe (2-15 October 2010).

For the chosen episodes, simulations with each model were performed with and without

considering the atmospheric aerosol effects. Three different configurations were requested: the first one which does not consider any aerosol effects feedbacks to meteorology (NRF; C11 fire and C21 dust episode); second, where only aerosol-radiation interactions are considered (ARI; C12 fire and C22 dust episode) and third, where aerosol-radiation-cloud interactions are considered (ARI+ACI; C13 fire and C23 dust episode)(this case could not be submitted by all of the participants). Although NRF case does not consider the aerosol effects and feedbacks, there is a standard aerosol assumption of some continental aerosol (250 cm^{-3} used by WRF-Chem in the absence of ACI for estimating cloud droplet number). On the other hand, ARI uses this constant value for accounting the interaction between aerosols and clouds, but allows the modification of the radiation budget by using the on-line estimated aerosols. Last, the ARI+ACI cases are based on simulated aerosol concentrations which interact both with radiation and aerosols. The common setup for the participating models and a unified output strategy allow analyzing the model output with respect to similarities and differences in the model response to the aerosol direct effect and aerosol-cloud interactions.

4.2.1 Participating models

An overview of the different models and their configurations is shown in Table 4.1, where in first row the model acronym is shown. The participating models shown here are COSMO-MUSCAT (Wolke et al., 2012) and WRF-Chem (Grell et al., 2005; Fast et al., 2006; Gustafson Jr et al., 2007; Chapman et al., 2009; Grell and Baklanov, 2011) with different chemistry and physics options and performed episodes. The horizontal grid spacing is around 25 km for most of the contributions. Only for the fire episode, the COSMO-MUSCAT simulations were made with a grid with of 0.125° (approximately 14 km) there is an additional WRF-Chem run with 9 km grid spacing. COSMO models use Kessler-type bulk microphysics (Doms et al., 2011) and WRF-Chem uses Morrison microphysics (Morrison et al., 2009), except for one contribution, that utilizes Lin (Lin et al., 1983). COSMO models use prognostic TKE (Doms et al., 2011) PBL. The YSU PBL scheme (Hong et al., 2006) was chosen for the WRF-Chem simulations. In general, the Modal Aerosol Dynamics Model for Europe (MADE) is applied (Ackermann et al., 1998) except for one WRF-Chem simulation, which uses the Model for Simulating Aerosol Interactions and Chemistry (MOSAIC)(4 bins) approach (Zaveri et al., 2008). For further information and details about the models, we refer to the work of Forkel et al. (2015); Im et al. (2015a,b); Baró et al. (2015). To enable the cross-comparison between models, the participating groups interpolated their model output to a common grid with 0.1° resolution.

Moreover, the ensemble of the available simulations has also been included in this compar-

Table 4.1: Modeling systems participating and their contributions to the case studies

		CS1	CS2	DE3	ES1	ES3
Lead Institution		UL, KIT/IMK-IFU*	UL, KIT/IMK-IFU*	IFT Leipzig	U. Murcia	UPM-ESMG
Model		WRF-Chem	WRF-Chem	COSMO-MUSCAT	WRF-Chem	WRF-Chem
Episode		Fire, Dust	Fire	Fire, Dust	Fire, Dust	Fire, Dust
Runs		NRF, ARI, ARI+ACI	NRF, ARI, ARI+ACI	NRF, ARI	NRF, ARI, ARI+ACI	NRF, ARI, ARI+ACI
Resolution		23 km	9.9 km	0.125°	23 km	23 km
Microphysics		Morrison	Morrison	Kessler-type bulk	Lin	Morrison
SW Radiation		RRTMG	RRTMG	δ -2-stream	RRTMG	RRTMG
LW Radiation		RRTMG	RRTMG	δ -2-stream	RRTMG	RRTMG
PBL/turbulence		YSU	YSU	Prognostic TKE	YSU	YSU
Biogenic model		MEGAN (Guenther et al., 2006)	MEGAN	Guenther et al. (1993)	MEGAN	MEGAN
Gas phase		RADM2 modified	RADM2 modified	RACM-MIM2	RADM2	CBMZ
Aerosol		MADE / SORGAM	MADE / SORGAM	Simpson et al. (2003)	MADE/SORGAM	MOSAIC 4 bins
Model reference		Grell et al. (2005); Forkel et al. (2015)	Grell et al. (2005); Forkel et al. (2015)	Wolke et al. (2012)	Grell et al. (2005)	Grell et al. (2005)

*Joint effort, also including ZAMG, RSE, UPM-ESMG.

ison, as recommended by several studies (Vautard et al., 2012; Jiménez-Guerrero et al., 2013; Landgren et al., 2014; Solazzo and Galmarini, 2015; Kioutsioukis et al., 2016), in order to check whether the design of an ensemble of simulations outperforms (or not) the skill of individual models.

4.2.2 Emissions and boundary conditions

For the EU domain, the anthropogenic emissions for the year 2009 (<http://www.gmes-atmosphere.eu/>) were applied by all modeling groups and are based on the TNO-MACC-II (Netherlands Organization for Applied Scientific Research, Monitoring Atmospheric Composition and Climate-Interim Implementation) framework (Kuenen et al., 2014; Pouliot et al., 2015). As described in Im et al. (2015a), annual emissions of CH₄, CO, NH₃, total non-methane volatile organic compounds (NMVOC), NO_x, PM₁₀ & PM_{2.5} and SO₂ from ten activity sectors are provided on a latitude/longitude grid of 1/8 × 1/16 resolution. Consistent temporal profiles (diurnal, day-of-week, seasonal) and vertical distributions were also made available to AQMEII and EuMetChem

participating groups for time disaggregation. The temporal profiles for the EU anthropogenic emissions were provided from Schaap et al. (2005). For further details, the reader is referred to Im et al. (2015a,b).

Hourly biomass burning emissions were provided by the Finnish Meteorological Institute (FMI) fire assimilation system (<http://is4fires.fmi.fi/>) (Sofiev et al., 2009). More details on the fire emissions and their uncertainties are discussed in Soares et al. (2015). The fire assimilation system provides only data for total PM emissions; the estimation of emissions for other species are described in Im et al. (2015b).

The chemical initial and boundary conditions were provided by the ECMWF IFS–MOZART model, which are available in 3–hour time intervals and provided in daily files with 8 times per file. They were run under the MACC-II project (Monitoring Atmospheric Composition and Climate- Interim Implementation) which uses an updated data set of anthropogenic emissions and compiles a satellite observations assimilations of O_3 , CO and NO_2 in the IFS-MOZART system.

4.2.3 Observational database

E-OBS (Haylock et al., 2008) version 11.0 has been used as the gridded observational database for maximum, mean and minimum temperature. E-OBS is a high-resolution European land-only daily gridded data set covering the period 1950-2014. The E-OBS 0.25° regular latitude-longitude grid has been used as the reference for validation. Thus, data from all model runs have been bilinearly interpolated onto the E-OBS grid. Since the resolution of the models is similar to that of E-OBS, the interpolation procedure is not expected to alter significantly our results.

4.2.4 Validation methodology

All the statistical measures are calculated at individual grid points. Only land grid points are considered in the analysis, since these are the only points where E-OBS contains information. Areas in grey indicate cells where E-OBS data are not available (southeastern part of the domain for the wildfires or southern part of the domain in the dust episode) or areas not covered by the modeling domain (southern part of the domain for the CS2 configuration).

We will use the notation V_{ipc}^k for a variable from model k at grid point i , on period p =fires,dust and case c =1 2, 3 representing no radiative feedbacks, ARI and ARI+ACI. If we use bracket notation for an average over a given index (e.g. $\langle \cdot \rangle_{pc}$, we can express the bias

at a given grid point as:

$$b_i^k = \left\langle V_{ipc}^k - O_{ip} \right\rangle_{pc} \quad (4.1)$$

where O_{ip} is the value observed. The model bias is the simplest measure of model performance.

The ensemble mean, $\left\langle V_{ipc}^k \right\rangle_k$, is usually considered as an additional simulation which compensates the errors of the different ensemble members. Even though this is a very simplistic view of the ensemble (which should be considered from a probabilistic point of view), it can be useful to reinforce the common signal of the different models in our analysis of the mean climate. Notice, however, that the ensemble mean is not a physical realization of any of the models, but just a statistical average (Knutti et al., 2010; Jiménez-Guerrero et al., 2013).

Then, the variability was assessed on the hourly series (V_{ipc}^k). The ability to represent the variability can be decomposed into:

- the ability to represent its size, which can be represented by the standard deviation of the series:

$$sd[V]_i^k = \sqrt{\left\langle \left(V_{ipc}^k \right)^2 \right\rangle_{pc}} \quad (4.2)$$

and can be compared to that of the observations $sd[O]_{ip}$, and

- the ability to represent the hourly variations, which can be represented by the linear determination coefficient (ρ^2) with the observations.

$$\rho_i^{2,k} = \frac{\left\langle V_{ipc}^k O_{ip} \right\rangle_{pm}^2}{\left\langle \left(V_{ipc}^k \right)^2 \right\rangle_{pm} \left\langle \left(O_{ip} \right)^2 \right\rangle_{pc}} \quad (4.3)$$

The latter ability can only be expected on simulations nested into “perfect” boundary conditions such as those considered in this study.

Finally, pattern agreement between simulated and observed data was quantified in a Taylor diagram by means of the spatial correlation (r) and the ratio between simulated and observed standard deviations, $V_i^k \equiv \left\langle V_{ipc}^k \right\rangle_{pc}$

$$r^k = \frac{\left\langle \left(V_i^k - \left\langle V_i^k \right\rangle_i \right) \left(O_i - \left\langle O_i \right\rangle_i \right) \right\rangle_i}{\sqrt{\left\langle \left(V_i^k - \left\langle V_i^k \right\rangle_i \right)^2 \right\rangle_i \left\langle \left(O_i - \left\langle O_i \right\rangle_i \right)^2 \right\rangle_i}} \quad (4.4)$$

$$s^k = \sqrt{\frac{\left\langle \left(V_i^k - \left\langle V_i^k \right\rangle_i \right)^2 \right\rangle_i}{\left\langle \left(O_i - \left\langle O_i \right\rangle_i \right)^2 \right\rangle_i}} \quad (4.5)$$

This information can be summarized in a Taylor (2001) diagram, which is a polar plot, with radial coordinate s^k and angular coordinate related to r^k .

4.3 Results

4.3.1 Bias

The results for the daily bias of maximum, mean and minimum temperature have been obtained by calculating the bias of the daily mean series at each grid point of all the land grid points of the corresponding domain for the fires and dust episodes.

During the fire episode (Fig. 4.1 left column) there is a general underestimation of the maximum temperature in the base case (average domain values from -2.1 K in ES3-C11 to -1.2 K in DE3-C11). This is especially noticeable over several cells in Russia (up to -7 K). Conversely, a general overestimation is found in the west and northwest area of the domain (positive differences between $+1.0$ K in DE3-C11 to $+6.5$ K in ES1-C11). When introducing the ARI or ARI+ACI, model biases do not improve (mean variation of the bias of $+17.2\%$ in C12 and $+11.0\%$ in C13). This positive variation was expected because the cold bias of models for reproducing maximum temperature and the overall cooling effects of aerosols. However, the improvement of introducing aerosol-cloud interactions is remarkable with respect to the case of including just aerosol-radiation effects (the bias reduces 6.2% in ARI+ACI with respect to ARI simulations). During the dust episode (Fig. 4.1 right column) the analysis of the results is similar as for the fires case (averaged-domain underestimations around -1.0 K in DE-C11 to -0.56 K in ES-C21). Here the inclusion of ARI (C22) leads to a mean increase of the bias of $+10.2\%$, but ARI+ACI (C23) leads to a very limited improvement of the simulations with respect to the base case (C21), generally reductions of the bias around -0.4% .

A similar discussion can be made for mean temperature. During the fires episode (left column of Fig. 4.2) all runs (but DE3) tend to underestimate the domain-averaged mean temperature (biases ranging from -0.4 K in ES1-C11 to $+1.0$ in DE3-C11). Here, the ensemble (ENS) simulation clearly outperforms the individual simulations (bias of -0.2 K in ENS-C11). Again, the model skill does not improve for mean temperature when including ARI or ARI+ACI (bias increase by 46.0% and 56.2% , respectively for the fires episode) but in the case of DE3-C12 simulation (including ARI reduces the bias by -27.3%). During the dust episode (right column of Fig. 4.2), there is a general averaged overestimation of mean temperature ($+0.4$ in ES1-C21 to 0.8 K in DE3-C21).

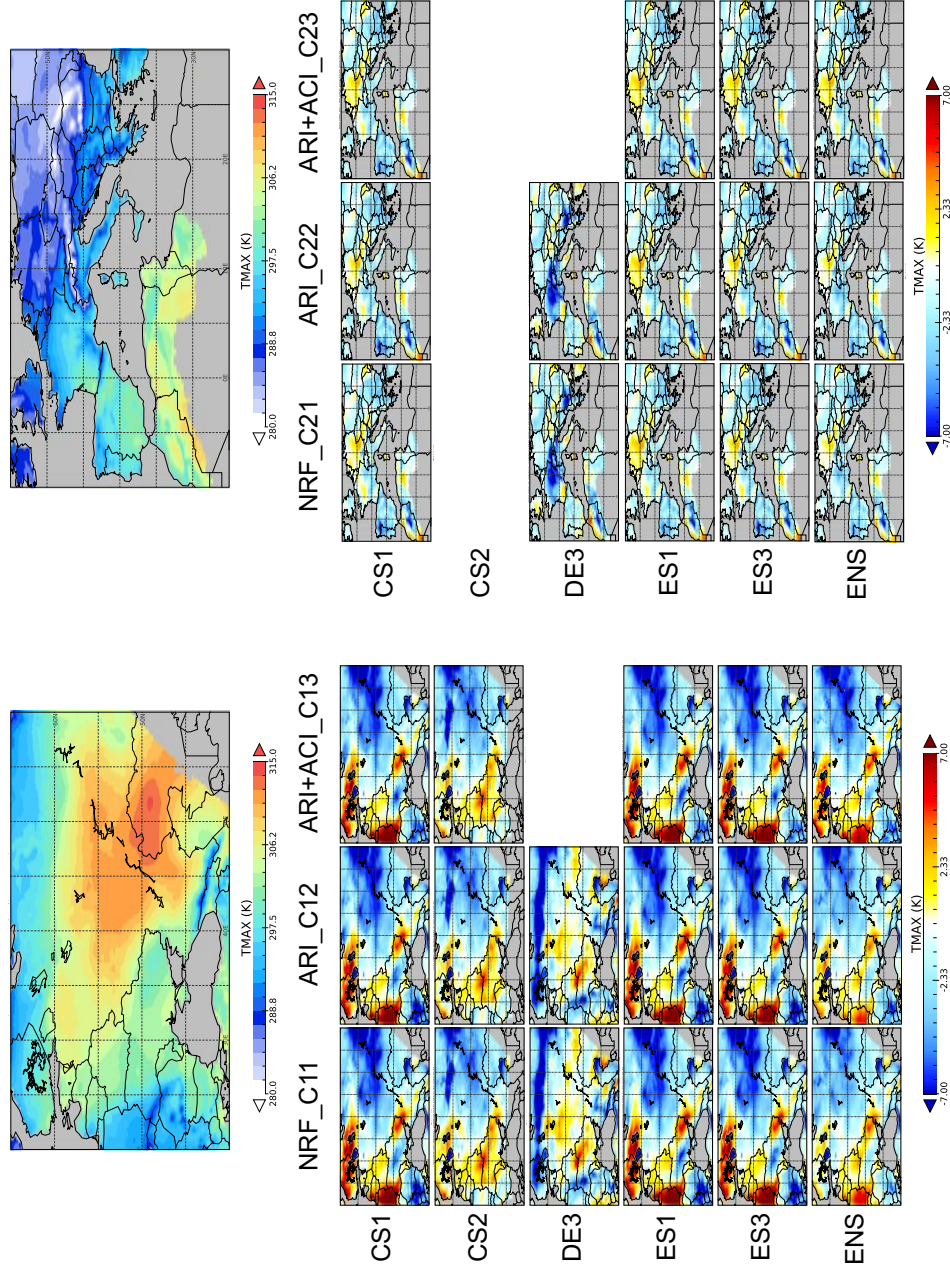


Figure 4.1: (Top row) Maximum temperature (TMAX) for the fires (left) and dust (right) episodes, as derived from E-OBS database (in K). The panel below represents the bias for the fires (left) and dust (right) episodes of each simulation with respect to the E-OBS database. NRF: no radiative feedbacks; ARI: aerosol-radiation interactions; ARI+ACI: as ARI including aerosol-cloud interactions.

Conversely to the fires episode, the inclusion of ARI and ARI+ACI improves the bias (reductions of this variable of -13.4% in C22 and -4.2% in C23). The reduction of the bias when including ARI+ACI is especially remarkable for the ensemble of simulations, where the bias decreases by -24.4% in ENS-C23.

Last, minimum temperature during the fire episodes is shown in the left column of Fig. 4.3. Here results are very different to analyze for improvements or worsening of the bias, since the domain-averaged errors are in the order of -0.01 K for WRF-based models in C11 and C12, so a very slight difference would lead to a percentage increase (or reduction) of the bias compared to the base case. However, for DE3-C11 the bias is larger (up to $+1.6$ K for minimum temperature averaged over all the domain) and the inclusion of ARI leads only to a small improvement (-1.5%). The dust case (right column of Fig. 4.3) shows a general overestimation of minimum temperature, with base-case biases ranging from $+0.5$ K in ES1-C21 to $+1.8$ K in DE3-C21. Here, the inclusion of ARI and ARI+ACI slightly improves the bias (reductions of -10.5% in C22 and -5.0% in C23). Here again, the improvement of the ENS-C22 and ENS-C23 simulations is larger than for the rest of the models (reductions of the bias of -29.7% and -38.2% for ARI and ARI+ACI, respectively).

The differences found in the maximum, mean and minimum temperature are related to what explained in section 4.1, according to other model evaluation studies. Since models underestimate surface temperature, the inclusion of the atmospheric aerosol feedbacks lead to a reduction on the surface temperature, leading to a worsening of the maximum temperature and an improvement on the minimum temperatures. In the case of mean temperatures, the effect will be balanced.

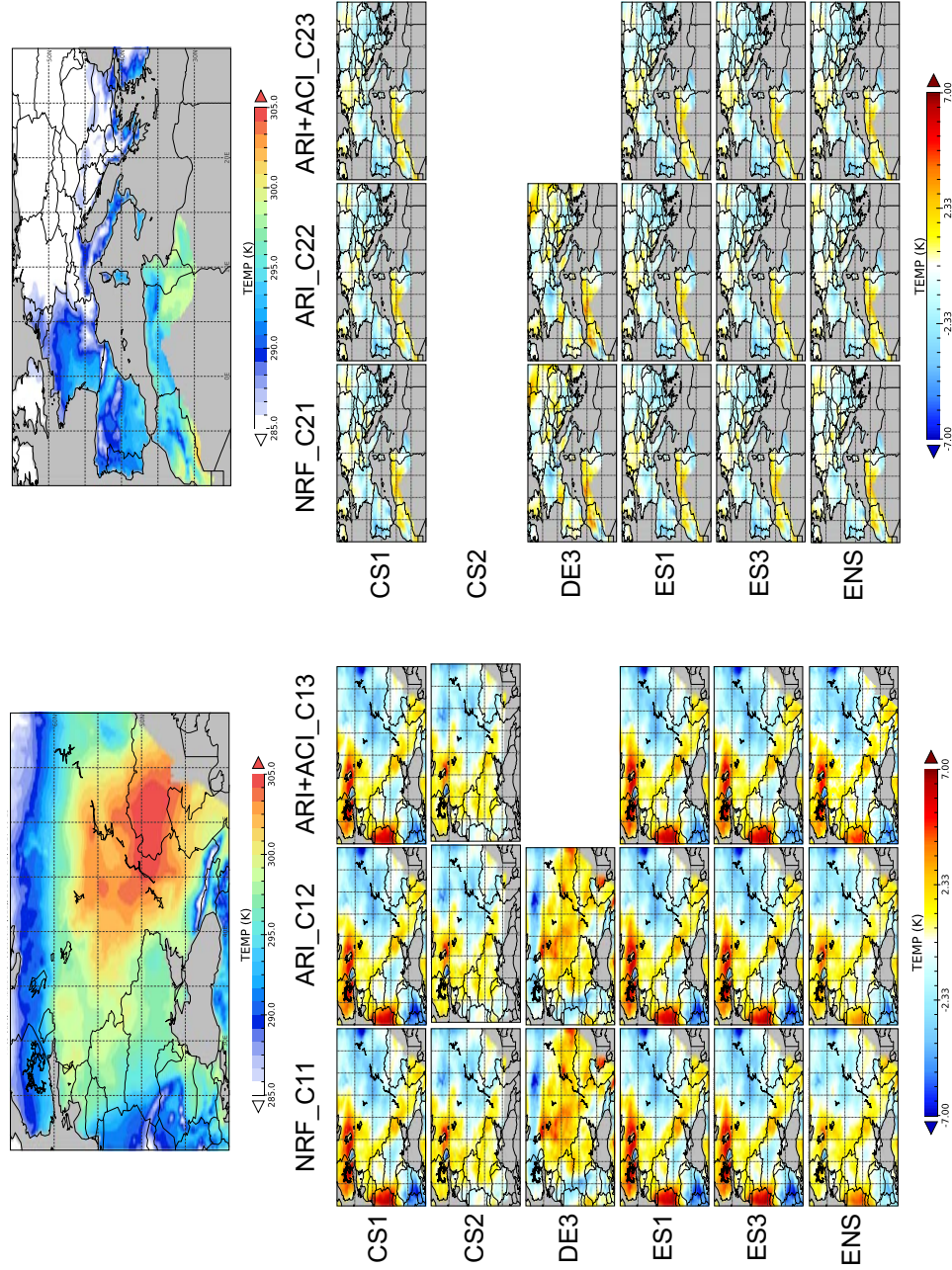


Figure 4.2: (Top row) Mean temperature (TEMP) for the fires (left) and dust (right) episodes, as derived from E-OBS database (in K). The panel below represents the bias for the fires (left) and dust (right) episodes of each simulation with respect to the E-OBS database. NRF: no radiative feedbacks; ARI: aerosol-radiation interactions; ARI+ACI: as ARI including aerosol-cloud interactions.

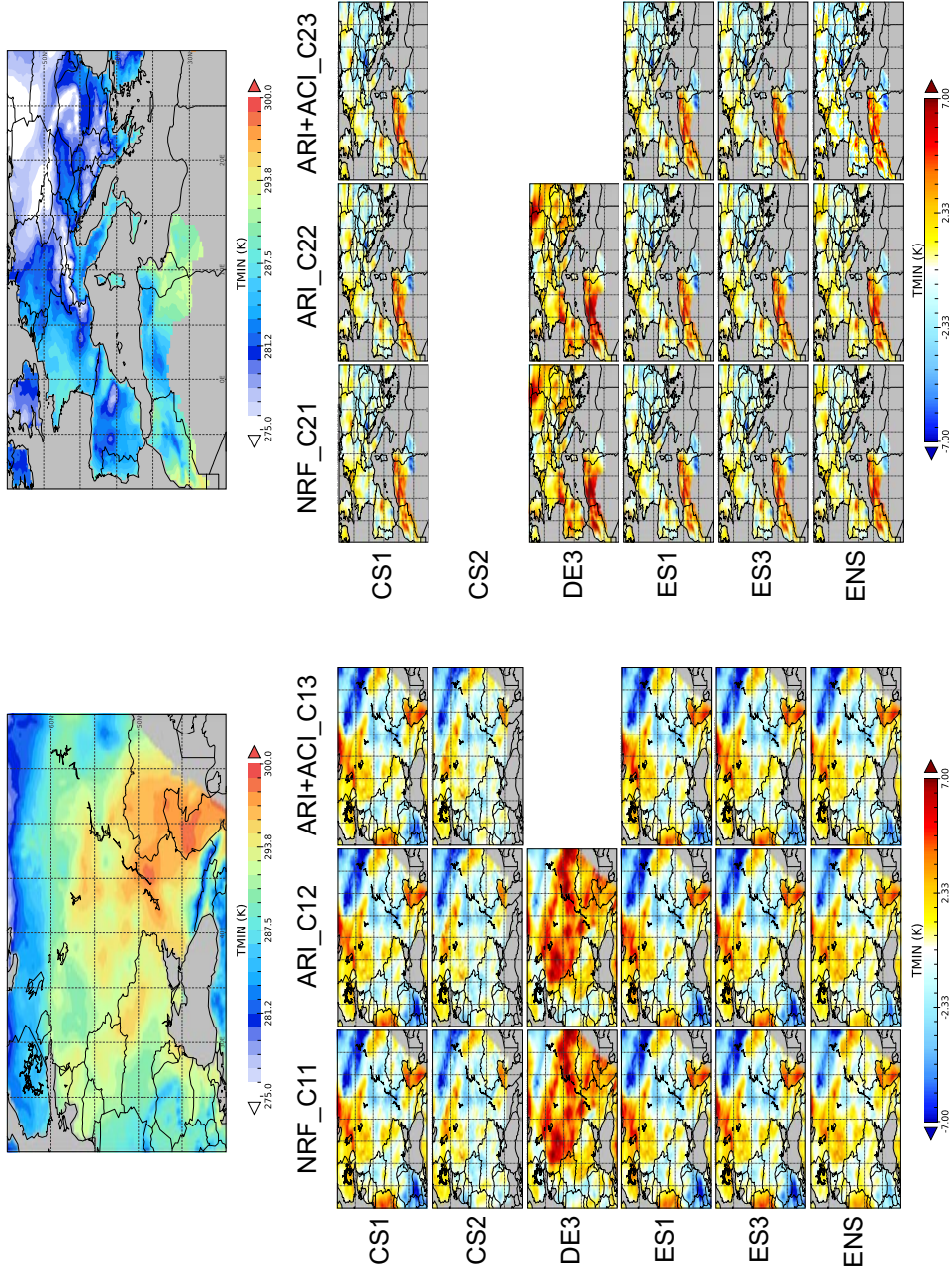


Figure 4.3: (Top row) Minimum temperature (TMIN) for the fires (left) and dust (right) episodes, as derived from E-OBS database (in K). The panel below represents the bias for the fires (left) and dust (right) episodes of each simulation with respect to the E-OBS database. NRF: no radiative feedbacks; ARI: aerosol-radiation interactions; ARI+ACI: as ARI including aerosol-cloud interactions.

4.3.2 Temporal correlation

The temporal correlation (estimated through the coefficient of determination, ρ^2) between simulated and observed series is shown in Fig. 4.4, 4.5 and 4.6 for mean maximum and mean minimum temperature, in that order. The first column in each panel represents the value of ρ^2 of the base case (C11 or C21) of each individual model (or the ensemble) with respect to the E-OBS database. The center (C12 or C22) and right (C13 and C23) columns indicate the increase (red values) or decrease (blue value) of the ρ^2 for each simulation with respect to the case not including feedbacks. Then, that gives an idea in the improvement (or not) in the skill of the model for representing the time evolution of our series when compared to the observations.

For maximum, mean and minimum temperature during the fires episode (left side of Fig. 4.4, 4.5 and 4.6, respectively), domain-averaged ρ^2 is higher than 0.5 for all models (0.52 in CS1-C11 minimum temperature to 0.78 in DE3-C11 mean temperature). In general, coefficients of determination are highest for mean temperature (0.60 to 0.78) and lowest for minimum temperature (0.50 to 0.56), presenting the ensemble always maximum values for ρ^2 (0.75, 0.79 and 0.61, respectively for maximum, mean and minimum temperature). The highest ρ^2 values are found over the north and west part of the domain (above 0.8 in mean temperature) and the lowest mainly over south and southeast area of the domain (under 0.2). According to the improvement with respect to C11 case, when analyzing the inclusion of the ARI and ARI+ACI a general improvement is observed for maximum and mean temperature, with positive values reaching up to 0.18 (domain-averaged values improve for individual models around 1% for maximum, 0.3% for mean temperature). Correlation with minima experiences a slight decrease (-0.4%) when including ARI or ARI+ACI for the ensemble mean.

During dust episode (right side of Fig. 4.4, 4.5 and 4.6), domain-averaged ρ^2 is higher than for the fires episode for all models and variables in the base case (0.76 in DE3-C21 minima to 0.90 in DE3-C21 mean temperature), with the ensemble again providing the highest correlation (values ranging from 0.88 for maximum, 0.91 for mean and 0.84 for minimum temperature). As well as before, the inclusion of the ARI and ARI+ACI shows an improvement over some areas in the order of 0.17 for mean and maximum temperature, with domain-averaged improvements of 0.3% in C22-C23 for maximum temperature, and 0.2% in C22-C23 for mean temperature and 0.1% in C23 for minimum temperature, with no improvement for C22 in this latter variable).

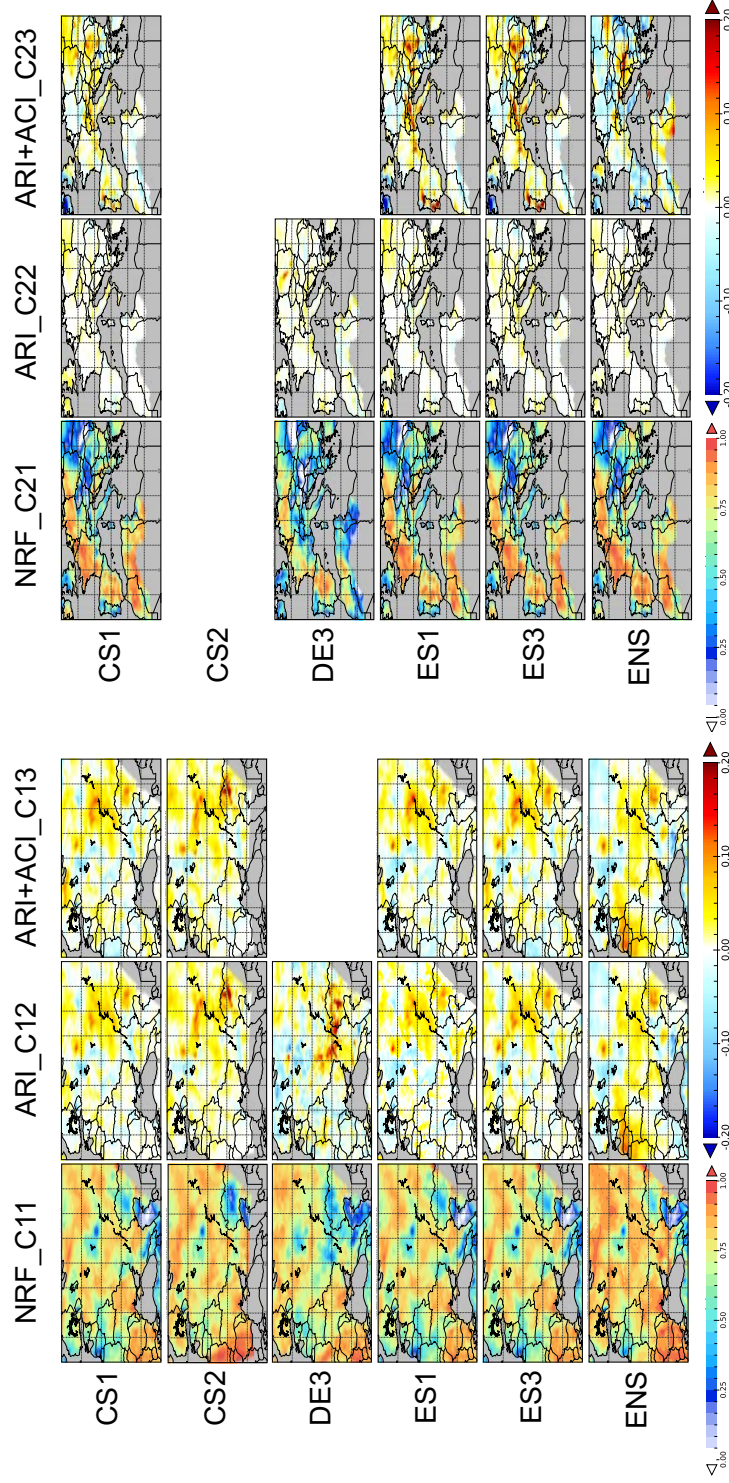


Figure 4.4: (Top row) Time determination coefficient (ρ^2) (model vs. E-OBS) of the maximum temperature (TMAX) for the fires (left panel) and dust (right panel) episodes. The first column in each panel below represents the value of ρ^2 of the no radiative feedback case with respect to the E-OBS database. The center and right columns indicate the increase (red values) or decrease (blue value) of each simulation with respect to the case not including feedbacks. NRF: no radiative feedbacks; ARI: aerosol-radiation interactions; ARI+ACI: as ARI including aerosol-cloud interactions.

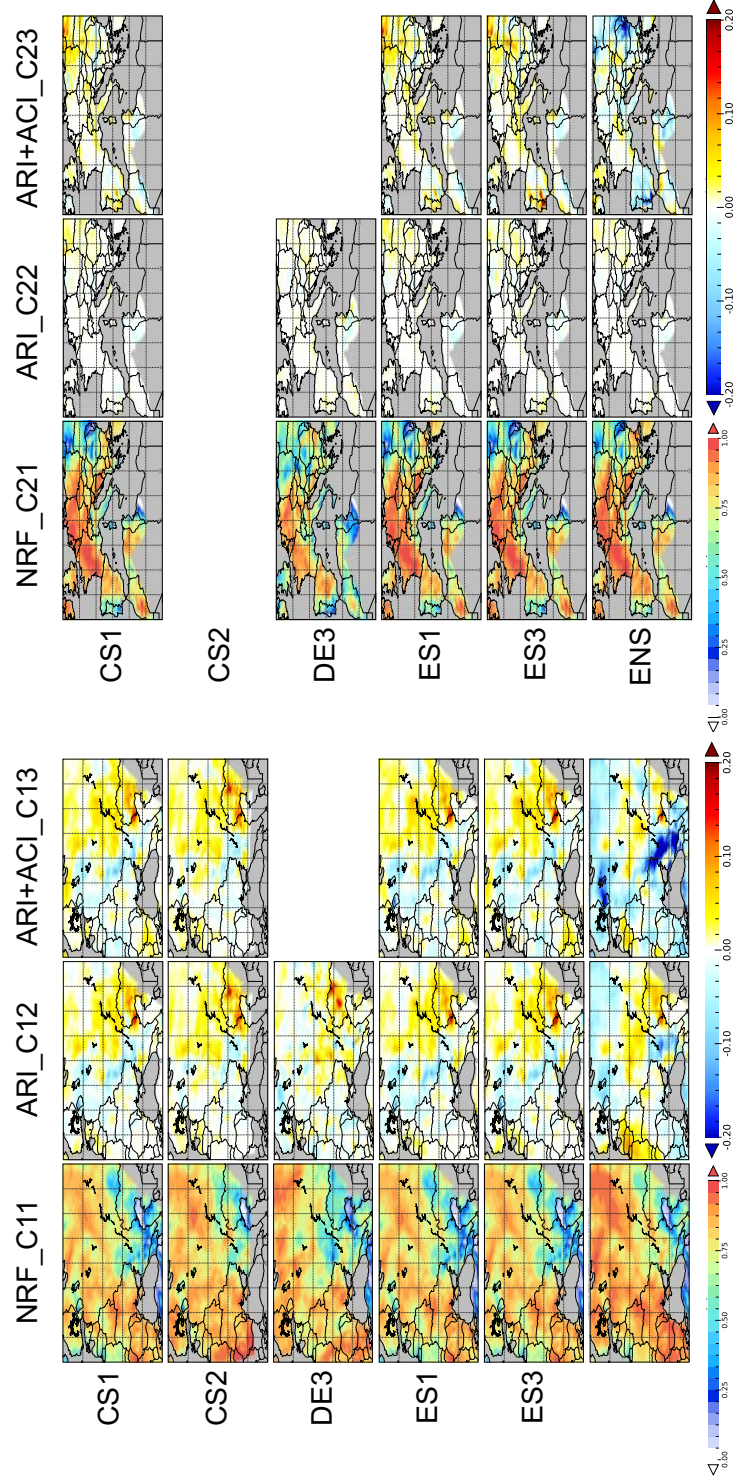


Figure 4.5: (Top row) Time determination coefficient (ρ^2) (model vs. E-OBS) of the mean temperature (TEMP) for the fires (left panel) and dust (right panel) episodes. The first column in each panel below represents the value of ρ^2 of the no radiative feedback case with respect to the E-OBS database. The center and right columns indicate the increase (red values) or decrease (blue value) of each simulation with respect to the case not including feedbacks. NRF: no radiative feedbacks; ARI: aerosol-radiation interactions; ARI+ACI: as ARI including aerosol-cloud interactions.

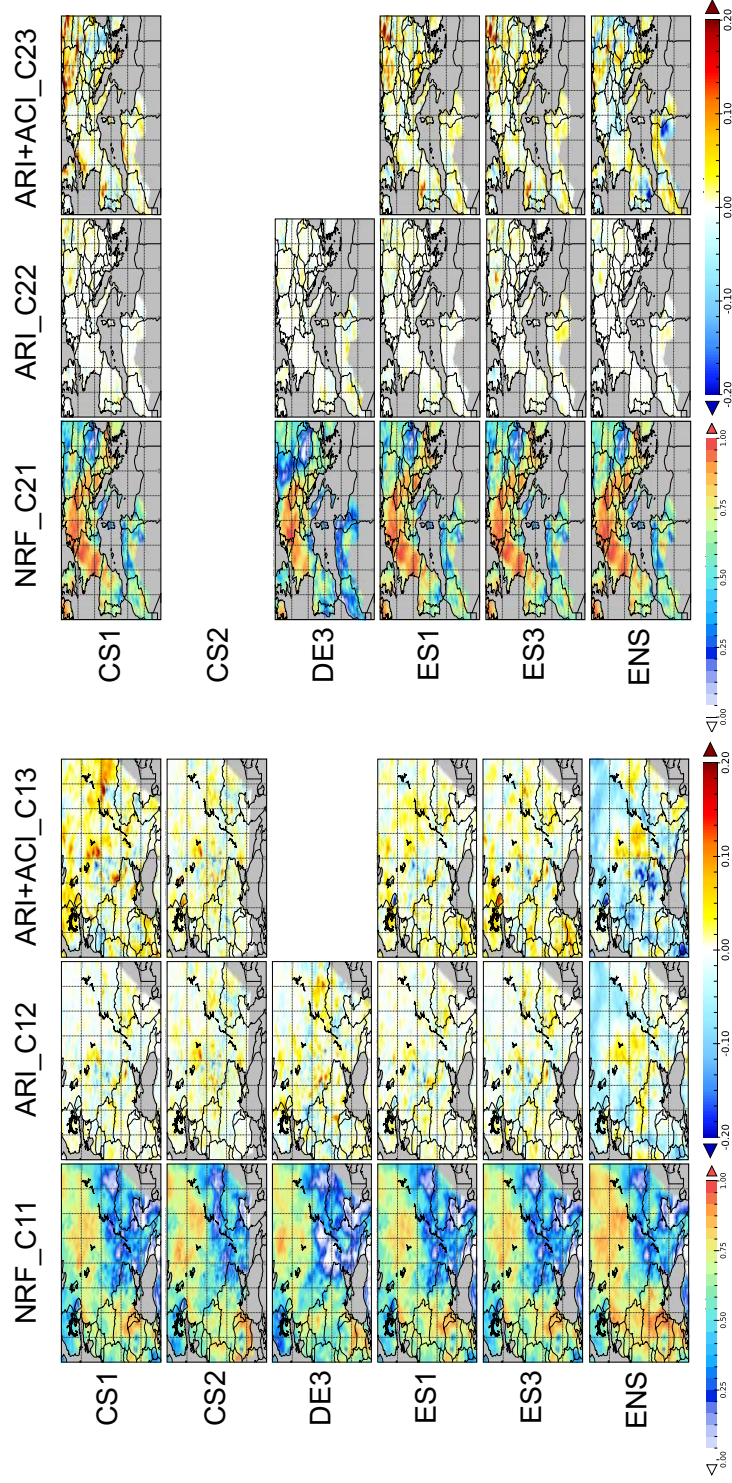


Figure 4.6: (Top row) Time determination coefficient (ρ^2) (model vs. E-OBS) of the minimum temperature (TMIN) for the fires (left panel) and dust (right panel) episodes. The first column in each panel below represents the value of ρ^2 of the no radiative feedback case with respect to the E-OBS database. The center and right columns indicate the increase (red values) or decrease (blue values) of each simulation with respect to the case not including feedbacks. NRF: no radiative feedbacks; ARI: aerosol-radiation interactions; ARI+ACI: as ARI including aerosol-cloud interactions.

4.3.3 Temporal variability

The results for the daily variability of maximum, mean and minimum temperature have been obtained by calculating the standard deviation of the daily mean series at each grid point of all the land grid points of the corresponding domain for the fires and dust episodes.

Considering maximum temperature, in the fires episode (left column of Fig. 4.7), all runs tend to slightly overestimate the standard deviation of maximum temperature for the base case (no radiative feedbacks), with biases of maximum temperature standard deviation varying between +1.28 K for DE3-C11 to +0.25 K for ES1-C11. The biases of the standard deviation are reduced by -22.6% (on average) when including the ARI, with reductions in the biases of the standard deviation ranging from -34.2% in ES1-C12 and -8.6% for DE3-C12. For the ARI+ACI simulations the average reduction of the bias is -41.21% (-56.9% for ES1-C13 and -24.40% for CS2-C13). The rest of the models and cases show an intermediate behavior for representing the variability, with the best skills always for the cases including the ARI+ACI interactions. Analogous results can be found for maximum temperature during the dust episode (right column of Fig. 4.7): the inclusion of aerosol feedbacks generally improve the representation of the temporal variability of maximum temperature, with an average reduction of the bias of the standard deviation of -5.9% (-16.6%) for ARI (ARI+ACI) simulations.

For mean temperature during the fires episode, (left column of Fig. 4.8) all runs tend to overestimate the standard deviation for the base case (no radiative feedbacks), with biases of mean temperature standard deviation between +0.2 to +1.1 K. As for the maximum temperature, the biases of the standard deviation are reduced on -41.8% (on average) when including the ARI and -66.5% for the ARI+ACI simulations, with reductions in the biases of the standard deviation ranging from -8.5% in the DE3-C12 simulation to -78.2% in the ES1-C13 case. Similar to the maximum temperature, the rest of the models and cases show an intermediate representation the variability of the mean temperature, with the best skills always for the cases including the ARI+ACI interactions. Results for the dust episode are shown in the right column of Fig. 4.8. The standard deviation tends to be overestimated by all models in the north of Africa and central Europe, and underestimated in the eastern part of the target domain. Overall, the inclusion of ARI does not lead to better skills of the models when representing the temporal variability ($+2.4\%$), and for ARI+ACI the skill improved only marginally (reductions of -0.6%).

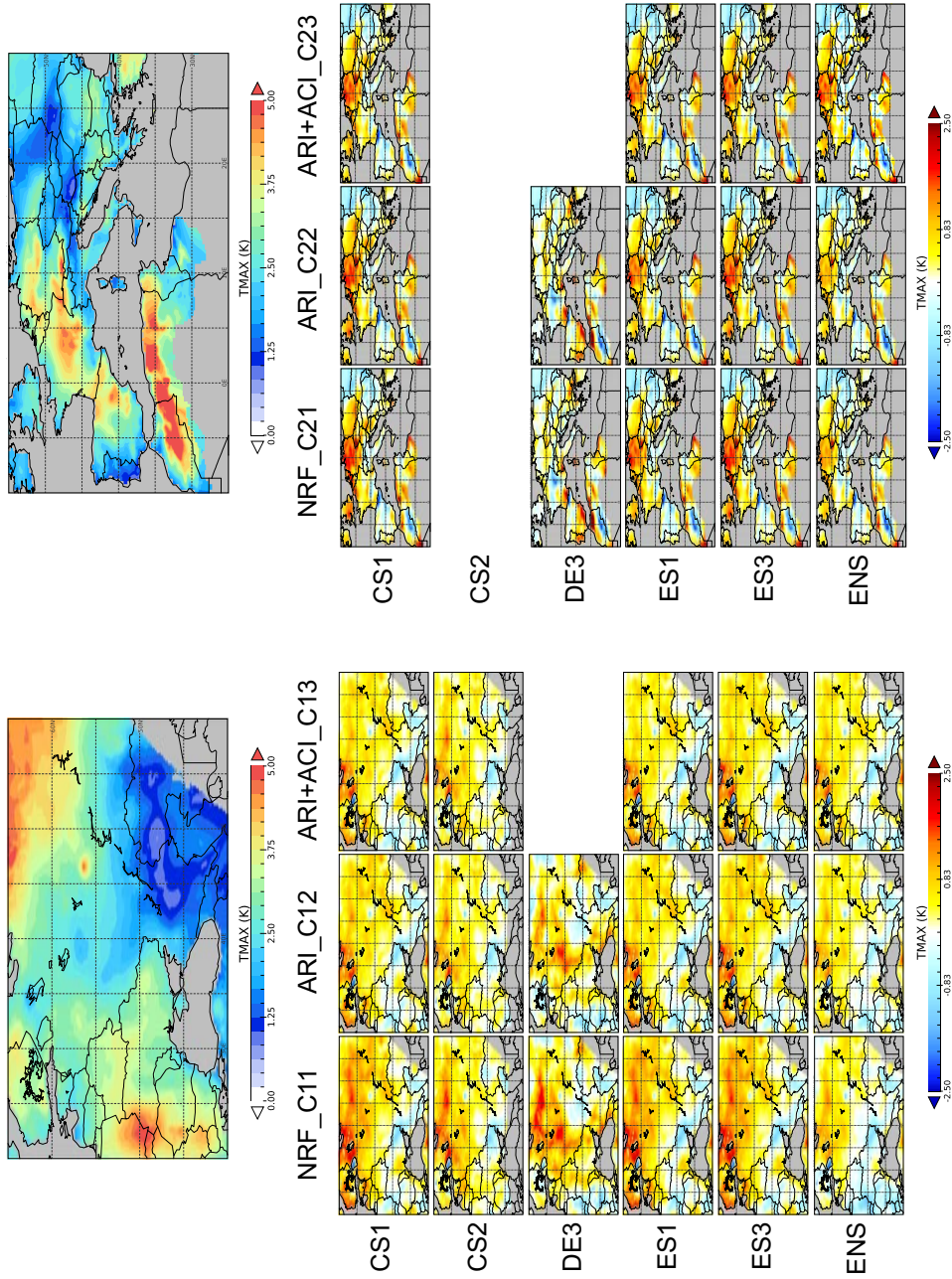


Figure 4.7: (Top row) Standard deviation (STD) of the maximum temperature (TMAX) for the fires (left) and dust (right) episodes, as derived from E-OBS database (in K). The panel below represents the bias for the standard deviation of the fires (left) and dust (right) episodes of each simulation with respect to the E-OBS database. NRF: no radiative feedbacks; ARI: aerosol-radiation interactions; ARI+ACI: as ARI including aerosol-cloud interactions.

With respect to the minimum temperature, for the fires episode (left column of Fig. 4.9) all runs tend to overestimate the standard deviation. Biases of the minimum temperature standard deviation range between +0.4 K for the WRF-Chem-based simulations and +1.0 K for DE3-C11. The high-resolution CS2-C11 simulation presents the lowest bias (+0.3 K).

If considering the biases of the standard deviation, there is a slight improvement when including ARI or ARI+ACI for the fires episode, while a slight worsening is depicted for the dust case. The variations in the biases of the standard deviation are on average -2.1% and -4.9% respectively for the ARI and ARI+ACI simulations ($+3.4\%$ and $+5.4\%$ for the dust episode).

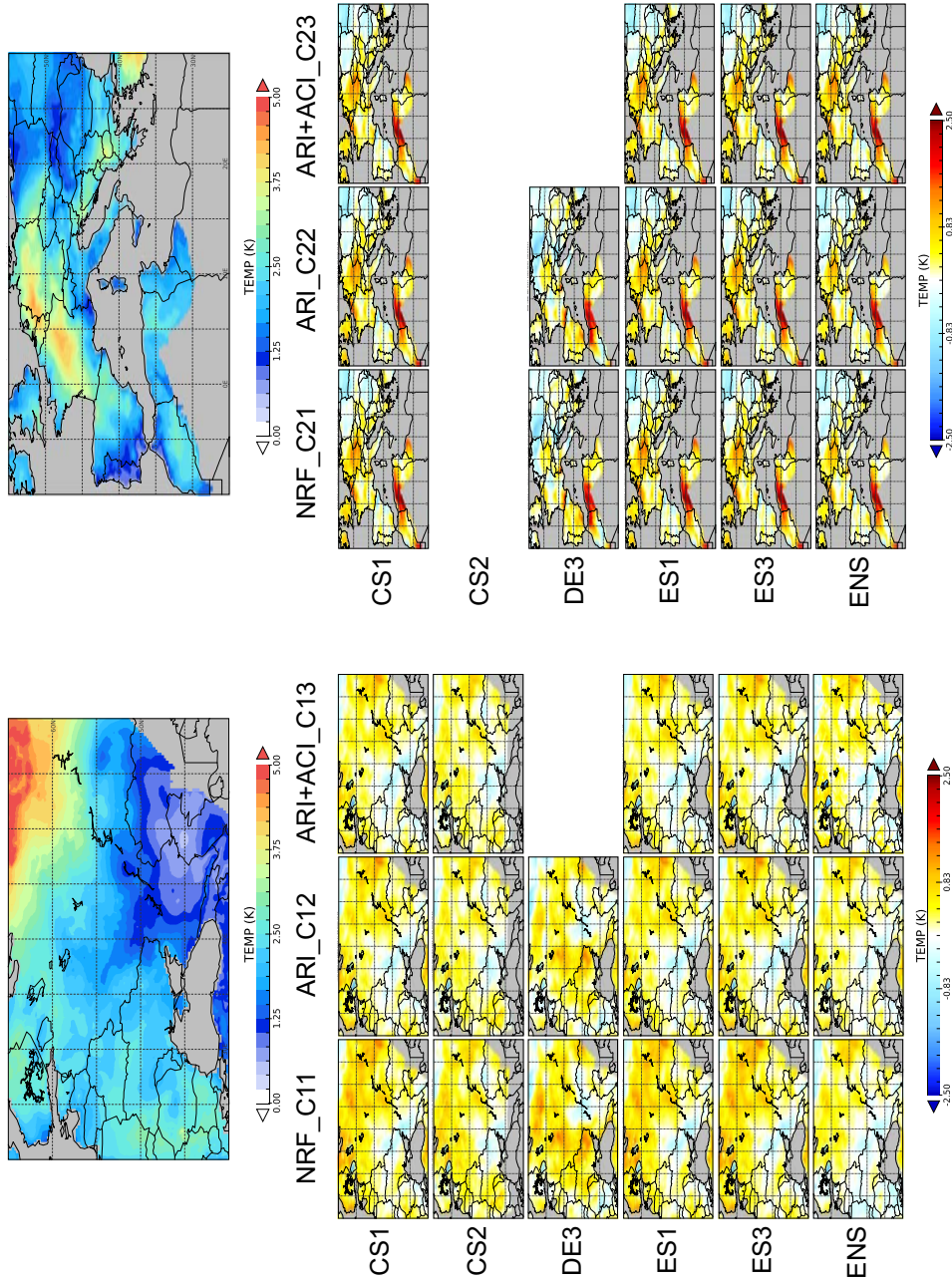


Figure 4.8: (Top row) Standard deviation (STD) of the mean temperature (TEMP) for the fires (left) and dust (right) episodes, as derived from E-OBS database (in K). The panel below represents the bias for the standard deviation of the fires (left) and dust (right) episodes of each simulation with respect to the E-OBS database. NRF: no radiative feedbacks; ARI: aerosol-radiation interactions; ARI+ACI: as ARI including aerosol-cloud interactions.

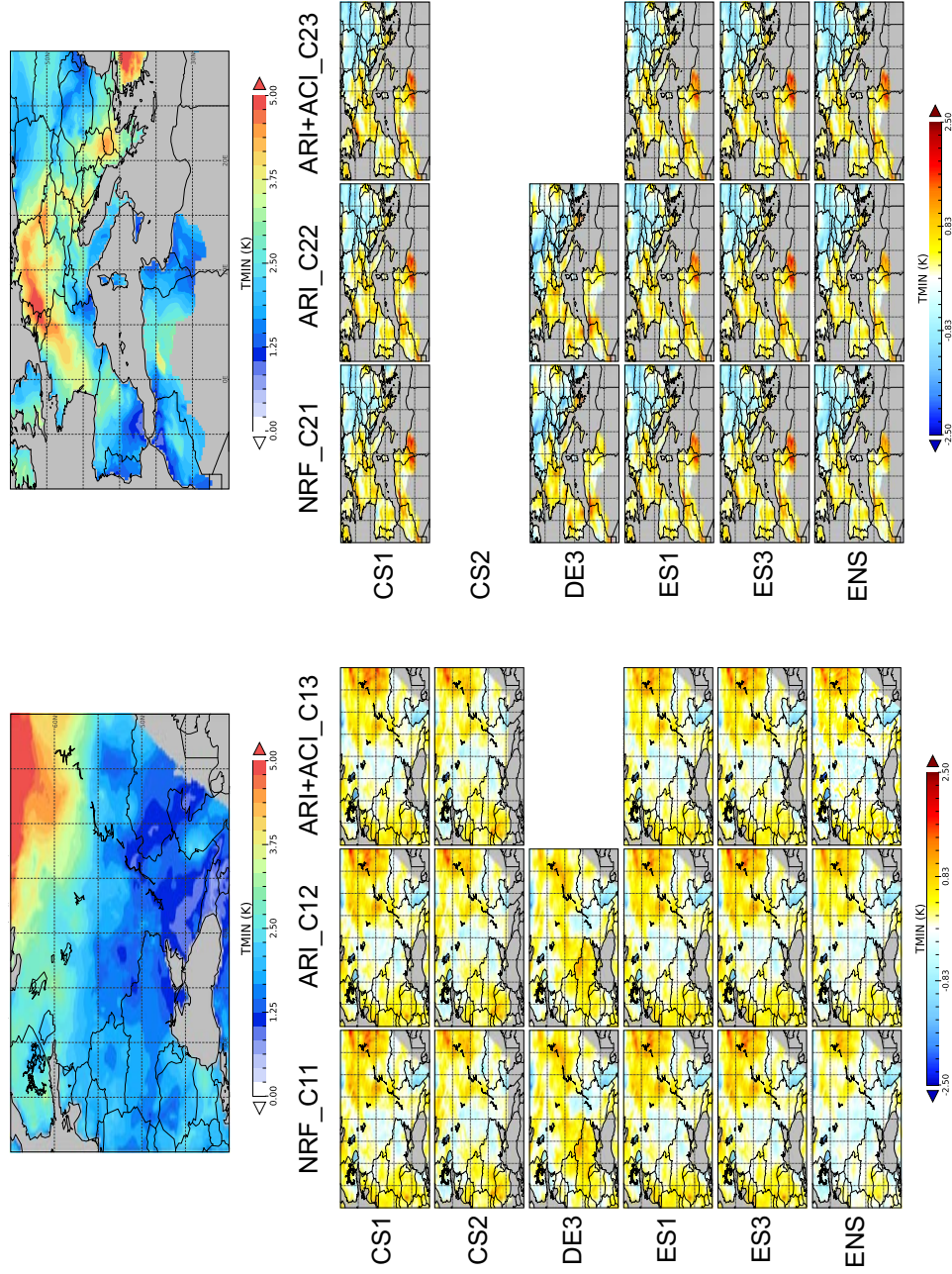


Figure 4.9: (Top row) Standard deviation (STD) of the minimum temperature (TMIN) for the fires (left) and dust (right) episodes, as derived from E-OBS database (in K). The panel below represents the bias for the standard deviation of the fires (left) and dust (right) episodes of each simulation with respect to the E-OBS database. NRF: no radiative feedbacks; ARI: aerosol-radiation interactions; ARI+ACI: as ARI including aerosol-cloud interactions.

4.3.4 Spatial variability

Taylor diagrams (Taylor, 2001) allow an easy comparison between the spatial and temporal patterns of two fields (Rauscher et al., 2010). In Fig. 4.10 shows the relative spatial standard deviation (radial distance from the origin) and the correlation (the cosine of the angular coordinate) with E-Obs. Model results with good performance in terms of spatial variability and correlation are located closer to the standard deviation ratio 1 and correlation 1, which corresponds to E-OBS (indicated by the small black asterisk). For maximum, mean and minimum temperature, the diverse models (and configurations) show a narrow spread in the representation of the spatial structure of the standard deviation.

With respect to the mean field of maximum temperature (left column in Fig. 4.10) all models perform well for the fires period (top row), with high spatial correlations (over 0.9) and a normalized standard deviation close to observations. However, the no radiative feedback configuration (C11 cases in Fig. 4.10) represent excessive spatial variability (standard deviation ratio over 1). The spatial variability of the daily standard deviation for the ARI simulations (asterisks in Fig. 4.10, C12 cases), as well as for ARI+ACI simulations (squares, C13 cases) is substantially improved, despite the spatial correlation remains practically constant for all models. Since there is a positive bias in the models when representing the spatial variability in the no radiative feedbacks simulations, the inclusion of radiative effects reduces the variability and therefore improves its spatial patterns. Analogous results can be found for the dust episode (bottom row, Fig. 4.10), with a larger agreement between models, and lower differences between C21, C22 and C23 cases (no feedbacks, ARI and ARI+ACI simulations, in that order).

With respect to the mean temperature (center column in Fig. 4.10), the models perform very similarly with each other, showing a high spatial correlation with the observations (over 0.9 for all models and cases), with a small overestimation of the spatial variability for the C11 (fire episode, no radiative feedbacks) case (top row), which improves when including the ARI and ARI+ACI interactions. Similarly, the spatial variability is slightly overestimated for the C21 (dust, no radiative feedbacks) case, except for the DE3 model. Generally, the models better capture the spatial structure of the variability during the fires and dust cases (Fig. 4.10, center column) when including the radiative feedbacks. The correlation is only slightly improved for the ARI and ARI+ACI cases (except for ENS simulations, which will be discussed below), and is always higher for the mean temperature than for maximum temperature. The minimum temperature (Fig. 4.10, right column) is captured with quality as the maximum and mean temperature.

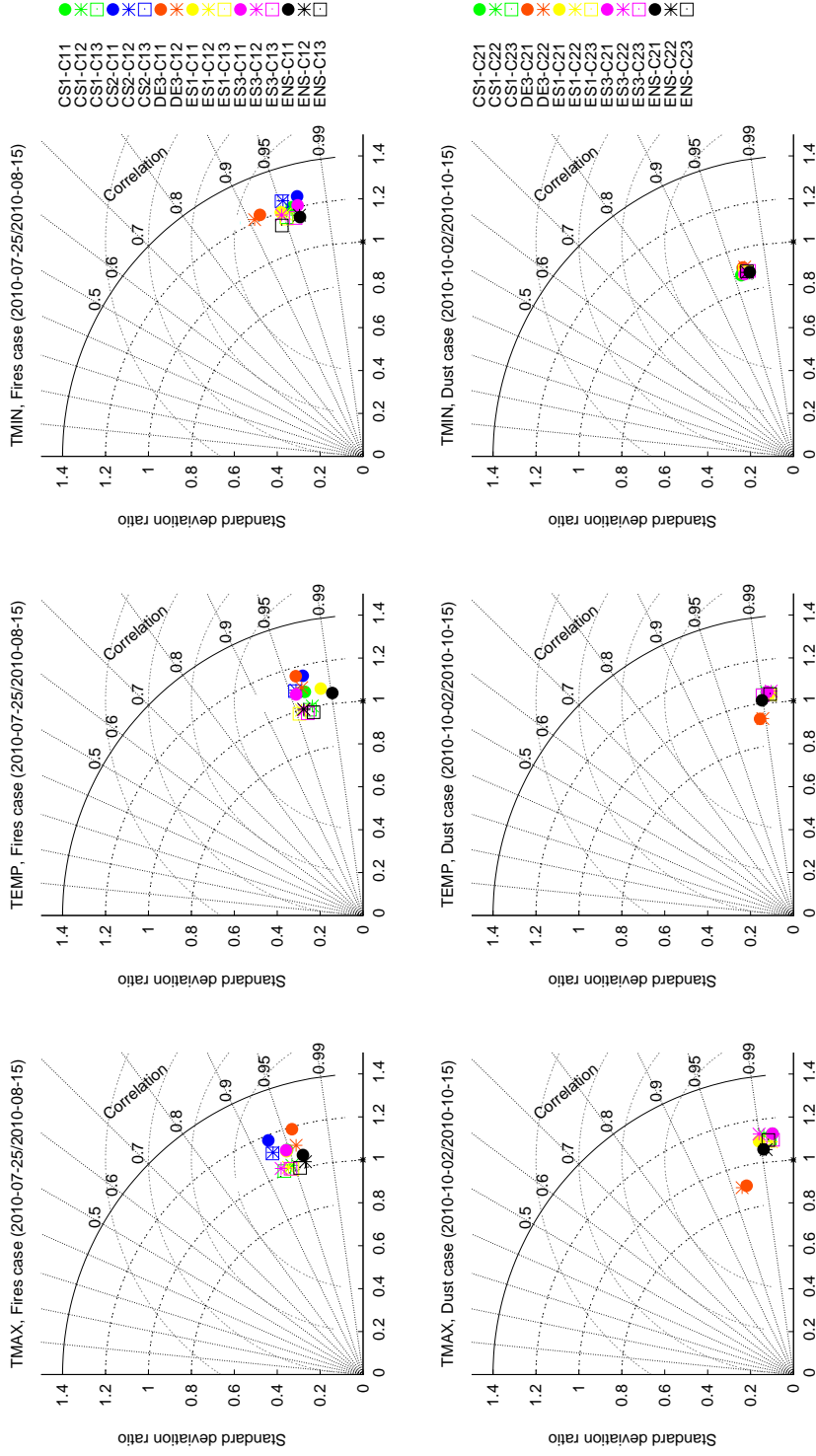


Figure 4.10: Taylor diagrams for (left) maximum temperature, (center) mean temperature, and (right) minimum temperature for the simulations included in the analysis. The top row represents the Taylor diagrams for the fires episode, while the bottom row stands for the dust episode. The cases included are: no radiative feedbacks (filled circle), ARI (asterisk) and ARI+ACI (empty squares). Each configuration is shown in a different color: CS1 (green), CS2 (dark blue), DE3 (red), ES1 (yellow), ES2 (red), ES3 (yellow), ENS (black) and ENS+ACI (empty squares).

While for the fire episode the models (in all cases) tend to provide a higher spatial variability than the observations, the spatial variability is underestimated for the dust episode, but with a high correlation (over 0.9) for both episodes. For this variable, the improvement of including the radiative feedbacks is not so evident, since the spatial variability does not generally improve for C12, C13, C22 or C23 cases with respect to the configuration without radiative feedbacks. Moreover, the correlation coefficient is even slightly reduced with the inclusion of ARI or ARI+ACI.

Last, the added value of considering the ensemble mean of all available simulations in each episode and case is clear for the fires episode, but not that obvious for the dust period. For the fire episode, the ensemble mean outperforms individual models in terms of the standard deviation and the correlation coefficient, especially for mean temperature, where the correlation increases up to 0.99 for the ENS-C11 case. The exception is found for the ENS-C13 for minimum temperature. Generally, the skill of most models improves when aerosol-meteorology interactions are taken into account

For the dust case, the ensemble mean outperforms the individual models for representing the standard deviation (that is, the spatial variability). However, the spatial correlation coefficient is somewhat reduced as compared to the individual models.

4.4 Summary and conclusions

This study shows a collective operational evaluation of the temperature at 2 meters (maximum, mean and minimum) simulated by the coupled chemistry and meteorology models under the umbrella of COST Action ES1004 for a wildfires and a dust episode in the year 2010. The meteorological parameters considered in this assessment are important to understand the effect of the aerosol interactions with clouds and radiation. In this sense, this study complements other several analysis (e.g. Brunner et al. (2015); Forkel et al. (2015); Makar et al. (2015a)) by analyzing whether the inclusion of the radiative feedbacks improves or not the representation of the temperature field (maximum, mean and minimum) in an ensemble of simulations.

Focusing on the bias, in both episodes there is a general underestimation of the studied variables, being most noticeable in maximum temperature. In general, there is not a straightforward conclusion with respect to the improvement (or not) of the bias when introducing aerosol radiative feedbacks. Broadly, the biases are improved when including ARI or ARI+ACI in the dust case, but no evident improvements are found for the heatwave/wildfires episode. Although the ensemble does not outperform the individual models (in general), the improvements found when including ARI and ARI+ACI are by far more remarkable for the ensemble than for the

individual models.

With respect to the temporal correlation, maximum and mean temperatures in the fires and dust episode show higher correlations over most of the domain when considering C11 case with respect to the E-OBS database than minimum temperature. During these episodes, a twofold conclusion can be obtained: (1) the ensemble of simulations always outperforms the representation of the temporal variability of the series; and (2) an improvement of the ρ^2 coefficient is found when considering ARI or ARI+ACI feedbacks (in both episodes).

Regarding the temporal variability, during the fire episode there is a general pronounced overestimation of the standard deviation of the studied variables. Here, the inclusion of aerosol feedbacks largely improves the representation of the temporal variability of the three studied variables (reduction of the bias of the standard deviation) showing the best skills for the cases including the ARI+ACI interactions, with a reduction of bias of the standard deviation by as much as 75%. Very similar results can be found for the dust episode. Generally, it is for the temporal variability where the inclusion of the aerosol radiative feedbacks shows the largest improvements and results in an added value of the computational effort made to include direct aerosol radiation interactions and aerosol cloud interactions in the models. Last, with respect to the spatial variability for maximum and mean temperature, the inclusion of radiative effects reduces the variability and improves the spatial patterns for both episodes. For the minimum temperature, the improvement of including the radiative feedbacks is less evident.

In order to further investigate the impact of including the aerosol interactions in online-coupled models, episodes with stronger effects on the ACI should be considered since the selected episodes during EuMetChem Cost Action were mainly related to ARI. Moreover, during the dust episode, most of the ARI+ACI differences found in the models with respect to the base case were found over the Mediterranean sea, but the observational data E-OBS only has values over land. Unfortunately part of the interpretation of the results may be missed due to the unavailability of this database over the ocean. Furthermore, it must be considered, that all results for the ARI+ACI cases were from WRF-Chem simulations.

There are still modeling issues regarding the representation of the field of temperature, where maximum temperatures are underestimated and minimum temperatures are overestimated and the inclusion of the aerosol feedbacks does not improve this situation. Nevertheless, in this study, a general improvement of the temporal variability and correlation has been seen. These improvements may be important not only for certain episodes, as analyzed here, by also for the representation of the climatology of temperatures. However, climatic-representative periods should be covered in further studies.

Chapter 5

How good are aerosol-cloud interactions represented in online-coupled regional models?

Baró, R., Stengel, M., Brunner, D., Curci, G., Hollmann, R., Forkel, R., Palacios-Peña, L., Savage, N., Schaap, M., Van der Gon, H., Hogrefe, C., Galmarini, S and Jiménez-Guerrero, P. How good are aerosol-cloud interactions represented in online-coupled regional models? Submitted to: Atmospheric Chemistry and Physics.

On-line coupled meteorology-chemistry models permit the description of the aerosol-radiation (ARI) and aerosol-cloud interactions (ACI). The effect of atmospheric aerosols remains uncertain in climate modeling. One of the reasons is their variability in time and space, which could modify cloud microphysics and impact cloud radiative properties and climate. Hence, the aim of this work is to assess the representation of the ARI+ACI interactions in regional-scale coupled models when simulating the climate-chemistry-cloud-radiation system. The evaluated simulations are run under the umbrella of the air quality model evaluation international initiative (AQMEII) Phase 2 (over 2010 and Europe) and include ARI+ACI interactions. The model simulations are evaluated against observational data from ESA Cloud_cci project. Results show an underestimation (overestimation) of cloud fraction (CFR) over land (ocean) areas, which could be related to satellite retrieval missing thin clouds. Lower bias and mean absolute error (MAE) are found in the ensemble mean. Cloud optical depth (COD) and cloud liquid ice path (CIP) generally underestimate over the whole domain. MAE was in line with the bias. Cloud liquid water path (CWP) broadly overestimates the bias. Temporal r points to a general positive correlation between models and satellite observations. Finally, the according to the spatial

variability CFR, has the best skill, whereas COD, CIP and CWP indicate a lower skill. The differences found can be attributed to differences in the microphysics schemes used, for instance, the number of ice hydrometeors has been seen to be relevant as well as the prognostic/diagnostic treatment of the CWP.

5.1 Introduction

The study of the atmospheric aerosol radiative effects and feedbacks with the climate system is nowadays one of the most important topics in climate science. Atmospheric aerosols vary in time and space and can lead to variations in cloud microphysics, which impact cloud radiative properties and climate. They influence the Earth's radiation budget by scattering and absorbing solar radiation, which turns into a reduction of incoming solar radiation and a cooling of the climate system. These processes have traditionally been called the aerosol direct effect but were renamed after the Fifth Report of the Intergovernmental Panel on Climate Change (IPCC AR5) (Boucher et al., 2013; Myhre et al., 2013b) as aerosol-radiation interactions (ARI). This term also encompasses the aerosol semi-direct effect, which has been seen as a rapid adjustment of the atmospheric state that follows aerosol-radiation interactions (Boucher, 2015). Last, aerosols serve as cloud condensation nuclei (CCN) influencing overall cloud radiative properties through interactions referred to as the first indirect effect or Twomey effect (Twomey, 1974, 1977). More aerosol particles lead to more cloud condensation nuclei resulting in an increase in the concentration of cloud droplets. When the cloud water is fixed, this is accompanied by a reduction in the cloud droplet size and an increase in the cloud reflectivity. Altogether results in less solar energy absorbed and a cooling of the climate system. Additionally, aerosols acting as CCN may affect precipitation efficiency, cloud life-time, and cloud thickness, thus further influencing weather and climate through the second indirect effect (Albrecht, 1989), also named cloud lifetime effect. The modification of cloud microphysical properties is expected to have an impact on cloud evolution, in particular in terms of the ability of clouds to generate droplets that are large enough to initiate precipitation. This effect is traditionally called the second aerosol indirect effect, but since the AR5 these indirect effects are called aerosol-cloud interactions (ACI). Those interactions are more uncertain due to complexity of the microphysical processes (Boucher and Lohmann, 1995; Schwartz and Benkovitz, 2002; Lohmann and Feichter, 2005).

There are different approaches to address the study of ACI, usually by means of combined methodologies of observations and/or modeling. In the field of observations/remote sensing, McComiskey et al. (2009) used the Atmospheric Radiation Measurement (ARM), focused on California area. They studied the albedo effect as the change in cloud droplet number con-

centration (CDNC) with aerosol concentration, resulting on a local radiative forcing of around -13 W m^{-2} (top-of-the-atmosphere). Liu et al. (2011a) also used ARM combined with GOES satellite measurements and derived theoretically an analytical relationship between the relative surface shortwave cloud radiative forcing, cloud fraction and cloud albedo. They noticed its utility for diagnosing deficiencies of cloud-radiation parameterizations in climate models.

Combining observations and modeling, Avey et al. (2007) used cloud retrievals from the Moderate Resolution Imaging Spectroradiometer (MODIS) and output from a tracer transport model (FLEXPART). They compared cloud and pollution fields in northeastern coast of United States, during 2004, under the umbrella of International Consortium for Atmospheric Research on Transport and Transformation (ICARTT) mission. Where the transport model indicates polluted air, cloud droplet effective radii is smaller and cloud optical depth (COD) is in some cases higher, at least close to primary source regions. Cloud perturbation is negligible when advection time varies ranges 4 ± 1 days, maybe due to wet-scavenging of CCN. Regarding the perturbation of cloud liquid water path (CWP) by pollution, they did not find any conclusive evidence. Menon et al. (2002), by means of the Goddard Institute for Space Studies (GISS) general circulation model, described the ACI regarding sulfate, organic carbon and sea salt. The result of the global mean aerosol indirect effect varies from -1.55 to -4.36 W m^{-2} in the simulations, considering the three types of aerosols. According to the authors, the preindustrial background aerosol burden gives a strong indirect effect, making a quite sensitive aerosol indirect effect result.

In the field of modeling, including aerosol interactions represents an important challenge in air quality/climate modeling. Additionally, it is also important for the development of integrated emissions control strategies for air quality management as well as climate change mitigation (Yu et al., 2013; Rosenfeld et al., 2014). Yang et al. (2011a) used the Weather Research Forecast coupled with chemistry (WRF-Chem) model in a study over the northern Chilean and southern Peruvian coasts during 15 October to 16 November 2008. They run a simulation including ACI and compared to other run with fixed CDNC and simplified cloud and aerosol treatments. When taking into account a complex ACI treatment, the temperature and humidity gradients are strengthened within the inversion layer; ACI inclusion also lowers the marine boundary layer depth. They also found that apart from a better skill when simulating aerosol properties, the coupled simulation of ACI improved cloud optical and microphysical properties. Moreover, a better agreement of mean top-of-atmosphere outgoing fluxes with observations was found in ACI simulation.

In the context of international initiatives, in AEROCOM (Quaas et al., 2009) ten different

general circulation models (GCMs) taking into account aerosol-radiation-cloud interactions were evaluated against satellite data. The authors computed statistical relationships between aerosol optical depth and various cloud and radiation quantities. Their results suggested that the second aerosol indirect effect has to be revised in GCMs (mainly regarding an autoconversion parameterisation). The Atmospheric Chemistry and Climate Model Intercomparison Project (ACCMIP) (Shindell et al., 2013) examined the short-lived drivers of climate change in current climate models. Ten ACCMIP models including aerosols, 8 of which also participated in the Coupled Model Intercomparison Project phase 5 (CMIP5) were evaluated. They studied the effective radiative forcing (ERF) which includes the direct + indirect effects. They pointed to an aerosol ERF of -1.17 W m^{-2} ; (ranging from -0.71 to -1.44 W m^{-2}) for the period 1850 to 2000.

In order to simulate realistically the chemistry-aerosol-cloud-radiation-climate interactions, fully online-coupled meteorology-atmospheric chemistry models are needed (Baklanov et al., 2008b; Zhang, 2008). Moreover, to build confidence in air quality-climate interaction studies, a thorough evaluation of integrated meteorology-atmospheric chemistry models is demanded, at both global and regional scales. Particularly, ACI continue to be one of the most important uncertainties in anthropogenic climate perturbations (Penner et al., 2006; Quaas et al., 2009). The air quality model evaluation international initiative (AQMEII)(Rao et al., 2011) emerged to promote policy-relevant research on regional air quality model evaluation across the atmospheric modeling communities in Europe and North America through the exchange of information on current practices and the identification of research priorities. It is coordinated by the European Joint Research Center (JRC) and U.S. Environmental Protection Agency (EPA). The first phase of AQMEII was focused on the evaluation of off-line coupled atmospheric models whereas during the second phase (Alapaty et al., 2012; Galmarini et al., 2015), the model assessment extended to on-line-coupled air quality models. Based on this, a coordinated exercise of Working Groups 2 and 4 of the COST Action ES1004 (EuMetChem, <http://eumetchem.info>) emerged, to take into account the radiative feedbacks of pollution during episodes with high loads of aerosols. In this sense, this study is conducted in the context of the second phase of AQMEII and and EuMetChem COST Action. An extensive model evaluation can be found in Brunner et al. (2015) for meteorological variables and according to ozone and particulate matter with an aerodynamic diameter smaller than $10 \mu\text{g m}^{-3}$ in Im et al. (2015a,b) respectively; but no information about aerosol-cloud processes from these initiatives is available in the scientific literature.

Under this umbrella, the main objective of this contribution is to assess the representation of the ARI+ACI interactions in regional-scale integrated models when simulating the climate-

chemistry-cloud-radiation system. Up to now, all the collective studies performed used global models; regional climate analysis do not usually take into account ARI+ACI. To the authors knowledge, this contribution is novel in the sense that comprises a collective analysis taking into account ARI+ACI in regional coupled models. It also complements the temperature collective analyses of Baró et al. (2017).

5.2 Methodology

The strategies used to analyze ACI in online-coupled models are described in this section. As stated in the introduction, the analyzed model outputs are the results run under the AQMEII Phase 2 initiative and EuMetChem COST Action. In order to analyze the skills of the coupled models which take into account ARI+ACI, simulations from different models with identical meteorological boundary conditions and anthropogenic emissions have been analyzed.

The common set-up for the participating models and a unified output strategy allow analyzing the model output with respect to similarities and differences in the model response to the aerosol-radiation and aerosol-cloud interactions. The studied variables are cloud fraction (CFR), cloud optical depth (COD), cloud ice path (CIP) and cloud water path (CWP). The target domain is Europe, and the analysis covers the whole year 2010 and its seasonality.

5.2.1 Model simulations

An overview of the one-year model simulations contributing to this study in the context of AQMEII Phase 2 is presented in Table 5.1. It includes 5 simulations conducted with the following models: LOTOS-EUROS (Sauter et al., 2012), UKCA (Savage et al., 2013) and WRF-Chem (Grell et al., 2005; Grell and Baklanov, 2011). To facilitate the cross-comparison between models, the participating groups interpolated their model output to a common grid with 0.25° resolution (but for NL2 model, which has a smaller grid).

According to the emissions and boundary conditions (Table 5.2), all simulations were driven by European Centre for Medium-Range Weather Forecasts (ECMWF) operational analyses (with data at 00 and 12 UTC) and with respective forecasts (at 3/6/9 etc hours), so that the time interval of meteorological fields used for boundary conditions was 3 hours. The chemical initial conditions (IC) were provided by the ECMWF IFS-MOZART model. According to the anthropogenic emissions used, they were provided by the Netherlands Organization for Applied Scientific Research (TNO). The dataset is a follow-on to the widely used TNO-MACC database (Pouliot et al., 2012). Biogenic emissions were estimated by the Model of Emissions of Gases and Aerosols from Nature (MEGAN) (Guenther et al., 2006) which were calculated online.

Fire emissions data were obtained from the IS4FIRE Project (<http://is4fires.fmi.fi>). The emission dataset is estimated by re-analysis of fire radiative power data obtained by MODIS instrument onboard of Aqua and Terra satellites. For further information regarding models parameterizations, the reader is referred to Brunner et al. (2015); Im et al. (2015a,b).

Table 5.1: Some of the AQMEII2 models features of the simulations studied.

Model Simulation	Model	Microphysics	Gas Phase	SW radiation	LW radiation	Aerosol	Aerosol feedbacks
ES1							
DE4	WRF Chem	Lin Morrison	RADM2 RADM2 integ1 RACM	RRTMG		MADE SORGAM	Yes
IT2						MADE VBS	
NL2	RACMO LOTOS-EUROS	Tiedke, Tompkins Neggers	CB-IV	RRTM		ISORROPIA II 2 bins	
UK4	METUM UKCA	Wilson & Ballard	RAQ	Edwards-Slingo		Classic	

Table 5.2: Source of the data used in the simulations inputs for the initial conditions (IC), boundary (BC) and aerosols emissions

Option	Data source
Meteo IC BC	ECMWF
Chemical IC BC	ECMWF IFS MOZART
Anthro. emissions	TNO-MACC
Biogenic emissions	MEGAN
Fire emissions	FMI

5.2.2 Observational data

In order to analyze the effect of different model settings on the representation of ARI+ACI, model data is compared and evaluated against satellite-based observations of cloud properties. In more detail, the satellite data used was generated by the ESA Cloud_cci project which is part of ESA’s Climate Change Initiative (CCI) programme (see Hollmann et al. (2013) for scientific aspects covered in the CCI programme). Several datasets are generated in Cloud_cci (Stengel et al., 2017), of which we used Level-3C data (monthly averages and histograms) of the Cloud_cci AVHRR-PM dataset (Stengel et al., 2016). The data was retrieved by employing the Community Cloud retrieval for Climate (CC4CL, Sus et al., 2017; Mcgarragh et al., 2017) using measurements of the Advanced Very High Resolution Radiometer (AVHRR) onboard the National Oceanic and Atmospheric Administration satellite No. 19 (NOAA-19). The Level 3C data has been used in this study, which has a spatial resolution of 0.5° Latitude/Longitude and represents monthly summary of instantaneous cloud property retrievals taken at 01:30 AM/PM local time. The dataset version used is v2.2, containing, compared to Stengel et al. (2017a) which described v2.0, two significant bug fixes: (1) correcting a miscalculation of BRDF components in condition of high solar zenith angles and/or snow/ice covered surfaces and (2) correcting look-up tables containing pre-calculated radiances as a function of ice cloud properties as well as viewing geometry and illumination condition. Both bug fixes lead to a significant reduction of random and systematic uncertainties of the data, in particular for the optical properties cloud effective radius and cloud optical thickness as well as therefrom derived cloud liquid and ice water path.

5.2.3 Evaluation methodology

Regarding the model evaluation methodology, satellite data is bilinearly interpolated to a common working grid covering the European domain. For evaluating cloud variables, model data is

postprocessed computing the monthly mean of the mean value from 13.00 to 14.00 PM. In order to perform the evaluation of the studied variables, we use several classical statistics according to Willmott et al. (1985), Willmott and Matsuura (2005) and Weil et al. (1992). We will compute the mean bias error (bias), the mean absolute error (MAE) and the correlation coefficient (r).

The bias (Eq. 5.1) is defined as:

$$MBE = \frac{1}{n} \sum_{i=1}^n e_i = \bar{P} - \bar{O} \quad (5.1)$$

Where e_i is the individual model-prediction errors usually defined as prediction (P_i) minus observations (O_i), and \bar{P} and \bar{O} are the model-predicted and observed means, respectively.

The MAE (Eq. 5.2) is defined as:

$$MAE = \frac{1}{n} \sum_{i=1}^n |e_i| \quad (5.2)$$

The standard deviation of the P_i (Eq. 5.3) is:

$$\sigma_P = \sqrt{\frac{1}{n} \sum_{i=1}^n (P_i - \bar{P})^2} \quad (5.3)$$

The standard deviation of the O_i (Eq. 5.4) is:

$$\sigma_O = \sqrt{\frac{1}{n} \sum_{i=1}^n (O_i - \bar{O})^2} \quad (5.4)$$

The r (Eq. 5.5) is:

$$r = \left[\frac{\frac{1}{N} \sum_{i=1}^n (O_i - \bar{O})(P_i - \bar{P})}{\sigma_O \sigma_P} \right] \quad (5.5)$$

Also, the standard deviation ratio is computed as σ_p/σ_o .

A satellite data mask for each monthly mean was done and applied to model data in order to compute the statistics over a coincident area. Last, mean values were computed and are shown in Section 5.3. Due to the monthly availability of the satellite data, the temporal coefficient of correlation is only shown for the whole year 2010. A satellite data mask with greater or equal to 6 values of satellite data -months- has been considered so that the correlation is only shown in grid points with at least 6 months of data).

5.3 Results

In the following section, the behaviour of the studied variables (CFR, COD, CIP and CWP) for the bias, MAE, temporal r and spatial variability are presented. They are obtained by calculating the corresponding statistic of the monthly mean series at each grid point of all the land grid points of the domain for each season as follows: January-February-March (JFM); April-May-June (AMJ); July-August-September (JAS); October-November-December (OND). All the figures have the same structure (but temporal r): top row represents the mean satellite values from ESA Cloud_cci and from left to right, the mean for the periods analyzed: 2010, JFM, AMJ, JAS and OND. The following rows (2 to 7) include the computed statistic for each model and the ensemble (ENS) mean, estimated as the average of all the available model simulations. With respect to temporal r , only the year correlation is shown (as explained in 5.2). First row shows the mean satellite data for the cloud variables (one in each column) for 2010, while the temporal r for each simulation is shown in the following rows.

5.3.1 Cloud fraction, CFR

Fig. 5.1 shows the bias and Fig. 5.2 the MAE for the variable CFR. In both cases, the first row shows the satellite CCI values, which are generally higher than 0 (except in some areas during JAS), with minimum values over the eastern Mediterranean which increase with latitude. The following rows show the bias and MAE of the different model simulations (Figs. 5.1 and 5.2 respectively). In Table 5.3, mean values of satellite, models and ENS are collected. For CFR, mean model values are close to satellite data, with a slight tendency for underestimation. Fig 5.1 generally points to an underprediction of CFR over land areas and an overestimation over the ocean. Individual model simulations present positive a bias range from +40% to over -35%. ES1 model depicts the highest underestimation (-40% mean bias) mainly over land areas. MAE (Fig. 5.2) is up to 40%, especially noticeable over central Europe and the Mediterranean Sea in ES1, and the rest of the models show lower MAE values (15%). DE4 and IT2 simulations show a high MAE over the Atlantic Ocean and North Africa with an error of 30%, coinciding with a positive bias of 30% (Fig.5.1). For the ENS mean (last row Fig 5.1), lower levels are found, with Biases ranging from 20% to -20%, outperforming the individual simulations (also for MAE). The positive bias is more pronounced during JAS, where mean satellite levels are lower (first row, Fig 5.1). This negative bias was expected because of the general trend of global and regional models to underestimate CCN (Wyant et al., 2015) and therefore cloud formation. On the other hand, overestimations found off-shore could be produced because satellite retrievals

missed thin clouds, making the models overestimate CFR since satellite did not totally capture them. Last, Fig. 5.3 represents mean satellite data for the cloud variables in the first row for 2010. The following rows cover the temporal r for each model simulation. For CFR, a positive temporal r prevails, with mean values of 0.7/0.8 and areas with values close to 0.9. Conversely, there are some areas over the sea, with negative correlation (around -0.5). This spatial pattern of the r coefficient is related to Fig. 5.1, where negative bias prevail over land areas and positive bias over sea. Generally, a positive correlation implies that when satellite CFR values increase (decrease) also model levels CFR increase (decrease) but models underestimate it, mainly over land area (Fig. 5.1).

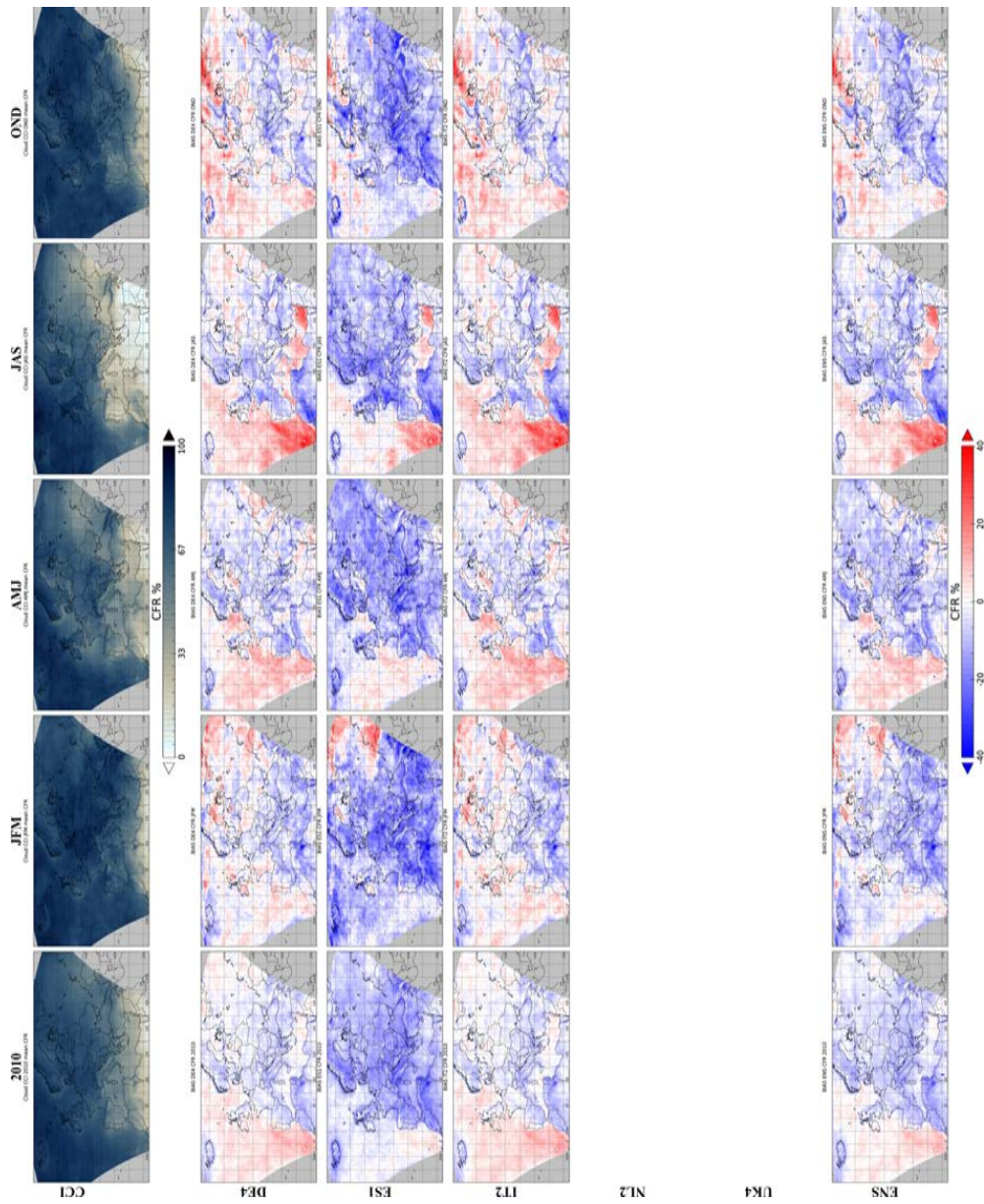


Figure 5.1: MEAN BIAS ERROR (bias) CFR. First row represents the mean satellite values of 2010, JFM, AMJ, JAS, OND. Following rows represent the bias of CFR for the same time periods.

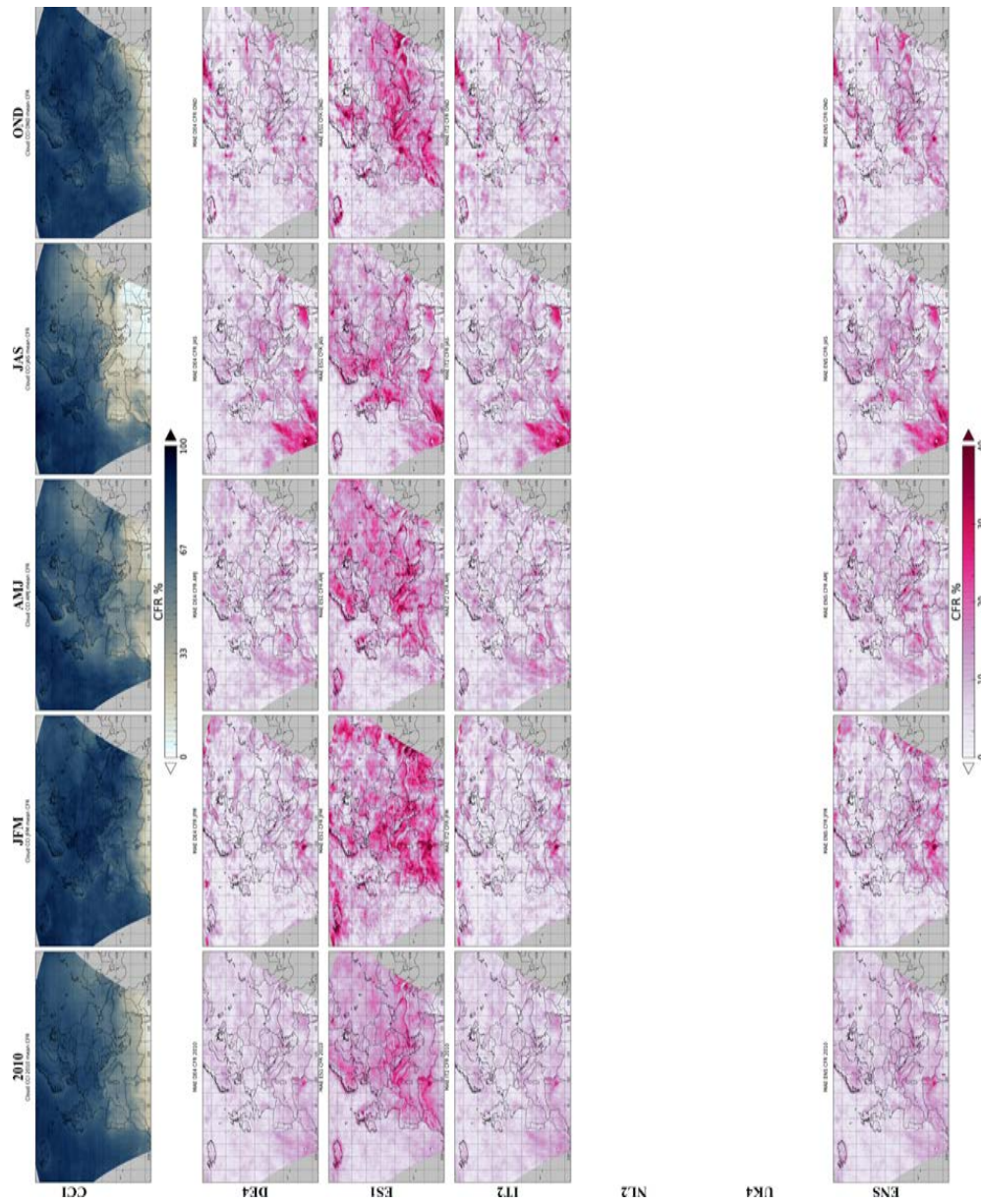


Figure 5.2: MEAN ABSOLUTE ERROR (MAE) CFR. First row represents the mean satellite values of 2010, JFM, AMJ, JAS, OND. Following rows represent the MAE of CFR for the same time periods.

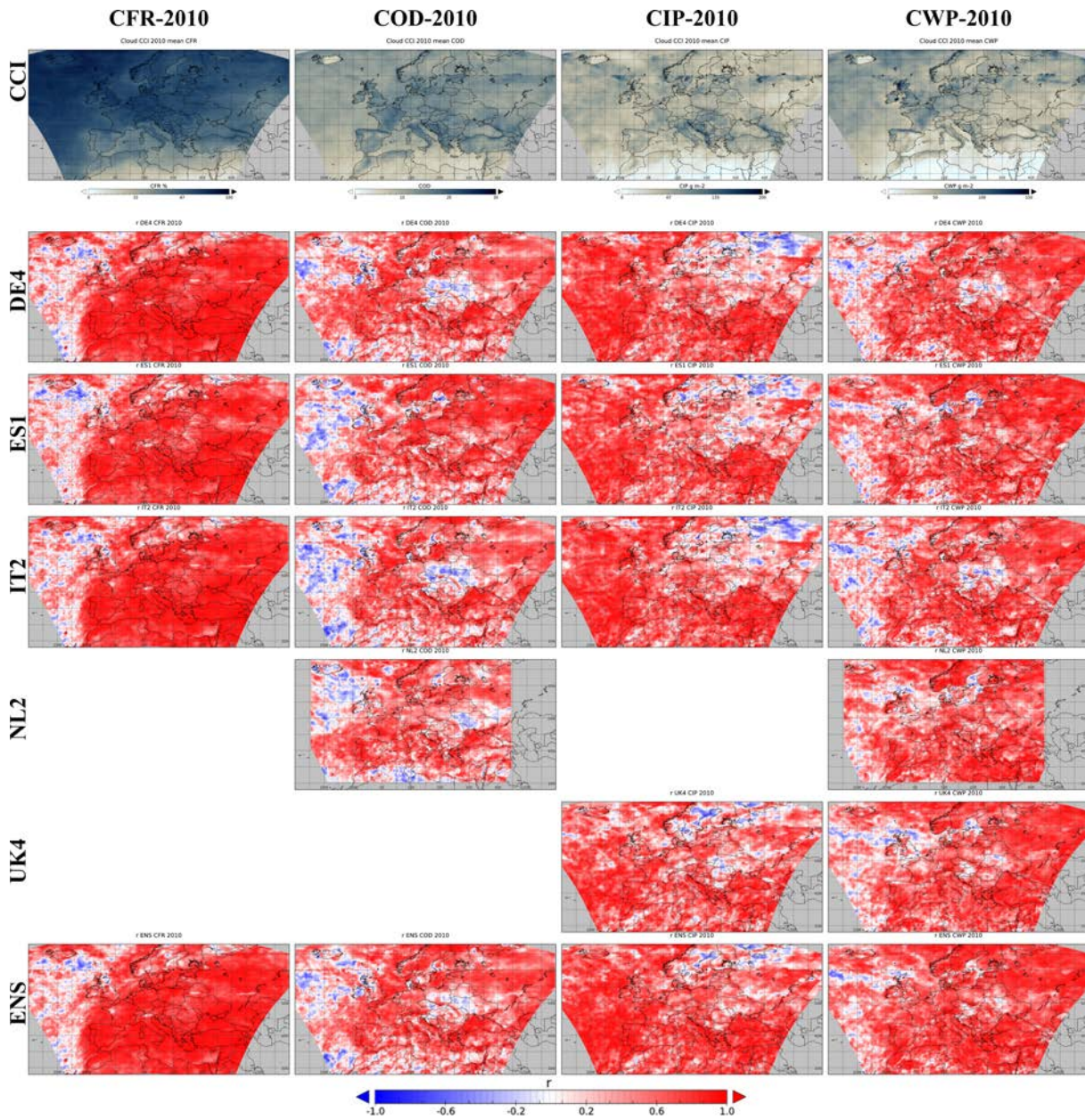


Figure 5.3: Temporal correlation (r) for the whole year 2010. First row represents the mean satellite values of 2010 where each column represents a cloud variable. Following rows show the r of each model and cloud variable.

Table 5.3: Mean Satellite, models and Ensemble values for CFR, COD, CIP and CWP.

	CFR MEAN VALUES				COD MEAN VALUES				CIP MEAN VALUES				CWP MEAN VALUES							
	2010	JFM	AMJ	JAS	OND	2010	JFM	AMJ	JAS	OND	2010	JFM	AMJ	JAS	OND	2010	JFM	AMJ	JAS	OND
CCI	62.5	70	60.8	53.3	67.2	11.4	10.3	11	10.5	14.5	52.2	63.3	42.2	36.2	74.8	42.3	36.3	36.3	39.6	59.8
DE4	60.3	68.2	57.9	50.2	64.9	7	8.1	6.1	5.4	8.2	15	19.1	13	9.8	18	43.2	48	37	35.8	51.6
ES1	53.6	60.3	50.6	46.3	57.1	3.2	3	3.2	3.2	3.5	7.1	9.2	6.4	4.7	8.2	28.1	24	25.2	27	29.4
IT2	60.6	68.2	58.5	50.6	65	6.5	7.4	6	5.1	7.3	15	19	13.2	10	18	41.8	45.9	37.6	35.1	48.6
NL2						1.5	1.5	1.3	1.5	1.5						58.8	53.4	52.2	64.5	65
UK4											42.5	57	35.3	25.7	52	44.3	42.2	41.6	44.7	48.9
ENS	58.1	65.2	55.5	49.8	61.8	4.6	5.1	4.2	4	5.3	19.5	25.5	16.7	12.3	23.5	40.8	40.7	37	39	46.6

5.3.2 Cloud optical depth, COD

Regarding COD, mean seasonal satellite values (first row, Fig 5.4) are up to 30, with the highest mean levels during the OND period. Lowest levels are found over northeastern part of the domain, with values under 10. Table 5.3, second column, indicates that in general lower mean models level are found compared to satellite data. This spatial pattern is clear the COD bias (Fig. 5.4), where there is a general underestimation of the monthly mean COD over the whole domain.

In general, higher negative bias is found during OND, showing NL2 the largest underestimation. During winter months (JFM), DE4 and IT2 show an overestimation over central Europe and some areas over the Atlantic ocean, coinciding with low levels of COD in the satellite. For WRF-Chem models, the differences appearing between models can be related to the different microphysics scheme (Table 5.1) used, Morrison (Morrison et al., 2009) in DE4 and IT2 and Lin scheme (Lin et al., 1983) in ES1. According to Baró et al. (2015), which studied the differences between these microphysics schemes, Morrison parameterization involved higher levels of droplet number mixing ratio.

The authors stated that, since cloud water was similar for Morrison and Lin simulations, the higher droplet number mixing ratio in Morrison indicates that cloud droplets have a lower diameter in Morrison than in Lin (especially during winter). Since COD measures the attenuation of the radiation due to the extinction by cloud droplets, smaller and more cloud droplets in Morrison scheme are more effective in scattering shortwave radiation, and could explain the positive biases found in DE4 and IT2 models. For the MAE (Fig. 5.5), highest values are found in winter and autumn months (JFM, OND), in line with the bias. Individual models have a MAE up to 35, being the largest MAE found in the NL2 model (as for bias). The differences found in NL2 model may again be related to its model microphysics scheme (Table 5.1) (Tiedtke, 1993; Tompkins et al., 2007; Neggers, 2009). Tompkins et al. (2007) tested the new scheme in the European Centre for Medium-Range Weather Forecasts (ECMWF), Integrated Forecasting System (IFS) model within two 7-member ensembles of 13-months. They compared with the ISCCP D2 retrievals, finding a reduction of the high-cloud cover leading to a lower COD. So, this is in accordance with the results found here, where this model presents the largest underestimations. For bias and MAE, again, ENS simulation outperforms the individual simulations (with maximum MAE values lower than 20). With respect to the temporal r (second column, Fig. 5.3), there is a general positive correlation with values up to 0.8 (mostly over land areas) and others with negative correlation over central Europe in DE4 and IT2 models, coincident with those areas where the bias is overestimated.

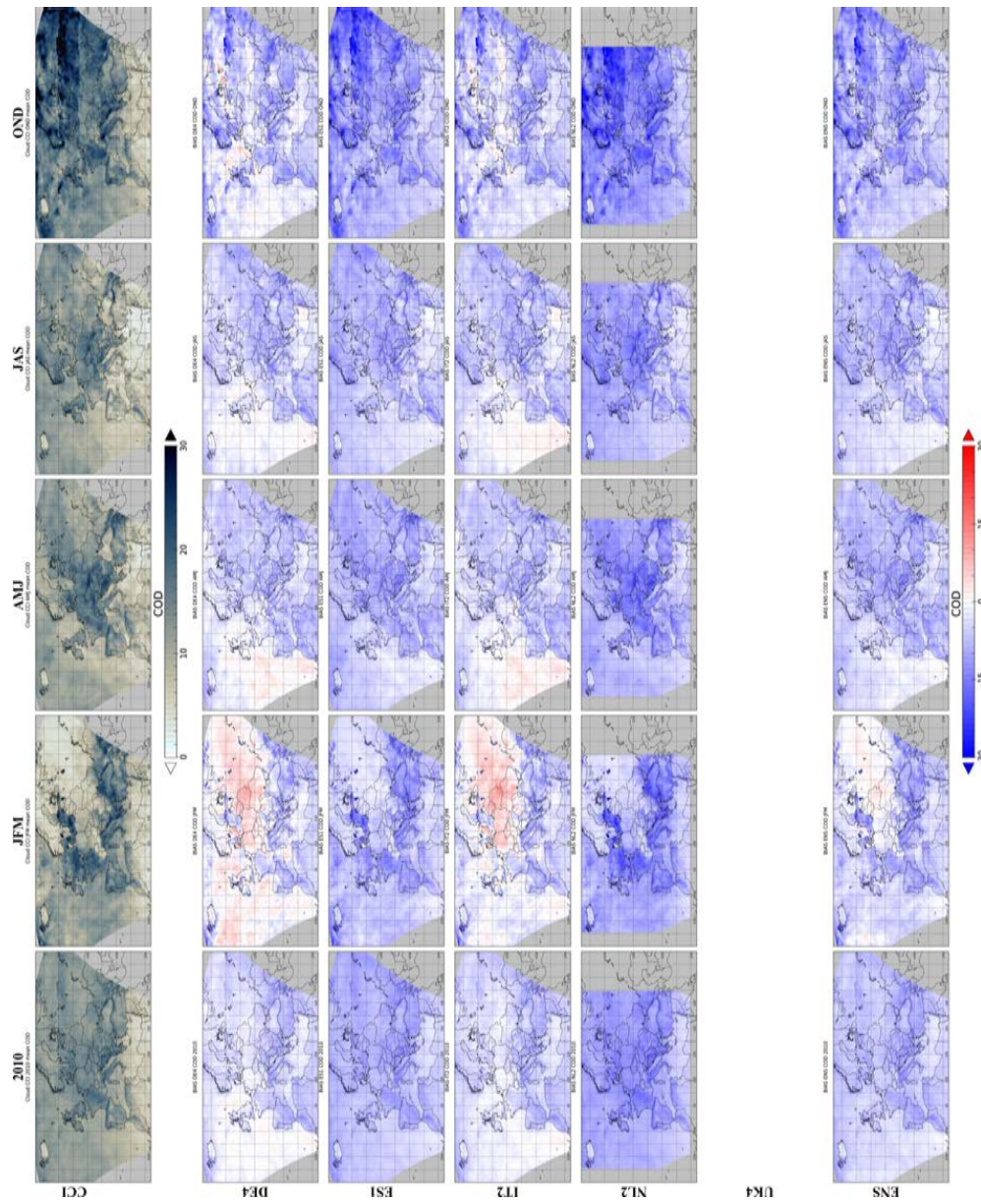


Figure 5.4: MEAN BIAS ERROR (bias) COD. First row represents the mean satellite values of 2010, JFM, AMJ, JAS, OND. Following rows represent the bias of COD for the same time periods.

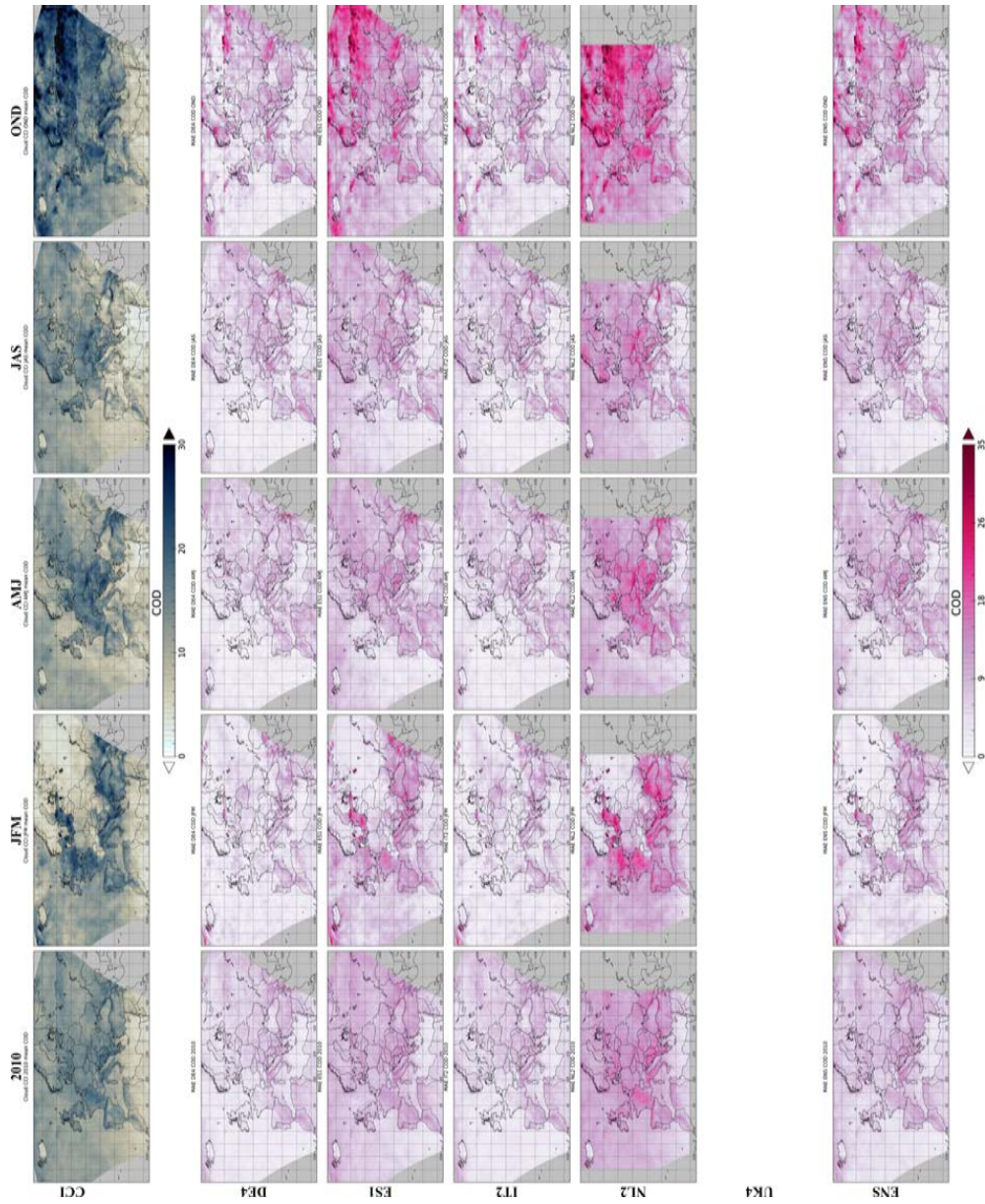


Figure 5.5: MEAN ABSOLUTE ERROR (MAE) COD. First row represents the mean satellite values of 2010, JFM, AMJ, JAS, OND. Following rows represent the MAE of COD for the same time periods.

5.3.3 Cloud ice path, CIP

With respect to CIP (Fig. 5.6), mean satellite levels (first row) are below 100 g m^{-2} but for some delimited areas during winter months (JFM, OND) and spring (AMJ), where high levels over 200 g m^{-2} can be found. Table 5.3, third column, reflects that mean models values are significantly lower compared to satellite retrievals for CIP. Therefore, CIP bias in Fig. 5.6 shows a general model underestimation but for UK4. WRF-Chem models (DE4, ES1, IT2) show negative biases between -80 and -50 g m^{-2} in different parts of the domain, depending on the season. The largest underestimations are found during JFM and OND (where mean satellite values were very high). On the other hand, UK4 overestimates CIP, with a positive bias of 80 g m^{-2} during JFM over central and northern Europe. During JFM, mean satellite data were around 50 g m^{-2} , which is best captured by the other models. UK4 also overestimates CIP during the rest of the year over some northern areas of the domain. The differences found here with respect to WRF-Chem models and UK4 could be related to the number of hydrometeors defined in each microphysics scheme. For both WRF-Chem microphysics (Lin et al., 1983; Morrison et al., 2009), 3 types of ice hydrometeors are considered whereas UK4 (Wilson and Ballard, 1999) only considers one. The fact that WRF-Chem simulations underestimate CIP, finding also an overestimation in UK4 model, could mean that the number of ice hydrometeors in the microphysics scheme is relevant for CIP representation. At the same time, ENS simulation outperforms the individual simulations since it compensates the UK4 model overestimation with the underestimations of the rest of the models. Regarding MAE, values are significantly higher during JFM and OND (Fig. 5.7), with an error over 80 g m^{-2} , shown in all the modelling results. This spatial pattern coincides with the areas with higher CIP levels in the mean satellite data as seen in Fig. 5.6. Temporal r (Fig. 5.3 shows positive r values around 0.7 and negative correlations between -0.5 and -0.6). Positive r is found in practically the entire domain whereas negative correlations are found in northern Europe (Scandinavian area and north of Russia).

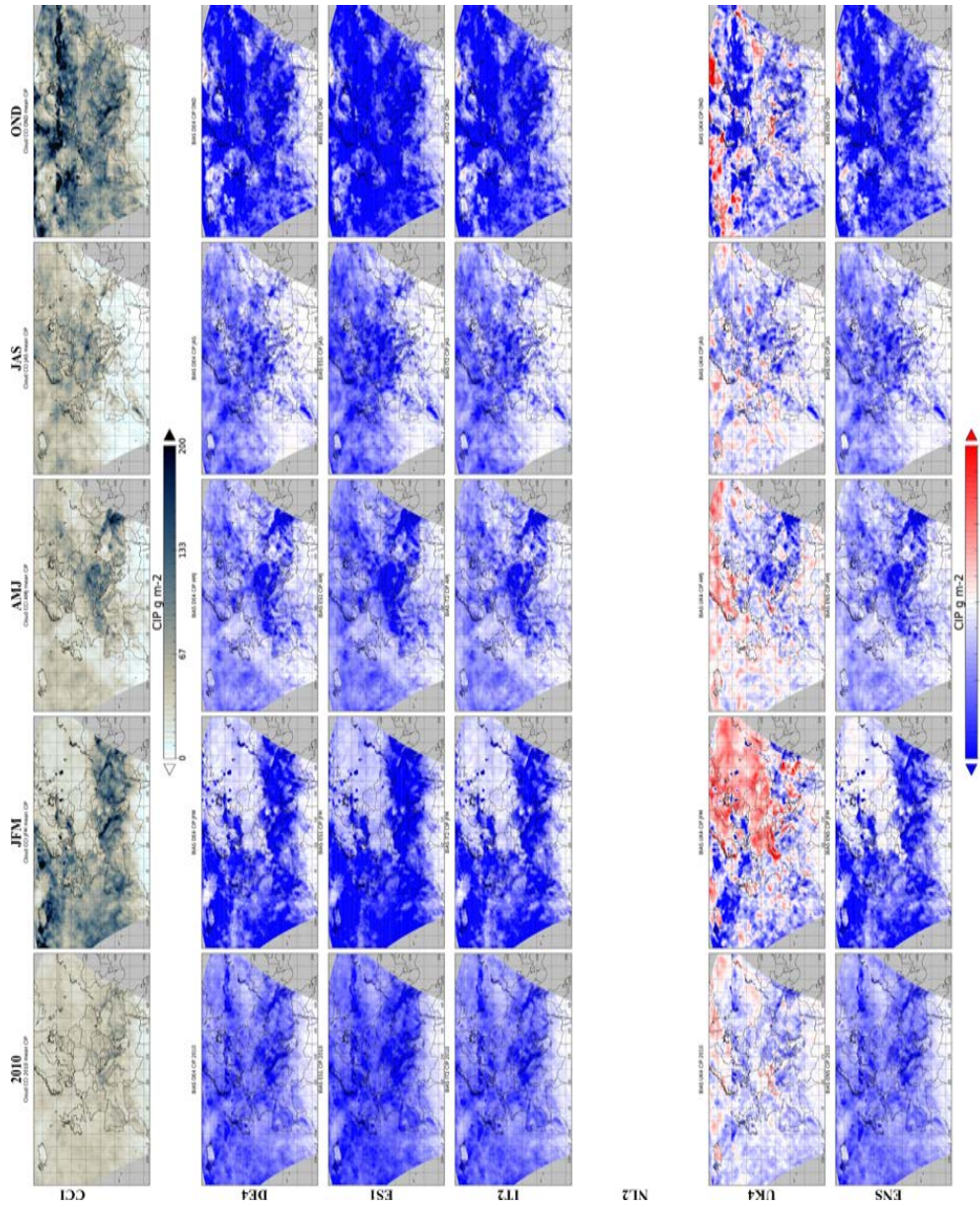


Figure 5.6: MEAN BIAS ERROR (bias) CIP. First row represents the mean satellite values of 2010, JFM, AMJ, JAS, OND. Following rows represent the bias of CIP for the same time periods.

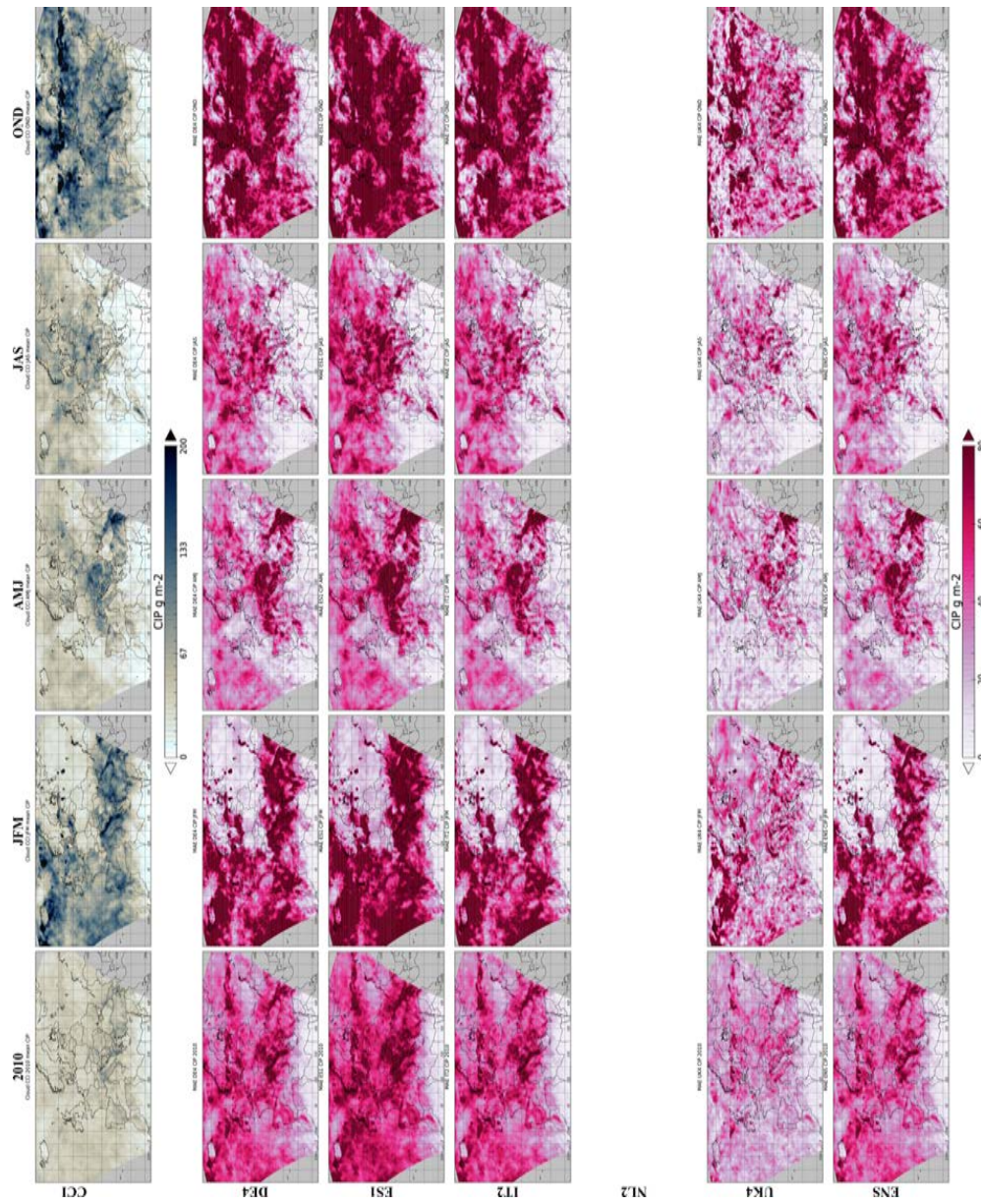


Figure 5.7: MEAN ABSOLUTE ERROR (MAE) CIP. First row represents the mean satellite values of 2010, JFM, AMJ, JAS, OND. Following rows represent the MAE of CIP for the same time periods.

5.3.4 Cloud water path, CWP

Lastly, bias and MAE values of CWP are shown in Fig. 5.8 and 5.9 respectively. Mean satellite levels (first row, Figs. 5.8 or 5.9) are below 100 g m^{-2} (as well as for CIP) but during winter months (JFM, OND) levels are higher than 150 g m^{-2} can be found (in JFM mainly in the North of Spain, some areas of the Mediterranean coast, France and North and Baltic Sea). As for CIP during OND, CWP is higher over the entire domain (but for the north of Africa). Kniffka et al. (2014) report CWP levels from space-based observations from the Spinning Enhanced Visible and Infrared Imager (SEVIRI) of less than 100 g m^{-2} in low clouds, 200 g m^{-2} in middle clouds. Also, satellite retrievals agree with those of Curry et al. (1990), who used data from the Nimbus 7 Scanning Multichannel Microwave Radiometer (SMMR), determining CWP for middle and low clouds (115 and 102 g m^{-2} , respectively) with a maximum value of 1070 g m^{-2} . Although mean satellite data seems to be in agreement with other studies, models shows higher CWP levels. Looking at mean model levels (last column, Table 5.3), these are higher compared to satellite levels, shown in Fig. 5.8 as a general overestimation of CWP (values up to $+50 \text{ g m}^{-2}$), mainly over the ocean, but for ES1 model. The model differences found here could be related to the treatment of the variable. For instance, in all the models included but UK4, CWP is treated as an prognostic variable whereas UK4 treats it as a diagnostic variable (Wilson and Ballard, 1999). Besides, as seen in section 5.3.2, within the WRF-Chem models and according to Baró et al. (2015), models with Morrison scheme have more droplets with smaller diameter compared to Lin scheme. This could also affect the representation of this variable, showing ES1 a model underestimation over most of the domain. Looking at the MAE (Fig. 5.9), the highest values are found in JFM and OND and Model NL2 shows the highest error, mainly over the Atlantic Ocean (50 g m^{-2}). According to Tiedtke (1993), a right representation of the CWP is important for high clouds, because it is directly related to the transparency or optically thickness. As stated in section 5.3.2, NL2 underestimates COD, (explained by the findings of Tompkins et al. (2007) when testing the scheme). No data is available for evaluating CIP or CWP over northern Africa. Temporal r (Fig. 5.3 shows a positive r value around 0.7 for most of the domain. Negative correlations prevail in the Atlantic Ocean and some parts in central Europe (up to -0.6).

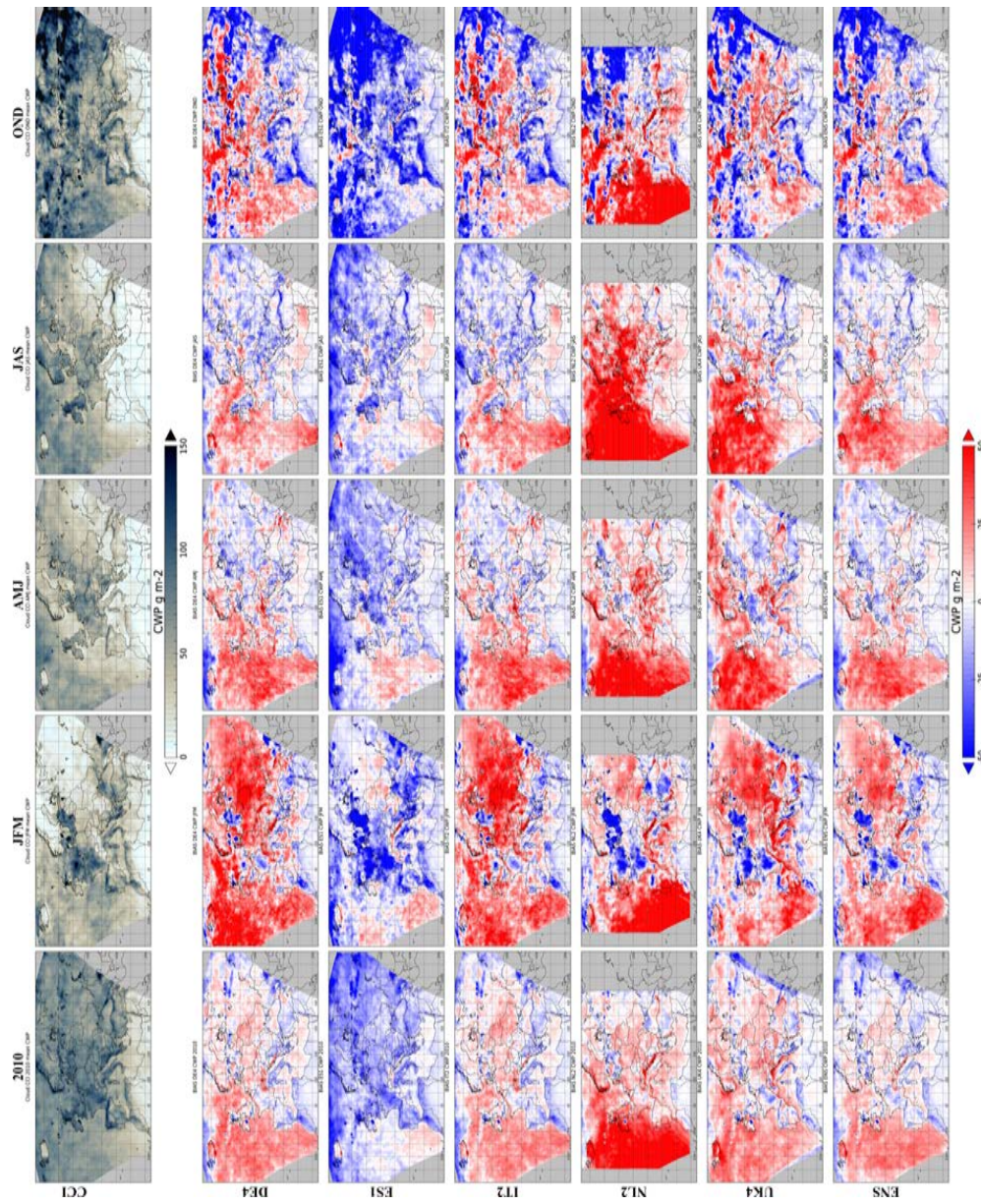


Figure 5.8: MEAN BIAS ERROR (BIAS) CWP. First row represents the mean satellite values of 2010, JFM, AMJ, JAS, OND. Following rows represent the bias of CWP for the same time periods.

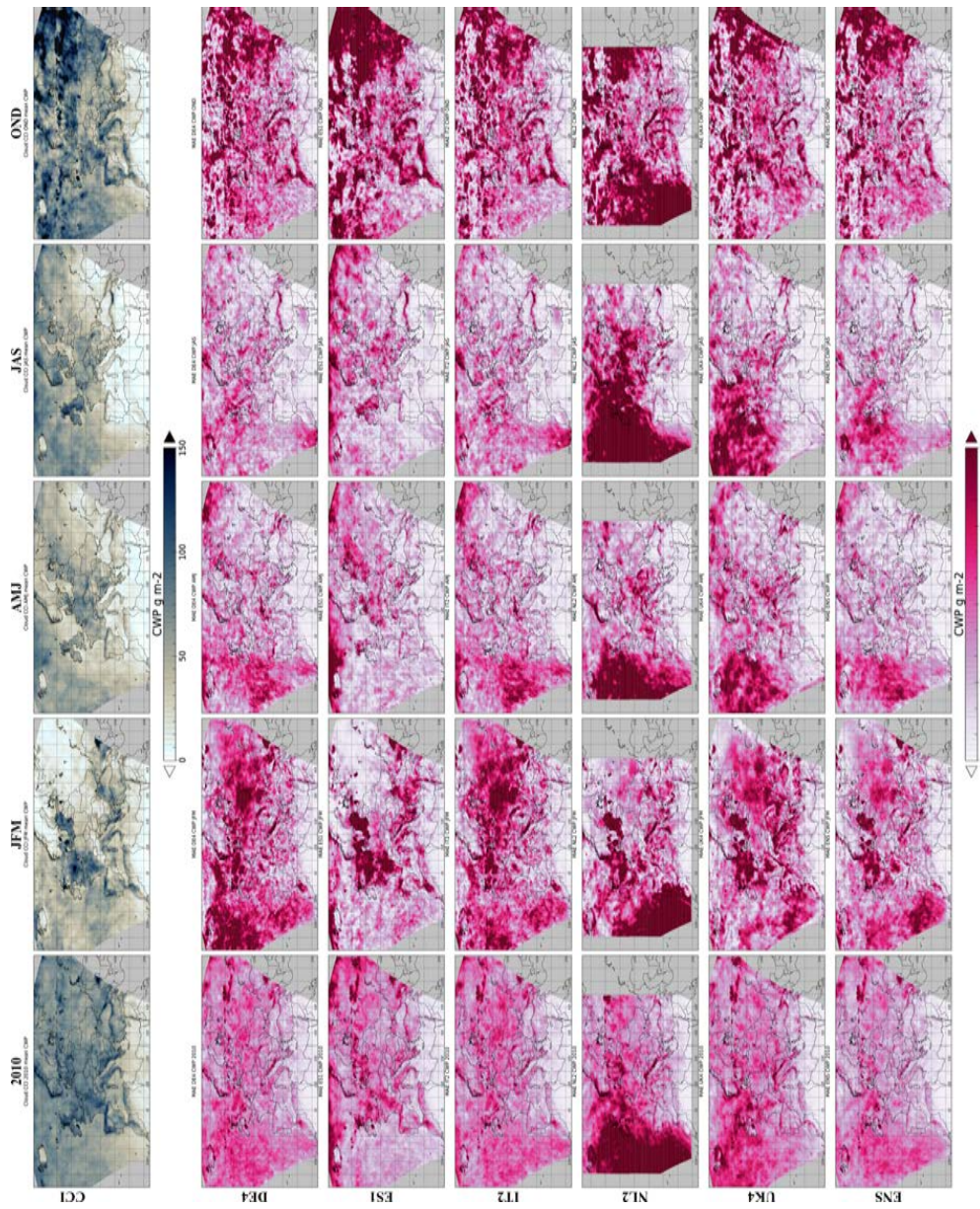


Figure 5.9: MEAN ABSOLUTE ERROR (MAE) CWP. First row represents the mean satellite values of 2010, JFM, AMJ, JAS, OND. Following rows represent the MAE of CWP for the same time periods.

5.3.5 Spatial correlation and variability

The spatial correlation and variability, averaged for year and target season, are summarized in Table 5.4 for each variable (CFR, COD, CIP and CWP, in that order). With respect to CFR, the seasonal correlation coefficients are very high (over 0.90 for each model and season, except for ES1 in wintertime, with $r = 0.89$). Year correlation coefficients range from 0.85 to 0.89, which indicates that the models have a good skill when capturing the spatial variability of the CFR. The ratio σ_P/σ_O gives an idea of the trend of the simulations to overestimate or underestimate the spatial variability (ratio over or under 1, respectively). All models present an accurate representativity of the spatial variability, with ratios very close to 1 for every season and also for the annual average. Also, all models have a very slight tendency to the overestimation of CFR spatial variability (σ_P/σ_O ranging from 1.01 to 1.07).

The spatial correlation coefficient for the rest of the variables indicates a lower skill for representing the spatial correlation of COD, CIP and CWP. All annual spatial r values are in the order of 0.6-0.7, ranging from the case of NL2 for COD (0.41) and CWP (0.44) on the bottom to the simulation of UK4 for CWP (0.73). These values are similar if seasonal correlation coefficients are observed, but in the case of CIP for summertime. The skill of the model for representing the spatial pattern of CIP is limited during JAS, with correlation coefficients ranging from 0.16 in UK4 to 0.35 in DE4 and IT2. Once again, the Morrison microphysics seems to outperform the rest of the simulations when representing the cloud ice path.

With respect to the spatial variability of COD, CIP and CWP, represented by the ratio σ_P/σ_O , important differences between the variables and models are found. For COD, ES1 and NL2 tend to underestimate its spatial variability, especially in the case of NL2, with values of σ_P/σ_O ranging from 0.09 in OND to 0.17 for summertime (JAS). The rest of the models present a good skill for reproducing the variability, with ratios which are slightly higher for the yearly-averaged values than for individual seasons. In the case of CIP, the spatial variability is pervasively estimated by all models and seasons (values σ_P/σ_O in the order of 0.1-0.2), except in the case of UK4, which just slightly underpredicts the variability (ratios around 0.8 except for OND, when this value decreases to 0.63).

Last, for the CWP, all models but ES1 slightly overestimate the spatial variability (σ_P/σ_O values around 1.0-1.3) for yearly-averaged values, winter and spring. In summer, this value is slightly overestimated by simulations not using WRF-Chem (NL2 and UK4), while for autumn (OND) all models tend to underpredict the spatial variability. In general, the best skills are found for DE4 simulations while the largest underestimations are present for ES1 simulations, which use the Lin microphysics scheme.

Table 5.4: Spatial correlation and standard deviation ratio values for CFR, COD, CIP and CWP over the periods: 2010, JFM, AMJ, JAS, OND. r : correlation coefficient; σ_P/σ_O : ratio between the standard deviation of the models (σ_P) and the observations (σ_O).

CFR										
	2010		JFM		AMJ		JAS		OND	
	r	σ_P/σ_O	r	σ_P/σ_O	r	σ_P/σ_O	r	σ_P/σ_O	r	σ_P/σ_O
DE4	0.89	1.06	0.94	1.01	0.94	1.02	0.94	1.07	0.95	1.06
ES1	0.87	1.05	0.89	1.03	0.91	1.05	0.92	1.03	0.92	1.06
IT2	0.88	1.07	0.94	1.03	0.94	1.03	0.94	1.07	0.95	1.07
NL2										
UK4										
ENS	0.85	1.06	0.93	1.04	0.92	1.04	0.93	1.05	0.94	1.07

COD										
	2010		JFM		AMJ		JAS		OND	
	r	σ_P/σ_O	r	σ_P/σ_O	r	σ_P/σ_O	r	σ_P/σ_O	r	σ_P/σ_O
DE4	0.68	1.12	0.62	1.05	0.59	1.07	0.66	0.94	0.71	0.85
ES1	0.67	0.55	0.69	0.46	0.57	0.61	0.66	0.55	0.73	0.38
IT2	0.68	1.07	0.57	0.99	0.56	1.06	0.59	0.89	0.73	0.81
NL2	0.41	0.16	0.39	0.10	0.34	0.16	0.51	0.17	0.47	0.09
UK4										
ENS	0.68	0.74	0.65	0.64	0.57	0.74	0.64	0.66	0.74	0.56

CIP										
	2010		JFM		AMJ		JAS		OND	
	r	σ_P/σ_O	r	σ_P/σ_O	r	σ_P/σ_O	r	σ_P/σ_O	r	σ_P/σ_O
DE4	0.62	0.24	0.53	0.20	0.64	0.30	0.35	0.26	0.58	0.16
ES1	0.60	0.10	0.43	0.09	0.58	0.12	0.31	0.12	0.53	0.07
IT2	0.62	0.24	0.52	0.20	0.63	0.30	0.35	0.26	0.58	0.16
NL2										
UK4	0.63	0.81	0.54	0.78	0.25	0.80	0.16	0.80	0.55	0.63
ENS	0.62	0.34	0.54	0.29	0.48	0.34	0.26	0.34	0.59	0.24

CWP										
	2010		JFM		AMJ		JAS		OND	
	r	σ_P/σ_O	r	σ_P/σ_O	r	σ_P/σ_O	r	σ_P/σ_O	r	σ_P/σ_O
DE4	0.68	1.08	0.57	1.14	0.67	1.12	0.76	0.90	0.65	0.85
ES1	0.66	0.69	0.53	0.69	0.64	0.76	0.77	0.67	0.65	0.48
IT2	0.66	1.04	0.56	1.09	0.64	1.11	0.72	0.87	0.66	0.81
NL2	0.44	1.31	0.28	1.32	0.56	1.34	0.72	1.49	0.39	0.87
UK4	0.73	1.10	0.62	0.97	0.69	1.22	0.78	1.19	0.74	0.76
ENS	0.65	1.03	0.56	0.97	0.68	1.07	0.76	0.99	0.66	0.72

5.4 Summary and conclusions

The presence or the absence of cloudiness must be well represented since clouds play an important role in the Earth's energy balance (Boucher et al., 2013; Myhre et al., 2013b). Hence, in this study a collective evaluation of the cloud variables CFR, COD, CIP and CWP has been shown. The simulations evaluated here were run by coupled chemistry and meteorology models in the context of the AQMEII Phase 2 initiative and EuMetChem COST Action for the year 2010. This study complements other collective analyses as Baró et al. (2017); Brunner et al. (2015); Makar et al. (2015b,a); Forkel et al. (2015) by adding an assessment of how coupled models represent ACI in an ensemble of simulations.

With respect to CFR, an underestimation (overestimation) of this variable is observed over land (ocean) areas. Individual model simulations present positive a bias close to 40% and a negative bias over -35% . MAE is up to 40%, especially noticeable over central Europe and the Mediterranean Sea in ES1 model. The rest of the models show lower MAE values (15%). DE4 and IT2 present a high MAE over the Atlantic Ocean and northern Africa, with an error around 30%, coincident with a positive bias of the same magnitude. For the ENS mean, lower CFR levels are found, with Biases ranging from 20% to -20% , outperforming the individual simulations (also for MAE). The positive bias is more pronounced during JAS, where mean satellite levels are lower. The negative bias could be due to the general underestimation in the representation of CCN by global and regional models (Wyant et al., 2015). On the other hand, overestimations found off-shore could be related to satellite retrieval missing thin clouds. A positive temporal coefficient of correlation r is dominant in the spatial pattern of this variable, with values close to 0.9. On the other hand, there are some areas over the ocean with negative correlation (around -0.5). This is similar to the bias, where a negative bias prevailed over land areas and a positive bias over the sea.

Regarding COD, lower mean model levels are found compared to satellite data resulting on a general underestimation of the monthly mean over the whole domain. In general, a higher negative bias is found during OND, with NL2 showing the largest underestimation. During winter, DE4 and IT2 have a trend for overestimation over central Europe and some areas over the Atlantic ocean, corresponding with low levels of COD as indicated by the satellite. These differences found in the WRF-Chem models may be related to the different microphysics scheme used (Morrison (Morrison et al., 2009) versus Lin (Lin et al., 1983)). In the former, cloud droplets have a lower diameter than Lin (especially during winter) (Baró et al., 2015), leading to a more effective extinction by cloud droplets. With respect to MAE higher levels

are found in winter months, in line with the bias. Individual models have a MAE up to 35, being higher for NL2 model (as for bias). The differences found in NL2 model may be related to the model microphysics scheme. Temporal r points to a general positive correlation between models and satellite observations, with values up to 0.8 (mostly over land areas). Some areas with a negative correlation over central Europe in DE4 and IT2 models are related to areas with a trend for overestimation.

There is an overall underestimation of the CIP but for UK4. The differences found here with respect to WRF-Chem models and UK4 could be related to the number of hydrometeors defined in each microphysics scheme. For both WRF-Chem microphysics, 3 types of ice hydrometeors are considered whereas UK4 (Wilson and Ballard, 1999) considers only one. So the underestimation found in UK4 model could mean that the number of ice hydrometeors is relevant. MAE values are significantly higher during JFM and OND (error of more than 80 g m^{-2}), shown in all the models results. This spatial pattern correlates with those areas with a higher mean CIP in the satellite. Temporal r shows positive correlation values around 0.7 and negative correlations between -0.5 and -0.6 . Positive r is found nearly over all the target domain whereas negatives correlations are found in northern Europe (Scandinavian countries and the north of Russia).

Despite mean satellite data seems to be in agreement with other studies (Kniffka et al., 2014), models shows higher CWP levels resulting in a general overestimation of CWP mainly over sea areas (but for ES1 model). The model differences found here could be related to the treatment of the variable, since for instance, all the models but for UK4, CWP is treated as an prognostic variable whereas UK4 treats it as a diagnostic variable (Wilson and Ballard, 1999). Besides, as seen in section 5.3.2, within the WRF-Chem models and according to Baró et al. (2015), models with Morrison scheme have more droplets with smaller diameter compared to Lin scheme. This could also affect the representation of this variable, showing an ES1 model underestimation over the most part of the domain. MAE highest levels were found in JFM and OND and Model NL2 shows the highest error, mainly over Atlantic Ocean, just as in bias. According to Tiedtke (1993), a right representation of the CWP is important for high clouds, due to its directly related to the transparency or optically thickness. Besides, as said in section 5.3.2, NL2 underestimates COD. Temporal r shows positive values around 0.7 for most of the domain. Negative correlations prevail in the Atlantic Ocean and some parts in center Europe (up to -0.6).

Finally, the seasonal and yearly correlation coefficients are very high for CFR (seasonal over 0.90, yearly over 0.85), which indicates that the models have a good skill when capturing the

spatial variability, whilst tender to slightly overestimate CFR spatial variability (value σ_P/σ_O ranging from 1.01 to 1.07). The rest of the variables, indicates a lower skill for representing the spatial correlation of COD, CIP and CWP. All annual spatial r values are in the order of 0.6-0.7. These values are similar if seasonal correlation coefficients are observed, but in the case of CIP for summertime. The skill of the model for representing the spatial pattern of CIP is limited during JAS, (correlation coefficients ranging from 0.16 to 0.35). Morrison microphysics seems to outperform the rest of the simulations when representing the cloud ice path. Important differences in the spatial variability between the variables and models are found. For COD, ES1 and NL2 tend to underestimate its spatial variability, especially in the case of NL2, with values of σ_P/σ_O ranging from 0.09 in OND to 0.17 for summertime (JAS). The rest of the models present a good skill for reproducing the variability, with ratios which are slightly higher for the yearly-averaged values. In the case of CIP, the spatial variability is pervasively estimated by all models and seasons, except for UK4, which slightly underpredicts the variability (ratios around 0.8 except for OND, when this value decreases to 0.63). For the CWP, all models but ES1 slightly overestimate the spatial variability (σ_P/σ_O values around 1.0-1.3) for yearly-averaged values, winter and spring. In summer. In general, the best skills are found for DE4 simulations while the largest underestimations are present for ES1 simulations (which use the Lin microphysics scheme).

According to Rosenfeld et al. (2014), an improvement in the understanding of ACI and their effects on climate is restricted by inadequate observational tools and models. The statistical effect of the aerosol on clouds is still a controversial matter given the limitations of the tools used in satellite, observation and in large or global-scale models (Stevens and Feingold, 2009).

A better understanding of the aerosol-cloud processes would reduce the uncertainty in anthropogenic climate forcing and provide a clear understanding and better predictions of the future impacts of aerosols on climate and weather (Rosenfeld et al., 2014). Observation systems have increasingly been used in the recent years, but improvements should be done (Seinfeld et al., 2016) since the large range of scales, and the fact that the various measuring systems, tend to address different scales. In Seinfeld et al. (2016) they compiled some large-scale field experiments planned to address aerosol-cloud-climate interactions. Overall, further comprehensive studies will be needed for a better understanding of these interactions and to help us to improve the knowledge of the climate and air quality interactions.

Chapter 6

Conclusions and future perspectives

The present Thesis contributes to characterize the uncertainties in the climate-chemistry-aerosol-cloud-radiation system associated with the aerosol direct and indirect radiative effects caused by aerosols over Europe, by employing an ensemble of fully-coupled climate and chemistry model simulations. As previously mentioned, the development of this Thesis has been done under the umbrella of the AQMEII Phase 2 and the EuMetChem COST Action ES1004, which have provided us with analytical tools to reach a better understanding of the air quality-climate interactions, and to also value the various physical and chemical processes incorporated in the coupled modeling systems. Moreover, we have taken advantage of the valuable database generated in this initiative.

Despite a detailed discussion of the results and conclusions have been included in the corresponding Chapters (from 2 to 5), here a summary of their most important aspects is presented. Moreover, recommendations for future work are also included.

6.1 General conclusions

The development of this Thesis has contributed to the state of the art in AQCI studies. Up to now, all the collective studies were based mainly on global models. Hence, this Thesis goes one step beyond studying the aerosol-radiation-cloud interactions through an ensemble of online-coupled regional models. After studying several episodes and the whole of 2010 by different online-coupled models, the inclusion of the aerosol feedbacks did not improve the bias, but its inclusion improved the spatio-temporal variability and correlation coefficients. These results confer value to the computational efforts made to include ARI and ACI in the models, which justifies the computational times and costs. This conclusion was reached from the partial conclusions that are disclosed below.

6.1.1 Sensitivity analysis of the microphysics scheme

Despite many aspects related to the microphysics processes are still not completely understood, it is well-known that they play an important role in how moist convection develops and evolves, and also in the radiative energy budget of the Earth–atmosphere system. Parameterization of cloud microphysics is a crucial part of fully–coupled meteorology–chemistry models. Considering this, the sensitivity of the selection of the microphysics scheme within WRF–Chem model has been assessed in **Chapter 2**. The impact on several variables is estimated when selecting two different microphysics parameterizations: Morrison (MORRAT) vs. Lin (LINES). This study covers the difference between the simulations for two 3–month periods (cold and a warm) during the year 2010, which thus allows a seasonal analysis.

- MORRAT provides a higher cloud water mixing ratio in winter, mainly over remote areas, where the CCN concentrations are lower; while LINES provides higher values over most polluted areas.
- MORRAT simulations indicate higher values for the droplet number mixing ratio during winter and summer for nearly all the simulation domains. This fact indicates that smaller and more numerous cloud droplets are simulated by the Morrison parameterization and therefore, this scheme is more effective for scattering shortwave radiation (as clearly observed when assessing both the differences in the mean upwelling shortwave flux and the downwelling shortwave flux at the bottom).
- The spatial pattern of differences for the droplet number mixing ratio and the 2–m temperature are highly correlated for wintertime. The MORRAT simulations with higher levels of cloud droplets allow less shortwave radiation to reach the ground, but also higher longwave radiation to be reflected towards the ground. Of these two effects, the latter prevails and, thus, the daily average temperature increases in northern areas (50°N to 70°N) in MORRAT compared to LINES.
- Despite the differences found in the behaviour of both simulations, the sensitivity of the results to microphysics scheme selection is very limited when comparing the results to observations.
- No significant benefits from selecting microphysics schemes can be derived from the results neither in northernmost areas nor in southern-Mediterranean Europe.
- Because of the limitations in this sensitivity analysis (restricted to just two simulations implemented into just one model), future research on this topic should be devoted to further

studies that examine the impact of aerosols on cloud properties using other microphysics and convective parameterizations, and also in other target domains.

6.1.2 Biomass burning aerosol impact on surface winds

As seen in **Chapter 1** the radiative effects of atmospheric aerosols are widely known to affect radiation, temperature, stability, clouds and precipitation through their radiative effects, which depend mainly on the aerosol optical properties. Wind fields affect aerosols levels by different processes, which result in wind-dependent emission over land or ocean (e.g. Boucher et al. (2013); Prijith et al. (2014); Li et al. (2015)). So **Chapter 3** covers the topic of the BB aerosol impacts on wind (and other meteorological variables). Apart from the studies of Jacobson and Kaufman (2006) and Péré et al. (2014), scientific literature about aerosol effects on wind is scarce. A reason of the lack of these studies could be the difficulty understanding the physical causes of the feedbacks between aerosols and winds.

The results shown in **Chapter 3** go one step beyond previous studies by including the online feedbacks between aerosols and meteorology in a regional climate-chemistry coupled model, and by solving online ARI in addition to ACI and, hence, considering aerosol feedbacks with meteorology).

- BB aerosols can affect surface winds not only where emission sources are located, but also further away from the release areas.
- Local winds decrease due to reduced SWDNB, which leads to drops in T2.
- Atmospheric stability increases when considering aerosol feedbacks, inducing a lower PBLH.
- Presence of BB aerosols in the atmosphere can change the SLP, by producing changes in mesoscale circulations and an increase of surface winds over distant regions.
- Considering BB aerosols feedbacks could play a key role when simulating surface winds.
- Including aerosols feedbacks when simulating surface winds could contribute to both weather prediction skills and improve climatological studies. For instance, better understanding of feedbacks between aerosols and winds could help the decision making on fires management and could condition the planning on wind energy.
- Albeit this promising conclusion, this work only analyzes one particular episode and more case studies will be needed to support these conclusions.

6.1.3 Atmospheric aerosol effects on temperature

The variable 2-m temperature considered in **Chapter 4** is crucial to understand the effect of the aerosol interactions with clouds and radiation. In this sense, this study complements other several other analyses (e.g. Brunner et al. (2015); Forkel et al. (2015); Makar et al. (2015a)) by analyzing whether the inclusion of the radiative feedbacks improves, or not, the representation of the temperature field (maximum, mean and minimum) in an ensemble of simulations by covering the COST Action ES1004 episodes. The two considered episodes are: the Russian heatwave and wildfires episode (25 July-15 August 2010) and a Saharan dust episode (2-15 October 2010).

- In both episodes, the bias in the studied variables is generally underestimated, and is more noticeable in maximum temperature. In general, there is not a straightforward conclusion about the improvement, or not, of the bias when introducing aerosol radiative feedbacks.
- Broadly speaking, the biases are improved when including ARI or ARI+ACI in the dust case, but no evident improvements have been found for the heatwave/wildfires episodes.
- Although the ensemble does not outperform the individual models in general, the improvements found when including ARI and ARI+ACI are by far more remarkable for the ensemble than for the individual models.
- Maximum and mean temperatures in the fires and dust episodes display higher temporal correlations over most of the domain when no aerosol effects feedbacks are considered, compared to the E-OBS database than minimum temperature.
 1. The ensemble of simulations always outperforms the representation of the temporal variability of the series
 2. The ρ^2 coefficient improves when considering the ARI or ARI+ACI feedbacks (in both episodes).
- During the fire episode, a generally marked overestimation of the standard deviation of the studied variables took place. Here, the inclusion of aerosol feedbacks largely improved the representation of the temporal variability of the three studied variables (reducing the bias of standard deviation), with the best skills shown for the cases that included the ARI+ACI interactions, with as much a 75% reduction in the bias of the standard deviation.

- During the dust episode, the inclusion of the aerosol radiative feedbacks for temporal variability displayed the greatest improvements and resulted in an added value of the computational efforts made to include direct aerosol radiation interactions and aerosol cloud interactions in models.
- For maximum and mean temperatures, the inclusion of radiative effects reduced the spatial variability and improved the spatial patterns for both episodes. For the minimum temperature, the improvement achieved by including the radiative feedbacks was less evident.
- To further investigate the impact of including the aerosol interactions in online-coupled models, episodes with stronger effects on the ACI should be considered as the episodes selected during EuMetChem Cost Action were related mainly to ARI.
- During the dust episode, most of the ARI+ACI differences found in the models compared to the base case were found over the Mediterranean Sea, but observational data E-OBS only has values over land. Unfortunately part of the interpretation of the results may have been missed due to the unavailability of this database over the ocean.
- Modeling issues still remain as to representing the temperature field, where maximum temperatures are underestimated and minimum temperatures are overestimated, and the inclusion of the aerosol feedbacks does not improve this situation. Nevertheless, in this study, a general improvement of the temporal variability and correlation has been seen. These improvements may be important for not only certain episodes, like those analyzed here, but also for representing the climatology of temperatures. However, climatic-representative periods should be covered in further studies.

6.1.4 Aerosol-cloud interactions representation in online-coupled models

The presence or the absence of the cloudiness must be well represented as clouds play an important role in the Earth's energy balance (Boucher et al., 2013; Myhre et al., 2013b). A better understanding of the aerosol-cloud processes would reduce the uncertainty in anthropogenic climate forcing and provide a clear understanding and better predictions of the future impacts of aerosols on climate and weather (Rosenfeld et al., 2014). This study shown in **Chapter 5**, complements other collective analysis such as Baró et al. (2017); Brunner et al. (2015); Forkel et al. (2015), Makar et al. (2015a,b), by adding an analysis of how coupled models represent ACI in an ensemble of simulations in the AQMEII Phase 2 and EuMetChem COST Action context.

- Underestimation (overestimation) of CFR is observed over land (ocean) areas. The latter could be related to satellite retrieval missing thin clouds. Lower bias and MAE are found in the ensemble mean.
- COD shown a general underestimation over the whole domain. MAE was in line with the bias.
- There is an overall underestimation of the CIP but for UK4. The differences found here could mean that the number of ice hydrometeors is relevant.
- Higher CWP mean model levels were found, which resulted in a general overestimation of CWP. Differences found in CWP could be related to the treatment of the variable (prognostic/diagnostic).
- Generally, temporal r points to a general positive correlation between models and satellite observations.
- CFR, has the best skill when capturing the spatial variability. COD, CIP and CWP indicate a lower skill for representing the spatial correlation.
- Differences found in models may be related to the different microphysics scheme used.
- High temporal correlation as well as good skill when capturing the spatial variability (specifically for CFR) has been seen. However, further comprehensive studies are needed for a better understanding of these interactions and to help us to improve the knowledge of the climate and air quality interactions.

6.2 Future works and development

As a future work, there are several aspects that would be of much interest to complement the results of this Thesis. Some of them are ongoing works and others are possible future research lines.

- As seen in **Chapter 2**, in order to model the indirect effects, the cloud scheme needs to be coupled with a double moment microphysical parameterization. One main limitation with using WRF–Chem when assessing ACI is that only couplings are computed in explicitly resolved clouds, rather than convective clouds simulated by cumulus parameterization (Chapman et al., 2009; Yang et al., 2011a). The works of Grell and Freitas (2014); Berg et al. (2015) have included aerosol interactions with parameterized clouds. However, these

developments were not available for when WRF-Chem was released at the time of writing this Thesis. Furthermore, according to Berg et al. (2015), high-resolution simulations using horizontal grid spacing less than 10 km can explicitly represent convective clouds and ACI. By considering the foregoing, future studies should be in line with using aerosol interactions with parameterized cloud with higher resolution.

- In line with the previous point, the aerosol–cloud–precipitation framework must be expanded to flexibly represent the effect of environmental conditions, in addition to the microphysics. We have started this line by quantifying the influence of including dust interactions on precipitation in a regional online-coupled climate/chemistry model over convective precipitation, as well as other cloud related variables. This work is presented in the European Geosciences Union (EGU) Conference, April 2017.
- This Thesis falls in line with the main objectives of the Project REPAIR (CGL2014-59677-R), funded by the Spanish Ministerio de Economía y Competitividad (MINECO) and by the FEDER European program, which is currently ongoing. Its main objective is to study the potential impact of an increased use of renewable energies, particularly wind and solar, on European climate and air quality in Europe until mid-century, through its role in mitigating projections of climate change that consider the interactions of aerosols and climatic system (radiative feedbacks). The undertaken of this Thesis has helped to set the basis for studying the air quality-climate interactions, using a regional online-coupled climate/chemistry model, which will serve to fulfill the objectives of REPAIR.
- In order to improve aerosol prediction, future studies should use data assimilation. Some studies (Pagowski et al., 2010; Liu et al., 2011b; Schwartz et al., 2012) have shown the improvements made by using aerosol and chemical data assimilation. Moreover, in the field of improving the aerosol representation by taking into account the aerosol feedbacks in online-coupled systems, Wang and Niu (2013) suggests the importance of taking into account the aerosol assimilation and radiation forcing in modeling aerosols.

Overall, we highlight the relevance of including aerosols feedbacks in the regional modeling field, as formerly stated by several authors (such as Forkel et al., 2015; Kong et al., 2015; Makar et al., 2015b; San José et al., 2015). Albeit a growing number of studies of meteorology and chemistry feedbacks employing online-coupled models are available in the scientific literature, further studies are needed in order to improve the representation of these interactions.

Bibliography

- Ackerman, S. A. (1997). Remote sensing aerosols using satellite infrared observations. *Journal of Geophysical Research: Atmospheres*, 102(D14):17069–17079.
- Ackermann, I. J., Hass, H., Memmesheimer, M., Ebel, A., Binkowski, F. S., and Shankar, U. (1998). Modal aerosol dynamics model for Europe: Development and first applications. *Atmospheric environment*, 32(17):2981–2999.
- AIAA (1999). *Guide to global aerosol models*. American Institute of Aeronautics and Astronautics, Reston, United States of America.
- Akay, A., Brereton, F., Cunado, J., Ferreira, S., Martinsson, P., Moro, M., and Ningal, T. F. (2013). Life Satisfaction and Air Quality in Europe. *Ecological Economics*, 88:1–10.
- Alapaty, K., Mathur, R., Pleim, J., Hogrefe, C., Rao, S. T., Ramaswamy, V., Galmarini, S., Schaap, M., Makar, P., Vautard, R., Makar, P., Baklanov, A., Kallos, G., Vogel, B., and Sokhi, R. (2012). New Directions: Understanding interactions of air quality and climate change at regional scales. *Atmospheric Environment*, 49:419–421.
- Albrecht, B. A. (1989). Aerosols, cloud microphysics, and fractional cloudiness. *Science*, 245(4923):1227–1230.
- Avey, L., Garrett, T. J., and Stohl, A. (2007). Evaluation of the aerosol indirect effect using satellite, tracer transport model, and aircraft data from the international consortium for atmospheric research on transport and transformation. *Journal of Geophysical Research: Atmospheres*, 112(D10).
- Baidya, S. and Sharp, J. (2013). Why atmospheric stability matters in wind assessment. *North America Windpower*, pages 29–29.
- Baklanov, A., Korsholm, U., Mahura, A., Petersen, C., and Gross, A. (2008a). ENVIRO-HIRLAM: on-line coupled modelling of urban meteorology and air pollution. *Advances in Science and Research*, 2(1):41–46.

- Baklanov, A., Korsholm, U., Woetmann, N., and Gross, A. (2008b). On-line coupling of chemistry and aerosols into meteorological models: advantages and prospective. Technical report, Project no. 516099. Danish Meteorological Institute (DMI), Copenhagen.
- Baklanov, A., Schlünzen, K., Suppan, P., Baldasano, J., Brunner, D., Aksoyoglu, S., Carmichael, G., Douros, J., Flemming, J., Forkel, R., Galmarini, S., Gauss, M., Grell, G., Hirtl, M., Joffre, S., Jorba, O., Kaas, E., Kaasik, M., Kallos, G., Kong, X., Korsholm, U., Kurganskiy, A., Kushta, J., Lohmann, U., Mahura, A., Manders-Groot, A., Maurizi, A., Moussiopoulos, N., Rao, S. T., Savage, N., Seigneur, C., Sokhi, R. S., Solazzo, E., Solomos, S., Sørensen, B., Tsegas, G., Vignati, E., Vogel, B., and Zhang, Y. (2014). Online coupled regional meteorology chemistry models in Europe: current status and prospects. *Atmospheric Chemistry and Physics*, 14(1):317–398.
- Baltensperger, U. (2010). Aerosol Composition and Radiative Properties. Lecture given at the WMO-BIPM Workshop, Geneva, Switzerland.
- Bangert, M., Kottmeier, C., Vogel, B., and Vogel, H. (2011). Regional scale effects of the aerosol cloud interaction simulated with an online coupled comprehensive chemistry model. *Atmospheric Chemistry and Physics*, 11(9):4411–4423.
- Baró, R., Jiménez-Guerrero, P., Balzarini, A., Curci, G., Forkel, R., Grell, G., Hirtl, M., Honzak, L., Langer, M., Pérez, J. L., Grell, G., Hirtl, M., Honzak, L., Langer, M., Pérez, J., Pirovano, G., José, R., Tuccella, P., Werhahn, J., and Zabkar, R. (2015). Sensitivity analysis of the microphysics scheme in WRF-Chem contributions to AQMEII phase 2. *Atmospheric Environment*, 115:620–629.
- Baró, R., Palacios-Peña, L., Baklanov, A., Balzarini, A., Brunner, D., Forkel, R., Hirtl, M., Honzak, L., Pérez, J. L., Pirovano, G., San José, R., Schröder, W., Werhahn, J., Wolke, R., Zabkar, R., and Jiménez-Guerrero, P. (2017). Regional effects of atmospheric aerosols on temperature: an evaluation of an ensemble of on-line coupled models. *Atmospheric Chemistry and Physics Discussions*, pages 1–35.
- Bellouin, N. (2013). Aerosol Modelling. Lecture given at the MACC II Summer School in Anglet, France.
- Berg, L., Shrivastava, M., Easter, R., Fast, J., Chapman, E., Liu, Y., and Ferrare, R. (2015). A new WRF-Chem treatment for studying regional-scale impacts of cloud processes on aerosol and trace gases in parameterized cumuli. *Geoscientific Model Development*, 8(2):409–429.

- Bergman, T., Kerminen, V. M., Korhonen, H., Lehtinen, K. J., Makkonen, R., Arola, A., Mielonen, T., Romakkaniemi, S., Kulmala, M., and Kokkola, H. (2011). Evaluation of the sectional aerosol microphysics module SALSA implementation in ECHAM5-HAM aerosol-climate model. *Geoscientific Model Development*, 4(4):3623–3690.
- Bian, H. and Prather, M. J. (2002). Fast-J2: Accurate simulation of stratospheric photolysis in global chemical models. *Journal of atmospheric chemistry*, 41(3):281–296.
- Bianconi, R., Galmarini, S., and Bellasio, R. (2004). Web-based system for decision support in case of emergency: ensemble modelling of long-range atmospheric dispersion of radionuclides. *Environmental Modelling & Software*, 19(4):401–411.
- Binkowski, F. S. (1999). The aerosol portion of Models-3 CMAQ. in Science Algorithms of the EPA Models-3 Community Multiscale Air Quality (CMAQ) Modeling System, edited by D.W. Byun and J.K.S. Ching, EPA. Technical report, EPA/600/R-99/030 Environmental Protection Agency, EPA. United States.
- Binkowski, F. S. and Roselle, S. J. (2003). Models-3 Community Multiscale Air Quality (CMAQ) model aerosol component 1. Model description. *Journal of geophysical research: Atmospheres*, 108(D6).
- Binkowski, F. S. and Shankar, U. (1995). The regional particulate matter model: 1. Model description and preliminary results. *Journal of Geophysical Research*, 100(D12):26191–26209.
- Bond, T. C., Doherty, S. J., Fahey, D., Forster, P., Berntsen, T., DeAngelo, B., Flanner, M., Ghan, S., Kärcher, B., Koch, D., Kinne, S., Kondo, Y., Quinn, P., Sarofim, M., Schultz, M., Schulz, M., Venkataraman, C., Zhang, H., Zhang, S., Bellouin, N., Guttikunda, S., Hopke, P., Jacobson, M., Kaiser, J., Klimont, Z., Lohmann, U., Schwarz, J., Shindell, D., Storelvmo, T., Warren, S., and Zender, C. (2013). Bounding the role of black carbon in the climate system: A scientific assessment. *Journal of Geophysical Research: Atmospheres*, 118(11):5380–5552.
- Boucher, O. (2015). *Atmospheric Aerosols: Properties and Climate Impacts*. Springer, Netherlands.
- Boucher, O. and Lohmann, U. (1995). The sulfate-CCN-cloud albedo effect. *Tellus B*, 47(3):281–300.
- Boucher, O., Randall, D., Artaxo, P., Bretherton, C., Feingold, G., Forster, P., Kerminen, V.-M., Kondo, Y., Liao, H., Lohmann, U., Rash, P., Satheesh, S., Sherwood, S., Stevens, B., and Zhang, X.-Y. (2013). Clouds and Aerosols. In: *Climate Change 2013: The Physical Science*

- basis. Contribution of Working Group I to the Fifth Assessment Report of the Intergovernmental Panel on Climate Change. *Cambridge University Press*, Cambridge, United Kingdom and New York, USA.
- Brasseur, G., Hauglustaine, D., Walters, S., Rasch, P., Müller, J.-F., Granier, C., and Tie, X. (1998). MOZART, a global chemical transport model for ozone and related chemical tracers: 1. model description. *Journal of Geophysical Research: Atmospheres (1984–2012)*, 103(D21):28265–28289.
- Brunner, D., Savage, N., Jorba, O., Eder, B., Giordano, L., Badia, A., Balzarini, A., Baró, R., Bianconi, R., Chemel, C., Curci, G., Forkel, R., Jiménez-Guerrero, P., Hirtl, M., Hodzic, A., Honzak, L., Im, U., Knote, C., Makar, P., Manders-Groot, A., van Meijgaard, E., Neal, L., Pérez, J. L., Pirovano, G., José, R. S., Schroder, W., Sokhi, R. S., Syrakov, D., Torian, A., Tuccella, P., Werhahn, J., Wolke, R., Yahya, K., Zabkar, R., Zhang, Y., Hogrefe, C., and Galmarini, S. (2015). Comparative analysis of meteorological performance of coupled chemistry-meteorology models in the context of AQMEII phase 2. *Atmospheric Environment*, 115:470 – 498.
- Buseck, P. and Schwartz, S. (2003). Tropospheric aerosols. *Treatise on geochemistry*, 4:91–142.
- Campbell, P., Zhang, Y., Yahya, K., Wang, K., Hogrefe, C., Pouliot, G., Knote, C., Hodzic, A., Jose, R. S., Perez, J. L., Guerrero, P. J., Baro, R., and Makar, P. (2015). A multi-model assessment for the 2006 and 2010 simulations under the Air Quality Model Evaluation International Initiative (AQMEII) Phase 2 over North America: Part I. Indicators of the sensitivity of o_3 and $\text{pm}_{2.5}$ formation regimes. *Atmospheric Environment*, 115:569 – 586.
- Carter, W. P. (2000). Implementation of the SAPRC-99 chemical mechanism into the Models-3 framework. Technical report, Environmental Protection Agency, EPA. United States.
- Chalmers, N., Highwood, E., Hawkins, E., Sutton, R., and Wilcox, L. (2012). Aerosol contribution to the rapid warming of near-term climate under RCP 2.6. *Geophysical Research Letters*, 39, L18709, doi:10.1029/2012GL052848.
- Chand, D., Wood, R., Anderson, T., Satheesh, S., and Charlson, R. (2009). Satellite-derived direct radiative effect of aerosols dependent on cloud cover. *Nature Geoscience*, 2(3):181–184.
- Chang, J., Middleton, P., Stockwell, W., Walcek, C., Pleim, J., Landsford, H., Binkowski, F., Madronich, S., Seaman, N., Stauffer, D., Byun, D., McHenry, J., Samson, P., and Hass, H. (1990). The regional acid deposition model and engineering model. Technical report, National Acid Precipitation Assessment Program, NAPAP Report 4, Washinton D.C.

- Chapman, E. G., Gustafson Jr, W., Easter, R. C., Barnard, J. C., Ghan, S. J., Pekour, M. S., and Fast, J. D. (2009). Coupling aerosol-cloud-radiative processes in the WRF-Chem model: Investigating the radiative impact of elevated point sources. *Atmospheric Chemistry and Physics*, 9(3):945–964.
- Charlson, R., Schwartz, S., Hales, J., Cess, R., Coakley, J., Hansen, J., and Hofmann, D. (1992). Climate forcing by anthropogenic aerosols. *Science*, 255(5043):423–430.
- Chin, M., Rood, R. B., Lin, S. J., Müller, J. F., and Thompson, A. M. (2000). Atmospheric sulfur cycle simulated in the global model GOCART: Model description and global properties. *Journal of Geophysical Research*, 105(D20):24671–24687.
- Chou, M. D. and Suarez, M. J. (1994). An efficient thermal infrared radiation parameterization for use in general circulation models. Technical report, NASA Technical Memorandum, Washintong D.C.
- Chou, M. D. and Suarez, M. J. (1999). A solar radiation parameterization for atmospheric studies. Technical report, NASA Technical Memorandum, Washintong D.C.
- Chou, M. D., Suarez, M. J., Liang, X. Z., Yan, M. M. H., and Cote, C. (2001). A thermal infrared radiation parameterization for atmospheric studies. Technical report, NASA Technical Memorandum, Washintong D.C.
- Chubarova, N., Nezval, Y., Sviridenkov, I., Smirnov, A., and Slutsker, I. (2012). Smoke aerosol and its radiative effects during extreme fire event over Central Russia in summer 2010. *Atmospheric Measurement Techniques*, 5(3):557–568.
- Chung, C. E. (2012). *Aerosol direct radiative forcing: a review*. INTECH Open Access Publisher.
- Collins, M., Arblaster, J., Dufresne, J. L., Fichefet, T., Friedlingstein, P., Gao, X., Gutowski, W., Johns, T., Krinner, G., Shongwem, M., Tebaldi, C., Weaver, A., and Wehner, M. (2013). Long-term Climate Change: Projections, Commitments and Irreversibility. In: Climate Change 2013: The Physical Science basis. Contribution of Working Group I to the Fifth Assessment Report of the Intergovernmental Panel on Climate Change. *Cambridge University Press*, Cambridge, United Kingdom and New York, USA.
- Collins, W. D., Rasch, P. J., Boville, B. A., Hack, J. J., McCaa, J. R., Williamson, D. L., Briegleb, B. P., Bitz, C. M., Lin, S. J., and Zhang, M. (2006). The formulation and atmospheric simulation of the Community Atmosphere Model version 3 (CAM3). *Journal of Climate*, 19(11):2144–2161.

- Curci, G., Hogrefe, C., Bianconi, R., Im, U., Balzarini, A., Baró, R., Brunner, D., Forkel, R., Giordano, L., Hirtl, M., Honzak, L., Jiménez-Guerrero, P., Knote, C., Langer, M., Makar, P., Pirovano, G., Pérez, J., San José, R., Syrakov, D., Tuccella, P., Werhahn, J., Wolke, R., Zabkar, R., Zhang, J., and Galmarini, S. (2015). Uncertainties of simulated aerosol optical properties induced by assumptions on aerosol physical and chemical properties: An AQMEII-2 perspective. *Atmospheric Environment*, 115:541–552.
- Curry, J. A., Ardeel, C. D., and Tian, L. (1990). Liquid water content and precipitation characteristics of stratiform clouds as inferred from satellite microwave measurements. *Journal of Geophysical Research: Atmospheres*, 95(D10):16659–16671.
- Curtius, J. (2006). Nucleation of atmospheric aerosol particles. *Comptes Rendus Physique*, 7(9):1027–1045.
- De Meij, A., Pozzer, A., Pringle, K., Tost, H., and Lelieveld, J. (2012). EMAC model evaluation and analysis of atmospheric aerosol properties and distribution with a focus on the mediterranean region. *Atmospheric Research*, 114:38–69.
- Denman, K. L., Brasseur, G., Chidthaisong, A., Ciais, P., Cox, P. M., Dickinson, R. E., Hauglustaine, D., Heinze, C., Holland, E., Jacob, D., Lohmann, U., Ramachandran, S., da Silva Dias, P., Wofsy, S., and Zhang, X. (2007). Couplings between changes in the climate system and biogeochemistry. In: *Climate Change 2007: The Physical Science Basis. Contribution of Working Group I to the Fourth Assessment Report of the Intergovernmental Panel on Climate Change*. Cambridge University Press, Cambridge, United Kingdom and New York, USA.
- Dodge, M. C. (2000). Chemical oxidant mechanisms for air quality modeling: critical review. *Atmospheric Environment*, 34(12):2103–2130.
- Doms, G., Förstner, J., Heise, E., Herzog, H., Mironov, D., Raschendorfer, M., Reinhardt, T., Ritter, B., Schrodin, R., Schulz, J., and Vogel, G. (2011). A description of the nonhydrostatic regional COSMO model. *Part II: Physical Parameterization*.
- Dubovik, O. and King, M. D. (2000). A flexible inversion algorithm for retrieval of aerosol optical properties from Sun and sky radiance measurements. *Journal of Geophysical Research*, 105(D16):20673–20696.
- Easter, R. C., Ghan, S. J., Zhang, Y., Saylor, R. D., Chapman, E. G., Laulainen, N. S., Abdul-Razzak, H., Leung, L. R., Bian, X., and Zaveri, R. A. (2004). MIRAGE: Model

- description and evaluation of aerosols and trace gases. *Journal of Geophysical Research*, 109, D20, doi:10.1029/2004JD004571.
- EEA (2010). The European Environment. State and outlook 2010. European environmental agency, Copenhagen.
- Emmerson, K. and Evans, M. (2009). Comparison of tropospheric gas-phase chemistry schemes for use within global models. *Atmospheric Chemistry and Physics*, 9(5):1831–1845.
- Fast, J. D., Gustafson Jr, W. I., Easter, R. C., Zaveri, R. A., Barnard, J. C., Chapman, E. G., Grell, G. A., and Peckham, S. E. (2006). Evolution of ozone, particulates, and aerosol direct radiative forcing in the vicinity of Houston using a fully coupled meteorology-chemistry-aerosol model. *Journal of Geophysical Research*, 111(D21):D21305.
- Fels, S. B. and Schwarzkopf, M. D. (1975). The simplified exchange approximation: A new method for radiative transfer calculations. *Journal of the Atmospheric Sciences*, 32(7):1475–1488.
- Forkel, R., Balzarini, A., Baró, R., Bianconi, R., Curci, G., Jiménez-Guerrero, P., Hirtl, M., Honzak, L., Lorenz, C., Im, U., Pérez, J. L., Pirovano, G., José, R. S., Tuccella, P., Werhahn, J., and Zabkar, R. (2015). Analysis of the WRF-Chem contributions to AQMEII phase2 with respect to aerosol radiative feedbacks on meteorology and pollutant distributions. *Atmospheric Environment*, 115:630 – 645.
- Forkel, R., Brunner, D., Baklanov, A., Balzarini, A., Hirtl, M., Honzak, L., Jiménez-Guerrero, P., Jorba, O., Pérez, J., San José, R., Schröder, W., Tsegas, G., Werhahn, J., Wolke, R., and Zabkar, R. (2016). A Multi-model case study on aerosol feedbacks in online coupled chemistry-meteorology models within the COST Action ES1004 EuMetChem. In *Air Pollution Modeling and its Application XXIV*, pages 23–28. Springer, Switzerland.
- Forkel, R., Werhahn, J., Hansen, A. B., McKeen, S., Peckham, S., Grell, G., and Suppan, P. (2012). Effect of aerosol-radiation feedback on regional air quality. A case study with WRF-Chem. *Atmospheric Environment*, 53:202–211.
- Forster, P., Ramaswamy, V., Artaxo, P., Berntsen, T., Betts, R., Fahey, D. W., Haywood, J., Lean, J., Lowe, D. C., Myhre, G., Nganga, J., Prinn, R., Raga, G., Schulz, M., and Van Dorland, R. (2007). Changes in atmospheric constituents and in radiative forcing. In: *Climate Change 2007: The Physical Science Basis. Contribution of Working Group I to the Fourth Assessment Report of the Intergovernmental Panel on Climate Change*. Cambridge University Press, Cambridge, United Kingdom and New York, United States of America.

- Galmarini, S., Bianconi, R., Appel, W., Solazzo, E., Mosca, S., Grossi, P., Moran, M., Schere, K., and Rao, S. (2012). ENSEMBLE and AMET: Two systems and approaches to a harmonized, simplified and efficient facility for air quality models development and evaluation. *Atmospheric environment*, 53:51–59.
- Galmarini, S., Hogrefe, C., Brunner, D., Makar, P., and Baklanov, A. (2015). Preface. *Atmospheric Environment*, 53(115):340–344.
- Gery, M. W., Whitten, G. Z., Killus, J. P., and Dodge, M. C. (1989). A photochemical kinetics mechanism for urban and regional scale computer modeling. *Journal of Geophysical Research*, 94(D10):12925–12956.
- Ghan, S. J. and Easter, R. C. (2006). Impact of cloud-borne aerosol representation on aerosol direct and indirect effects. *Atmospheric Chemistry and Physics*, 6(12):4163–4174.
- Ghan, S. J., Leung, L. R., Easter, R. C., and Abdul-Razzak, H. (1997). Prediction of cloud droplet number in a general circulation model. *Journal of Geophysical Research: Atmospheres*, 102(D18):21777–21794.
- Ghan, S. J. and Schwartz, S. E. (2007). Aerosol properties and processes: A path from field and laboratory measurements to global climate models. *Bulletin of the American Meteorological Society*, 88(7):1059–1083.
- Giordano, L., Brunner, D., Flemming, J., Hogrefe, C., Im, U., Bianconi, R., Badia, A., Balzarini, A., Baró, R., Chemel, C., Curci, G., Forkel, R., Jiménez-Guerrero, P., Hirtl, M., Hodzic, A., Honzak, L., Jorba, O., Knote, C., Kuenen, J., Makar, P., Manders-Groot, A., Neal, L., Pérez, J., Pirovano, G., Pouliot, G., José, R. S., Savage, N., Schlöder, W., Sokhi, R., Syrakov, D., Torian, A., Tuccella, P., Werhahn, J., Wolke, R., Yahya, K., Zabkar, R., Zhang, Y., and Galmarini, S. (2015). Assessment of the {MACC} reanalysis and its influence as chemical boundary conditions for regional air quality modeling in aqmeii-2. *Atmospheric Environment*, 115:371 – 388.
- Goosse, H. P., Barriat, Y., Lefebvre, W., Loutre, M. F., and Zunz, V. (2009). *Introduction to climate dynamics and climate modeling*. Date of consult: 12/20/2013. Available through <http://www.climate.be/textbook>.
- Grell, G. and Baklanov, A. (2011). Integrated modeling for forecasting weather and air quality: A call for fully coupled approaches. *Atmospheric Environment*, 45(38):6845–6851.

- Grell, G. A. and Dévényi, D. (2002). A generalized approach to parameterizing convection combining ensemble and data assimilation techniques. *Geophysical Research Letters*, 29(14):38–1.
- Grell, G. A. and Freitas, S. R. (2014). A scale and aerosol aware stochastic convective parameterization for weather and air quality modeling. *Atmospheric Chemistry and Physics*, 14(10):5233–5250.
- Grell, G. A., Peckham, S. E., Schmitz, R., McKeen, S. A., Frost, G., Skamarock, W. C., and Eder, B. (2005). Fully coupled “online” chemistry within the WRF model. *Atmospheric Environment*, 39(37):6957–6975.
- Griffin, R. J., Dabdub, D., and Seinfeld, J. H. (2002). Secondary organic aerosol 1. Atmospheric chemical mechanism for production of molecular constituents. *Journal of Geophysical Research*, 107, D17, doi:10.1029/2001JD000541.
- Gualtieri, G. and Secci, S. (2011). Comparing methods to calculate atmospheric stability-dependent wind speed profiles: A case study on coastal location. *Renewable Energy*, 36(8):2189–2204.
- Guenther, A., Karl, T., Harley, P., Wiedinmyer, C., Palmer, P. I., and Geron, C. (2006). Estimates of global terrestrial isoprene emissions using MEGAN (Model of Emissions of Gases and Aerosols from Nature). *Atmospheric Chemistry and Physics*, 6(11):3181–3210.
- Guenther, A., Zimmermanharley, P., Monson, R., and Fall, R. (1993). Isoprene and monoterpene rate variability: model evaluations and sensitive analyses. *J. Geophys. Res*, 98:10799–10808.
- Gustafson Jr, W. I., Chapman, E. G., Ghan, S. J., Easter, R. C., and Fast, J. D. (2007). Impact on modeled cloud characteristics due to simplified treatment of uniform cloud condensation nuclei during NEAQS 2004. *Geophysical Research Letters*, 34(19):L19809.
- Hansen, J., Johnson, D., Lacis, A., Lebedeff, S., Lee, P., Rind, D., and Russell, G. (1981). Climate impact of increasing atmospheric carbon dioxide. *Science*, 213(4511):957–966.
- Hansen, J., Sato, M., and Ruedy, R. (1997). Radiative forcing and climate response. *Journal of Geophysical Research: Atmospheres*, 102(D6):6831–6864.
- Hansen, J. e., Sato, M., Ruedy, R., Nazarenko, L., Lacis, A., Schmidt, G., Russell, G., Aleinov, I., Bauer, M., Bauer, S., Bell, N., Cairns, B., Canuto, V., Chandler, M., Cheng, Y., Del Genio, A., Faluvegi, G., Fleming, E., Friend, A., Hall, T., Jackman, C., Kelley, M., Kiang, N., Koch,

- D., Lean, J., Lerner, J., Lo, K., Menon, S., Miller, R., Minnis, P., Novakov, T., Oinas, V., Perlwitz, J., Perlwitz, J., Rind, D., Romanou, A., Shindell, D., Stone, P., Sun, S., Tausnev, N., Thresher, D., Wielicki, B., Wong, T., Yao, M., and Zhang, S. (2005). Efficacy of climate forcings. *Journal of Geophysical Research: Atmospheres*, 110(D18).
- Hauck, H., Berner, A., Frischer, T., Gomiscek, B., Kundi, M., Neuberger, M., Puxbaum, H., and Preining, O. (2004). AUPHEP-Austrian project on health effects of particulates-general overview. *Atmospheric Environment*, 38(24):3905–3915.
- Haylock, M., Hofstra, N., Klein Tank, A., Klok, E., Jones, P., and New, M. (2008). A European daily high-resolution gridded data set of surface temperature and precipitation for 1950–2006. *Journal of Geophysical Research: Atmospheres*, 113(D20).
- Haywood, J. and Boucher, O. (2000). Estimates of the direct and indirect radiative forcing due to tropospheric aerosols: A review. *Reviews of Geophysics*, 38(4):513–543.
- He, S. and Carmichael, G. R. (1999). Sensitivity of photolysis rates and ozone production in the troposphere to aerosol properties. *Journal of Geophysical Research*, 104(D21):26307–26324.
- Herman, M., Deuzé, J., Devaux, C., Goloub, P., Bréon, F., and Tanré, D. (1997). Remote sensing of aerosols over land surfaces including polarization measurements and application to POLDER measurements. *Journal of Geophysical Research: Atmospheres*, 102(D14):17039–17049.
- Hinds, W. C. (1999). *Aerosol technology: properties, behavior, and measurement of airborne particles*. John Wiley and Sons, New York, United States of America.
- Holben, B., Tanre, D., Smirnov, A., Eck, T., Slutsker, I., Abuhassan, N., Newcomb, W., Schafer, J., Chatenet, B., Lavenu, F., Kaufman, Y., Vande Castle, J., Setzer, A., Markham, B., Clark, D., Frouin, R., Halthore, R., Karneli, A., O’Neill, N., Pietras, C., Pinker, R., Voss, K., and Zibordi, G. (2001). An emerging ground-based aerosol climatology: Aerosol optical depth from AERONET. *Journal of Geophysical Research*, 106(D11):12067–12097.
- Hollmann, R., Merchant, C., Saunders, R., Downy, C., Buchwitz, M., Cazenave, A., Chuvieco, E., Defourny, P., de Leeuw, G., Forsberg, R., Holzer-Popp, T., Paul, F., Sandven, S., Sathyendranath, S., Van Roozendaal, M., and W, W. (2013). The ESA climate change initiative: Satellite data records for essential climate variables. *Bulletin of the American Meteorological Society*, 94(10):1541–1552.

- Hong, S.-Y., Noh, Y., and Dudhia, J. (2006). A new vertical diffusion package with an explicit treatment of entrainment processes. *Monthly Weather Review*, 134(9):2318–2341.
- Hong, S. Y. and Pan, H. L. (1996). Nonlocal boundary layer vertical diffusion in a medium-range forecast model. *Monthly weather review*, 124(10):2322–2339.
- Hsu, N., Bettenhausen, C., and Sayer, A. (2011). Time series of monthly average AOD at 550 nm over the Washington, D.C. Region. Technical report, NASA. Washintong D.C.
- Iacono, M. J., Delamere, J. S., Mlawer, E. J., Shephard, M. W., Clough, S. A., and Collins, W. D. (2008). Radiative forcing by long-lived greenhouse gases: Calculations with the AER radiative transfer models. *Journal of Geophysical Research: Atmospheres*, 113(D13).
- Im, U., Bianconi, R., Solazzo, E., Kioutsioukis, I., Badia, A., Balzarini, A., Baró, R., Bellasio, R., Brunner, D., Chemel, C., Curci, G., Flemming, J., Forkel, R., Giordano, L., Jiménez-Guerrero, P., Hirtl, M., Hodzic, A., Honzak, L., Jorba, O., Knote, C., Kuenen, J. J., Makar, P. A., Manders-Groot, A., Neal, L., Pérez, J. L., Pirovano, G., Pouliot, G., Jose, R. S., Savage, N., Schroder, W., Sokhi, R. S., Syrakov, D., Torian, A., Tuccella, P., Werhahn, J., Wolke, R., Yahya, K., Zabkar, R., Zhang, Y., Zhang, J., Hogrefe, C., and Galmarini, S. (2015a). Evaluation of operational on-line-coupled regional air quality models over Europe and North America in the context of AQMEII phase 2. Part I: Ozone. *Atmospheric Environment*, 115:404–420.
- Im, U., Bianconi, R., Solazzo, E., Kioutsioukis, I., Badia, A., Balzarini, A., Baró, R., Bellasio, R., Brunner, D., Chemel, C., Curci, G., van der Gon, H. D., Flemming, J., Forkel, R., Giordano, L., Jiménez-Guerrero, P., Hirtl, M., Hodzic, A., Honzak, L., Jorba, O., Knote, C., Makar, P. A., Manders-Groot, A., Neal, L., Perez, J. L., Pirovano, G., Pouliot, G., Jose, R. S., Savage, N., Schroder, W., Sokhi, R. S., Syrakov, D., Torian, A., Tuccella, P., Wang, K., Werhahn, J., Wolke, R., Zabkar, R., Zhang, Y., Zhang, J., Hogrefe, C., and Galmarini, S. (2015b). Evaluation of operational online-coupled regional air quality models over Europe and North America in the context of AQMEII phase 2. Part II: Particulate matter. *Atmospheric Environment*, 115:421 – 441.
- Isaksen, I., Midtbo, K., Sunde, J., and Crutzen, P. (1977). A simplified method to include molecular scattering and reflection in calculations of photon fluxes and photodissociation rates. *Geophysica Norvegica*, 31:11–26.
- Jacob, D. (1999). *Introduction to atmospheric chemistry*. Princeton University Press, Princeton, New Jersey, United States of America.

- Jacobson, M. Z. (1994). *Developing, Coupling, and Applying a Gas, Aerosol, Transport, and Radiation Model to Study Urban and Regional Air Pollution*. PhD thesis, University of California, Los Angeles.
- Jacobson, M. Z. (2001a). GATOR-GCMM: 2. A study of daytime and nighttime ozone layers aloft, ozone in national parks, and weather during the SARMAP Field Campaign. *Journal of Geophysical Research*, 106(D6):5403–5420.
- Jacobson, M. Z. (2001b). GATOR-GCMM: A global-through urban-scale air pollution and weather forecast model: 1. Model design and treatment of subgrid soil, vegetation, roads, rooftops, water, sea ice, and snow. *Journal of Geophysical Research*, 106(D6):5385–5401.
- Jacobson, M. Z. (2001c). Strong radiative heating due to the mixing state of black carbon in atmospheric aerosols. *Nature*, 409(6821):695–697.
- Jacobson, M. Z. and Kaufman, Y. J. (2006). Wind reduction by aerosol particles. *Geophysical Research Letters*, 33(24).
- Jérez, S., Mántavez, J. P., Jiménez-Guerrero, P., Gómez-Navarro, J. J., Lorente-Plazas, R., and Zorita, E. (2013). A multi-physics ensemble of present-day climate regional simulations over the Iberian Peninsula. *Climate dynamics*, 40(11-12):3023–3046.
- Jiménez-Guerrero, P., Montávez, J., Domínguez, M., Romera, R., Fita, L., Fernández, J., Cabos, W., Liguori, G., and Gaertner, M. (2013). Mean fields and interannual variability in RCM simulations over Spain: the ESCENA project. *Climate Research*, 57(3):201–220.
- Jorba, O., Pérez, C., Haustein, K., Janjic, Z., Dabdub, D., Baldasano, J. M., Badia, A., and Spada, M. (2010). Status of development and firsts results at global scale of NMMB/BSC-CHEM: an online multiscale air quality model. In *EGU General Assembly Conference Abstracts*, volume 12, page 5228.
- Joseph, J. H., Wiscombe, W., and Weinman, J. (1976). The delta-eddington approximation for radiative flux transfer. *Journal of the Atmospheric Sciences*, 33(12):2452–2459.
- Kazil, J., Stier, P., Zhang, K., Quaas, J., Kinne, S., O’Donnell, D., Rast, S., Esch, M., Ferrachat, S., Lohmann, U., and Feichter, J. (2010). Aerosol nucleation and its role for clouds and earth’s radiative forcing in the aerosol-climate model ECHAM5-HAM. *Atmospheric Chemistry and Physics*, 10(22):10733–10752.
- Kennedy, I. M. (2007). The health effects of combustion-generated aerosols. *Proceedings of the Combustion Institute*, 31(2):2757–2770.

- Kent, G., McCormick, M., and Schaffner, S. (1991). Global optical climatology of the free tropospheric aerosol from 1.0- μm satellite occultation measurements. *Journal of Geophysical Research: Atmospheres*, 96(D3):5249–5267.
- Kinne, S., Schulz, M., Textor, C., Guibert, S., Balkanski, Y., Bauer, S. E., Berntsen, T., Berglen, T. F., Boucher, O., Chin, M., Collins, W., Dentener, F., Diehl, T., Easter, R., Feichter, J., Fillmore, D., Ghan, S., Ginoux, P., Gong, S., Grini, A., Hendricks, J., Herzog, M., Horowitz, L., Isaksen, I., Iversen, T., Kirkevåg, A., Kloster, S., Koch, D., Kristjansson, J. E., Krol, M., Lauer, A., Lamarque, J. F., Lesins, G., Liu, X., Lohmann, U., Montanaro, V., Myhre, G., Penner, J., Pitari, G., Reddy, S., Seland, O., Stier, P., Takemura, T., and Tie, X. (2006). An AeroCom initial assessment—optical properties in aerosol component modules of global models. *Atmospheric Chemistry and Physics*, 6(7):1815–1834.
- Kioutsioukis, I., Im, U., Solazzo, E., Bianconi, R., Badia, A., Balzarini, A., Baró, R., Bellasio, R., Brunner, D., Chemel, C., Curci, G., van der Gon, H. D., Flemming, J., Forkel, R., Giordano, L., Jiménez-Guerrero, P., Hirtl, M., Jorba, O., Manders-Groot, A., Neal, L., Pérez, J. L., Pirovano, G., San Jose, R., Savage, N., Schroder, W., Sokhi, R. S., Syrakov, D., Tuccella, P., Werhahn, J., Wolke, R., Hogrefe, C., and Galmarini, S. (2016). Insights into the deterministic skill of air quality ensembles from the analysis of AQMEII data. 16(24):15629–15652.
- Kniffka, A., Stengel, M., Lockhoff, M., Bennartz, R., and Hollmann, R. (2014). Characteristics of cloud liquid water path from SEVIRI onboard the Meteosat Second Generation 2 satellite for several cloud types. *Atmospheric Measurement Techniques*, 7(4):887–905.
- Knote, C., Tuccella, P., Curci, G., Emmons, L., Orlando, J. J., Madronich, S., Baró, R., Jiménez-Guerrero, P., Luecken, D., Hogrefe, C., Forkel, R., Werhahn, J., Hirtl, M., Pérez, J. L., José, R. S., Giordano, L., Brunner, D., Yahya, K., and Zhang, Y. (2015). Influence of the choice of gas-phase mechanism on predictions of key gaseous pollutants during the AQMEII Phase 2 intercomparison. *Atmospheric Environment*, 115:553 – 568.
- Knutti, R., Furrer, R., Tebaldi, C., Cermak, J., and Meehl, G. A. (2010). Challenges in combining projections from multiple climate models. *Journal of Climate*, 23(10):2739–2758.
- Kong, X., Forkel, R., Sokhi, R. S., Suppan, P., Baklanov, A., Gauss, M., Brunner, D., Barò, R., Balzarini, A., Chemel, C., Curci, G., Jiménez-Guerrero, P., Hirtl, M., Honzak, L., Im, U., Pérez, J. L., Pirovano, G., San Jose, R., Schlünzen, K. H., Tsegas, G., Tuccella, P., Werhahn, J., Zabkar, R., and Galmarini, S. (2015). Analysis of meteorology–chemistry interactions dur-

- ing air pollution episodes using online coupled models within AQMEII phase-2. *Atmospheric Environment*, 115:527–540.
- Konovalov, I., Beekmann, M., Kuznetsova, I., Yurova, A., and Zvyagintsev, A. (2011). Atmospheric impacts of the 2010 Russian wildfires: integrating modelling and measurements of an extreme air pollution episode in the Moscow region. *Atmospheric Chemistry and Physics*, 11(19):10031–10056.
- Kuenen, J., Visschedijk, A., Jozwicka, M., and Denier Van der Gon, H. (2014). TNO-MACC_II emission inventory; a multi-year (2003–2009) consistent high-resolution European emission inventory for air quality modelling. *Atmospheric Chemistry and Physics*, 14(20):10963–10976.
- Kulmala, M., Hämeri, K., Aalto, P., Mäkelä, J., Pirjola, L., Nilsson, E. D., Buzorius, G., Rannik, Ü., Maso, M., Seidl, W., Hoffman, T., Janson, R., Hansson, H., Viisanen, Y., Laaksonen, A., and O’dowd, C. (2001). Overview of the international project on biogenic aerosol formation in the boreal forest (BIOFOR). *Tellus B*, 53(4):324–343.
- Kumar, R., Barth, M. C., Pfister, G. G., Naja, M., and Brasseur, G. P. (2013). WRF-Chem simulations of a typical pre-monsoon dust storm in northern India: influences on aerosol optical properties and radiation budget. *Atmospheric Chemistry and Physics*, 13(8):21837–21881.
- Lacis, A. A. and Hansen, J. (1974). A parameterization for the absorption of solar radiation in the earth’s atmosphere. *Journal of the Atmospheric Sciences*, 31(1):118–133.
- Landgren, O. A., Haugen, J. E., and Førland, E. J. (2014). Evaluation of regional climate model temperature and precipitation outputs over Scandinavia. *Climate Research*, 60(3):249–264.
- Lattuati, M. (1997). *Contribution à l’étude du bilan de l’ozone troposphérique à l’interface de l’Europe et de l’Atlantique Nord: modélisation lagrangienne et mesures en altitude*. PhD thesis, Université Paris.
- Legrand, M., Bertrand, J., Desbois, M., Menenger, L., and Fouquart, Y. (1989). The potential of infrared satellite data for the retrieval of saharan-dust optical depth over africa. *Journal of Applied Meteorology*, 28(4):309–319.
- Li, G., Wang, Y., and Zhang, R. (2008). Implementation of a two-moment bulk microphysics scheme to the WRF model to investigate aerosol-cloud interaction. *Journal of Geophysical Research: Atmospheres*, 113(D15).

- Li, S., Wang, T., Xie, M., Han, Y., and Zhuang, B. (2015). Observed aerosol optical depth and angstrom exponent in urban area of Nanjing, China. *Atmospheric Environment*.
- Li, Z., Lee, K.-H., Wang, Y., Xin, J., and Hao, W.-M. (2010). First observation-based estimates of cloud-free aerosol radiative forcing across China. *Journal of Geophysical Research: Atmospheres*, 115(D7).
- Liao, H., Yung, Y. L., and Seinfeld, J. H. (1999). Effects of aerosols on tropospheric photolysis rates in clear and cloudy atmospheres. *Journal of Geophysical Research*, 104(D19):23697–23.
- Lin, Y.-L., Farley, R. D., and Orville, H. D. (1983). Bulk parameterization of the snow field in a cloud model. *Journal of Climate and Applied Meteorology*, 22(6):1065–1092.
- Liu, H., Crawford, J. H., Considine, D. B., Platnick, S., Norris, P. M., Duncan, B. N., Pierce, R. B., Chen, G., and Yantosca, R. M. (2009). Sensitivity of photolysis frequencies and key tropospheric oxidants in a global model to cloud vertical distributions and optical properties. *Journal of Geophysical Research*, 114, D10, doi:10.1029/2008JD011503.
- Liu, Y., Daum, P. H., and McGraw, R. L. (2005). Size truncation effect, threshold behavior, and a new type of autoconversion parameterization. *Geophysical research letters*, 32(11).
- Liu, Y., Wu, W., Jensen, M., and Toto, T. (2011a). Relationship between cloud radiative forcing, cloud fraction and cloud albedo, and new surface-based approach for determining cloud albedo. *Atmospheric Chemistry and Physics*, 11(14):7155–7170.
- Liu, Z., Liu, Q., Lin, H.-C., Schwartz, C. S., Lee, Y.-H., and Wang, T. (2011b). Three-dimensional variational assimilation of MODIS aerosol optical depth: Implementation and application to a dust storm over East Asia. *Journal of Geophysical Research: Atmospheres*, 116(D23).
- Lohmann, U. and Feichter, J. (2005). Global indirect aerosol effects: a review. *Atmospheric Chemistry and Physics*, 5(3):715–737.
- Lorente-Plazas, R., Jiménez, P. A., Dudhia, J., and Montávez, J. P. (2016). Evaluating and improving the impact of the atmospheric stability and orography on surface winds in the WRF model. *Monthly Weather Review*, 144(7):2685–2693.
- Lovett, G. M., Tear, T. H., Evers, D. C., Findlay, S. E., Cosby, B. J., Dunscomb, J. K., Driscoll, C. T., and Weathers, K. C. (2009). Effects of air pollution on ecosystems and biological diversity in the eastern United States. *Annals of the New York Academy of Sciences*, 1162(1):99–135.

- Lurmann, F. W., Carter, W. P., and Coyner, L. A. (1987). A surrogate species chemical reaction mechanism for urban-scale air quality simulation models. Technical report, EPA/600/3-87/014a. Environmental Protection Agency, EPA. United States.
- Madronich, S. (1987). Photodissociation in the atmosphere: Actinic flux and the effects of ground reflections and clouds. *Journal of Geophysical Research*, 92(D8):9740–9752.
- Madronich, S. and Weller, G. (1990). Numerical integration errors in calculated tropospheric photodissociation rate coefficients. *Journal of Atmospheric Chemistry*, 10(3):289–300.
- Makar, P., Gong, W., Hogrefe, C., Zhang, Y., Curci, G., Zabkar, R., Milbrandt, J., Im, U., Balzarini, A., Baró, R., Bianconi, R., Cheung, P., Forkel, R., Gravel, S., Hirtl, M., Honzak, L., Hou, A., Jiménez-Guerrero, P., Langer, M., Moran, M., Pabla, B., Pérez, J., Pirovano, G., José, R. S., Tuccella, P., Werhahn, J., Zhang, J., and Galmarini, S. (2015a). Feedbacks between air pollution and weather, Part 2: Effects on chemistry. *Atmospheric Environment*, 115:499–526.
- Makar, P., Gong, W., Milbrandt, J., Hogrefe, C., Zhang, Y., Curci, G., Zabkar, R., Im, U., Balzarini, A., Baró, R., Bianconi, R., Cheung, P., Forkel, R., Gravel, S., Hirtl, M., Honzak, L., Hou, A., Jiménez-Guerrero, P., Langer, M., Moran, M., Pabla, B., Pérez, J., Pirovano, G., José, R. S., Tuccella, P., Werhahn, J., Zhang, J., and Galmarini, S. (2015b). Feedbacks between air pollution and weather, Part 1: Effects on weather. *Atmospheric Environment*, 115:442–469.
- Mann, G. W., Carslaw, K. S., Ridley, D. A., Spracklen, D. V., Pringle, K. J., Merikanto, J., Korhonen, H., Schwarz, J. P., Lee, L. A., Manktelow, P. T., Woodhouse, M. T., Schmidt, A., Breider, T. J., Emmerson, K. M., Reddington, C. L., Chipperfield, M. P., and Pickering, S. J. (2012). Intercomparison of modal and sectional aerosol microphysics representations within the same 3-D global chemical transport model. *Atmospheric Chemistry and Physics*, 12(10):4449–4476.
- Mashayekhi, R. and Sloan, J. (2013). Effects of aerosols on precipitation in north-eastern North America. *Atmospheric Chemistry and Physics*, 13(10):27937–27969.
- Mathur, R., Pleim, J., Wong, D., Otte, T., Gilliam, R., Roselle, S., Young, J., Binkowski, F., and Xiu, A. (2010). The WRF-CMAQ integrated on-line modeling system: development, testing, and initial applications. *Air Pollution Modeling and Its Application*, 20:155–160.
- Maurizi, A., D'Isidoro, M., and Mircea, M. (2011). BOLCHEM: An integrated system for

- atmospheric dynamics and composition. In *Integrated Systems of Meso-Meteorological and Chemical Transport Models*, pages 89–94. Springer, Berlin Heidelberg.
- McComiskey, A., Feingold, G., Frisch, A. S., Turner, D. D., Miller, M. A., Chiu, J. C., Min, Q., and Ogren, J. A. (2009). An assessment of aerosol-cloud interactions in marine stratus clouds based on surface remote sensing. *Journal of Geophysical Research: Atmospheres*, 114(D9).
- Mcgarragh, G., Poulsen, C., Thomas, G., Povey, A., Sus, O., Schlundt, C., Stapelberg, S., Proud, S., Christensen, M., Stengel, M., and Grainger, R. (2017). The Community Cloud retrieval for CLimate (CC4cL). Part II: The optimal estimation algorithm. *To be submitted to Atmospheric Measurement Techniques*.
- Meier, J., Tegen, I., Heinold, B., and Wolke, R. (2012). Direct and semi-direct radiative effects of absorbing aerosols in Europe: Results from a regional model. *Geophysical Research Letters*, 39, L09802, doi:10.1029/2012GL050994(9).
- Menon, S., Genio, A. D. D., Koch, D., and Tselioudis, G. (2002). Gcm simulations of the aerosol indirect effect: Sensitivity to cloud parameterization and aerosol burden. *Journal of the atmospheric sciences*, 59(3):692–713.
- Menon, S., Unger, N., Koch, D., Francis, J., Garrett, T., Sednev, I., Shindell, D., and Streets, D. (2008). Aerosol climate effects and air quality impacts from 1980 to 2030. *Environmental Research Letters*, 3, 024004 doi:10.1088/1748-9326/3/2/024004(2).
- Mishra, A. K., Koren, I., and Rudich, Y. (2015). Effect of aerosol vertical distribution on aerosol-radiation interaction: A theoretical prospect. *Heliyon*, 1(2):e00036.
- Mitchell, D. L., Rasch, P., Ivanova, D., McFarquhar, G., and Nousiainen, T. (2008). Impact of small ice crystal assumptions on ice sedimentation rates in cirrus clouds and gcm simulations. *Geophysical Research Letters*, 35(9).
- Mlawer, E. and Clough, S. (1998). Shortwave and longwave enhancements in the rapid radiative transfer model. In *Proceedings of the Seventh Atmospheric Radiation Measurement (ARM) Science Team Meeting, Rep. CONF-970365*.
- Mlawer, E. J., Taubman, S. J., Brown, P. D., Iacono, M. J., and Clough, S. A. (1997). Radiative transfer for inhomogeneous atmospheres: RRTM, a validated correlated-k model for the longwave. *Journal of Geophysical Research*, 102(D14):16663–16682.
- Monahan, E. C. and Mac Niocaill, G. (1986). *Oceanic Whitecaps: And Their Role in Air-Sea Exchange Processes*. D. Reidel Publishing Company, Dordrecht, Holland.

- Morcrette, J., Jones, L., Kaiser, J., Benedetti, A., and Boucher, O. (2007). Toward a forecast of aerosols with the ecmwf integrated forecast system. *ECMWF Newsl*, 114:15–17.
- Morcrette, J.-J., Barker, H., Cole, J., Iacono, M., and Pincus, R. (2008). Impact of a new radiation package, McRad, in the ECMWF Integrated Forecasting System. *Monthly Weather Review*, 136(12):4773–4798.
- Morrison, H., Thompson, G., and Tatarskii, V. (2009). Impact of cloud microphysics on the development of trailing stratiform precipitation in a simulated squall line: Comparison of one-and two-moment schemes. *Monthly Weather Review*, 137(3):991–1007.
- Myhre, G., Samset, B. H., Schulz, M., Balkanski, Y., Bauer, S., Berntsen, T. K., Bian, H., Bellouin, N., Chin, M., Diehl, T., Easter, R. C., Feichter, J., Ghan, S. J., Hauglustaine, D., Iversen, T., Kinne, S., Kirkevåg, A., Lamarque, J.-F., Lin, G., Liu, X., Lund, M. T., Luo, G., Ma, X., van Noije, T., Penner, J. E., Rasch, P. J., Ruiz, A., Seland, Ø., Skeie, R. B., Stier, P., Takemura, T., Tsigaridis, K., Wang, P., Wang, Z., Xu, L., Yu, H., Yu, F., Yoon, J.-H., Zhang, K., Zhang, H., and Zhou, C. (2013a). Radiative forcing of the direct aerosol effect from Aerocom Phase II simulations. *Atmospheric Chemistry and Physics*, 13(4):1853–1877.
- Myhre, G., Shindell, D., Breon, F.-M., Collins, W., Fuglestvedt, J., Huang, J., Koch, D., Lamarque, J.-F., Lee, D., Mendoza, B., Nakajima, T., Robock, A., Stephens, G., Takemura, T., and H, Z. (2013b). Anthropogenic and Natural Radiative Forcing. In: *Climate Change 2013: The Physical Science Basis. Contribution of Working Group I to the Fifth Assessment Report of the Intergovernmental Panel on Climate Change*. Cambridge University Press, Cambridge, United Kingdom and New York, USA.
- Nagaraja Rao, C., Stowe, L., and McClain, E. (1989). Remote sensing of aerosols over the oceans using AVHRR data Theory, practice and applications. *International Journal of Remote Sensing*, 10(4-5):743–749.
- Nakajima, T., Tanaka, M., and Yamauchi, T. (1983). Retrieval of the optical properties of aerosols from aureole and extinction data. *Applied Optics*, 22(19):2951–2959.
- Neggers, R. A. (2009). A dual mass flux framework for boundary layer convection. part ii: Clouds. *Journal of the Atmospheric Sciences*, 66(6):1489–1506.
- Neu, J. L., Prather, M. J., and Penner, J. E. (2007). Global atmospheric chemistry: Integrating over fractional cloud cover. *Journal of Geophysical Research*, 112, D11306, doi:10.1029/2006JD008007.

- Ogren, J., Andrews, E., McComiskey, A., Sheridan, P., Jefferson, A., and Fiebig, M. (2006). New insights into aerosol asymmetry parameter. In *Proceedings of the Sixteenth ARM Science Team Meeting, Albuquerque, United States of America*.
- Ogren, J. A. (1995). A systematic approach to in situ observations of aerosol properties. In *Aerosol Forcing of Climate, edited by Charlson, R.J., and Heintzenberg, J.*, pages 215–226. John Wiley and Sons, New York, United States of America.
- Okuda, T., Isobe, R., Nagai, Y., Okahisa, S., Funato, K., and Inoue, K. (2015). Development of a high-volume pm 2.5 particle sampler using impactor and cyclone techniques. *Aerosol and Air Quality Research*, 15(3):759–767.
- Pagowski, M., Grell, G., McKeen, S., Peckham, S., and Devenyi, D. (2010). Three-dimensional variational data assimilation of ozone and fine particulate matter observations: some results using the Weather Research and Forecasting–Chemistry model and Grid-point Statistical Interpolation. *Quarterly Journal of the Royal Meteorological Society*, 136(653):2013–2024.
- Peckham, S. E., Grell, G. A., McKeen, S. A., Barth, M., Pfister, G., Wiedinmyer, C., Fast, J. D., Gustafson, W. I., Ghan, S. J., Zaveri, R., Easter, R., Barnard, K., Chapman, E., Hewson, M., Schmitz, R., Salzmann, M., Beck, V., and Freitas, S. (2012). *WRF-Chem Version 3.4 User's Guide*. US Department of Commerce, National Oceanic and Atmospheric Administration, Oceanic and Atmospheric Research Laboratories, Global Systems Division, United States.
- Penner, J. E., Quaas, J., Storelvmo, T., Takemura, T., Boucher, O., Guo, H., Kirkevåg, A., Kristjánsson, J. E., and Seland, Ø. (2006). Model intercomparison of indirect aerosol effects. *Atmospheric Chemistry and Physics*, 6(11):3391–3405.
- Péré, J., Bessagnet, B., Mallet, M., Waquet, F., Chiapello, I., Minvielle, F., Pont, V., and Menut, L. (2014). Direct radiative effect of the Russian wildfires and its impact on air temperature and atmospheric dynamics during August 2010. *Atmospheric Chemistry and Physics*, 14(4):1999–2013.
- Péré, J., Bessagnet, B., Pont, V., Mallet, M., and Minvielle, F. (2015). Influence of the aerosol solar extinction on photochemistry during the 2010 Russian wildfires episode. *Atmospheric Chemistry and Physics Discussions*, 15(5):7057–7087.
- Petzold, A., Ogren, J. A., Fiebig, M., Laj, P., Li, S.-M., Baltensperger, U., Holzer-Popp, T., Kinne, S., Pappalardo, G., Sugimoto, N., Wehrli, C., Wiedensohler, A., and Zhang, X. (2013). Recommendations for reporting "black carbon" measurements. *Atmospheric Chemistry and Physics*, 13(16):8365–8379.

- Pierangelo, C., Chédin, A., Heilliette, S., Jacquinet-Husson, N., and Armante, R. (2004). Dust altitude and infrared optical depth from AIRS. *Atmospheric Chemistry and Physics*, 4(7):1813–1822.
- Planton, S. and Maynard, K. (2004). Météo france prism model adaptation. PRISM Report Series-10.
- Pope, C. A., Ezzati, M., and Dockery, D. W. (2009). Fine-particulate air pollution and life expectancy in the United States. *New England Journal of Medicine*, 360(4):376–386.
- Pósfai, M., Anderson, J. R., Buseck, P. R., and Sievering, H. (1999). Soot and sulfate aerosol particles in the remote marine troposphere. *Journal of Geophysical Research*, 104(D17):21685–21693.
- Pósfai, M. and Buseck, P. R. (2010). Nature and climate effects of individual tropospheric aerosol particles. *Annual Reviews*, 38:17–43.
- Pouliot, G., Pierce, T., Denier van der Gon, H., Schaap, M., Moran, M., and Nopmongcol, U. (2012). Comparing emission inventories and model-ready emission datasets between Europe and North America for the AQMEII project. *Atmospheric Environment*, 53:4–14.
- Pouliot, G., van der Gon, H. A. D., Kuenen, J., Zhang, J., Moran, M. D., and Makar, P. A. (2015). Analysis of the emission inventories and model-ready emission datasets of Europe and North America for phase 2 of the AQMEII project. *Atmospheric Environment*, 115:345–360.
- Prather, M. J. (2002). Lifetimes of atmospheric species: Integrating environmental impacts. *Geophysical Research Letters*, 29, doi: 10.1029/2002GL016299.
- Prijith, S., Aloysius, M., and Mohan, M. (2014). Relationship between wind speed and sea salt aerosol production: A new approach. *Journal of Atmospheric and Solar-Terrestrial Physics*, 108:34–40.
- Prospero, J. M., Ginoux, P., Torres, O., Nicholson, S. E., and Gill, T. E. (2002). Environmental characterization of global sources of atmospheric soil dust identified with the Nimbus 7 Total Ozone Mapping Spectrometer (TOMS) absorbing aerosol product. *Reviews of Geophysics*, 40(1).
- Quaas, J., Ming, Y., Menon, S., Takemura, T., Wang, M., Penner, J. E., Gettelman, A., Lohmann, U., Bellouin, N., Boucher, O., Sayer, A. M., Thomas, G. E., McComiskey, A., Feingold, G., Hoose, C., Kristjánsson, J. E., Liu, X., Balkanski, Y., Donner, L. J., Ginoux,

- P. A., Stier, P., Grandey, B., Feichter, J., Sednev, I., Bauer, S. E., Koch, D., Grainger, R. G., Kirkevåg, A., Iversen, T., Seland, Ø., Easter, R., Ghan, S. J., Rasch, P. J., Morrison, H., Lamarque, J.-F., Iacono, M. J., Kinne, S., and Schulz, M. (2009). Aerosol indirect effects—general circulation model intercomparison and evaluation with satellite data. *Atmospheric Chemistry and Physics*, 9(22):8697–8717.
- Ramanathan, V. and Carmichael, G. (2008). Global and regional climate changes due to black carbon. *Nature Geoscience*, 1(4):221–227.
- Ramanathan, V., Crutzen, P., Kiehl, J., and Rosenfeld, D. (2001a). Aerosols, climate, and the hydrological cycle. *science*, 294(5549):2119–2124.
- Ramanathan, V., Crutzen, P. J., Lelieveld, J., Mitra, A. P., Althausen, D., Anderson, J., Andreae, M. O., Cantrell, W., Cass, G. R., Chung, C. E., Clarke, A. D., Coakley, J. A., Collins, W. D., Conant, W. C., Dulac, F., Heintzenberg, J., Heymsfield, A. J., Holben, B., Howell, S., Hudson, J., Jayaraman, A., Kiehl, J. T., Krishnamurti, T. N., Lubin, D., McFarquhar, G., Novakov, T., Ogren, J. A., Podgorny, I. A., Prather, K., Priestley, K., Prospero, J. M., Quinn, P. K., Rajeev, K., Rasch, P., Rupert, S., Sadourny, R., Satheesh, S. K., Shaw, G. E., Sheridan, P., and Valero, F. P. J. (2001b). Indian Ocean Experiment: An integrated analysis of the climate forcing and effects of the great Indo-Asian haze. *Journal of Geophysical Research*, 106(D22):28371–28398.
- Ramanathan, V. and Downey, P. (1986). A nonisothermal emissivity and absorptivity formulation for water vapor. *Journal of Geophysical Research*, 91(D8):8649–8666.
- Ramanathan, V. and Feng, Y. (2009). Air pollution, greenhouse gases and climate change: Global and regional perspectives. *Atmospheric Environment*, 43(1):37–50.
- Randall, D. A., Wood, R. A., Bony, S., Colman, R., Fichet, T., Fyfe, J., Kattsov, V., Pitman, A., Shukla, J., Srinivasan, J., Stouffer, R., Sumi, A., and Taylor, K. (2007). Climate models and their evaluation. In: *Climate Change 2007: The Physical Science Basis. Contribution of Working Group I to the Fourth Assessment Report of the Intergovernmental Panel on Climate Change*. Cambridge University Press, Cambridge, United Kingdom and New York, USA.
- Rao, S. T., Galmarini, S., and Puckett, K. (2011). Air Quality Model Evaluation International Initiative (AQMEII): advancing the state of the science in regional photochemical modeling and its applications. *Bulletin of the American Meteorological Society*, 92(1):23–30.

- Rauscher, S. A., Coppola, E., Piani, C., and Giorgi, F. (2010). Resolution effects on regional climate model simulations of seasonal precipitation over Europe. *Climate Dynamics*, 35(4):685–711.
- Real, E. and Sartelet, K. (2011). Modeling of photolysis rates over Europe: impact on chemical gaseous species and aerosols. *Atmospheric Chemistry and Physics*, 11(4):1711–1727.
- Remer, L. A., Kaufman, Y., Tanré, D., Mattoo, S., Chu, D., Martins, J. V., Li, R.-R., Ichoku, C., Levy, R., Kleidman, R., Eck, T., Vermote, E., and Holben, B. (2005). The MODIS aerosol algorithm, products, and validation. *Journal of the atmospheric sciences*, 62(4):947–973.
- Rosenfeld, D., Lohmann, U., Raga, G. B., O’Dowd, C. D., Kulmala, M., Fuzzi, S., Reissell, A., and Andreae, M. O. (2008). Flood or drought: How do aerosols affect precipitation? *science*, 321(5894):1309–1313.
- Rosenfeld, D., Sherwood, S., Wood, R., and Donner, L. (2014). Climate effects of aerosol-cloud interactions. *Science*, 343(6169):379–380.
- Rutledge, S. A. and Hobbs, P. V. (1984). The mesoscale and microscale structure and organization of clouds and precipitation in midlatitude cyclones. XII: A diagnostic modeling study of precipitation development in narrow cold-frontal rainbands. *Journal of the Atmospheric Sciences*, 41(20):2949–2972.
- Saarikoski, S. (2008). *Chemical mass closure and source-specific composition of atmospheric particles*. PhD thesis, Finnish Meteorological Institute, Helsinki.
- San José, R., Pérez, J., Balzarini, A., Baró, R., Curci, G., Forkel, R., Galmarini, S., Grell, G., Hirtl, M., Honzak, L., Im, U., Jiménez-Guerrero, P., Langer, M., Pirovano, G., Tuccella, P., Werhahn, J., and Zabkar, R. (2015). Sensitivity of feedback effects in CBMZ/MOSAIC chemical mechanism. *Atmospheric Environment*, 115:646–656.
- Sanap, S. D., Ayantika, D. C., Pandithurai, G., and Niranjana, K. (2014). Assessment of the aerosol distribution over Indian subcontinent using CMIP5 models. *Atmospheric Environment*, In Press, Accepted Manuscript, doi: 10.1016/j.atmosenv.2014.01.017.
- Sanderson, M. G., Collins, W. J., Johnson, C. E., and Derwent, R. G. (2006). Present and future acid deposition to ecosystems: The effect of climate change. *Atmospheric Environment*, 40(7):1275–1283.

- Sarwar, G., Luecken, D., Yarwood, G., Whitten, G. Z., and Carter, W. P. (2008). Impact of an updated carbon bond mechanism on predictions from the CMAQ modeling system: Preliminary assessment. *Journal of Applied Meteorology and Climatology*, 47(1):3–14.
- Sathe, A., Gryning, S.-E., and Peña, A. (2011). Comparison of the atmospheric stability and wind profiles at two wind farm sites over a long marine fetch in the North Sea. *Wind Energy*, 14(6):767–780.
- Sauter, F., van der Swaluw, E., Manders-Groot, A., Kruit, R. W., Segers, A., and Eskes, H. (2012). LOTOS-EUROS v1.8 Reference Guide. TNO. *TNO report TNO-060-UT-2012-01451*.
- Savage, N., Agnew, P., Davis, L., Ordóñez, C., Thorpe, R., Johnson, C., O'Connor, F., and Dalvi, M. (2013). Air quality modelling using the met office unified model (AQUM OS24-26): model description and initial evaluation. *Geoscientific Model Development*, 6(2):353–372.
- Schaap, M., Roemer, M., Boersen, G., Timmermans, R., and Builtjes, P. (2005). LOTOS-EUROS: Documentation. TNO report B&O-A. Technical report, 2005-296, Apeldoorn.
- Schell, B., Ackermann, I. J., Hass, H., Binkowski, F. S., and Ebel, A. (2001). Modeling the formation of secondary organic aerosol within a comprehensive air quality model system. *Journal of Geophysical Research*, 106(D22):28275–28293.
- Schulz, M., Textor, C., Kinne, S., Balkanski, Y., Bauer, S., Berntsen, T., Berglen, T., Boucher, O., Dentener, F., Guibert, S., Isaksen, I. S. A., Iversen, T., Koch, D., Kirkevåg, A., Liu, X., Montanaro, V., Myhre, G., Penner, J. E., Pitari, G., Reddy, S., Seland, Ø., Stier, P., and Takemura, T. (2006). Radiative forcing by aerosols as derived from the AeroCom present-day and pre-industrial simulations. *Atmospheric Chemistry and Physics*, 6(12):5225–5246.
- Schwartz, C. S., Liu, Z., Lin, H.-C., and McKeen, S. A. (2012). Simultaneous three-dimensional variational assimilation of surface fine particulate matter and MODIS aerosol optical depth. *Journal of Geophysical Research: Atmospheres*, 117(D13).
- Schwartz, S. E. and Benkovitz, C. M. (2002). Influence of anthropogenic aerosol on cloud optical depth and albedo shown by satellite measurements and chemical transport modeling. *Proceedings of the National Academy of Sciences*, 99(4):1784–1789.
- Schwarzkopf, M. D. and Fels, S. B. (1991). The simplified exchange method revisited: An accurate, rapid method for computation of infrared cooling rates and fluxes. *Journal of Geophysical Research*, 96(D5):9075–9096.

- Seinfeld, J. H., Bretherton, C., Carslaw, K. S., Coe, H., DeMott, P. J., Dunlea, E. J., Feingold, G., Ghan, S., Guenther, A. B., Kahn, R., Kraucunas, I., Kreidenweis, S., Molina, M., Nenes, A., Penner, J., Prather, K., Ramanathan, V., Ramaswamy, V., Rasch, P., Ravishankara, A., Rosenfeld, D., Stephens, G., and Wood, R. (2016). Improving our fundamental understanding of the role of aerosol-cloud interactions in the climate system. *Proceedings of the National Academy of Sciences*, 113(21):5781–5790.
- Seinfeld, J. H. and Pandis, S. N. (2006). *Atmospheric chemistry and physics: from air pollution to climate change*. John Wiley and Sons, New Jersey, United States of America.
- Shaw, G. E. (1983). Sun Photometry. *Bulletin of the American Meteorological Society*, 64(1):4–10.
- Shindell, D. T., Lamarque, J.-F., Schulz, M., Flanner, M., Jiao, C., Chin, M., Young, P. J., Lee, Y. H., Rotstayn, L., Mahowald, N., Milly, G., Faluvegi, G., Balkanski, Y., Collins, W. J., Conley, A. J., Dalsoren, S., Easter, R., Ghan, S., Horowitz, L., Liu, X., Myhre, G., Nagashima, T., Naik, V., Rumbold, S. T., Skeie, R., Sudo, K., Szopa, S., Takemura, T., Voulgarakis, A., Yoon, J.-H., and Lo, F. (2013). Radiative forcing in the ACCMIP historical and future climate simulations. *Atmospheric Chemistry and Physics*, 13(6):2939–2974.
- Simpson, D., Andersson-Sköld, Y., and Jenkin, M. E. (1993). Updating the chemical scheme for the EMEP MSC-W oxidant model: current status. Norwegian Meteorological Institute. Meteorological Synthesizing Centre-West, Norway.
- Simpson, D., Fagerli, H., Jonson, J., Tsyro, S., Wind, P., and Tuovinen, J. (2003). The EMEP Unified Eulerian Model. Model Description. EMEP MSC-W Report 1/2003. *The Norwegian Meteorological Institute, Oslo, Norway*.
- Skamarock, W. C., Klemp, J. B., Dudhia, J., Gill, D. O., Barker, D. M., Duda, M. G., Huang, X.-Y., Wang, W., and Powers, J. G. (2008). A description of the advanced research WRF version 3. *NCAR technical note*, 475:113.
- Skamarock, W. C., Klemp, J. B., Dudhia, J., Gill, D. O., Barker, D. M., Wang, W., and Powers, J. G. (2005). A description of the advanced research WRF version 2. Technical report, DTIC Document.
- Soares, J., Sofiev, M., and Hakkarainen, J. (2015). Uncertainties of wild-land fires emission in AQMEII phase 2 case study. *Atmospheric Environment*, 115:361–370.

- Sofiev, M., Vankevich, R., Lotjonen, M., Prank, M., Petukhov, V., Ermakova, T., Koskinen, J., and Kukkonen, J. (2009). An operational system for the assimilation of the satellite information on wild-land fires for the needs of air quality modelling and forecasting. *Atmospheric Chemistry and Physics*, 9(18):6833–6847.
- Solazzo, E. and Galmarini, S. (2015). A science-based use of ensembles of opportunities for assessment and scenario studies. *Atmospheric Chemistry and Physics*, 15(5):2535–2544.
- Spracklen, D. V., Pringle, K. J., Carslaw, K. S., Chipperfield, M. P., and Mann, G. W. (2005). A global off-line model of size-resolved aerosol microphysics: I. Model development and prediction of aerosol properties. *Atmospheric Chemistry and Physics*, 5(8):2227–2252.
- Stanhill, G. and Cohen, S. (2001). Global dimming: a review of the evidence for a widespread and significant reduction in global radiation with discussion of its probable causes and possible agricultural consequences. *Agricultural and Forest Meteorology*, 107(4):255–278.
- Stanier, C. O., Khlystov, A. Y., and Pandis, S. N. (2004). Ambient aerosol size distributions and number concentrations measured during the Pittsburgh Air Quality Study (PAQS). *Atmospheric Environment*, 38(20):3275–3284.
- Stengel, M., Stapelberg, M., Schlundt, C., Poulsen, C., and Hollmann, R. (2016). ESA Cloud Climate Change Initiative (ESA Cloud_cci) data: AVHRR-PM CLD_PRODUCTS v2.0. *Deutscher Wetterdienst, 2016*.
- Stengel, M., Stapelberg, M., Sus, O., Schlundt, C., Poulsen, C., Thomas, G., Christensen, M., Henken, C., Preusker, R., Fischer, J., Devasthale, A., Willmott, U., Karlsson, K.-G., McGarragh, G., Povey, A., Grainger, D., Proud, S., Meirink, J., Feofilov, A., Bennartz, R., Bojanowski, J., and Hollmann, R. (2017). Cloud property datasets retrieved from AVHRR, MODIS, AATSR and MERIS in the framework of the Cloud_cci project. *To be submitted to Earth System Science Data*.
- Stensrud, D. J. (2007). *Parameterization schemes: keys to understanding numerical weather prediction models*. Cambridge University Press, New York.
- Steppeler, J., Doms, G., Schättler, U., Bitzer, H., Gassmann, A., Damrath, U., and Gregoric, G. (2003). Meso-gamma scale forecasts using the nonhydrostatic model LM. *Meteorology and Atmospheric Physics*, 82(1):75–96.
- Stevens, B. and Feingold, G. (2009). Untangling aerosol effects on clouds and precipitation in a buffered system. *Nature*, 461(7264):607–613.

- Stevens, B., Lenschow, D. H., Vali, G., Gerber, H., Bandy, A., Blomquist, B., Brenguier, J., Bretherton, C., Burnet, F., and Campos, T. (2003). Dynamics and chemistry of marine stratocumulus-DYCOMS-II. *Bulletin of the American Meteorological Society*, 84(5):579–593.
- Stocker, T., Dahe, Q., Plattner, G.-K., Alexander, L., Allen, S., NL, B., Bréon, F.-M., Church, J., Cubasch, U., Emori, S., Forster, P., Friendlingstein, P., Gillett, N., Gregory, J., Hartmann, D., Jansen, E., Kirtman, B., Knutti, R., Kanikicharla, K., Lemke, P., Marotze, J., Masson-Delmotte, V., Meehl, G., Mokhov, I., Rhein, M., Rojas, M., Sabine, C., Shindell, D., Talley, L., Vaughan, D., and Xie, S.-P. (2013). Technical Summary. In: *Climate Change 2013: The Physical Science Basis. Contribution of Working Group I to the Fifth Assessment Report (AR5) of the Intergovernmental Panel on Climate Change*. Cambridge University Press, Cambridge, United Kingdom and New York, USA.
- Stockwell, W. R., Kirchner, F., Kuhn, M., and Seefeld, S. (1997). A new mechanism for regional atmospheric chemistry modeling. *Journal of Geophysical Research*, 102(D22):25847–25879.
- Stockwell, W. R., Middleton, P., Chang, J. S., and Tang, X. (1990). The second generation regional acid deposition model chemical mechanism for regional air quality modeling. *Journal of Geophysical Research*, 95(D10):16343–16.
- Sus, O., Jerg, M., Poulsen, C., Thomas, G., Stapelberg, S., MCGarragh, G., Povey, A., Schlundt, C., Stengel, M., and Hollmann, R. (2017). The Community Cloud retrieval for CLimate (CC4CL). Part I: A framework applied to multiple satellite imaging sensors. *To be submitted to Atmospheric Measurement Techniques*.
- Taketani, F., Miyakawa, T., Takashima, H., Komazaki, Y., Pan, X., Kanaya, Y., and Inoue, J. (2016). Shipborne observations of atmospheric black carbon aerosol particles over the arctic ocean, bering sea, and north pacific ocean during september 2014. *Journal of Geophysical Research: Atmospheres*, 121(4):1914–1921.
- Tanré, D., Bréon, F., Deuzé, J., Dubovik, O., Ducos, F., François, P., Goloub, P., Herman, M., Lifermann, A., and Waquet, F. (2011). Remote sensing of aerosols by using polarized, directional and spectral measurements within the A-Train: the PARASOL mission. *Atmospheric Measurement Techniques*, 4(7):1383–1395.
- Tao, W.-K., Simpson, J., and McCumber, M. (1989). An ice-water saturation adjustment. *Monthly Weather Review*, 117(1):231–235.
- Taylor, K. E. (2001). Summarizing multiple aspects of model performance in a single diagram. *Journal of Geophysical Research: Atmospheres*, 106(D7):7183–7192.

- Tie, X., Madronich, S., Walters, S., Zhang, R., Rasch, P., and Collins, W. (2003). Effect of clouds on photolysis and oxidants in the troposphere. *Journal of Geophysical Research*, 108, D20, doi:10.1029/2003JD003659.
- Tiedtke, M. (1993). Representation of clouds in large-scale models. *Monthly Weather Review*, 121(11):3040–3061.
- Tomasi, C., Fuzzi, S., and Kokhanovsky, A. (2016). *Atmospheric Aerosols: Life Cycles and Effects on Air Quality and Climate*. John Wiley & Sons, Weinheim, Germany.
- Tompkins, A. M., Gierens, K., and Rädcl, G. (2007). Ice supersaturation in the ECMWF integrated forecast system. *Quarterly Journal of the Royal Meteorological Society*, 133(622):53–63.
- Twitty, J. (1975). The inversion of aureole measurements to derive aerosol size distributions. *Journal of the Atmospheric Sciences*, 32(3):584–591.
- Twohy, C. H., Petters, M. D., Snider, J. R., Stevens, B., Tahnk, W., Wetzcl, M., Russell, L., and Burnet, F. (2005). Evaluation of the aerosol indirect effect in marine stratocumulus clouds: Droplet number, size, liquid water path, and radiative impact. *Journal of Geophysical Research: Atmospheres*, 110(D8).
- Twomey, S. (1974). Pollution and the planetary albedo. *Atmospheric Environment*, 8(12):1251–1256.
- Twomey, S. (1977). The influence of pollution on the shortwave albedo of clouds. *Journal of the Atmospheric Sciences*, 34(7):1149–1152.
- Twomey, S. (1991). Aerosols, clouds and radiation. *Atmospheric Environment. Part A. General Topics*, 25(11):2435–2442.
- Vautard, R., Moran, M. D., Solazzo, E., Gilliam, R. C., Matthias, V., Bianconi, R., Chemel, C., Ferreira, J., Geyer, B., Hansen, A. B., Jericevic, A., Prank, M., Segers, A., Silver, J., Werhahn, J., Wolke, R., Rao S, T., and Galmarini, S. (2012). Evaluation of the meteorological forcing used for the air quality model evaluation international initiative (AQMEII) air quality simulations. *Atmospheric Environment*, 53:15–37.
- Wang, H. and Niu, T. (2013). Sensitivity studies of aerosol data assimilation and direct radiative feedbacks in modeling dust aerosols. *Atmospheric Environment*, 64:208 – 218.
- Wang, K., Yahya, K., Zhang, Y., Hogrefe, C., Pouliot, G., Knote, C., Hodzic, A., Jose, R. S., Perez, J. L., Jiménez-Guerrero, P., Baro, R., Makar, P., and Bennartz, R. (2015). A multi-model assessment for the 2006 and 2010 simulations under the Air Quality Model Evaluation

- International Initiative (AQMEII) Phase 2 over North America: Part II. Evaluation of column variable predictions using satellite data. *Atmospheric Environment*, 115:587 – 603.
- Weil, J., Sykes, R., and Venkatram, A. (1992). Evaluating air-quality models: review and outlook. *Journal of Applied Meteorology*, 31(10):1121–1145.
- Welsch, H. (2007). Environmental welfare analysis: A life satisfaction approach. *Ecological Economics*, 62(3):544–551.
- Wesely, M. L. (1989). Parameterization of surface resistances to gaseous dry deposition in regional-scale numerical models. *Atmospheric Environment*, 23(6):1293–1304.
- Wharton, S. and Lundquist, J. K. (2012). Atmospheric stability affects wind turbine power collection. *Environmental Research Letters*, 7(1):014005.
- Whitby, E. R. and McMurry, P. H. (1997). Modal aerosol dynamics modeling. *Aerosol Science and Technology*, 27(6):673–688.
- Whitten, G. Z., Heo, G., Kimura, Y., McDonald-Buller, E., Allen, D. T., Carter, W. P., and Yarwood, G. (2010). A new condensed toluene mechanism for Carbon Bond: CB05-TU. *Atmospheric Environment*, 44(40):5346–5355.
- Wild, O. and Prather, M. J. (2000). Excitation of the primary tropospheric chemical mode in a global three-dimensional model. *Journal of Geophysical Research*, 105(D20):24647–24660.
- Wilks, D. S. (2011). *Statistical methods in the atmospheric sciences*, volume 100. Academic press, London, United Kingdom.
- Willmott, C. J., Ackleson, S. G., Davis, R. E., Feddema, J. J., Klink, K. M., Legates, D. R., O'Donnell, J., and Rowe, C. M. (1985). Statistics for the evaluation and comparison of models. *Journal of Geophysical Research*, 90(C5):8995–9005.
- Willmott, C. J. and Matsuura, K. (2005). Advantages of the mean absolute error (MAE) over the root mean square error (RMSE) in assessing average model performance. *Climate Research*, 30(1):79–82.
- Wilson, D. R. and Ballard, S. P. (1999). A microphysically based precipitation scheme for the UK Meteorological Office Unified Model. *Quarterly Journal of the Royal Meteorological Society*, 125(557):1607–1636.
- WMO (2003). WMO/GAW Aerosol Measurement Procedures Guidelines and Recommendations. Technical report, GAW No. 153. World Meteorological Organization, WMO. Geneva.

- Wolke, R., Hellmuth, O., Knoth, O., Schröder, W., Heinrich, B., and Renner, E. (2004). The chemistry-transport modeling system LM-MUSCAT: Description and CityDelta applications. In *Air Pollution Modeling and Its Application XVI*, pages 427–439. Kluwer Academic/Plenum Publishers, New York.
- Wolke, R., Schröder, W., Schrödner, R., and Renner, E. (2012). Influence of grid resolution and meteorological forcing on simulated European air quality: a sensitivity study with the modeling system cosmo-muscat. *Atmospheric environment*, 53:110–130.
- Wyant, M. C., Bretherton, C. S., Wood, R., Carmichael, G. R., Clarke, A., Fast, J., George, R., Gustafson Jr., W. I., Hannay, C., Lauer, A., Lin, Y., Morcrette, J.-J., Mulcahy, J., Saide, P. E., Spak, S. N., and Yang, Q. (2015). Global and regional modeling of clouds and aerosols in the marine boundary layer during VOCALS: the VOCA intercomparison. *Atmospheric Chemistry and Physics*, 15(1):153–172.
- Yang, H. and Levy II, H. (2004). Sensitivity of photodissociation rate coefficients and O₃ photochemical tendencies to aerosols and clouds. *Journal of Geophysical Research*, 109, D24, doi:10.1029/2004JD005032.
- Yang, Q., Gustafson Jr, W., Fast, J. D., Wang, H., Easter, R. C., Morrison, H., Lee, Y.-N., Chapman, E. G., Spak, S., and Mena-Carrasco, M. (2011a). Assessing regional scale predictions of aerosols, marine stratocumulus, and their interactions during VOCALS-REx using WRF-Chem. *Atmospheric Chemistry and Physics*, 11(23):11951–11975.
- Yang, Q., Gustafson Jr, W., Fast, J. D., Wang, H., Easter, R. C., Morrison, H., Lee, Y.-N., Chapman, E. G., Spak, S., and Mena-Carrasco, M. (2011b). Assessing regional scale predictions of aerosols, marine stratocumulus, and their interactions during VOCALS-REx using WRF-Chem. *Atmospheric Chemistry and Physics*, 11(23):11951–11975.
- Yarwood, G., Jung, J., Heo, G., Whitten, G. Z., Mellberg, J., and Estes, M. (2010). CBM06 Version 6 of the Carbon Bond Mechanism. 9th Annual CMAS Conference, Chape Hill, NC. October 11-13.
- Yarwood, G., Rao, S., Yocke, M., and Whitten, G. (2005). Updates to the Carbon Bond chemical mechanism: CB05. Final report. Technical report, RT-0400675 Environmental Protection Agency, EPA. United States.
- Yu, F., Luo, G., and Ma, X. (2012). Regional and global modeling of aerosol optical properties with a size, composition, and mixing state resolved particle microphysics model. *Atmospheric Chemistry and Physics*, 12(13):5719–5736.

- Yu, S., Mathur, R., Pleim, J., Wong, D., Gilliam, R., Alapaty, K., Zhao, C., and Liu, X. (2013). Aerosol indirect effect on the grid-scale clouds in the two-way coupled WRF-CMAQ: model description, development, evaluation and regional analysis. *Atmospheric Chemistry and Physics*, page 25649.
- Yu, S. and Zhang, Y. (2011). An examination of the effects of aerosol chemical composition and size on radiative properties of multi-component aerosols. *Atmospheric Climate Science*, 1:19–32.
- Zanis, P. (2009). A study on the direct effect of anthropogenic aerosols on near surface air temperature over southeastern Europe during summer 2000 based on regional climate modeling. *Annales Geophysicae*, 27(10):3977–3988.
- Zaveri, R. A., Easter, R. C., Fast, J. D., and Peters, L. K. (2008). Model for simulating aerosol interactions and chemistry (MOSAIC). *Journal of Geophysical Research*, 113, D13204, doi:10.1029/2007JD008782.
- Zaveri, R. A. and Peters, L. K. (1999). A new lumped structure photochemical mechanism for large-scale applications. *Journal of Geophysical Research*, 104(D23):30387–30415.
- Zhang, B., Wang, Y., and Hao, J. (2015). Simulating aerosol–radiation–cloud feedbacks on meteorology and air quality over eastern china under severe haze conditions in winter. *Atmospheric Chemistry and Physics*, 15(5):2387–2404.
- Zhang, K., Wan, H., Wang, B., Zhang, M., Feichter, J., and Liu, X. (2010). Tropospheric aerosol size distributions simulated by three online global aerosol models using the M7 microphysics module. *Atmospheric Chemistry and Physics*, 10(13):6409–6434.
- Zhang, Y. (2008). Online-coupled meteorology and chemistry models: history, current status, and outlook. *Atmospheric Chemistry and Physics*, 8(11):2895–2932.
- Zhang, Y., Pun, B., Vijayaraghavan, K., Wu, S.-Y., Seigneur, C., Pandis, S. N., Jacobson, M. Z., Nenes, A., and Seinfeld, J. H. (2004). Development and application of the model of aerosol dynamics, reaction, ionization, and dissolution (MADRID). *Journal of Geophysical Research*, 109(D1):1341–1353.
- Zhang, Y., Seigneur, C., Seinfeld, J. H., Jacobson, M. Z., and Binkowski, F. S. (1999). Simulation of aerosol dynamics: A comparative review of algorithms used in air quality models. *Aerosol Science and Technology*, 31(6):487–514.